

A mathematical derivation of zero-temperature 2D superconductivity from microscopic Bardeen-Cooper-Schrieffer model

Jacques Magnen^a and Jérémie Unterberger^b

^aCentre de Physique Théorique,¹ Ecole Polytechnique,
91128 Palaiseau Cedex, France
jacques.magnen@cpht.polytechnique.fr

^bInstitut Elie Cartan,² Université de Lorraine,
B.P. 239, F – 54506 Vandœuvre-lès-Nancy Cedex, France
jeremie.unterberger@univ-lorraine.fr

Starting from H. Fröhlich's second-quantized Hamiltonian for a d -dimensional electron gas in interaction with lattice phonons describing the quantum vibrations of a metal, we present a rigorous mathematical derivation of the superconducting state, following the principles laid out originally in 1957 by J. Bardeen, L. Cooper and J. Schrieffer. As in the series of papers written on the subject in the 90es [22], [25], [24], [23], [56], [17], [18], of which the present paper is a continuation, the representation of ions as a uniform charge background allows for a $(1 + d)$ -dimensional fermionic quantum-field theoretic reformulation of the model at equilibrium. For simplicity, we restrict in this article to $d = 2$ dimensions and zero temperature, and disregard effects due to electromagnetic interactions. Under these assumptions, we prove transition from a Fermi liquid state to a superconducting state made up of Cooper pairs of electrons at an energy level $\Gamma_\phi \sim \hbar\omega_D e^{-\pi/m\lambda}$ equal to the mass gap, expressed in terms of the Debye frequency ω_D , electron mass m and coupling constant λ . The dynamical $U(1)$ -symmetry breaking produces at energies lower than the energy gap Γ_ϕ a Goldstone boson, a non-massive particle described by an effective $(2 + 1)$ -dimensional non-linear sigma-model, whose parameters and correlations are computed. The proof relies on a mixture of general concepts and tools (multi-scale cluster expansions, Ward identities), adapted to this quantum many-body problem with its extended infra-red singularity located on the

¹Laboratoire associé au CNRS UMR 7644

²Laboratoire associé au CNRS UMR 7502. J. Unterberger acknowledges the support of the ANR, via the ANR project ANR-16-CE40-0020-01.

Fermi circle, and a specific $1/N$ -expansion giving the leading diagrams at intermediate energies. Ladder diagrams are proved to provide the leading behavior in the infra-red limit, in agreement with mean-field theory predictions.

Some insights about expected extensions of our method to a rigorous study of real-world, low-temperature superconductivity are provided.

Keywords: BCS theory, constructive field theory, renormalization, cluster expansions, non-linear sigma-model, Goldstone boson, low-temperature superconductivity, Cooper pairs, Ward identities, Bethe-Salpeter kernel, Fermi liquids.

Mathematics Subject Classification (2010): 81T08, 81V70, 82D55.

Contents

0	Introduction	3
0.1	The Bardeen-Cooper-Schrieffer model of electrons and phonons	3
0.2	Constructive approaches for superconductivity	7
0.3	Our results	15
0.4	Outline and notations	23
1	The gap equation	26
1.1	Green functions and Nambu formalism	28
1.2	Symmetry-broken Grassman Gaussian measure	30
1.3	Multi-scale analysis	31
1.4	Bubble diagrams and fermion four-point function in Cooper channel	34
1.5	The gap equation at lowest order	40
1.6	The pre-Goldstone boson propagator	42
1.7	Energy gap and Goldstone boson	46
2	Fermionic theory	59
2.1	Angular decompositions	59
2.2	Dressed action	66
2.3	Cluster expansions	75
2.3.1	Horizontal cluster expansion	79
2.3.2	Single-scale bounds	82
2.3.3	Bubble resummations	90
2.3.4	Momentum-decoupling expansion and displacement of external legs	94
2.3.5	Mayer expansion	96
2.4	Multi-scale bounds and fermionic fixed-point	98

3	Low-energy theory for Cooper pairs	104
3.1	A heuristic introduction	106
3.2	Complementary expansion	109
3.3	Ward identities	130
3.4	Bosonic fixed-point procedure and low-energy multi-scale bounds	137
3.5	Proof of Theorem 2: Cooper pair n -point functions	145
3.6	Proof of Theorem 3: fermion quasi-exponential decay	146
3.7	Proof of Theorem 4: phase transition	147
3.8	Proof of Theorem 5: local transverse behavior of the Goldstone boson	147
4	Generalizations and perspectives	151
5	Appendix	152
5.1	Grassmann integrals	152
5.2	Integration by parts formulas	152
5.3	Local bounds for determinants	154
5.4	Cooper pair bubble and Σ -kernel estimates	156
5.5	Error terms for Ward identities	160
5.6	Mayer expansion	162
	Index of notations	163

0 Introduction

0.1 The Bardeen-Cooper-Schrieffer model of electrons and phonons

The Bardeen-Cooper-Schrieffer (BCS) theory has proved extremely successful at predicting the main characteristic features of conventional, low-temperature superconductivity of metals such as tin, lead, aluminium... see e.g. textbooks [65], [12], [67], [68]. The original objective of the Nobel prizes in their ground-breaking paper [3] was to account for the formation of a condensate of *Cooper pairs*, bound states made of pairs of electrons which behave like bosons, and are in particular responsible for the Meissner effect ³. The explanation for this bound-state is the existence of an effective *attractive force* between pairs of electrons due to the quantum oscillations of the ionic lattice. This remarkable effect can be easily understood starting from H. Fröhlich's [30, 31] second-quantized Hamiltonian \mathcal{H} , depending on a constant $\gamma \neq 0$,

³to which is traditionally attributed the spectacular magnetic levitation. However, disorder-induced vortex trapping supercurrents are more directly responsible for this effect in real materials [5].

$$\begin{aligned} \mathcal{H} := & \int_V d^d \mathbf{x} \bar{\psi}_\sigma(\mathbf{x}) \left\{ -\frac{\hbar^2 \nabla^2}{2m} - \mu \right\} \psi_\sigma(\mathbf{x}) \\ & + \gamma \int_V d^d \mathbf{x} \bar{\psi}_\sigma(\mathbf{x}) \psi_\sigma(\mathbf{x}) \phi(\mathbf{x}) \end{aligned} \quad (0.1)$$

where Einstein's implicit summation convention is used for spin states $\sigma = \{\uparrow, \downarrow\}$. This Hamiltonian involves:

- an *electron field* $\psi_\sigma = (\psi_\uparrow, \psi_\downarrow)$ describing a spin 1/2, mass m , fermionic particle with dispersion relation $\epsilon(\mathbf{k}) := \frac{\hbar^2 |\mathbf{k}|^2}{2m} - \mu$, where μ is a chemical potential regulating the density;
- a *phonon field*, namely, a bosonic quasi-particle describing the oscillations of the lattice,

$$\phi(\mathbf{x}) := \sum_{\mathbf{k}} \left(\frac{\hbar \omega(\mathbf{k})}{2V} \right)^{1/2} [c_{\mathbf{k}} e^{i\mathbf{k} \cdot \mathbf{x}} + c_{\mathbf{k}}^\dagger e^{-i\mathbf{k} \cdot \mathbf{x}}] \Theta(\omega_D - \omega(\mathbf{k})) \quad (0.2)$$

with dispersion relation $\omega(\mathbf{k}) := c|\mathbf{k}|$, where Θ is a smoothed Heaviside function. The superconducting material is assumed to take up a roughly cubic volume $V \subset \mathbb{R}^d$ ($d \geq 1$) with $|V| \approx L^d$, implying a discrete sum over momenta \mathbf{k} roughly multiples of $2\pi/L$. The sum is really a finite sum over momenta \mathbf{k} such that $\omega(\mathbf{k}) < \omega_D$ or equivalently $|\mathbf{k}| < k_D := \frac{\omega_D}{c}$, where k_D^{-1} is roughly equal to the mean spacing between ions. The frequency ω_D is called *Debye frequency*. We shall eventually restrict to space dimension $d = 2$ (possible extension to $d = 3$ is briefly discussed in section 4), but let us keep d arbitrary till then.

In practice, only electrons with momentum \mathbf{k} close to the Fermi circle

$$\Sigma_F := \{|\mathbf{k}| = k_F\}, \quad k_F := \hbar^{-1} \sqrt{2m\mu} \quad (0.3)$$

defined by the vanishing of the energy $\epsilon(\cdot)$ participate in the interactions. We *assume* here that

$$\hbar\omega_D \ll \mu, \quad (0.4)$$

a condition satisfied in usual materials (see discussion in [26], §37), and consider only couplings of the phonon field to electrons with momentum \mathbf{k} such that

$$\epsilon(\mathbf{k}) = O(\hbar\omega_D), \quad (0.5)$$

i.e. to electrons with momenta in an annulus of radius $\delta|\mathbf{k}| \approx \frac{\hbar\omega_D}{\mu} k_F$ around the Fermi circle. The reader may read with profit the classical book by A. Fetter and J. Walecka [26] for: the second quantization formalism applied to interacting many-particle systems (Chapter 1); phonons interacting with electrons (Chapter 12), see in particular §45 where a value for γ is derived in terms of the bulk compressibility of the ionic background seen as an elastic medium; fundamental properties of superconductors, and a semi-rigorous explanation of these using the above model (0.1), see Chapter

13, following arguments due to Bardeen, Cooper and Schrieffer and detailed computations done by L. P. Gor'kov using finite temperature Green's functions [39]. For a more mathematical, modern presentation of 3D BCS theory, see the series of papers by R. Frank, C. Hainzl, E. Hamza, B. Schlein, R. Seiringer and J. P. Solovej [44], [28], [42], [43] where the Ginzburg-Landau theory is derived in an \hbar -small vicinity of the critical temperature by minimizing in the semi-classical limit a functional introduced by A. J. Leggett [51] (called BCS functional) built out of quasi-free trial states.

At zero temperature, the lowest energy state of the system is obtained by filling the energy levels up to μ , i.e. summing over all $\mathbf{k} \in \frac{2\pi}{L}\mathbb{Z}$ such that $|\mathbf{k}| < k_F$. The self-consistent quadratic approximation of \mathcal{H} introduced by Bogoliubov [7, 8] involves elementary excitations known as quasi-particles, with a minimum energy Γ_ϕ known as the *energy gap*, see e.g. [2], §6.4. A phenomenologically important parameter is the density of states at the Fermi surface (compare to [26], p. 333), at temperature $T = 0$, $N(0) \equiv N(T = 0) = \frac{2}{2\pi} k_F \frac{dk}{d\epsilon} \Big|_{\epsilon=\mu} = \frac{m}{\pi\hbar^2}$. Fetter and Walecka find the following value for the energy gap Γ_ϕ in *three* dimensions:

$$\Gamma_\phi \approx \hbar\omega_D e^{-1/N(0)\gamma^2}. \quad (0.6)$$

This energy gap may also be interpreted as a critical temperature $T_c := \Gamma_\phi/k_B$, where k_B is the Boltzmann constant. In 2D, however, the critical temperature is known to be zero because of the celebrated Mermin-Wagner theorem, which forbids continuous symmetry-breaking for any $T > 0$. At $T = 0$, the theory is effectively $(1 + 2)$ -dimensional, as we shall presently see, so the Mermin-Wagner theorem does not apply.

In this article, we use the well-known equivalence (shown by going over to interaction picture and using Wick's theorem) of the quantum model with a functional integral representation in terms of Grassmann fields $\psi, \bar{\psi}$ living in a $(1 + d)$ -dimensional space. The supplementary coordinate τ plays formally the rôle of an *imaginary time*, since dynamics are retrieved (at least formally) by letting $t := -i\tau$. Space-time points are denoted by $\xi = (\tau, \mathbf{x})$. We consider here only vacuum expectation values at zero temperature. Let us consider the infinite volume limit $V \rightarrow \mathbb{R}^3$, so that $\mathbf{p} \equiv \hbar\mathbf{k}$ becomes a continuous momentum variable; and integrate out the phonon field (see [26], §46). Then the ground-state expectation $\left\langle \left(\prod_{i=1}^n \bar{\psi}_{\sigma_i}(\mathbf{x}_i) \right) \left(\prod_{i'=1}^n \psi_{\sigma_{i'}}(\mathbf{x}'_{i'}) \right) \right\rangle$ becomes the Grassmann integral

$$G_n \left((\mathbf{x}_i)_{i=1,\dots,n}, (\mathbf{x}'_{i'})_{i'=1,\dots,n} \right) \equiv \frac{1}{\mathcal{Z}_\lambda} \int d\mu(\psi, \bar{\psi}) \left(\prod_{i=1}^n \bar{\psi}_{\sigma_i}(0, \mathbf{x}_i) \right) \left(\prod_{i'=1}^n \psi_{\sigma_{i'}}(0, \mathbf{x}'_{i'}) \right) e^{-\frac{1}{\hbar}\mathcal{V}(\psi, \bar{\psi})} \quad (0.7)$$

which may be expressed in terms of the normalized Grassmann measure

$$d\mu_\lambda(\psi, \bar{\psi}) := \frac{1}{\mathcal{Z}_\lambda} e^{-\frac{1}{\hbar}\mathcal{V}(\psi, \bar{\psi})} d\mu(\psi, \bar{\psi}), \quad (0.8)$$

where:

- $\psi = \psi(\xi)$, $\bar{\psi} = \bar{\psi}(\xi)$ are now fields living in $(1 + d)$ -dimensional space-time with coordinate $\xi \equiv (\tau, \mathbf{x})$;
- $d\mu(\psi, \bar{\psi})$ is a Grassmann Gaussian measure with covariance kernel given by the inverse of the quadratic form B_0 ,

$$B_0(\psi, \bar{\psi}) := \int dp \bar{\psi}_\sigma(-p)(ip^0 - e(\mathbf{p}))\psi_\sigma(p) \quad (0.9)$$

for fields $\psi, \bar{\psi}$ with Fourier support satisfying the cut-off condition

$$e(\mathbf{p}) \equiv \epsilon\left(\frac{\mathbf{p}}{\hbar}\right) = \frac{|\mathbf{p}|^2}{2m} - \mu = O(\hbar\omega_D), \quad (0.10)$$

see (0.5). A precise definition of the model will be given only at the end of section 1 (see Definition 1.1). It is enough to say here that the measure involves only Fourier scales $\geq j_D$, i.e. momenta (p_0, \mathbf{p}) such that $|p^0| = O(2^{-j_D}\mu)$, $|\mathbf{p} - p_F| = O(2^{-j_D}p_F)$, where $p_F \equiv \hbar k_F$ and

$$j_D \equiv \lfloor \log_2(\mu/\hbar\omega_D) \rfloor \geq 0 \quad (0.11)$$

by (0.4);

- and the interaction $\mathcal{V}(\psi, \bar{\psi})$, formally defined in Fourier coordinates as

$$\int \prod_{i=1}^4 dp_i \delta(p_1 + p_2 - p_3 - p_4) \bar{\psi}_\uparrow(p_1) \psi_\uparrow(p_3) \langle p_1, p_2 | U | p_3, p_4 \rangle \bar{\psi}_\downarrow(p_2) \psi_\downarrow(p_4) \quad (0.12)$$

for a general, spin-neutral two-body potential U written in second-quantized form using the positive electron density operator $\bar{\psi}_\sigma \psi_\sigma$, may be chosen in this context in the form

$$\begin{aligned} \mathcal{V}(\psi, \bar{\psi}) := & \int \prod_{i=1}^4 dp_i \delta(p_1 + p_2 - p_3 - p_4) \bar{\psi}_\uparrow(p_1) \psi_\uparrow(p_3) \\ & \left(-\lambda \tilde{\Theta}(\hbar\omega_D - \omega((\mathbf{p}_1 - \mathbf{p}_3))/\hbar) \frac{\omega^2((\mathbf{p}_1 - \mathbf{p}_3)/\hbar)}{(p_1^0 - p_3^0)^2 + \omega^2((\mathbf{p}_1 - \mathbf{p}_3)/\hbar)} + \frac{r_0}{r_B} \hat{v}(\mathbf{p}_1 - \mathbf{p}_3) \right) \bar{\psi}_\downarrow(p_2) \psi_\downarrow(p_4) \end{aligned} \quad (0.13)$$

where \hat{v} is (the Fourier transform of) a static, rotation-invariant, spin-neutral two-body potential, say, with high enough infra-red cut-off (see discussion in section 4), and $\frac{r_0}{r_B} \equiv \frac{r_0}{\hbar^2/m\epsilon^2}$ (mean interparticle spacing, divided by the Bohr radius) is assumed to be $\ll 1$, corresponding to a high-density (also called: *degenerate*) regime of the electron gas, see [26], §3. Up to inessential issues regarding cut-offs (with $\tilde{\Theta} \approx \Theta^2$ but not quite), (0.1) reduces exactly to this model if one sets $\hat{v} \equiv 0$ and lets

$$\lambda = \gamma^2. \quad (0.14)$$

The well-known and essential observation is that the above kernel $\frac{\omega^2((\mathbf{p}_1-\mathbf{p}_3)/\hbar)}{(p_1^0-p_3^0)^2+\omega^2((\mathbf{p}_1-\mathbf{p}_3)/\hbar)}$ is > 0 , bounded above by 1, and ≈ 1 in average, under our cut-off conditions. In practice, we shall simply replace $\frac{\omega^2((\mathbf{p}_1-\mathbf{p}_3)/\hbar)}{(p_1^0-p_3^0)^2+\omega^2((\mathbf{p}_1-\mathbf{p}_3)/\hbar)}$ by 1, implying an *attractive* δ -interaction between electrons. We still denote by \mathcal{V} the corresponding interaction,

$$\mathcal{V}(\psi, \bar{\psi}) = -\lambda \int \prod_{i=1}^4 dp_i \delta(p_1+p_2-p_3-p_4) \bar{\psi}_\uparrow(p_1) \psi_\uparrow(p_3) \tilde{\Theta}(\hbar\omega_D - e(\mathbf{p}_1-\mathbf{p}_3)) \bar{\psi}_\downarrow(p_2) \psi_\downarrow(p_4) \quad (0.15)$$

and argue in section 4 that a small enough, short-ranged two-body potential \hat{v} can be added to \mathcal{V} without altering the general conclusions, provided the overall effect near the Fermi sphere remains that of an *attractive* potential.

Let us mention the following result by W. Kohn and J. M. Luttinger [47, 52]: in $d = 3$ dimensions, they proved that for essentially *any* arbitrary, even *purely repulsive*, rotation-invariant interaction, the scattering amplitude for pairs of quasi-particles of opposite momenta had poles on the Fermi surface, implying the possibility of creation of a superconducting bound state in large enough *odd* angular momentum sectors. This is shown by analyzing the sign of non-zero angular momentum second-order contributions such as those of Fig. 1.7.2, which however vanish for $d = 2$. On the other hand, in $d = 2$ dimensions, J. Feldman, H. Knörrer, R. Sinclair and E. Trubowitz [20] proved that third-order contributions, namely, *triangle diagrams*

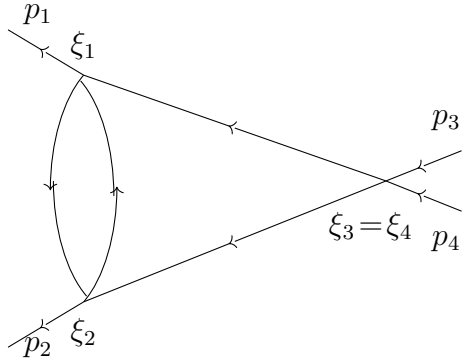


Fig. 0.1. Triangle diagram.

created superconducting bound states in the angular momentum sector $\ell = 1$. Hence one can expect that our conclusions extend to very general, not purely attractive interactions.

0.2 Constructive approaches for superconductivity

Constructive methods (actually, *multi-scale cluster expansions*), see e.g. [1, 19, 33, 34, 21, 35, 36, 54, 55, 60, 61, 70, 71], consist in implementing rigorously Wilson's renormalization group ideas developed to study small perturbations of Gaussian models. In

the case at hand, correlation functions are computed by averaging w.r. to a Grassmann Gaussian measure $d\mu(\psi, \bar{\psi})$ perturbed by a quartic interaction $e^{\lambda \int d\tau d\mathbf{x} (\bar{\psi}_\uparrow \psi_\uparrow)(\tau, \mathbf{x})(\bar{\psi}_\downarrow \psi_\downarrow)(\tau, \mathbf{x})}$, with λ *small enough*. The bare covariance is infra-red singular on the set ($p^0 = 0, |\mathbf{p}| = p_F$). In principle, bare parameters of the model, m, μ, λ , become running coupling constants m^j, μ^j, λ^j through the renormalization procedure. In our case, λ is not renormalized (see below why), and the model is directly rewritten in terms of its renormalized parameters $m^* := \lim_{j \rightarrow +\infty} m^j, \mu^* := \lim_{j \rightarrow +\infty} \mu^j$ and

$$p_F^* := \sqrt{2m^*\mu^*}. \quad (0.16)$$

The first step consists in splitting the covariance of the measure according to the distance to the singularity; namely, one rewrites $\psi, \bar{\psi}$ as sums of independent fields, $\psi = \sum_j \psi^j, \bar{\psi} = \sum_j \bar{\psi}^j$ ($j \geq 0$), whose covariance is supported on the set $|\mathbf{p}^0| + \frac{p_F^*}{\mu^*} \left| |\mathbf{p}| - p_F^* \right| \approx 2^{-j} \mu$. Splitting each field of each vertex into its components, and splitting accordingly perturbative graphs by letting scale indices *grow from the top to the bottom* (see e.g. Fig. 2.3.1), one gets the following picture: *high-momentum diagrams* of lowest scale j (i.e. with all covariance indices $\leq j$) are *quasi-local* w.r. to *low-momentum diagrams* of highest scale $k \gg j$. For λ small enough, this allows the sum of *all* perturbative graphs of lowest scale j to be resummed into effective corrections to low-momentum vertices, amounting to a scale-by-scale renormalization of parameters. Graphs of a given scale j are resummed using a cluster expansion; as well-known, for *fermionic* theories, the exponential of the interaction may be expanded to infinity, see e.g. [55], [61]. The above scheme works provided effective corrections can be shown to remain small; in particular, if the running coupling constant remains $o(1)$. In the present case, however, the running coupling constant becomes large around some transition scale (logarithm of the inverse of the energy gap) called j_ϕ , implying that the perturbation around the Grassmann Gaussian measure is not pertinent any more. This is interpreted as the formation of a *bound state* made up of *Cooper pairs*. Instead of merely relying on perturbation theory, the idea is therefore to *resum* explicitly a class of four-point diagrams, forming the *Bethe-Salpeter kernel*, which contribute to this *non-perturbative* effect. The sum – mathematically, a kernel denoted $\Sigma_{\perp, \perp}(\tau, \mathbf{x}; \tau', \mathbf{x}')$, one of the components of a two-by-two matrix-valued kernel Σ –, may be interpreted as the two-point function of the bound state. The leading behavior of this kernel may be captured by looking simply at the geometric series of *ladder (bubble) diagrams*, which can be explicitly computed. These two-point functions turn out to be the only non-massive (i.e. long-range) ones, hence they give the main contribution to the theory at large scale, an effective *bosonic* theory in the same class as the $U(1)$ *non-linear sigma model*. The underlying non-massive boson may be called *Goldstone boson*, by reference to the general theory of continuous symmetry-breaking (see discussion of Regime II below), and the kernel $\Sigma_{\perp, \perp}$ *Goldstone boson propagator*, the other non-vanishing component, $\Sigma_{//, //}$, being massive. A full understanding of the model at all scales can be obtained by considering "mixed" diagrams featuring both fermionic propagators and vertices, and some bound-state two-point

functions. Contrary to fermionic vertices, though, Σ -kernels must not be systematically expanded, but rather (as for most non-massive bosonic models, see e.g. [21]) through some careful cluster expansion.

Let us emphasize one specific aspect of the present model, which ultimately explains why non-perturbative effects can be dealt with at an analytical level. The *small parameter* here is the expected mean value of the interaction, restricted to some *scale* j and integrated over a scaled box $\Delta^j \subset \mathbb{R}^{1+d}$ with sides of length $\approx 2^j$, $\lambda I^j(\Delta^j) = O(m\lambda)$ up to spurious logarithmic corrections, see (2.23), (2.26), independently of the choice of the scale j defined for typical momenta as $\lfloor \log(\mu/|p^0|) \rfloor$ or $\lfloor \log(p_F/|\mathbf{p}| - p_F) \rfloor$, which reflects the fact that the theory near the Fermi sphere is *just renormalizable (independently of space dimension)*. Note that this very fact is actually not straightforward, and more easily established in $d = 2$ dimensions than for $d = 3$ (see brief discussion in section 4). Therefore *we restrict to $d = 2$ in the sequel*. n -point functions within a given scale will be reexpressed in terms of a geometric-like entire series in the *non-dimensional parameter*

$$g := m\lambda, \quad (0.17)$$

hence converge *provided*

$$g \ll 1. \quad (0.18)$$

(2.26) is based on the "sector-counting proposition", see Proposition 2.5, which may be rephrased as follows (see [23]): *The theory near the Fermi surface (in this context, Fermi circle) may be with remarkable accuracy reformulated after a scale-dependent rescaling as a large N vector model with action*

$$\sim N \int d\xi \left(\sum_{\alpha_1=1}^N (\bar{\psi}_{\uparrow}^{\alpha_1} \bar{\psi}_{\downarrow}^{\alpha_1})(\xi) \right) \left(\sum_{\alpha_2=1}^N (\psi_{\uparrow}^{\alpha_2} \psi_{\downarrow}^{\alpha_2})(\xi) \right), \quad (0.19)$$

$\xi = (\tau, \mathbf{x})$, where the fields $\psi_{\uparrow,\downarrow}^{\alpha}$, $\bar{\psi}_{\uparrow,\downarrow}^{\alpha}$ ($\alpha = \alpha_{1,2}$) are fermion fields restricted to a given momentum angular sector indexed by α and rescaled in such a way that $\sum_{\alpha=1}^N \langle (\bar{\psi}_{\sigma}^{\alpha} \psi_{\sigma}^{\alpha})(\xi) \rangle \sim 1$. The momentum-scale dependent number $N \equiv N_j = 2^j$ increases exponentially as one gets nearer to the Fermi circle defined by $j = +\infty$. Expanding the interaction and using Wick's theorem yields Feynman diagrams made up of vertices and fermion loops, each in a given angular sector, which may be thought of as a "color". Performing the sum over colors produces *for generic vertices* a factor $O(N)$ per fermion loop, and $O(1/N)$ per vertex. Alternatively, following a fermion loop, one can prove that *there is at most one sum over sectors per vertex* in a given diagram. Then dominant diagrams in an $1/N$ -expansion are *chains of bubbles* (see §1.4), as confirmed perturbatively by a Feynman diagram expansion; the simplicity of the theory is due to the fact that chains of bubbles make up a geometric series which can be resummed explicitly. The idea of the "1/N-expansion" is old and has been used in many different contexts; we refer the reader to [48] and [46] respectively for a rigorous analysis of the N -component Gross-Neveu and non-linear sigma model.

Instead of N -component vectors, one sometimes also considers large $N \times N$ -matrices, either in the context of random matrices or Schrödinger operators [6], [58] – in connection to two-dimensional gravity [14], since leading terms are then planar diagrams – or as an approximation to gauge theories, following a seminal paper by 't Hooft, see [66] or [29], chap. 7 for a review of two-dimensional quantum-field theory models in this limit. R. Gurau, V. Rivasseau et al. have also applied these ideas to tensor field models, see [40], [41].

Under Hypothesis (0.18), the following scenario – in accordance with the original idea by Bardeen, Cooper and Schrieffer, but going beyond mean-field regime predictions, which are valid only for an infinitesimal interaction, physically, in an ideally degenerate regime, see below (0.5) – was explored in the 90's by various theoretical physicists, including one of the authors of the present work, see articles by M. Disertori, J. Feldman, J. Magnen, V. Rivasseau, E. Trubowitz [22], [25], [24], [23], [56], [16],[17], [18], [15]. Notations are as follows: energy and momentum scales are labeled by an integer index j ranging from j_D to $+\infty$; typical energies p^0 , resp. transverse momenta $|\mathbf{p}| - p_F$ of scale j are $\approx 2^{-j}\mu$, resp. $\approx 2^{-j}p_F$. The highest scale $j_D \geq 0$ is defined in agreement with the above cut-off hypotheses (0.4), (0.5). Physical parameters, in particular, the electron mass, the coupling constant and the Fermi radius (or, equivalently, the chemical potential) are renormalized à la Wilson, defining scale parameters m^j, λ^j, μ^j . *Three energy regimes were singled out:*

- (i) **(Regime I, high-energy regime)** At *high enough energy*, i.e. for j *small enough*, no bound states can form, and electrons are still in their normal, Fermi liquid phase, where they behave essentially like free fermions, see [16]. The scale-by-scale renormalization of the model à la Wilson yields the following flow for the coupling constant,

$$\lambda^{j+1} - \lambda^j \approx (\lambda^j)^2 \left[\mathcal{A}_0^{j \rightarrow}(\Upsilon_{3,diag}) - \mathcal{A}_0^{(j-1) \rightarrow}(\Upsilon_{3,diag}) \right] \quad (0.20)$$

where $\Upsilon_{3,diag}$ is the amputated Cooper pair bubble diagram of §1.4 (see Fig. 1.4.3), and $\mathcal{A}_0^{j \rightarrow}(\Upsilon_{3,diag})$ is the evaluation at zero external momentum of $\Upsilon_{3,diag}$ computed for internal momenta of scale $\leq j$, see §1.4. The difference $(\mathcal{A}_0^{j \rightarrow} - \mathcal{A}_0^{(j-1) \rightarrow})(\Upsilon_{3,diag})$ is approximately scale independent (which is essentially tantamount to saying that the theory is just renormalizable) and $\approx \frac{m}{\pi}$. As long as $\lambda \mathcal{A}_0^{j \rightarrow}(\Upsilon_{3,diag})$ remains $o(1)$, the solution of the flow equation is well approximated by

$$(\lambda^j)^{-1} \simeq \lambda^{-1} - \mathcal{A}_0^{j \rightarrow}(\Upsilon_{3,diag}) \quad (0.21)$$

or equivalently,

$$\lambda^j \simeq \frac{\lambda}{1 - \lambda \mathcal{A}_0^{j \rightarrow}(\Upsilon_{3,diag})}. \quad (0.22)$$

Just a few scales above a transition scale j_ϕ defined by $\lambda \mathcal{A}_0^{(j_\phi-1) \rightarrow}(\Upsilon_{3,diag}) < 1 < \lambda \mathcal{A}_0^{j_\phi \rightarrow}(\Upsilon_{3,diag})$, the renormalized coupling constant $m\lambda^j \approx 1$ becomes large.

Thus the above perturbative regime analysis breaks down. Since (as shown in §1.4) $\mathcal{A}_0^{j \rightarrow}(\Upsilon_{3,diag}) \sim \frac{m}{\pi}(j - j_D)$, the above condition holds for

$$j_\phi = j_D + \frac{\pi}{\lambda m} + O(1). \quad (0.23)$$

This defines an energy level for the transition,

$$\Gamma_\phi \approx 2^{-j_\phi} \mu. \quad (0.24)$$

Let us add here some necessary precisions. Because one renormalizes in the vicinity of the Fermi circle, which is an *extended singularity*, it is easy to see that leading corrections to the vertex are "pinched" diagrams of the form

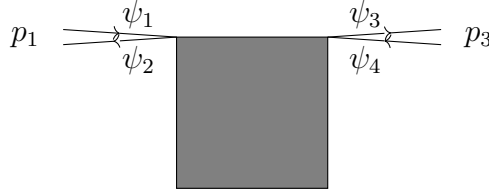


Fig. 0.2. Bethe-Salpeter kernel.

(see Fig. 1.7.5 for details), $\psi_i = \psi, \bar{\psi}$ ($i = 1, \dots, 4$) with external momenta $p_1 = (0, \mathbf{p}_1), p_3 = (0, \mathbf{p}_3)$ near the Fermi circle, depending only on the relative angle $(\widehat{\mathbf{p}_1, \mathbf{p}_3})$. *Two-particle irreducible* diagrams of this type *with Cooper pair external structure*, i.e. with $\psi_1\psi_2, \psi_3\psi_4 = \bar{\psi}_\uparrow\bar{\psi}_\downarrow, \psi_\downarrow\psi_\uparrow$, form the so-called *Bethe-Salpeter kernel*, which may be summed into a geometric series. Now, the bare theory has an ultra-local, *angle-independent* vertex $-\lambda(\bar{\psi}\psi)^2$, and Cooper pair bubbles lead to angle-independent, *s-wave* corrections. However, more complicated diagrams with extra vertices lead to *angle-dependent* corrections, that may be seen as effective *p-wave, d-wave, etc.* effective vertices. To leading order these do not interfere, because they are orthogonal Fourier modes. Hence we get instead of (0.20) an infinite series of flows,

$$\lambda_s^{j+1} - \lambda_s^j \approx (\lambda_s^j)^2 \left[\mathcal{A}_0^{j \rightarrow}(\Upsilon_{3,diag}) - \mathcal{A}_0^{(j-1) \rightarrow}(\Upsilon_{3,diag}) \right] \quad (0.25)$$

compare with (0.20), and

$$\begin{aligned} \lambda_p^{j+1} - \lambda_p^j &\approx (\lambda_p^j)^2 \left[\mathcal{A}_0^{j \rightarrow}(\Upsilon_{3,diag}) - \mathcal{A}_0^{(j-1) \rightarrow}(\Upsilon_{3,diag}) \right] + O((\lambda^j)^3), \\ \lambda_d^{j+1} - \lambda_d^j &\approx (\lambda_d^j)^2 \left[\mathcal{A}_0^{j \rightarrow}(\Upsilon_{3,diag}) - \mathcal{A}_0^{(j-1) \rightarrow}(\Upsilon_{3,diag}) \right] + O((\lambda^j)^3), \quad \dots \end{aligned} \quad (0.26)$$

The difference between (0.25) and (0.26) is that $\lambda_s^{j_D} = \lambda$ whereas $\lambda_n^{j_D} = 0$, $n = p, d, \dots$. Thus coupling constants other than λ_s increase much more slowly, with leading term at scale $j \ll j_\phi$ bounded by the sum $\sum_{k=j_D}^j O((\lambda_s^k)^3) \approx \frac{1}{(j_\phi - j)^2}$, whereas $\lambda_s^j \approx \frac{1}{j_\phi - j}$. This is not sufficient to conclude (see discussion in §1.7, and around eq. (3.35)), but strongly hints at an *s*-wave superconducting behavior.

(ii) **(Regime II, near transition scale)**

In regimes II and III, that is, around and below the gap energy, the phonon field ϕ , initially centered around 0, is seen by semi-perturbative arguments to choose a more favorable position on a circle of radius $\approx \Gamma_\phi$, which *breaks the $U(1)$ fermionic charge symmetry* $\begin{pmatrix} \psi(\xi) \\ \bar{\psi}(\xi) \end{pmatrix} \mapsto \begin{pmatrix} e^{i\alpha}\psi(\xi) \\ \bar{\psi}(\xi)e^{-i\alpha} \end{pmatrix}$. At a semi-rigorous level, this can be seen using a *Hubbard-Stratonovich transform*,

$$e^{-\mathcal{V}} = \int d\mu(\Gamma) e^{-\int_V d\xi \begin{pmatrix} \bar{\psi}_\uparrow \\ \psi_\downarrow \end{pmatrix}^t (\xi) \Gamma(\xi) \begin{pmatrix} \psi_\uparrow \\ \bar{\psi}_\downarrow \end{pmatrix} (\xi)}, \quad (0.27)$$

$\Gamma(\xi) \equiv \begin{pmatrix} 0 & \Gamma^*(\xi) \\ \Gamma(\xi) & 0 \end{pmatrix}$, where $d\mu(\Gamma)$ is the probability measure on complex-valued fields $\Gamma \equiv \Gamma_1 + i\Gamma_2 : V \rightarrow \mathbb{C} \simeq \mathbb{R}^2$ defined by

$$\int d\mu(\Gamma) \Gamma_i(\xi) \Gamma_{i'}(\xi') = \lambda \delta_{i,i'} \delta(\xi - \xi'), \quad (0.28)$$

corresponding to a quadratic action $\frac{1}{2}\lambda^{-1} \int d\xi |\Gamma(\xi)|^2$. This formula is very much related to the original BCS interaction in $\bar{\psi}_\sigma \psi_\sigma \phi$, see (0.1), but now the random potential ϕ has become an *off-diagonal Hermitian matrix* Γ , *coupling Cooper pairs* $(\bar{\psi}_\uparrow, \bar{\psi}_\downarrow)$ or $(\psi_\uparrow, \psi_\downarrow)$. Fermionic charge symmetries translate into rotations $\Gamma(\xi) \mapsto e^{2i\alpha}\Gamma(\xi)$ of the Γ -field. The fact that the values of the field Γ concentrate statistically on a small neighborhood of a circle is by itself a good argument to try to split locally Γ into the sum of a tangential component Γ_{tang} (parallel to the circle) and a transversal (orthogonal) component Γ_{transv} ; from simpler models with the same symmetries, see e.g. [49], §13.3.1 for an example inspired by the Glashow-Salam-Weinberg model of electroweak interactions, it is understood by elementary computations that the tangential, resp. transversal components should be massless, resp. massive. The tangential component is traditionally called *Goldstone boson* by reference to the well-known Goldstone's theorem [38] stating that *for every spontaneously broken continuous symmetry, a given theory must contain a massless particle*. Here we find as effective theory a non-linear sigma model, see e.g. [57], Chapter 11 and §13.3. Applying Gaussian integrations by parts on the measure (0.27), one easily sees that n -point functions of the *Goldstone boson* Γ are directly related to $2n$ -point functions of

electron pairs in the *Cooper pair channel*, $\bar{\psi}_\uparrow\bar{\psi}_\downarrow$ or $\psi_\downarrow\psi_\uparrow$. Integrating instead w.r. to the *fermions* yields now a *bosonic theory in terms of* Γ , with total (i.e., quadratic part + interaction) action

$$\mathcal{F}(\Gamma) = \frac{1}{2}\lambda^{-1} \int d\xi \left\{ |\Gamma(\xi)|^2 - \log \det(\text{Id} - C\Gamma)(\xi) \right\} \quad (0.29)$$

up to cut-offs, where C is the covariance kernel of the fermions. Using the identity $\log \det(\text{Id} - A) = \text{Tr} \log(\text{Id} - A) = -\text{Tr} \left(A + \frac{A^2}{2} + \frac{A^3}{3} + \dots \right)$, noting that odd powers do not contribute to the trace, assuming Γ to be *constant*, and dividing by the volume, one obtains the so-called *effective potential*, $\mathcal{S}(\Gamma)$, for which an explicit formula was obtained in [22], section 4,

$$\mathcal{S}(\Gamma) = \mathcal{S}(|\Gamma|) = \frac{1}{2}\lambda^{-1}|\Gamma|^2 - (2\pi)^{-3} \int dp \log \left(1 + \frac{|\Gamma|^2}{(p^0)^2 + (\epsilon(\mathbf{p}))^2} \right) \quad (0.30)$$

with an ultra-violet cut-off in p at $|p^0|, |\mathbf{p}| \approx \hbar\omega_D$. (The exact correspondence is $\mathcal{S}(\Gamma) \sim (\hbar\omega_D)^2 \mathcal{E} \left(\left(\frac{\Gamma}{g\hbar\omega_D} \right)^2 \right)$ in the notations of [22], p. 48, with $g \equiv \sqrt{\lambda}$). By construction, $\mathcal{S}(\Gamma)$ is due to the *ladder diagrams* obtained by resumming Cooper pair bubble diagrams, see §1.4. Searching for the minimum $\Gamma_\phi = \text{argmin}(\mathcal{S})$ of \mathcal{S} gives an implicit equation, known as the **gap equation**, which coincides with the one found in mean-field theory, i.e. starting from the Bogoliubov-De Gennes Hamiltonian, see e.g. [2], §6.4, and the one given in our §1.5. The solution of the gap equation is

$$|\Gamma| \sim \Gamma_\phi \sim \hbar\omega_D e^{-\pi/\lambda m}, \quad (0.31)$$

where Γ_ϕ is as in (0.24) and (0.6).

As was already well understood from the $1/N$ -asymptotic expansion in previous work on the subject, dominant contributions due to ladder diagrams are actually the *only* divergent ones, thus explaining in particular the essential fact that *only electron pairs in the Cooper channel contribute to the superconductive phase*.

Allowing $\Gamma = \Gamma(\xi)$ to fluctuate, one obtains an action for tangential fluctuations $\Gamma_{tang}(\xi)$ which is roughly $\approx \frac{1}{g_\phi} \int d\xi |\nabla \Gamma_{tang}(\xi)|^2$, in Fourier,

$$\approx \frac{1}{g_\phi} \int dq \left((q^0)^2 + v_\phi^2 |\mathbf{q}|^2 \right) |\hat{\Gamma}_{tang}(q)|^2, \quad (0.32)$$

where $g_\phi \approx \frac{\Gamma_\phi^2}{m}$ and

$$v_\phi \approx v_F := \frac{p_F}{m} \quad (0.33)$$

(Fermi velocity) is a velocity, see e.g. [23].

Although $d = 2$, the zero-temperature theory is effectively a $(1 + 2)$ -dimensional theory. Hence Mermin-Wagner's argument does not apply, and infinitesimal bulk or boundary terms are in principle enough to imply a symmetry-breaking in some direction θ , by which we mean that

$$\Gamma \sim \Gamma_\phi e^{i\theta} + \text{fluctuation}. \quad (0.34)$$

- (iii) **(Regime III, low-energy regime)** Around the transition scale, the Goldstone boson favors a position on a circle of radius Γ_ϕ , thus conferring the electron an effective squared mass $\sim \Gamma_\phi > 0$ which dominates the kinetic energy term. Thus electrons are "hooked up" to a fixed scale $\simeq j_\phi$: Regime III may be thought of *from the point of view of unpaired fermions* as a *single scale* extending from j_ϕ to $+\infty$. Dominant low-momentum contributions to Feynman diagrams come therefore exclusively from the Goldstone boson. Now, Ward identities associated to the (broken) $U(1)$ number symmetry prove (more or less as in the case of diagrams with low-momentum photons in quantum electrodynamics) that such diagrams vanish up to error terms coming from cut-off effects, which decrease exponentially as one lowers the energy scale. Thus, below an energy level

$$j'_\phi = j_\phi + o(\ln(1/g)), \quad (0.35)$$

the effective coupling constant of diagrams is once again small enough to sum series produced by the cluster expansion. Contrary to individual fermions, the Goldstone boson (or equivalently, electron pairs in the Cooper channel) remains non-massive in the *Euclidean infra-red* defined *not by the vicinity to the Fermi circle*, but by the *vicinity to 0*.

Unfortunately, the writing of the above program stopped at the end of the 90'es somewhere between Regime I and Regime II for lack of a sound mathematical proof, due to technical difficulties coming mainly from the necessity of integrating simultaneously the fermion fields $\psi, \bar{\psi}$ and the Goldstone boson field Γ . At each scale j , one had to distinguish "small-field", perturbative regions, from "large-field" regions, which could be handled only through large deviation arguments. In theory, the idea was to split the Γ -field into the sum of a "fast" perturbation field Γ_f with scale index $\leq j$, and of a "slow" background field Γ_b with scale index $> j$, giving a local orientation and making it possible to define a "tangential" and a "transversal" component. In the small field region, Γ_f is small, and Γ_b minimizes to a good approximation the effective potential computed with the contributions of the scales $\leq j$. The main difficulty was to prove that a given region was "small-field" with high probability.

Also, both the implementation of Ward identities and the use of the $1/N$ -expansion are awkward in this representation, requiring partial integrations of the bosonic field in order to go back to a purely fermionic representation. Finally, integrating out fermions in order to deal with the infra-red behavior of the boson field naturally leads

to functional determinants such as (0.29) which are delicate to define properly and handle in combination with cluster decompositions (see the above cited paper [46] by C. Kopper for a successful result in this direction for a *scalar* intermediate boson field).

Our strategy here is different; let us describe it briefly, highlighting differences with previous attempts. We introduce by hand a fixed symmetry-breaking term ("adding and subtracting" it) with a given, arbitrary but fixed, orientation θ (see (0.34)), and a module computed by a fixed-point argument; this spares us the trouble of having to define a local orientation around every point. Thus the transversal, resp. tangential, direction is *parallel* ($//$), resp. *perpendicular* (\perp), to θ . We carefully avoid introducing the Goldstone field in the first place, producing instead through an explicit expansion an effective, non-local interaction kernel $\Sigma_{\perp,\perp}$ in the perpendicular (\perp) direction, called *Goldstone boson propagator*, which is obtained by resumming a geometric series made up of alternating Cooper pair bubble diagrams and Bethe-Salpeter kernels, themselves sums of two-particle irreducible diagrams as in Fig. 0.2; the $\Sigma_{\perp,\perp}$ -kernel may be interpreted as the propagator of a bosonic particle which is never introduced. Decomposing fields into angular sectors, we are able to prove that the two-point function of Cooper pairs diverge only in the *s*-wave. Then – taking the *s*-wave projection – we write down in terms of $\Sigma_{\perp,\perp}$ an exact, non-perturbative version of the gap equation mentioned in the discussion of the neighborhood of the transition scale (see Regime II above). The actual value of the gap Γ_ϕ is shown to be close to the mean-field one (0.31) by a fixed-point argument. Cooper pair two-point functions are shown to be proportional to the $\Sigma_{\perp,\perp}$ -kernel, itself roughly inverse of the conjectural action associated to tangential fluctuations of the Γ -field (again, see Regime II).

Proceeding this way, we fill this important gap in the literature, thus hopefully laying the foundational stones of a rigorous mathematical analysis of 2D and 3D low-temperature superconductivity from first principles, going beyond Ginzburg-Landau theory. We also conjecture that our methods will help understand related models featuring a dynamical symmetry-breaking transition in a large N regime, like 3D Anderson's model in its delocalized phase, or the integer quantum Hall effect.

0.3 Our results

Instead of singling out three regimes, we proceed as follows.

A. (fermionic regime, or high-momentum theory) We *choose* a value for j_ϕ such

that (0.23) holds, and consider the fermionic theory directly with *effective parameters* $\Gamma_\phi \approx \hbar\omega_D e^{-\pi/m\lambda}$, $m^* \approx m$, $\mu^* \approx \mu$, namely, we modify the Grassmann Gaussian measure $d\mu(\psi, \bar{\psi})$ of eq. (0.9) by multiplying it with the exponential of a quadratic weight,

$$d\mu_\theta^*(\psi, \bar{\psi}) \propto e^{-\int d\xi \begin{pmatrix} \bar{\psi}_\uparrow \\ \bar{\psi}_\downarrow \end{pmatrix}^t (\xi) \left\{ \mathbb{F}(\theta) + \left(\frac{1}{m} - \frac{1}{m^*}\right) \frac{|\nabla|^2}{2} + (\mu^* - \mu) \right\} \begin{pmatrix} \psi_\uparrow \\ \psi_\downarrow \end{pmatrix} (\xi)} d\mu(\psi, \bar{\psi}) \quad (0.36)$$

where $\xi = (\tau, \mathbf{x})$, and $\mathbb{F}(\theta) = \begin{pmatrix} 0 & \Gamma^* \\ \Gamma & 0 \end{pmatrix} \equiv \begin{pmatrix} 0 & \Gamma_\phi e^{-i\theta} \\ \Gamma_\phi e^{i\theta} & 0 \end{pmatrix}$, $\theta \in \mathbb{R}/2\pi\mathbb{Z}$ is a *constant* off-diagonal, Hermitian matrix; see Definition 1.1 for a precise definition. Up to cut-offs, the covariance kernel of $d\mu_\theta^*$ is the inverse of the quadratic form

$$B(\psi, \bar{\psi}) = \int dp \begin{pmatrix} \bar{\psi}_\uparrow(-p) \\ \bar{\psi}_\downarrow(-p) \end{pmatrix}^t \left\{ ip^0 - e^*(p)\sigma^3 - \mathbb{F} \right\} \begin{pmatrix} \psi_\uparrow(p) \\ \psi_\downarrow(p) \end{pmatrix}, \quad (0.37)$$

compare with (0.9), where $e^*(p) := \frac{|p|^2}{2m^*} - m^*$ is the effective (or renormalized) dispersion relation. This extra term is compensated by subtracting it to the interaction, which takes the form of a bare, scale j_D counterterm $\delta\mathcal{V}_\theta := \int d\xi \delta\mathcal{V}_\theta(\xi)$ added to the interaction \mathcal{V} defined in (0.15), namely,

$$\delta\mathcal{V}_\theta(\xi) = - \begin{pmatrix} \bar{\psi}_\uparrow \\ \bar{\psi}_\downarrow \end{pmatrix}^t (\xi) \left\{ \delta\mathbb{F}^{j_D} + \frac{\delta m^{j_D}}{(m^*)^2} \frac{|\nabla|^2}{2} + \delta\mu^{j_D} \right\} \begin{pmatrix} \psi_\uparrow \\ \psi_\downarrow \end{pmatrix} (\xi),$$

and

$$\delta\mathbb{F}^{j_D} := \mathbb{F}(\theta), \quad \frac{\delta m^{j_D}}{(m^*)^2} := \frac{1}{m} - \frac{1}{m^*}, \quad \delta\mu^{j_D} := \mu^* - \mu. \quad (0.38)$$

Because of the ultra-violet, scale j_D cut-off, the resulting measure

$$d\mu_{\theta;\lambda}(\psi, \bar{\psi}) := \frac{1}{\mathcal{Z}_\lambda^*} e^{-(\mathcal{V} + \delta\mathcal{V}_\theta)} d\mu_\theta^*(\psi, \bar{\psi}) \quad (0.39)$$

depends on θ , on Γ_ϕ , on m^* and on μ^* . In particular – as will be shown –, it induces an infinite-volume symmetry-breaking precisely in the direction θ . Then we study the renormalization flow from scale j_D to scale $j'_\phi = j_\phi + o(\ln(1/g))$. Fermions are shown to become massive at energy scales $\simeq j_\phi$, making it possible to integrate out fermions with energy scales $> j_\phi$ as if they were of the same scale, *provided* they do not form Cooper pairs with low transfer momentum.

The considerable difference with the above discussion of Regime I is that, should one start from $\Gamma = 0$, then the number symmetry would imply that Γ is *not* renormalized: the fact that $\Gamma \neq 0$ in average is a *non-perturbative* effect. Proceeding that way, the symmetry-breaking would be read only indirectly through the apparition of a large, renormalized coupling constant depending on the momentum angular sectors of its four legs, favoring $\bar{\psi}_\uparrow\psi_\downarrow, \psi_\downarrow\psi_\uparrow$ in Cooper channels. These, in turn, might be subtracted by changing the value of Γ . Our approach looks much simpler.

Let us remark at this point that another (maybe physically more natural) procedure would have led to an equivalent effective, large-scale behavior. Namely, we could have chosen a lattice ultra-violet cut-off with lattice constant a on a large volume $V \subset \mathbb{R} \times \mathbb{R}^2 = \text{span}(\mathbf{e}_0, \mathbf{e}_1, \mathbf{e}_2)$, with inverse covariance kernel $\mathcal{A}(\psi, \bar{\psi}) := \sum_i \left(\frac{1}{2}(\bar{\psi}_\sigma(\xi_i)\psi_\sigma(\xi_i + a\mathbf{e}_0) - \bar{\psi}_\sigma(\xi_i + a\mathbf{e}_0)\psi_\sigma(\xi_i)) - \frac{1}{4m} \sum_{j=1,2} (\bar{\psi}_\sigma(\xi_i + a\mathbf{e}_j) - \bar{\psi}_\sigma(\xi_i))(\psi_\sigma(\xi_i + a\mathbf{e}_j) - \psi_\sigma(\xi_i)) - \mu \bar{\psi}_\sigma(\xi_i)\psi_\sigma(\xi_i) \right)$. Adding $\sum_i \begin{pmatrix} \bar{\psi}_\uparrow \\ \bar{\psi}_\downarrow \end{pmatrix}^t(\xi_i) \Gamma(\theta) \begin{pmatrix} \psi_\uparrow \\ \psi_\downarrow \end{pmatrix}(\xi_i)$ to $\mathcal{A}(\cdot)$, and subtracting the same term to \mathcal{V} , would have led back formally to the initial theory – up to boundary terms on ∂V . Then it would have been natural to add to the interaction an infinitesimal bulk term, $\mathcal{V} + \delta\mathcal{V}_\theta \rightarrow \mathcal{V} + \delta\mathcal{V}_\theta + \sum_i \begin{pmatrix} \bar{\psi}_\uparrow \\ \bar{\psi}_\downarrow \end{pmatrix}^t(\xi_i) \begin{pmatrix} 0 & \varepsilon e^{-i\theta} \\ \varepsilon e^{i\theta} & 0 \end{pmatrix} \begin{pmatrix} \psi_\uparrow \\ \psi_\downarrow \end{pmatrix}(\xi_i)$ and let

$$d\mu_{\theta;\lambda}(\psi, \bar{\psi}) := \lim_{\varepsilon \rightarrow 0^+} \lim_{|V| \rightarrow \infty} d\mu_{\theta;\lambda}^{\varepsilon;V}(\psi, \bar{\psi}) \quad (0.40)$$

where $d\mu_{\theta;\lambda}^{\varepsilon;V}(\psi, \bar{\psi})$ is the normalized measure obtained by modifying \mathcal{V} as indicated. Our (unproven but unlikely to be difficult) claim is that models (0.39) and (0.40) have the same infra-red behavior.

B. (bosonic regime, or low-energy theory) Diagrams involving a small number (≤ 6) of low-momentum Cooper pairs are a priori divergent, because the Goldstone boson propagator is not integrable (see Theorem 2 below). *Ward identities*, however, imply that these are actually convergent. On the other hand, it would be a very bad idea to reorganize the series of perturbations in such a way as to produce systematically *all* Goldstone bosons, since this would lead to a local accumulation of low-momentum bosonic fields which cannot be controlled perturbatively. Thus what is needed here is a complementary, multi-scale Cooper pair expansion procedure producing only a limited number of Goldstone bosons. This procedure makes it possible to give at last the large scale behavior of n -point functions of the theory.

Let us now present the main results of our article. Our starting point, namely, the symmetry-broken measure $d\mu_{\theta;\lambda}$, is equal to the measure defined in (0.39), with a precise choice of cut-offs. First, we have:

Theorem 1 (construction of the model). *Assume $g := \lambda m > 0$ is small enough. Consider the Grassmann measure $d\mu_{\theta;\lambda}$ of Definition 1.1, re-expressed in terms of modified parameters Γ_ϕ, m^*, μ^* . Denote by $\langle \cdot \rangle_{\theta;\lambda}$ the expectation of a fermionic functional with respect to $d\mu_{\theta;\lambda}$. Let*

$$j_\phi := \lfloor j_D + \frac{\pi}{\lambda m} \rfloor \quad (0.41)$$

and

$$j'_\phi := j_\phi + \lfloor \frac{1}{4} \ln(1/g) \rfloor. \quad (0.42)$$

Then, for an adequate choice of parameters such that

$$\Gamma_\phi \approx \hbar\omega_D e^{-\pi/m\lambda} \approx 2^{-j_\phi} \mu, \quad m^* = m(1 + O(g^2)), \quad \mu^* = \mu(1 + O(g)), \quad (0.43)$$

the renormalization flow is well-defined down to scale $j'_\phi - 1$, leading to vanishing renormalized counterterms $\delta\mu^{j'_\phi}, \delta m^{j'_\phi}$, and a small value of $\delta\Gamma^{j'_\phi} = O(g\Gamma_\phi)$. The coefficient of p^0 in the effective covariance kernel, see (0.29), is $iZ^{j'_\phi}$, with $Z^{j'_\phi} = 1 + O(g^2)$. The parameters m^*, μ^* , together with the pre-gap energy $\Gamma^{(j'_\phi-1)\rightarrow}$ – defined as solution of an approximate gap equation, see Definition 1.2 – are fixed simultaneously by a fixed-point argument.

Theorem 1 covers exactly the fermionic theory of **A.**, and spans the entire section 2. Because fermions become massive in the infra-red region, the "true" effective mass (defined in terms of decay of fermionic two-point functions, see Theorem 3) is not directly accessible (it is given in terms of the distance to the real axis of the first pole of the Fourier-transformed two-point function). Nevertheless, m^*, μ^* may be thought as *effective parameters* giving the essentially *exact location of the renormalized Fermi circle*. Going slightly *beyond* scale j_ϕ , down to scale j'_ϕ – which is required for technical reasons pertaining to the *bosonic regime* – can only improve the precision. As for the scale j'_ϕ counterterm coefficient $\delta\Gamma^{j'_\phi}$, thanks to its supplementary $O(g)$ prefactor, it is sufficiently close to 0 to enter only as a small, single-scale correction to the value of Γ_ϕ , which is chosen so as to satisfy the gap equation (see Theorem 2). The gap energy may equivalently be expressed in terms of the renormalized mass, $\Gamma_\phi \approx \hbar\omega_D e^{-\pi/m^*\lambda}$ since $e^{-\frac{\pi}{\lambda}|\frac{1}{m} - \frac{1}{m^*}|} = O(1)$.

Cooper pairs are defined as linear combinations of electron pairs in Cooper channel, $(\bar{\psi}_\uparrow\bar{\psi}_\downarrow)(\xi)$ and $(\psi_\downarrow\psi_\uparrow)(\xi)$, which may be represented in matrix form as $\begin{pmatrix} \bar{\psi}_\uparrow \\ \psi_\downarrow \end{pmatrix}^t \Gamma \begin{pmatrix} \psi_\uparrow \\ \bar{\psi}_\downarrow \end{pmatrix}$ where $\Gamma = \begin{pmatrix} 0 & \Gamma^* \\ \Gamma & 0 \end{pmatrix}$ is an arbitrary off-diagonal Hermitian matrix. Cooper pairs in the (\perp, \perp) channel, i.e. with associated matrix $\Gamma^\perp = \Gamma_\phi \begin{pmatrix} 0 & e^{-i(\theta+\frac{\pi}{2})} \\ e^{i(\theta+\frac{\pi}{2})} & 0 \end{pmatrix}$, are dominant only in the low-momentum regime (Regime II and III, or **B.** in our terminology), so relevant observables are averages of these composite fields in a large volume, or correlations at distances $|\tau - \tau'| + \frac{m^*}{p_F}|\mathbf{x} - \mathbf{x}'| \gtrsim \Gamma_\phi^{-1}$.

Theorem 2 (gap equation, Cooper pair correlations at large scale).

(i) The gap equation for $d\mu_{\theta,\lambda}^*$ (see Remark below Theorem 1), defined by fixed point as the value of Γ_ϕ for which the local part of the fermionic two-point function vanishes, see Definition 3.2, has a unique solution

$$\Gamma_\phi \approx \hbar\omega_D e^{-\pi/m\lambda}. \quad (0.44)$$

(ii) Fix Γ_ϕ as in (i), and consider the associated theory with measure $d\mu_{\theta;\lambda}^*$. Let $\xi_1 \neq \dots \neq \xi_{2n}$ ($n \geq 1$). If ε is a two-by-two matrix, we define for $\eta > 0$ (small)

$$\begin{aligned} & : \left(\left(\begin{array}{c} \bar{\psi}_\uparrow \\ \bar{\psi}_\downarrow \end{array} \right)^t \varepsilon \left(\begin{array}{c} \psi_\uparrow \\ \psi_\downarrow \end{array} \right) \right) (\eta^{-1}\xi_i) : = \\ & \left(\left(\begin{array}{c} \bar{\psi}_\uparrow \\ \bar{\psi}_\downarrow \end{array} \right)^t \varepsilon \left(\begin{array}{c} \psi_\uparrow \\ \psi_\downarrow \end{array} \right) \right) (\eta^{-1}\xi_i) - \left\langle \left(\begin{array}{c} \bar{\psi}_\uparrow \\ \bar{\psi}_\downarrow \end{array} \right)^t \varepsilon \left(\begin{array}{c} \psi_\uparrow \\ \psi_\downarrow \end{array} \right) \right\rangle_{\theta;\lambda}. \end{aligned} \quad (0.45)$$

Then $2n$ -point functions of Cooper pairs have the following asymptotic large-scale behavior:

$$\begin{aligned} & \left\langle \prod_{i=1}^{2n} : \left(\left(\begin{array}{c} \bar{\psi}_\uparrow \\ \bar{\psi}_\downarrow \end{array} \right)^t \mathbb{F}^\perp \left(\begin{array}{c} \psi_\uparrow \\ \psi_\downarrow \end{array} \right) \right) (\eta^{-1}\xi_i) : \right\rangle_{\theta;\lambda} \sim_{\eta \rightarrow 0} (1 + o(1)) \cdot \\ & \cdot \lambda^{-2n} \sum_{(i_1, i_2), \dots, (i_{2n-1}, i_{2n})} \prod_{k=1}^n \{ \Gamma_\phi^2 \Sigma_{\perp, \perp} (\eta^{-1}(\xi_{i_{2k-1}} - \xi_{i_{2k}})) \}, \end{aligned} \quad (0.46)$$

where $\mathbf{\Gamma}^\perp := \Gamma_\phi \begin{pmatrix} e^{-i(\theta + \frac{\pi}{2})} \\ e^{i(\theta + \frac{\pi}{2})} \end{pmatrix}$ is perpendicular to $\mathbf{\Gamma}^{\prime\prime} := \Gamma_\phi \begin{pmatrix} e^{-i\theta} \\ e^{i\theta} \end{pmatrix}$; the sum ranges over all pairings $\{ \{i_1, i_2\}, \dots, \{i_{2n-1}, i_{2n}\} \}$ of indices, and the two-by-two matrix kernel Σ , whose entry $\Sigma_{\perp, \perp} = \frac{1}{\Gamma_\phi^2} {}^t \mathbf{\Gamma}^\perp \Sigma \mathbf{\Gamma}^\perp$ in the (\perp, \perp) -channel is interpreted as propagator of the Goldstone boson, is defined and studied in §3.2 and 3.4. In particular, see (3.11) and (3.75), if $\xi \neq 0$,

$$\Sigma_{\perp, \perp}(\eta^{-1}\xi) \sim_{\eta \rightarrow 0} \eta \frac{g_\phi / 4\pi v_\phi}{\sqrt{|\mathbf{x}|^2 + v_\phi^2 \tau^2}} \left(1 + O\left(\frac{\eta}{\Gamma_\phi (|\tau| + |\mathbf{x}|/v_\phi)} \right) \right), \quad (0.47)$$

where

$$v_\phi \approx v_F^* \equiv \frac{p_F^*}{m^*} \quad (0.48)$$

is roughly equal to the (renormalized) Fermi velocity v_F^* ; and

$$g_\phi \approx \frac{\Gamma_\phi^2}{m^*}. \quad (0.49)$$

The kernel Σ is not integrable, in the sense that the integral $\int_{\mathbb{R}^3} d\xi \Sigma_{\perp, \perp}(\xi - \xi')$ diverges.

The gap parameter Γ_ϕ , as well as the Goldstone boson parameters v_ϕ, g_ϕ , are obtained as limits of scale-dependent converging series, $(\Gamma^{j+\rightarrow})_{j+\geq j'_\phi}$, $(v_\phi^{j+\rightarrow})_{j+\geq j'_\phi}$, $(g_\phi^{j+\rightarrow})_{j+\geq j'_\phi}$, see Definition 3.4 and §3.4.

Remark 1. The Fourier transform of $\Sigma_{\perp,\perp}$, as follows by straightforward computations from (0.47), is of the form

$$\Sigma_{\perp,\perp}(q) \sim_{q \rightarrow 0} \frac{g_\phi}{(|q|^0)^2 + (v_\phi |\mathbf{q}|)^2} \quad (0.50)$$

and *diverges* for $q = 0$. Quite remarkably, the fact that $\Sigma_{\perp,\perp}$ *has a pole precisely at* $q = 0$, implying a non-massive behavior, is shown by a *Ward identity* (see §3.3) to be *equivalent to the gap equation*. We actually use most of the time the latter characterization in terms of $\Sigma_{\perp,\perp}$ as a definition of the gap equation, a convenient choice for estimates.

Remark 2. Error terms $o(1)$ in Theorem 2 (ii) go to 0 as $g \rightarrow 0$. Details of the proof, see in particular (2.123) in section 2 and (3.76) in section 3, give error terms denoted by " $o(1)$ " which are bounded by $O(g^{1/4})$ or equivalently $O(2^{-(j'_\phi - j_\phi)})$; a more detailed computation of lowest-order terms would allow to replace $O(g^{1/4})$ by $O(g)$. The leading order of Γ_ϕ in (i), on the other hand, depends both on the ultra-violet cut-off and on subleading diagrams.

Remark 3. The above Theorem only involves the (\perp, \perp) -component of Σ . Intermediate computations produce a two-by-two matrix propagator Σ , diagonal in the basis $(\Gamma^{//}, \Gamma^\perp)$. However, the other diagonal coefficient $\Gamma_\phi^2 \Sigma_{//, //}(\xi - \xi') = {}^t \Gamma^{//} \Sigma \Gamma^{//}(\xi - \xi')$ is *massive*, which translates into a quasi-exponential decay at large distances, similar to that of the fermions. This case is studied alongside the case of isolated fermions in Theorem 3 below.

We can now tentatively recast our results in terms of the Hubbard-Stratonovich transformed theory (0.27) involving the complex boson field $\Gamma = \Gamma(\xi)$. Namely, by Gaussian integration by parts (see Appendix), n -point functions of the Γ -field are in one-to-one correspondence with the Cooper pair n -point functions of (0.46), from which we can conclude (leaving aside mathematical rigor) to the following. The Goldstone boson Γ behaves like a non-massive particle described by a non-linear sigma model with coupling constant $g_\phi \approx \frac{\Gamma_\phi^2}{m^*}$ having the dimension of an energy, namely, the statistical weight for a function Γ with values on the circle $\{|\Gamma| = \Gamma_\phi\}$ is $\sim e^{-\frac{1}{g_\phi} \int d\xi |\nabla \Gamma(\xi)|^2}$, where $\nabla := \begin{pmatrix} \partial_\tau \\ v_\phi \nabla \end{pmatrix}$. In rescaled, non-dimensional units, $(\tau, \mathbf{x}, \Gamma) \rightarrow (\tau', \mathbf{x}', \Gamma') := (\Gamma_\phi \tau, p_c \mathbf{x}, \Gamma_\phi^{-1} \Gamma)$, with $p_c = \frac{\Gamma_\phi}{v_\phi}$, the weight for Γ becomes $\sim e^{-\frac{1}{g'_\phi} \int d\xi' |\nabla' \Gamma'(\xi')|^2}$ with

$$g'_\phi = \frac{g_\phi}{\Gamma_\phi v_\phi^2} \approx \frac{\Gamma_\phi}{\mu} \ll 1. \quad (0.51)$$

This is the signature of a weakly coupled, super-critical $(1+2)$ -dimensional non-linear sigma model, known (at least perturbatively) to be a free theory at large scales (see e.g. [57], §13.3), from which the qualitative behavior (0.46) can be expected. Note, however, that the interaction between Cooper pairs is mediated by *massive* individual electrons.

Theorem 3 (isolated electrons). *n*-point functions of electrons which are not in the (\perp, \perp) Cooper pair channel decay quasi-exponentially at large distance with a decay rate $\approx \Gamma_\phi$, namely, for every $n \geq 0$, there exists $C_n > 0$ such that, if $\xi \neq \xi'$,

$$\left| \langle \bar{\psi}_\sigma(\eta^{-1}\xi)\psi_{\sigma'}(\eta^{-1}\xi') \rangle_{\theta;\lambda} \right| \leq C_n (p_F^*)^2 \delta_{\sigma,\sigma'} \left(1 + \Gamma_\phi \eta^{-1} (|\tau - \tau'| + \frac{m^*}{p_F^*} |\mathbf{x} - \mathbf{x}'|) \right)^{-n} \quad (0.52)$$

and similarly,

$$\left| \langle : (\bar{\psi}_\uparrow \psi_\uparrow)(\eta^{-1}\xi) : : (\bar{\psi}_\uparrow \psi_\uparrow)(\eta^{-1}\xi') : \rangle_{\theta;\lambda} \right| \leq C_n (p_F^*)^4 \left(1 + \Gamma_\phi \eta^{-1} (|\tau - \tau'| + \frac{m^*}{p_F^*} |\mathbf{x} - \mathbf{x}'|) \right)^{-n}. \quad (0.53)$$

and, letting $\mathbb{T} // := \Gamma_\phi \begin{pmatrix} 0 & e^{-i\theta} \\ e^{i\theta} & 0 \end{pmatrix}$,

$$\left| \langle : (\bar{\Psi} \mathbb{T} // \Psi)(\eta^{-1}\xi) : : (\bar{\Psi} \mathbb{T} // \Psi)(\eta^{-1}\xi') : \rangle_{\theta;\lambda} \right| \leq C_n (p_F^*)^4 \left(1 + \Gamma_\phi \eta^{-1} (|\tau - \tau'| + \frac{m^*}{p_F^*} |\mathbf{x} - \mathbf{x}'|) \right)^{-n}. \quad (0.54)$$

Remark. We fall short of proving *exponential decay* for two-point functions of electrons. This is mainly due to our choice of cut-offs for the Gaussian covariance kernel, which yields *quasi-exponentially* decaying scaled kernels. However, non-Gaussian cut-offs of the form $\chi^j(p/\mu) = e^{-2^{2j}\mu^{-2}[(p^0)^2 + (e(\mathbf{p}))^2 + \Gamma_\phi^2]} - e^{-2^{2(j+1)}\mu^{-2}[(p^0)^2 + (e(\mathbf{p}))^2 + \Gamma_\phi^2]}$, similar to those used in [15], would produce *exponentially* decaying kernels, and most likely allow us to prove an exponential decay in $e^{-\Gamma_\phi(1+o(1))\eta^{-1}(|\tau - \tau'| + \frac{m^*}{p_F^*} |\mathbf{x} - \mathbf{x}'|)}$, resp. $e^{-2\Gamma_\phi(1+o(1))\eta^{-1}(|\tau - \tau'| + \frac{m^*}{p_F^*} |\mathbf{x} - \mathbf{x}'|)}$ for two-point, resp. four-point functions, instead of the quasi-exponential decay factors $\left(1 + \Gamma_\phi \eta^{-1} (|\tau - \tau'| + \frac{m^*}{p_F^*} |\mathbf{x} - \mathbf{x}'|) \right)^{-n}$ in (0.52), resp. (0.53), implying that the *effective mass* of electrons is $\approx \Gamma_\phi$.

Let us add a few comments. Cooper pairs are the main observables at low energy. On the other hand, isolated electrons have become *massive*. The large-scale behavior of isolated fermions and Cooper pairs written down in Theorem 3 points out to a *superconductive phase*, qualitatively different from the *normal phase*, which is that of the free electron gas obtained for $\lambda = 0$, or more generally of Fermi liquids. Namely, for $\lambda = 0$ (i.e. in the *normal phase*), specializing to vanishing τ -coordinates, the one-point density kernel is proved by a standard computation (see (5.32) and (5.33)),

$$\left| \langle \bar{\psi}_\sigma(0, \eta^{-1}\mathbf{x}) \psi_{\sigma'}(0, \eta^{-1}\mathbf{x}') \rangle_{\lambda=0} \right| \approx_{\eta \rightarrow 0} (p_F^*)^{1/2} \delta_{\sigma,\sigma'} |\eta^{-1}(\mathbf{x} - \mathbf{x}')|^{-3/2}, \quad (0.55)$$

and the density-density correlation kernel (connected two-point function)

$$\left| \langle : (\bar{\psi}_\uparrow \psi_\uparrow)(0, \eta^{-1}\mathbf{x}) : : (\bar{\psi}_\uparrow \psi_\uparrow)(0, \eta^{-1}\mathbf{x}') : \rangle_{\lambda=0} \right| \approx_{\eta \rightarrow 0} p_F^* |\eta^{-1}(\mathbf{x} - \mathbf{x}')|^{-3}. \quad (0.56)$$

These correlation functions decrease polynomially at large distances, to be compared with the quasi-exponential decrease exhibited in Theorem 3. Two-point functions of Cooper pairs in arbitrary channels behave similarly with a *cubic* inverse distance decrease,

$$\left\langle \prod_{i=1}^2 : \left(\begin{pmatrix} \bar{\psi}_\uparrow \\ \bar{\psi}_\downarrow \end{pmatrix} \right)^t \mathbb{F}(\theta_i) \begin{pmatrix} \psi_\uparrow \\ \psi_\downarrow \end{pmatrix} : \right\rangle_{\lambda=0} = O_{\eta \rightarrow 0} \left(p_F^* |\eta^{-1}(\mathbf{x} - \mathbf{x}')|^{-3} \right), \quad (0.57)$$

where $\mathbb{F}(\theta_i) := \Gamma_\phi \begin{pmatrix} 0 & e^{-i\theta_i} \\ e^{i\theta_i} & 0 \end{pmatrix}$, $\theta_i \in \mathbb{R}/2\pi\mathbb{Z}$, $i = 1, 2$, as opposed to the *linear* inverse distance decrease shown in Theorem 2 for the superconductive phase.

Theorem 4 (phase transition). *Let $\theta, \theta_1 \in \mathbb{R}/2\pi\mathbb{Z}$ and $\xi_1 \in \mathbb{R} \times \mathbb{R}^2$. Then*

$$\langle (\bar{\Psi} \mathbb{F}(\theta_1) \Psi)(\xi_1) \rangle_{\theta; \lambda} = \frac{c}{\lambda} \text{Tr}(\mathbb{F}(\theta_1) \mathbb{F}(\theta)) \quad (0.58)$$

with $c = 1 + o(1)$.

This is in agreement with the mean-field prediction for the average of Cooper pairs in a superconducting ground-state oriented in direction θ , namely, e.g.

$$\langle \bar{\psi}_\uparrow \bar{\psi}_\downarrow + \psi_\downarrow \psi_\uparrow \rangle_{\theta=0; \lambda} \sim \frac{\Gamma_\phi}{\lambda} \text{Tr}((\sigma^1)^2) = 2 \frac{\Gamma_\phi}{\lambda}, \quad \langle \bar{\psi}_\uparrow \bar{\psi}_\downarrow - \psi_\downarrow \psi_\uparrow \rangle_{\theta=0; \lambda} = 0 \quad (0.59)$$

if $\theta = 0$. Thus an infinitesimally small "Cooper magnetic field" (i.e. parameter conjugate to Cooper pair field, not to be confused with a true magnetic field pairing to individual electrons) in a given direction θ is enough to orient Cooper pairs in that direction.

In the following theorem, we consider the integral X_Ω of a Cooper pair field over a space-time domain Ω "comparable" to a scale j_ϕ box. Polynomial and exponential moments of X_Ω , i.e. expectations $\langle P(X_\Omega) \rangle_{\theta; \lambda}$, $\langle e^{cX_\Omega} \rangle_{\theta; \lambda}$ may be computed as the integral w.r. to a probability measure denoted by $\mathbb{P}_{\theta; \lambda}$, e.g. $\langle e^{cX_\Omega} \rangle_{\theta; \lambda} = \int d\mathbb{P}_{\theta; \lambda}(x) e^{cx}$. Then upper bounds for quantities $\mathbb{P}_{\theta; \lambda}[X_\Omega < \eta] \equiv \int_{-\infty}^\eta d\mathbb{P}_{\theta; \lambda}(x)$, $\mathbb{P}_{\theta; \lambda}[X_\Omega > \eta] \equiv \int_\eta^{+\infty} d\mathbb{P}_{\theta; \lambda}(x)$, may be interpreted as large deviation estimates.

Theorem 5 (local transverse behavior of Goldstone bosons).

Let $\Omega \subset \mathbb{R} \times \mathbb{R}^2$ be a domain such that $\{\xi = (\tau, \mathbf{x}) \mid \Gamma_\phi \left(|\tau| + \frac{m^}{p_F^*} |\mathbf{x}| \right) \leq c\} \subset \Omega \subset \{\xi = (\tau, \mathbf{x}) \mid \Gamma_\phi \left(|\tau| + \frac{m^*}{p_F^*} |\mathbf{x}| \right) \leq C\}$, where $0 < c < C$ are constants, and*

$$X_\Omega := \text{Re} \int_\Omega d\xi (\bar{\Psi} \sigma(\theta) \Psi)(\xi), \quad (0.60)$$

where $\sigma(\theta) := \cos(\theta)\sigma^1 + \sin(\theta)\sigma^2 = \begin{pmatrix} 0 & e^{-i\theta} \\ e^{i\theta} & 0 \end{pmatrix}$ is a linear combination of off-diagonal Pauli matrices, see (1.19). Let

$$\bar{X}_\Omega := \int d\mu_{\theta;\lambda} X_\Omega(\theta) = |\Omega| \langle (\bar{\Psi}\sigma(\theta)\Psi)(0) \rangle_{\theta;\lambda} = 2|\Omega| \frac{\Gamma_\phi}{\lambda} (1 + o(1)). \quad (0.61)$$

Then, for $\eta > 0$ small enough,

$$\mathbb{P}_{\theta;\lambda}[|X_\Omega - \bar{X}_\Omega| > \eta \frac{\Gamma_\phi}{\lambda} \text{Vol}(\Omega)] \lesssim e^{-g_\perp \eta^2} \quad (0.62)$$

where

$$g_\perp \approx \frac{\mu}{\Gamma_\phi} \approx 2^{j_\phi}. \quad (0.63)$$

This is in general agreement with mean-field estimates for the curvature of the effective potential \mathcal{S} (see (0.30)) near its minimum,

$$\mathcal{S}(|\Gamma|) \sim \frac{m}{4\pi} \left\{ -(\hbar\omega_D)^2 e^{-2\pi/m\lambda} + 2(|\Gamma| - \Gamma_\phi)^2 \right\} \quad (0.64)$$

in a neighborhood of Γ_ϕ , see [22]. Namely, the field $\Gamma(\xi)$ may be considered as roughly constant over Ω . Through the correspondence between the Cooper pair field and its conjugate field Γ , one may assimilate the event $\{|X_\Omega - \bar{X}_\Omega| > \eta \frac{\Gamma_\phi}{\lambda} \text{Vol}(\Omega)\}$ with the event $\{||\Gamma(\xi)| - \Gamma_\phi| > \eta \Gamma_\phi, \xi \in \Omega\}$, which has probability $\lesssim e^{-\frac{m}{2\pi} \text{Vol}(\Omega) \eta^2 \Gamma_\phi^2} \approx e^{-g_\perp \eta^2}$. For larger domains Ω , the large deviation rate $-\log\left(\mathbb{P}\left[\int_\Omega d\xi \left||\Gamma(\xi)| - \Gamma_\phi| > \eta \Gamma_\phi \text{Vol}(\Omega)\right]\right)$ is expected from (0.64) to increase linearly in $\text{Vol}(\Omega)$.

0.4 Outline and notations

The paper is organized as follows.

Section 1 is a long, introductory section, where we gradually introduce notations, recall standard facts about the BCS model, reformulate the initial model as a multi-scale model, and evaluate bubble diagrams. Main points are *Definition 1.1*, where our model is precisely defined, and §1.7, where a two-by-two matrix-valued kernel Σ – whose (\perp, \perp) -component is interpreted as *propagator of the Goldstone boson* – and a *gap equation* are introduced in perturbative terms (*Definition 1.9*). Section §1.7 goes well beyond mean-field theory, but remains perturbative; hence the way in which the gap energy Γ_ϕ and the Σ -kernel are defined differs in details from the non-perturbative definition of section 3. The precise construction in section 3 is heavily inspired from, but does not rely upon, the one in §1.7, so details in §1.7 are not really important, and the whole subsection – apart from the *displacement procedure*, which is accurately described there – may be skipped from a mathematical point of view. Yet we hope that §1.7 will help the reader find his way through the much more technical section 3.

Section 2 is dedicated to the *high-momentum* or *fermionic theory* (part **A.** of our scheme). It relies mainly on *expansions*. Formally, these apply to the *dressed* model, see *Definition 2.6*, which interpolates between the coupled model of section 1 and a fully-decoupled model. The horizontal (cluster) and momentum-decoupling (vertical) expansions implement the decoupling between degrees of freedom required to renormalize the diverging contributions, and show convergence of the series obtained by formally expanding $e^{-\mathcal{V}} = \sum_{n \geq 0} (-1)^n \frac{\mathcal{V}^n}{n!}$. A simple bubble resummation procedure provides the "1/N-argument" required to control the series in the neighborhood of the transition scale.

Section 3 is concerned with the *low-momentum* or *bosonic theory* (part **B.**) As in QED, Ward identities are proved, which show that – despite the fact that Goldstone bosons is non-massive – all diagrams are infra-red convergent. By a careful complementary multi-scale expansion of Cooper pairs, n -point functions are rewritten in terms of a sum over multi-scale trees with vertices connected by $\Sigma_{\perp, \perp}$ -kernels. The end of the section is dedicated to the proof of the Theorems stated in §0.3.

Perspectives are presented in section 4.

Finally, some technical lemmas are collected in section 5.

Important notations. The reader will find many more notations in the body of the article. We hope that this selection will help the reader find his way through the article and prevent any confusion. A more comprehensive index of notations with reference pages is given at the end of the text.

Following the physicists' convention, the star (*) denotes *complex conjugation*. Alternatively, *real* parameters with a star (*) denote *effective parameters*; Gaussian measures and covariance kernels with a star are computed with the effective parameters.

The gap parameter Γ_ϕ is a positive real number.

– Space-time points are typically denoted by $\xi = (\tau, \mathbf{x})$, $\tau \in \mathbb{R}$, $\mathbf{x} \in \mathbb{R}^2$.

– *Fermions* are denoted either by $\psi = (\psi_\sigma)_{\sigma=\uparrow, \downarrow} = \begin{pmatrix} \psi_\uparrow \\ \psi_\downarrow \end{pmatrix}$, $\bar{\psi} = (\bar{\psi}_\sigma)_{\sigma=\uparrow, \downarrow} = (\bar{\psi}_\uparrow \ \bar{\psi}_\downarrow)$ or $\Psi = (\Psi_\sigma)_{\sigma=\uparrow, \downarrow} = \begin{pmatrix} \psi_\uparrow \\ \bar{\psi}_\downarrow \end{pmatrix}$, $\bar{\Psi} = (\bar{\Psi}_\sigma)_{\sigma=\uparrow, \downarrow} = (\bar{\psi}_\uparrow \ \psi_\downarrow)$. The latter are *Nambu spinors*, which mix ψ and $\bar{\psi}$ -components. Thus *Cooper pairings* are (depending on the context) written as $\psi_\downarrow \psi_\uparrow, \bar{\psi}_\uparrow \bar{\psi}_\downarrow$ or $\bar{\Psi}_\downarrow \Psi_\uparrow, \bar{\Psi}_\uparrow \Psi_\downarrow$, or (in matrix notation) $\bar{\Psi} \begin{pmatrix} 0 & 0 \\ 1 & 0 \end{pmatrix} \Psi$, $\bar{\Psi} \begin{pmatrix} 0 & 1 \\ 0 & 0 \end{pmatrix} \Psi$, combining into $\bar{\Psi} \sigma^{1,2} \Psi$ (in terms of Pauli matrices, see (1.19)), or more generally, using an off-diagonal hermitian matrix, $\bar{\Psi} \Gamma \Psi$, where $\Gamma := \begin{pmatrix} 0 & \Gamma^* \\ \Gamma & 0 \end{pmatrix}$, with $\Gamma \in \mathbb{C}$. If $\Gamma = \Gamma_\phi e^{i\theta}$, resp. $\Gamma_\phi e^{i(\theta + \frac{\pi}{2})}$, then we note $\Gamma \equiv \Gamma^{//} = \Gamma(\theta)$, $\Gamma \equiv \Gamma^{//} = \Gamma(\theta)$, resp. $\Gamma^\perp, \Gamma^\perp$. We also consider the

complex-valued vector $\mathbf{\Gamma} = \begin{pmatrix} \Gamma^* \\ \Gamma \end{pmatrix}$, in particular, $\mathbf{\Gamma}^{\prime\prime}$ and $\mathbf{\Gamma}^\perp$. Seeing Γ either as a complex number, a vector or a matrix will turn out to be useful. In particular, $\frac{1}{2}\text{Tr}(\mathbb{F}\mathbb{F}') = \frac{1}{2}(\mathbf{\Gamma}, \mathbf{\Gamma}') = \text{Re}(\Gamma(\Gamma')^*)$ is the scalar product of \mathbb{F} with \mathbb{F}' , or indifferently $\mathbf{\Gamma}$ with $\mathbf{\Gamma}'$, or Γ with Γ' . All quantities are equivariant w.r. to rotations by an angle θ' , acting as follows,

$$\mathbb{F}(\theta) \mapsto \begin{pmatrix} e^{-i\theta'} & \\ & e^{i\theta'} \end{pmatrix} \mathbb{F} \begin{pmatrix} e^{i\theta'} & \\ & e^{-i\theta'} \end{pmatrix} = \mathbb{F}(\theta+2\theta'), \quad \mathbf{\Gamma}(\theta) \mapsto \begin{pmatrix} e^{-i\theta'} & \\ & e^{i\theta'} \end{pmatrix} \mathbf{\Gamma}(\theta) = \mathbf{\Gamma}(\theta+\theta') \quad (0.65)$$

and $\Gamma(\theta) \mapsto \Gamma(\theta)e^{i\theta'} = \Gamma(\theta + \theta')$.

– Part **A.** is dedicated in a large part to a *multi-scale analysis*, in which power-counting is directly dependent on the *vicinity to the Fermi circle*. Thus the *norm* on momenta,

$$|p| := \sqrt{(p^0)^2 + \left(\frac{p_F^*}{m^*}p_\perp\right)^2} \quad (0.66)$$

with $p_\perp := |\mathbf{p}| - p_F^*$, measures the distance to the (extended to $(1+2)$ -dimensional description) Fermi circle defined by $p^0 = 0$, $|\mathbf{p}| = p_F^*$. Dualizing, we let

$$|\xi| := \sqrt{|\tau|^2 + \left(\frac{m^*}{p_F^*}|\mathbf{x}\right)^2}. \quad (0.67)$$

– On the other hand, the analysis in part **B.** focuses on *Cooper pairs* with *small* total momentum \mathbf{q} , entering into fermionic diagrams of **A.** as a small *transfer momentum*. Therefore, the *Euclidean norm* adapted to this context,

$$|q|_+ := \sqrt{(q^0)^2 + (v_\phi|\mathbf{q}|)^2} \quad (0.68)$$

vanishes when $q = 0$. Dualizing, we let

$$|\xi|_+ := \sqrt{|\tau|^2 + (|\mathbf{x}|/v_\phi)^2}. \quad (0.69)$$

Note that $|p|$ and $|p|_+$ are as different as can be. In order to further avoid confusions, we systematically denote *electron momenta* by the letter p and *Cooper pair momenta* by the letter q . On the other hand, $|\xi| \approx |\xi|_+$ may be used interchangeably most of the time.

– A fermion momentum p has *scale* $j \in \{j_D, \dots, j'_\phi\}$ if $|p| \approx 2^{-j}\mu$. A Cooper pair momentum q has *Euclidean scale* j_+ ($j_+ \geq j'_\phi$) if $|q|_+ \approx 2^{-j_+}\mu$. Momentum cut-offs χ^j , resp. $\chi_+^{j_+}$ select momenta of scale j , resp. Euclidean scale j_+ , namely $\chi^j(p)$, resp. $\chi^{j_+}(q)$ vanish except if $|p| \approx 2^{-j}\mu$, resp. $|q|_+ \approx 2^{-j_+}\mu$. The sum $\chi^{j \rightarrow} := \sum_{k \leq j} \chi^k$, resp. $\chi^{-j} := \sum_{k \geq j} \chi^k$ are infra-red, resp. ultra-violet cut-offs; similarly for $\chi_+^{j_+ \rightarrow} :=$

$\sum_{k_+ \leq j_+} \chi_+^{k_+}$, resp. $\chi_+^{\rightarrow j_+} := \sum_{k_+ \geq j_+} \chi_+^{k_+}$. Infra-red, resp. ultra-violet cut-off fermion fields are similarly denoted by $\psi^{j \rightarrow}, \bar{\psi}^{j \rightarrow}, \Psi^{j \rightarrow}, \bar{\Psi}^{j \rightarrow}$, resp. $\psi^{\rightarrow j}, (\bar{\psi})^{\rightarrow j}, \Psi^{\rightarrow j}, (\bar{\Psi})^{\rightarrow j}$.

– The amplitude of an amputated Feynman diagram Υ is denoted by $\mathcal{A}(\Upsilon)$. Letting $\xi_{int,i}, i = 1, \dots, N_{int}$, resp. $\xi_{ext,i}, i = 1, \dots, N_{ext}$ be the location of the internal, resp. external vertices of Υ , $\mathcal{A}(\Upsilon)$ is equal to the integral $(\prod_{i=2}^{N_{ext}} \int d\xi_{ext,i})(\prod_{i=1}^{N_{int}} \int d\xi_{int,i})$ of the product of the internal vertices by the internal propagators. Because of translation invariance, the location $\xi_{ext,1}$ of one of the external vertices has been kept fixed. Restricting to propagators of momentum scales $\leq j$, one obtains instead a scale j infra-red cut-off amplitude denoted by $\mathcal{A}^{j \rightarrow}(\Upsilon)$.

– A *Cooper pair with momentum q* (or equivalently, a pair of electrons in Cooper channel) is an integrated composite field $\int d\xi e^{-i(q,\xi)}(\psi_\downarrow \psi_\uparrow)(\xi)$ or $\int d\xi e^{-i(q,\xi)}(\bar{\psi}_\uparrow \bar{\psi}_\downarrow)(\xi)$ with total momentum q such that $|q|_+ \lesssim \Gamma_\phi$. Such fields are the main subject of part **B.**. However, they also contribute in an unessential way to the analysis of part **A.**, since they can enter even high-energy diagrams as external legs of fermion loops, though with a very small relative volume. By abuse of language, we shall sometimes also speak of "Cooper pairs" even when the total momentum q is such that $|q|_+ \gg \Gamma_\phi$; such pairs are simply unphysical quantities entering as virtual particles into diagrams.

– Sign conventions regarding Grassmann integrals are recalled in Appendix, §5.1.

– Finally, $N_0 := 8$ is a constant. Bounds for multi-scale polymers with $< N_0$, resp. $\geq N_0$ external legs proceed differently due to the complicated angular dependence of external legs.

Acknowledgements. One of us (J. Magnen) would like to express his warmest and most sincere thanks to J. Feldman, V. Rivasseau and E. Trubowitz for extended discussions on the topics of this article and related subjects.

1 The gap equation

This long section starts with a series of reformulations of the initial model defined by the Grassmann measure

$$d\mu_\lambda(\psi, \bar{\psi}) = \frac{1}{\mathcal{Z}_\lambda} e^{-\mathcal{V}(\psi, \bar{\psi})} d\mu(\psi, \bar{\psi}); \quad (1.1)$$

recall that $d\mu(\psi, \bar{\psi})$ is Grassmann Gaussian measure cut-off at some scale j_D , with covariance kernel given (up to cut-off issues) by the operator $(ip^0 - e(\mathbf{p}))^{-1}$, see (0.9), and

$$\mathcal{V}(\psi, \bar{\psi}) := -\lambda \int \prod_{i=1}^4 dp_i \delta(p_1 + p_2 - p_3 - p_4) \bar{\psi}_\uparrow(p_1) \psi_\uparrow(p_3) \bar{\psi}_\downarrow(p_2) \psi_\downarrow(p_4) \quad (1.2)$$

see (0.15), again up to cut-off issues. The issue is to motivate and define precisely the symmetry-broken Grassmann measure $d\mu_{\theta;\lambda}$ (see Theorems in the Introduction) defining the model.

Let us describe informally the various stages:

- first (see §1.1), the $U(1)$ -number (charge) symmetry $(\psi, \bar{\psi}) \rightarrow (e^{i\theta}\psi, \bar{\psi}e^{-i\theta})$ is *broken* at energies comparable to the energy gap (i.e. in Regime II), yielding a non-zero value in the ground state for products of *spin-neutral* annihilation operators, for instance

$$\langle (\bar{\psi}_\uparrow \bar{\psi}_\downarrow + \psi_\downarrow \psi_\uparrow)(\xi) \rangle_{\theta=0;\lambda} \approx 2 \frac{\Gamma_\phi}{\lambda}. \quad (1.3)$$

This is a direct consequence of the fact that *Cooper pairs*, i.e. *neutral* pairs of electrons $\bar{\psi}_\uparrow \bar{\psi}_\downarrow, \psi_\downarrow \psi_\uparrow$ form bound states. On the other hand, non spin-neutral bound states do not form. This motivates the introduction of *Nambu fields* $(\Psi, \bar{\Psi})$. The well-known Bogolioubov-De Gennes-Gor'kov mean-field, quadratic Hamiltonian [7, 8] (which we do not discuss here) is diagonalized in a rotated basis expressed in terms of $\bar{\Psi}$, and the mean-field ground-state is similarly obtained from the normal state ground-state by applying products of $\bar{\Psi}$'s, see e.g. [2], §6.4.

- second (see §1.2), the Cooper pair contribution to effective action is written in the Nambu basis in terms of an off-diagonal matrix $\int d\xi \bar{\Psi}(\xi) \begin{pmatrix} 0 & \Gamma^* \\ \Gamma & 0 \end{pmatrix} \Psi(\xi)$, where the *energy gap* $\Gamma_\phi := |\Gamma|$ (coinciding with the above ground state expectation value) satisfies a consistency equation called *gap equation* (discussed later on). Pauli matrices help encode the separation of Γ into its real/imaginary parts. This leads to a modified Grassmann Gaussian measure $d\mu_\theta^*(\Psi, \bar{\Psi})$ with covariance kernel $C_\theta^*(p)$ in the form of a rational function, whose denominator is bounded near the Fermi circle. Its inverse Fourier transform therefore decreases exponentially at large distances like $O(e^{-c\Gamma_\phi|\xi|_+})$, with $|\xi|_+ := \sqrt{|\tau|^2 + (\frac{|\mathbf{x}|}{v_\phi})^2}$. Thus the energy gap also plays the rôle of an inverse correlation length for the fermions.

- further (see §1.3), the energy gap Γ_ϕ (as follows from the analysis in [24]) may be defined (neglecting small corrections due to scales $\geq j'_\phi$) as *minus the inverse of the off-diagonal interacting Green function* evaluated at (p^0, \mathbf{p}) such that $p^0 = 0$ and \mathbf{p} is located on the Fermi sphere. However, the *radius p_F of the Fermi sphere* – defined as the singular locus of the theory – must be *renormalized*. Since renormalization is implemented à la Wilson as a flow of the parameters m, μ, Γ_ϕ of the theory, we actually rewrite the model in terms of its effective (i.e. far infra-red) parameters $m^* := m^{j'_\phi}, \mu^* := \mu^{j'_\phi}$ and Γ_ϕ . This implies introducing quadratic counterterms proportional to m^*, μ^*, Γ_ϕ at bare scale j_D . If m^*, μ^* have been chosen correctly, then counterterms $\delta m^{j'_\phi}, \delta \mu^{j'_\phi}$ for parameters m, μ vanish. Now, the flow is computed using a *multi-scale decomposition* of the fields,

$$\Psi := \sum_{j \geq j_D} \Psi^j, \quad \bar{\Psi} := \sum_{j \geq j_D} \bar{\Psi}^j \quad (1.4)$$

Scale j counter-terms are then determined by computing two-point functions of the scale j infra-red cut-off theory with external momenta located on the renormalized Fermi circle. The above arguments explain *why* the precise form of the UV cut-off (0.4) (in itself largely irrelevant) is not fixed from the beginning, but rather as part of (1.4).

The model used as basis for discussion in the present article is that introduced in §1.3, though (for pedagogical reasons) some of its features are specified only in §2.1. As for the rest of the section, it is dedicated to the study of the *gap equation*.

Starting with perturbation theory, we discuss in §1.4 and §1.5 *ladder diagrams* (see [26], §11), which we call here for obvious diagrammatic reasons *bubble diagrams*. The evaluation of these diagrams with transfer momentum close to zero yields the main contribution to the energy gap Γ_ϕ . As a concession to the mean-field approximation scheme, we resum ladder diagrams (see §1.6) in an intermediate step, and deduce the approximate value for Γ_ϕ known in textbooks. In our rigorous approach, the sum of ladder diagrams plays a quintessential rôle – as we shall see, ladder diagrams in their *Cooper pairing channel* are alone responsible for the superconducting transition, other diagrams yielding only finite corrections – but does not give the exact value of Γ_ϕ .

The last subsection (§1.7) – which lies half-way between mean-field theory and rigorous arguments – shows how to re-sum *perturbatively* all diagrams forming the Goldstone boson propagator $\Sigma_{\perp,\perp}$ (the task is done beyond perturbation theory in §3.2). The series is formed by alternating bubble diagrams with two-point irreducible diagrams forming the *Bethe-Salpeter kernel*. Definition 1.9 defines Γ_ϕ as the value of the parameter Γ such that $\Sigma_{\perp,\perp}$ diverges when $q = 0$, a requirement that – as mentioned in a Remark in the introduction – is equivalent to the exact gap equation. This means that Goldstone bosons, as expected, are not massive. The diagram series naturally forms a two-by-two, diagonal matrix kernel $\Sigma = \begin{pmatrix} \Sigma_{//, //} & 0 \\ 0 & \Sigma_{\perp, \perp} \end{pmatrix}$, whose (\perp, \perp) component is shown to be *massive*, contrary to $\Sigma_{\perp, \perp}$.

1.1 Green functions and Nambu formalism

The main quantity controlling the electron pairing is the 2×2 Green function,

$$G(\tau, x; \tau', x') := \begin{pmatrix} \langle \psi_\uparrow(\tau, x) \bar{\psi}_\uparrow(\tau', x') \rangle & \langle \psi_\uparrow(\tau, x) \psi_\downarrow(\tau', x') \rangle \\ \langle \bar{\psi}_\downarrow(\tau, x) \psi_\uparrow(\tau', x') \rangle & \langle \bar{\psi}_\downarrow(\tau, x) \psi_\downarrow(\tau', x') \rangle \end{pmatrix} \quad (1.5)$$

In terms of the so-called *Nambu fields*,

$$\Psi(\cdot) := \begin{pmatrix} \psi_{\uparrow} \\ \psi_{\downarrow} \end{pmatrix}, \quad \bar{\Psi}(\cdot) := \begin{pmatrix} \bar{\psi}_{\uparrow} & \psi_{\downarrow} \end{pmatrix} \quad (1.6)$$

the above matrix is simply the tensor quantity $\langle \Psi(\tau, \mathbf{x}) \otimes \bar{\Psi}(\tau', \mathbf{x}') \rangle_c$. The particle number symmetry

$$(\psi, \bar{\psi})(\xi) \longrightarrow (e^{i\theta}\psi, \bar{\psi}e^{-i\theta}) \quad (1.7)$$

is broken by Cooper pairing. However, the remaining symmetries, namely, $SU(2)$ *spin symmetry*

$$(\psi, \bar{\psi})(\xi) \longrightarrow (g\psi, \bar{\psi}g^{-1})(\xi), \quad g \in SU(2), \quad (1.8)$$

invariance under CT *involution*

$$(\psi, \bar{\psi}) \longrightarrow (i\bar{\psi}, i\psi) \quad (1.9)$$

and spatial rotational invariance imply (see [24], Lemma II.1) that $G = \begin{pmatrix} G_{1,1} & G_{1,2} \\ G_{2,1} & G_{2,2} \end{pmatrix}$ is rotationally invariant, and (in Fourier coordinates)

$$G_{1,1}(p^0, \mathbf{p}) = \left(G_{1,1}(-p^0, \mathbf{p}) \right)^*, \quad G_{2,2}(p^0, \mathbf{p}) = -G_{1,1}(-p^0, \mathbf{p}) \quad (1.10)$$

$$G_{1,2}(p^0, \mathbf{p}) = \left(G_{2,1}(-p^0, \mathbf{p}) \right)^*. \quad (1.11)$$

In particular, $G(p^0 = 0, \mathbf{p})$ is a Hermitian matrix of the form $\begin{pmatrix} a & b \\ b^* & -a \end{pmatrix}$ with $a \in \mathbb{R}$.

In this language, the quadratic part of the action, see (0.9), is (up to the ultra-violet cut-off)

$$\mathcal{A}_0(\Psi, \bar{\Psi}) = \int dp \bar{\Psi}(-p) \left(ip^0 \mathbb{1} - e(\mathbf{p})\sigma^3 \right) \Psi(p) \quad (1.12)$$

So the Grassmann Gaussian measure $d\mu(\Psi, \bar{\Psi})$ obtained by letting $\lambda = 0$ is characterized (again, up to UV cut-off) by

$$C_0 := G(\lambda = 0) = \frac{1}{ip^0 \mathbb{1} - e(\mathbf{p})\sigma^3} = \begin{pmatrix} [ip^0 - e(\mathbf{p})]^{-1} & 0 \\ 0 & [ip^0 + e(\mathbf{p})]^{-1} \end{pmatrix}. \quad (1.13)$$

Then the interaction $\mathcal{V}(\psi, \bar{\psi})$, see (1.2), rewrites as $\mathcal{V}(\Psi, \bar{\Psi}) \equiv \int_V d\xi \mathcal{V}(\Psi, \bar{\Psi}; \xi)$, with

$$\mathcal{V}(\Psi, \bar{\Psi}; \xi) := -\lambda (\bar{\Psi} \sigma^i \Psi)^2(\xi) \quad (1.14)$$

where $i = 1, 2$ or 3 indifferently (since the square depends only on the determinant of the matrix inserted between $\bar{\Psi}$ and Ψ). Choosing σ^1, σ^2 or more generally $\sigma(\theta) := \cos(\theta) \sigma^1 + \sin(\theta) \sigma^2$ emphasizes the rôle of Cooper pairings in a given direction θ .

1.2 Symmetry-broken Grassman Gaussian measure

The BCS phase transition and the above symmetry considerations suggest that we:

- (i) substitute to the bare dispersion relation $e(\mathbf{p})$ the **effective dispersion relation**,

$$e^*(\mathbf{p}) = \frac{|\mathbf{p}|^2}{2m^*} - \mu^* \quad (1.15)$$

in terms of the **effective parameters** μ^*, m^* where:

$$\boxed{\delta\mu := \mu^* - \mu, \quad |\delta\mu| = O(g)\mu \ll \mu} \quad (1.16)$$

is the **Fermi sphere radius renormalization**; and

$$\boxed{\delta m := \frac{m}{m^*}(m^* - m), \quad |\delta m| = O(g^2)m \ll m} \quad (1.17)$$

is the **mass renormalization** defined in such a way that $\frac{\delta m}{m^2} = \frac{1}{m} - \frac{1}{m^*}$;

- (ii) and rewrite the functional integral in terms of the unknown renormalized parameters μ^*, m^* and unknown gap $\Gamma_\phi \neq 0$ as

$$\begin{aligned} d\mu_{\theta;\lambda}(\Psi, \bar{\Psi}) &= \frac{1}{\mathcal{Z}_\lambda^*} e^{-\mathcal{V}(\Psi, \bar{\Psi})} \\ &\exp\left(+ \int dp \bar{\Psi}(-p) \left(\Gamma_1(\theta)\sigma^1 + \Gamma_2(\theta)\sigma^2 + \frac{\delta m}{m^2} \frac{|\mathbf{p}|^2}{2} + \delta\mu \right) \Psi(p)\right) d\mu_\theta^*(\Psi, \bar{\Psi}), \end{aligned} \quad (1.18)$$

where:

- $$\sigma^1 = \begin{pmatrix} 0 & 1 \\ 1 & 0 \end{pmatrix}, \quad \sigma^2 = \begin{pmatrix} 0 & -i \\ i & 0 \end{pmatrix}, \quad \sigma^3 = \begin{pmatrix} 1 & 0 \\ 0 & -1 \end{pmatrix} \quad (1.19)$$

are the usual Pauli matrices, and $\begin{pmatrix} \Gamma_1(\theta) \\ \Gamma_2(\theta) \end{pmatrix} = \begin{pmatrix} \cos \theta & -\sin \theta \\ \sin \theta & \cos \theta \end{pmatrix} \begin{pmatrix} \Gamma_\phi \\ 0 \end{pmatrix} =$

$\Gamma_\phi \begin{pmatrix} \cos \theta \\ \sin \theta \end{pmatrix}$ is a vector in \mathbb{R}^2 of norm Γ_ϕ pointing in the direction θ ;

- $d\mu_\theta^*(\Psi, \bar{\Psi})$ is the free Grassmann measure characterized by its covariance kernel,

$$\boxed{C_\theta^* := \frac{1}{ip^0 \mathbb{1} - e^*(\mathbf{p})\sigma^3 - \Gamma(\theta)} = -\frac{ip^0 \mathbb{1} + e^*(\mathbf{p})\sigma^3 + \Gamma(\theta)}{(p^0)^2 + (e_{|\Gamma|}^*(\mathbf{p}))^2},} \quad (1.20)$$

and

$$e_{|\Gamma|}^*(\mathbf{p}) := \text{sgn}(e^*(\mathbf{p})) \sqrt{e^*(\mathbf{p})^2 + |\Gamma|^2}. \quad (1.21)$$

In (1.20), $\Gamma(\theta) := \Gamma_1(\theta)\sigma^1 + \Gamma_2(\theta)\sigma^2 = \begin{pmatrix} 0 & \bar{\Gamma}(\theta) \\ \Gamma(\theta) & 0 \end{pmatrix}$ is an off-diagonal Hermitian matrix, in conformity with (1.11).

Let us emphasize that the measure $\exp\left(+\int dp \bar{\Psi}(-p)\left(\Gamma_1(\theta)\sigma^1 + \Gamma_2(\theta)\sigma^2 + \frac{\delta m}{m^2} \frac{|\mathbf{p}|^2}{2} + \delta\mu\right)\Psi(p)\right) d\mu_\theta^*(\Psi, \bar{\Psi})$ is by construction *independent* of Γ_ϕ and θ , and equal to the original measure $d\mu_\lambda(\psi, \bar{\psi})$ of (0.8), *up to error terms due to the ultra-violet cut-off*.

1.3 Multi-scale analysis

Let $p_F^* := \sqrt{2m^*\mu^*}$ be the radius of the effective Fermi circle

$$\Sigma_F^* := \{|\mathbf{p}| = p_F^*\}, \quad (1.22)$$

defined by $e^*(\mathbf{p}) = 0$ for $|\mathbf{p}| = p_F^*$. Near the Fermi circle, one has

$$e^*(\mathbf{p}) \sim \frac{de^*}{dp} \Big|_{p_F^*} p_\perp = \frac{p_F^*}{m^*} p_\perp \quad (1.23)$$

where $p_\perp := |\mathbf{p}| - p_F^*$ is a signed measure of the distance of \mathbf{p} to the Fermi circle. Let \mathbf{p}_D be some momentum such that $e^*(\mathbf{p}_D) \equiv \hbar\omega_D$, see Assumption (0.5). Given the form of the denominator of C_θ^* , see (1.20), it is natural to impose the UV cut-off conditions $\max(|p^0|, e^*(\mathbf{p})) \lesssim e^*(\mathbf{p}_D) = \hbar\omega_D$; namely, it can easily be seen that the region $|p^0| \gg \hbar\omega_D \gtrsim \frac{p_F^*}{m^*} |p_\perp|$ plays practically no rôle in the theory. Assumption (0.4) $\hbar\omega_D \ll \mu$ implies

$$p_{D,\perp} \sim \frac{d|\mathbf{p}|}{de^*} \Big|_{|\mathbf{p}|=p_F^*} \hbar\omega_D = \frac{m^*}{p_F^*} \hbar\omega_D \ll \frac{2m^*}{(p_F^*)^2} \mu^* p_F^* = p_F^*. \quad (1.24)$$

A generic point in $V \subset \mathbb{R} \times \mathbb{R}^2$ will in general be denoted by $\xi = (\tau, \mathbf{x})$, or $\xi' = (\tau', \mathbf{x}')$, $\xi_k = (\tau_k, \mathbf{x}_k)$, etc. By convention $(p, \xi) = p^0\tau - \mathbf{p} \cdot \boldsymbol{\xi}$ is the Minkowski scalar product, while

$$\boxed{|p| := \sqrt{(p^0)^2 + \left(\frac{p_F^*}{m^*} p_\perp\right)^2}, \quad |\xi| := \sqrt{|\tau|^2 + \left(\frac{m^*}{p_F^*} |\mathbf{x}|\right)^2}} \quad (1.25)$$

is a homogeneous norm chosen in such a way that $|p| \sim e^*(\mathbf{p})$ if $p = (0, \mathbf{p})$ is close to the Fermi circle, see (1.23).

Remark. Note that $|p|$ has nothing to do with the Euclidean norm $|p|_+ \approx \sqrt{(p^0)^2 + \left(\frac{p_F^*}{m^*} |\mathbf{p}|\right)^2}$ used in the low-momentum regime (see section 3).

Eq. (1.24) yields some upper momentum scale $j_D \gg 0$ for p^0 and p_\perp ,

$$|p^0| \lesssim 2^{-j_D} \mu, \quad |p_\perp| \lesssim 2^{-j_D} p_F, \quad j_D := \log_2(\mu/\hbar\omega_D). \quad (1.26)$$

Finally, we note that $e_{|\Gamma|}^*(\mathbf{p}) \sim e^*(\mathbf{p}) \sim \frac{p_F^*}{m^*} p_\perp$ for $|\Gamma| \ll \frac{p_F^*}{m^*} |p_\perp| \lesssim 2^{-j_D} \mu$. Thus

$$j_\phi := \lfloor \log_2(\mu/|\Gamma|) \rfloor = \ln(1/g) + O(1) \quad (1.27)$$

fixes an *energy scale associated to the phase transition*. On the other hand, if $|p| \ll |\Gamma|$, then $e_{|\Gamma|}^*(\mathbf{p}) \approx |\Gamma|$ is essentially constant; thus, when $\lambda = 0$ (i.e. for the free theory), all momenta p such that $|p| \ll |\Gamma|$ may be treated as being of the same scale. It turns out *not* to be the case for the interacting theory. In order to make the bridge between the high- and the low-momentum regimes, we fix a *lower* energy scale $j'_\phi \geq j_\phi$,

$$j'_\phi := j_\phi + O(\ln(1/g)). \quad (1.28)$$

In this section, we only discuss momenta p such that

$$2^{-j'_\phi} \mu \lesssim |p| \lesssim 2^{-j_D} \mu. \quad (1.29)$$

We now define a multi-scale version of our model according to the above principles. Fix some smooth function $\chi : \mathbb{R}_+ \rightarrow [0, 1]$ supported on $[\frac{1}{2}, \frac{3}{2}]$ such that $\sum_{j \in \mathbb{Z}} \chi^j \equiv 1$ on \mathbb{R}_+ , where $\chi^j(\cdot) := \chi(2^j \cdot)$. Assume $\chi^j(\cdot) \equiv \sum_\alpha \chi^{j,\alpha}(\cdot)$ is further decomposed as a finite sum of smooth functions such that $\text{supp}(\chi^{j,\alpha}) \subset \text{supp}(\chi^j)$; the $\chi^{j,\alpha}$ will be specified only in §2.1 (with α indexing momentum angular sectors), since it does not matter at this stage. Let

$$\boxed{\chi^{j \rightarrow} := \sum_{k=j_D}^j \chi^k, \quad \chi^{\rightarrow j} := \sum_{k=j}^{+\infty} \chi^k, \quad j_D \leq j \leq j'_\phi} \quad (1.30)$$

so that $\chi^{j \rightarrow}(|p|/\mu) \approx \mathbf{1}_{|p| \gtrsim 2^{-j} \mu}$ is a scale j infra-red cut-off (coupled with a scale j_D UV cut-off), resp. $\chi^{\rightarrow j}(|p|/\mu) \approx \mathbf{1}_{|p| \lesssim 2^{-j} \mu}$ is a scale j UV cut-off. Define as in [25] the 2×2 matrix-valued kernel

$$\boxed{C_\theta^j(\xi, \xi') := \int \frac{d^3 p}{(2\pi)^3} \frac{e^{i(p, \xi - \xi')}}{ip^0 - e^*(\mathbf{p})\sigma_3 - \Gamma(\theta)} \chi^j(|p|/\mu), \quad j_D \leq j < j'_\phi} \quad (1.31)$$

$$\boxed{C_\theta^{j'_\phi}(\xi, \xi') := \int \frac{d^3 p}{(2\pi)^3} \frac{e^{i(p, \xi - \xi')}}{ip^0 - e^*(\mathbf{p})\sigma_3 - \Gamma(\theta)} \chi^{\rightarrow j'_\phi}(|p|/\mu)} \quad (1.32)$$

and similarly (assuming $\chi^{\rightarrow j'_\phi}(\cdot) = \sum_\alpha \chi^{\rightarrow j'_\phi, \alpha}(\cdot)$)

$$\boxed{C_\theta^{j,\alpha}(\xi, \xi') := \int \frac{d^3 p}{(2\pi)^3} \frac{e^{i(p, \xi - \xi')}}{ip^0 - e^*(\mathbf{p})\sigma_3 - \Gamma(\theta)} \chi^{j,\alpha}(|p|/\mu), \quad j_D \leq j < j'_\phi} \quad (1.33)$$

$$\boxed{C_\theta^{j'_\phi, \alpha}(\xi, \xi') := \int \frac{d^3 p}{(2\pi)^3} \frac{e^{i(p, \xi - \xi')}}{ip^0 - e^*(\mathbf{p})\sigma_3 - \Gamma(\theta)} \chi^{-j'_\phi, \alpha}(p/\mu)}, \quad (1.34)$$

and let $(\Psi^{j, \alpha})_{j_D \leq j \leq j'_\phi}, (\bar{\Psi}^{j, \alpha})_{j_D \leq j \leq j'_\phi}$ be independent free spin 1/2 fermion fields, either on \mathbb{R}^3 or on a finite volume V , with covariance kernel

$$\int d\mu_\theta^*(\Psi^{j, \alpha}, \bar{\Psi}_\alpha^j) \Psi^{j, \alpha}(\xi) \bar{\Psi}^{j', \alpha'}(\xi') \equiv \delta_{j, j'} \delta_{\alpha, \alpha'} C_\theta^{j, \alpha}(\xi, \xi'). \quad (1.35)$$

If V is a finite volume, then $C_\theta^{j, \alpha}(\xi, \xi')$ is simply extended outside of $V \times V$ by 0. Let

$$\Psi^j := \sum_\alpha \Psi^{j, \alpha}, \quad \bar{\Psi}^j := \sum_\alpha \bar{\Psi}^{j, \alpha}. \quad (1.36)$$

Then

$$\Psi(\cdot) := \sum_{j=j_D}^{j'_\phi} \Psi^j(\cdot), \quad \bar{\Psi}(\cdot) := \sum_{j=j_D}^{j'_\phi} \bar{\Psi}^j(\cdot) \quad (1.37)$$

has covariance kernel

$$C_\theta^*(\xi, \xi') = \sum_{j=j_D}^{j'_\phi} \sum_\alpha C_\theta^{j, \alpha}(\xi, \xi') = \sum_{j=j_D}^{j'_\phi} C_\theta^j(\xi, \xi'). \quad (1.38)$$

Its Fourier transform $C_\theta^*(p)$ is equal to $\frac{1}{ip^0 - e^*(\mathbf{p})\sigma_3 - \Gamma(\theta)}$ for $|p| \ll \hbar\omega_D$.

Summarizing: for $j_D \leq j < j'_\phi$, C_θ^j is given by an integral over momenta p such that $|p| \approx \max(|p^0|, |e^*(\mathbf{p})|) \approx 2^{-j}\mu$, or equivalently: $\max(|\mathbf{p}|, \frac{m^*}{p_F}|p^0|) \approx 2^{-j}p_F^*$.

Definition 1.1 (Grassmann measure) (i) Let

$$d\mu_{\theta; \lambda}(\Psi, \bar{\Psi}) = \frac{1}{Z_\lambda^*} e^{-\mathcal{L}_\theta(\Psi, \bar{\Psi})} d\mu_\theta^*(\Psi, \bar{\Psi}) \quad (1.39)$$

where $d\mu_\theta^*(\Psi, \bar{\Psi}) = d\mu_\theta^*((\Psi^j)_{j_D \leq j \leq j'_\phi}, (\bar{\Psi}^j)_{j_D \leq j \leq j'_\phi})$ is the Grassmann Gaussian measure associated to the fields $(\Psi^j)_{j_D \leq j \leq j'_\phi}, (\bar{\Psi}^j)_{j_D \leq j \leq j'_\phi}$ as in (1.31), (1.37), and

$$\mathcal{L}_\theta(\cdot) \equiv \int d\xi \mathcal{L}_\theta(\cdot; \xi), \quad (1.40)$$

$$\boxed{\mathcal{L}_\theta(\Psi, \bar{\Psi}; \xi) := \lambda(\bar{\Psi}\Psi)^2(\xi) + \sum_{j=j_D}^{j'_\phi} \sum_\alpha \bar{\Psi}^{j, \alpha}(\xi) \left(\Gamma(\theta) - \left(\frac{\delta m}{m^2} \frac{|\nabla|^2}{2} + \delta\mu \right) \sigma^3 \right) \Psi^{j, \alpha}(\xi)} \quad (1.41)$$

(ii) (same with scale j infra-red cut-off) For $j_D \leq j \leq j'_\phi$, we let

$$d\mu_{\theta;\lambda}(\Psi^{j\rightarrow}, \bar{\Psi}^{j\rightarrow}) = \frac{1}{\mathcal{Z}_\lambda^{j\rightarrow}} e^{-\mathcal{L}_\theta(\Psi^{j\rightarrow}, \bar{\Psi}^{j\rightarrow})} d\mu_\theta^*(\Psi^{j\rightarrow}, \bar{\Psi}^{j\rightarrow}) \quad (1.42)$$

where $d\mu_\theta^*(\Psi^{j\rightarrow}, \bar{\Psi}^{j\rightarrow}) = d\mu_\theta^*((\Psi^k)_{j_D \leq k \leq j}, (\bar{\Psi}^k)_{j_D \leq k \leq j})$ is the Grassmann Gaussian measure associated to the fields $(\Psi^k)_{j_D \leq k \leq j}, (\bar{\Psi}^k)_{j_D \leq k \leq j}$ as in (1.31), (1.37), and

$$\mathcal{L}_\theta^{\rightarrow j}(\cdot) \equiv \int d\xi \mathcal{L}_\theta^{\rightarrow j}(\cdot; \xi), \quad (1.43)$$

$$\mathcal{L}_\theta^{\rightarrow j}(\Psi^{j\rightarrow}, \bar{\Psi}^{j\rightarrow}; \xi) := \lambda(\bar{\Psi}^{j\rightarrow} \Psi^{j\rightarrow})^2(\xi) + \sum_{k=j_D}^j \sum_{\alpha} \bar{\Psi}^{k,\alpha}(\xi) \left(\Gamma(\theta) - \left(\frac{\delta m}{m^2} \frac{|\nabla|^2}{2} + \delta\mu \right) \sigma^3 \right) \Psi^{k,\alpha}(\xi)$$

(1.44)

The whole point in introducing the $\Psi^{j,\alpha}$'s at this very early stage is that the quadratic part \mathcal{L}_θ in the above Definition is diagonal in that basis.

Up to change of normalization constant \mathcal{Z}_λ^* , $d\mu_\lambda(\Psi^{j\rightarrow}, \bar{\Psi}^{j\rightarrow})$ is simply obtained from $d\mu(\Psi, \bar{\Psi})$ by letting $\Psi^k, \bar{\Psi}^k \equiv 0$ for $k > j$. In practice, this j -dependent measure will result from the momentum-decoupling expansion and renormalization by replacing $\Psi, \bar{\Psi}$ with $\Psi(t^j; \cdot) := \sum_{k=j_D}^j \Psi^k(\cdot) + t^j \sum_{k>j} \Psi^k(\cdot)$, $\bar{\Psi}(t^j; \cdot) := \sum_{k=j_D}^j \bar{\Psi}^k(\cdot) + t^j \sum_{k>j} \bar{\Psi}^k(\cdot)$ and letting $t^j = 0$. It is the right place to mention that these infra-red cut-off theories enjoy the same invariance properties as the original theory, see §1.1, which is crucial for the renormalization step (see §2.3).

1.4 Bubble diagrams and fermion four-point function in Cooper channel

We primarily consider in this subsection the simplest Feynman diagrams of the theory – the *bubble diagrams*. Feynman rules can be found in Chapter 46 of the book by Fetter and Walecka [26]. The amplitude of an amputated bubble diagram Υ , computed using the free Grassmann measure C_θ^* , is denoted in whole generality by $\mathcal{A}_q(\Upsilon)$, where q is the external momentum flowing into the diagram, or $\mathcal{A}_q(\Gamma, \Upsilon_3)$ if one wishes to emphasize the dependence on the parameter Γ . Replacing C_θ^* with $(C_\theta^*)^{j\rightarrow} := \sum_{k=j_D}^j C_\theta^k$, one obtains the scale j infra-red cut-off evaluation $\mathcal{A}_q^{j\rightarrow}(\Upsilon)$.

The symmetry-broken theory with gap parameter $\Gamma \in \mathbb{C}$ involves

- **diagonal or normal propagators**, $\bar{\psi}_{\sigma_1} \longrightarrow \psi_{\sigma_2}$ evaluated as $-\delta_{\sigma_1, \sigma_2} \frac{i\mathbf{p}^0 + e^*(\mathbf{p})}{(p^0)^2 + (e^*(\mathbf{p}))^2}$.

Graphically, we orient such propagators using arrows from $\bar{\psi}$ to ψ , following the convention of e.g. quantum electrodynamics, in order to follow fermion loops;

- **off-diagonal or symmetry-broken propagators**,

$$\frac{\psi_{\sigma_1} \times \psi_{\sigma_2}}{\quad} \quad \frac{\bar{\psi}_{\sigma_1} \times \bar{\psi}_{\sigma_2}}{\quad}$$

evaluated as $-\delta_{\sigma_1, \sigma_2} \frac{\Gamma^*(\theta)}{(p^0)^2 + (e_{|\Gamma|}^*(\mathbf{p}))^2}$, resp. $-\delta_{\sigma_1, \sigma_2} \frac{\Gamma(\theta)}{(p^0)^2 + (e_{|\Gamma|}^*(\mathbf{p}))^2}$. Such propagators are non-oriented. Because we introduced them by hand in the Gaussian measure, they exist even in Regime I, i.e. above the gap energy, but they are very *small* for scales $j \ll j_\phi$ due to the coefficient $|\Gamma| = \Gamma_\phi = O(2^{-j_\phi})$ in the numerator.

The names *diagonal* and *off-diagonal* refer to the location of these quantities inside the two-by-two free Green function $G|_{\lambda=0}$, see (1.5).

• **Γ -counterterms** \rightarrow \blacksquare Γ coming from the term $\int dp \bar{\Psi}(-p) \Gamma(\theta) \Psi(p)$ in (1.18).

In subsequent computations, we rewrite diagonal propagators as follows,

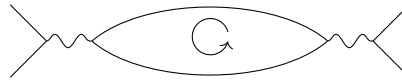
$$\boxed{\frac{ip^0 + e^*(\mathbf{p})}{(p^0)^2 + (e_{|\Gamma|}^*(\mathbf{p}))^2} = \frac{1}{-ip^0 + e_{|\Gamma|}^*(\mathbf{p})} - \frac{\delta e^*(\mathbf{p})}{(p^0)^2 + (e_{|\Gamma|}^*(\mathbf{p}))^2}} \quad (1.45)$$

with

$$\delta e^*(\mathbf{p}) := e_{|\Gamma|}^*(\mathbf{p}) - e^*(\mathbf{p}) \sim \begin{cases} \frac{1}{2} \frac{p_F^*}{m^*} \left(\frac{\Gamma_\phi}{p_\perp}\right)^2 p_\perp & (|p_\perp| \gg \Gamma_\phi) \\ \frac{\Gamma_\phi}{|p_\perp|} p_\perp & (|p_\perp| \lesssim \Gamma_\phi). \end{cases} \quad (1.46)$$

The integration measure $dp = dp^0 d\mathbf{p}$ for angle-independent quantities is of the two-dimensional form $2\pi|\mathbf{p}| dp^0 dp_\perp \sim 2\pi p_F dp^0 dp_\perp$. Thus the theory is *effectively* 1 + 1-*dimensional* in the neighborhood of the Fermi sphere; this remarkable fact actually holds true for any dimension $d \geq 2$.

Vacuum polarization bubbles. In an intermediate boson picture, where density fields $\bar{\psi}_\downarrow \psi_\downarrow$, $\bar{\psi}_\uparrow \psi_\uparrow$ interact via a delta-potential represented by a wavy line, such bubbles may be represented as



yielding a renormalization of the intermediate boson.

Bubble diagrams are evaluated without taking into account the usual (-1) -factor per loop, characteristic of fermionic theories. One obtains *three possibilities*:

• The *normal* $(\psi, \bar{\psi})$ -*bubble diagram* Υ_1

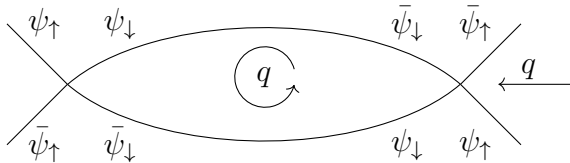


Fig. 1.4.1. Normal bubble diagram Υ_1 .

is evaluated up to error terms (see (1.45) and below) as

$$\mathcal{A}_q^{j \rightarrow}(\Upsilon_1) = - \int \frac{\chi^{j \rightarrow}(|p+q|/\mu) \chi^{j \rightarrow}(|p|/\mu) dp}{\left(i(p^0 + q^0) + e_{|\Gamma|}^*(\mathbf{p} + \mathbf{q}) \right) \left(ip^0 + e_{|\Gamma|}^*(\mathbf{p}) \right)} \quad (1.47)$$

A naive power-counting argument in terms of the integration measure, also valid for the Cooper-pair bubble $\Upsilon_{3,diag}$ below, yields

$$|\mathcal{A}_0^{j \rightarrow}(\Upsilon_1)| \lesssim \int dp^0 d\mathbf{p} \frac{(\chi^{j \rightarrow}(p))^2}{|p|^2} \sim 2\pi p_F \int_{2^{-j}\mu < |p| < 2^{-j_D}\mu} \frac{dp^0 dp_\perp}{|p|^2} \sim m^* \int_{2^{-j}\mu}^{2^{-j_D}\mu} \frac{d|p|}{|p|} \approx \sum_{j=j_D}^{j_\phi} m^*, \quad (1.48)$$

a logarithmically divergent integral. However, $\mathcal{A}_0^{j \rightarrow}(\Upsilon_1)$ is UV convergent, as can be seen from a contour deformation into the upper/lower half-plane of the integral in p^0 . Namely, $\int \frac{dp^0}{(ip^0 + e_{|\Gamma|}^*(\mathbf{p}))^2} = i \int dp^0 \frac{d}{dp^0} \left(\frac{1}{ip^0 + e_{|\Gamma|}^*(\mathbf{p})} \right) = 0$, so (by integration by parts in p^0 and parity in p^0)

$$\mathcal{A}_0^{j \rightarrow}(\Upsilon_1) = i \int \frac{\frac{d}{dp^0} ((\chi^{j \rightarrow}(|p|/\mu))^2) dp}{ip^0 + e_{|\Gamma|}^*(\mathbf{p})}. \quad (1.49)$$

Now, $\frac{d}{dp^0}(\chi^{j \rightarrow}(|p|/\mu))$ vanishes except for momenta p of scales $j_D + O(1)$ or $j + O(1)$, which thus suppresses the diverging sum over scales. Generalizing, we let q be a small transfer momentum, $|q|_+ \ll 2^{-j}\mu$, and subtract $\mathcal{A}_0^{j \rightarrow}(\Upsilon_1)$, yielding

$$\mathcal{A}_q^{j \rightarrow}(\Upsilon_1) = \int dp \frac{iq^0 + (e_{|\Gamma|}^*(\mathbf{p} + \mathbf{q}) - e_{|\Gamma|}^*(\mathbf{p}))}{\left(i(p^0 + q^0) + e_{|\Gamma|}^*(\mathbf{p} + \mathbf{q}) \right) \left(ip^0 + e_{|\Gamma|}^*(\mathbf{p}) \right)^2} \chi^{j \rightarrow}(|p|/\mu) \chi^{j \rightarrow}(|p+q|/\mu) \quad (1.50)$$

with $q^0, e_{|\Gamma|}^*(\mathbf{p} + \mathbf{q}) - e_{|\Gamma|}^*(\mathbf{p}) = O(\frac{|q|_+}{|p|})|p|$. Restricting the integration domain to momenta p of scale k and moving the contour in p^0 to a distance $\approx 2^{-k}\mu$ from the real axis yields $\mathcal{A}_q^{j \rightarrow}(\Upsilon_1) = \sum_{k=j_D}^j \mathcal{A}_q^k(\Upsilon_1)$, with $\mathcal{A}_q^k(\Upsilon_1) = m^* O(\frac{|q|_+}{2^{-k}\mu})$, summing to $O(1)$.

The same bound may also be obtained by noting that $i(p^0 + q^0) - e_{|\Gamma|}^*(\mathbf{p} + \mathbf{q}) \simeq i(p^0 + q^0) - \frac{p_F^*}{m^*}(p_\perp + q_\perp)$, $q_\perp := \frac{\mathbf{q} \cdot \mathbf{p}}{|\mathbf{p}|}$, and

$$\begin{aligned} & \left(iq^0 - \frac{p_F^*}{m^*} q_\perp \right) \frac{1}{\left(i(p^0 + q^0) - \frac{p_F^*}{m^*} (p_\perp + q_\perp) \right) \left(ip^0 - \frac{p_F^*}{m^*} p_\perp \right)} \\ &= \frac{1}{ip^0 - \frac{p_F^*}{m^*} p_\perp} - \frac{1}{i(p^0 + q^0) - \frac{p_F^*}{m^*} (p_\perp + q_\perp)} \end{aligned} \quad (1.51)$$

which vanishes by translation invariance upon integration in p up to cut-off issues; we skip details since we do not need a second argument, but refer the reader to Ward

identities in quantum electrodynamics which can be proved in a similar way, see e.g. [57].

Error terms involve the subtracted terms, $\frac{\delta e^*(\mathbf{p})}{(p^0)^2 + (e_{|\Gamma|}^*(\mathbf{p}))^2}$ or $\frac{\delta e^*(\mathbf{p}+\mathbf{q})}{(p^0+q^0)^2 + (e_{|\Gamma|}^*(\mathbf{p}+\mathbf{q}))^2}$ or both. However, the small factor $\frac{\Gamma_\phi}{|p_\perp|}$ appearing in (1.46) transforms the logarithmically divergent estimates (1.48) into a convergent integral; the same argument holds for Υ_3 below.

- The *off diagonal* or *symmetry-broken* $(\psi, \bar{\psi})$ -bubble diagrams $\Upsilon_{3,off}, \Upsilon'_1$

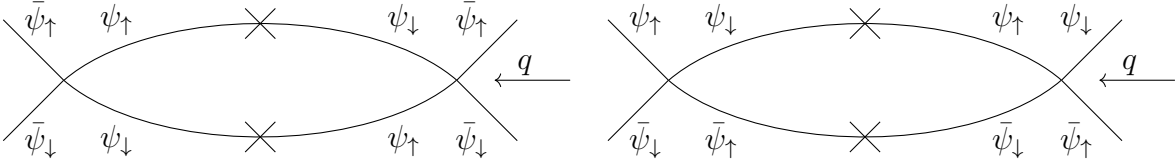


Fig. 1.4.2. Symmetry broken bubble diagrams $\Upsilon_{3,off}$, resp. Υ'_1 (from left to right).

are evaluated at zero external momentum as

$$\mathcal{A}_0^{j \rightarrow}(\Gamma, \Upsilon_{3,off}) = -\bar{\Gamma}^2 \int \frac{\chi^{j \rightarrow}(|p|/\mu) dp}{(p_0^2 + (e_{|\Gamma|}^*(\mathbf{p}))^2)^2}, \quad \mathcal{A}_0^{j \rightarrow}(\Upsilon'_1) = |\Gamma|^2 \int \frac{\chi^{j \rightarrow}(|p|/\mu) dp}{(p_0^2 + (e_{|\Gamma|}^*(\mathbf{p}))^2)^2} \quad (1.52)$$

which are equal by simple scaling to a constant times $(\frac{\Gamma}{\mu})^2$, resp. $(\frac{|\Gamma|}{\mu})^2$ times $2^{2j} m^* (1 + O((2^{-(j-j_D)})^2))$. Letting $|\Gamma| \equiv \Gamma_\phi \approx 2^{-j_\phi} \mu$ and summing over scales $j_D \leq j \leq j_\phi$ (in this computation one may simply set $j'_\phi = j_\phi$), one gets

$$O(m^*) \sum_{j \leq j_\phi} 2^{-2(j_\phi - j)} = O(m^*), \quad (1.53)$$

a finite contribution.

The diagram $\Upsilon_{3,off}$ has a *Cooper pair external structure*; it connects a Cooper pair $\bar{\psi}_\uparrow \bar{\psi}_\downarrow$ to another one. Later on (see §1.7), following the Nambu convention, see (1.5), we shall denote with a lower index "diag" diagrams connecting a Cooper pair $\bar{\psi}_\uparrow \bar{\psi}_\downarrow$ to the adjoint pair $\psi_\downarrow \psi_\uparrow$ or conversely, and "off" diagrams connecting two Cooper pairs of the same kind. This accounts for the notation $\Upsilon_{3,off}$. On the other hand, Υ'_1 is a companion diagram to Υ_1 , connecting two conventional pairs $\bar{\psi} \psi$. Rewriting the product of two vertices

$$\{(\bar{\psi}_\uparrow \psi_\uparrow)(\xi)(\bar{\psi}_\downarrow \psi_\downarrow)(\xi)\} \{(\bar{\psi}_\uparrow \psi_\uparrow)(\xi')(\bar{\psi}_\downarrow \psi_\downarrow)(\xi')\} \quad (1.54)$$

in the form $(\bar{\psi}_\uparrow \bar{\psi}_\downarrow)(\xi) \{(\psi_\uparrow(\xi) \psi_\downarrow(\xi')) \cdot (\psi_\downarrow(\xi) \psi_\uparrow(\xi'))\} (\bar{\psi}_\uparrow \bar{\psi}_\downarrow)(\xi')$, one sees that $\mathcal{A}^{j \rightarrow}(\Gamma, \Upsilon_{3,off})$ is a contribution to the off-diagonal channel $(\psi_\uparrow \psi_\downarrow) \otimes (\bar{\psi}_\uparrow \bar{\psi}_\downarrow)$, equal to $e^{-2i\theta}$ times a quantity which is *negative*, equal to $-|\mathcal{A}_0^{j \rightarrow}(\Gamma, \Upsilon_{3,off})|$, when $q = 0$.

- The main diagram in BCS theory is the *Cooper pair bubble* $\Upsilon_{3,diag}$,

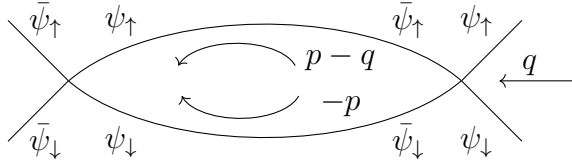
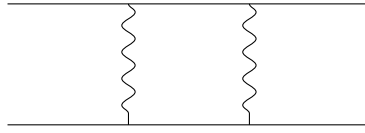


Fig. 1.4.3. Cooper pair bubble.

Remark. Ladder diagrams. In the intermediate boson picture as above, such bubbles take the form



where wiggling lines $\xi \rightsquigarrow \xi'$ represent the δ -interaction $\delta(\xi - \xi')$, and may be concatenated in the form of ladders of arbitrary length,



Fig. 1.4.4. Ladder diagram.

conventionally called *ladder diagrams* in connection to the Bethe-Salpeter kernel, see [26], or equivalently in the following dual form,



Fig. 1.4.5. Bubble chain.

The above Cooper pair bubble diagram is evaluated up to convergent error terms as

$$\mathcal{A}_q^{j \rightarrow}(\Gamma, \Upsilon_{3,diag}) = \frac{1}{(2\pi)^3} \int dp \frac{\chi^{j \rightarrow}(|p|/\mu) \chi^{j \rightarrow}(|p+q|/\mu)}{\left(i(p^0 + q_0) - e_{|\Gamma|}^*(\mathbf{p} + \mathbf{q})\right) \left(-ip^0 - e_{|\Gamma|}^*(\mathbf{p})\right)} \quad (1.55)$$

It is UV divergent: at zero external momenta,

$$\begin{aligned}
\mathcal{A}_0(\Gamma, \Upsilon_{3,diag}) &= \frac{1}{(2\pi)^3} \int dp |C_\theta^*(p)|^2 \\
&= \frac{1}{(2\pi)^3} \int \frac{dp}{|ip^0 - e_{|\Gamma|}^*(\mathbf{p})|^2} + O(m^*) \\
&= \frac{1}{(2\pi)^2} \int \frac{d\mathbf{p}}{|e_{|\Gamma|}^*(\mathbf{p})|} + O(m^*) \\
&= \frac{1}{2\pi} p_F^* \int_{-(2m^*/p_F^*)\hbar\omega_D}^{(2m^*/p_F^*)\hbar\omega_D} \frac{dp_\perp}{\sqrt{(\frac{p_F^*}{2m^*})^2 p_\perp^2 + |\Gamma|^2}} \left(1 + \frac{m^*}{p_F^*} O\left(\frac{p_\perp}{p_F^*}\right)\right) \\
&= \frac{m^*}{\pi} \left(\sinh^{-1} \frac{\hbar\omega_D}{|\Gamma|} + O(1) \right) \\
&= \frac{m^*}{\pi} \left(\log(\hbar\omega_D/|\Gamma|) + O(1) \right). \tag{1.56}
\end{aligned}$$

Rewriting (1.54) in the form $(\bar{\psi}_\uparrow \bar{\psi}_\downarrow)(\xi) \{ (\psi_\uparrow(\xi) \bar{\psi}_\uparrow(\xi')) \cdot (\psi_\downarrow(\xi) \bar{\psi}_\downarrow(\xi')) \} (\psi_\downarrow \psi_\uparrow)(\xi')$, one sees that $\mathcal{A}_q(\Gamma, \Upsilon_{3,diag})$ is a contribution to the diagonal channel $(\bar{\psi}_\uparrow \bar{\psi}_\downarrow) \otimes (\psi_\downarrow \psi_\uparrow)$, which is *positive* when $q = 0$.

This quantity diverges logarithmically in the neighbourhood of the Fermi circle when $\Gamma = 0$. The estimates (1.56) also holds for $\mathcal{A}_0^{j \rightarrow}(\Gamma, \Upsilon_{3,diag})$ when $|\Gamma| \approx 2^{-j\phi} \mu$ and $j \geq j_\phi + O(1)$. On the other hand, if $2^{-j} \mu \gg |\Gamma|$, then the above integral has an infra-red cut-off of scale j , so that

$$\mathcal{A}_0^{j \rightarrow}(\Gamma, \Upsilon_{3,diag}) \sim \frac{m^*}{\pi} (j - j_D) \tag{1.57}$$

is essentially independent of Γ .

Both the transfer momentum q and the infra-red cut-off at fermionic scale j play the rôle of an infra-red cut-off; the resulting effective IR cut-off fermionic scale is $k \simeq \min\left(j, \lfloor \log(\mu/|q|_+) \rfloor\right)$. In particular,

$$\mathcal{A}_q^{j \rightarrow}(\Gamma, \Upsilon_{3,diag}) \sim \mathcal{A}_0^{j \rightarrow}(\Gamma, \Upsilon_{3,diag}) \sim \frac{m^*}{\pi} (j - j_D) \tag{1.58}$$

if the transfer momentum is small, i.e. $|q|_+ \lesssim 2^{-j} \mu$.

On the other hand, as proved in Appendix, see §5.4, if $|q|_+ \gtrsim 2^{-j} \mu$,

$$|\mathcal{A}_q^{j \rightarrow}(\Gamma, \Upsilon_{3,diag}) - \mathcal{A}_0^{k \rightarrow}(\Gamma, \Upsilon_{3,diag})| \lesssim m^*, \quad k := \lfloor \log(\mu/|q|_+) \rfloor \tag{1.59}$$

so $\mathcal{A}_q^{j \rightarrow}(\Gamma, \Upsilon_{3,diag})$ is roughly equal to the evaluation of a bubble with zero transfer momentum and infra-red cut-off $\approx |q|_+$; the reason is that (say, for $q^0 = 0$), the integrand in \mathbf{p} (a generalization of (1.56)) vanishes when \mathbf{p} and $\mathbf{p} + \mathbf{q}$ are not on the same side of the Fermi sphere.

It is a remarkable fact *per se* that, due to symmetry-breaking, the above integral (1.56) has an effective cut-off, making the diagram finite.

1.5 The gap equation at lowest order

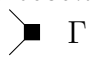
We consider here only the Cooper pair bubble diagram $\Upsilon_{3,diag}$ and interpret the gap equation as a self-consistent identity ensuring the vanishing of the one-point function in the direction θ .

We first *remark* that, as an immediate consequence of (1.20),

$$\lambda \int dp (C_\theta^*)_{12}(p) \simeq \lambda \Gamma \int dp |C_\theta^*(p)|^2 = \lambda \Gamma \mathcal{A}_0(\Upsilon_{3,diag}) \quad (1.60)$$

with error terms coming from $\delta e^*(\mathbf{p})$, see (1.45), graphically,

Fig. 1.5.1. Off-diagonal covariance is equal to Cooper pair bubble diagram.

The diagram on the left-hand side may be interpreted as *one* of the two *main contributions to the one-point function of the Goldstone boson*, the other coming from the counterterm insertion $-\Gamma(\psi_\downarrow\psi_\uparrow)(\xi)$ at ξ , . Then these two main contributions cancel provided

$$\boxed{\lambda \mathcal{A}_0(\Gamma, \Upsilon_{3,diag}) \simeq 1} \quad (1.61)$$

or equivalently, taking (1.57) into account,

$$\boxed{j_\phi - j_D = \frac{\pi}{g} + O(1)}. \quad (1.62)$$

This is the crudest approximation to the **gap equation**. Letting $\lambda \mathcal{A}_0(\Gamma, \Upsilon_{3,diag}) \equiv 1$ implies that the bubble series,

Fig. 1.5.2. Cooper pair bubble geometric series.

which is the leading order approximation of the Goldstone boson propagator, diverges at zero transfer momentum. These two properties – vanishing of the one-point function in the direction θ , singularity of the Goldstone boson propagator – remain simultaneously true beyond mean-field theory and even non-perturbatively, as we shall

see later on, see §1.7 and section 3. Whatever the exact value of Γ , and the cut-off scale $j'_\phi \geq j_\phi$, one has as soon as $|\Gamma| \approx \hbar\omega_D e^{-\pi/g}$

$$\lambda \mathcal{A}_0^{(j'_\phi-1)\rightarrow}(\Gamma, \Upsilon_{3,diag}) = 1 + O(g). \quad (1.63)$$

The infra-red behavior of chains of bubbles, and later on, of Goldstone boson propagators, are best understood after a change of basis, choosing for external structures the linear combinations $(\bar{\Psi}^{\Gamma//,\perp}\Psi) \otimes (\bar{\Psi}^{\Gamma//,\perp}\Psi)$ instead of the diagonal channels $(\bar{\psi}_\uparrow\bar{\psi}_\downarrow) \otimes (\psi_\downarrow\psi_\uparrow)$, $(\psi_\downarrow\psi_\uparrow) \otimes (\bar{\psi}_\uparrow\bar{\psi}_\downarrow)$ and the off-diagonal channels $(\bar{\psi}_\uparrow\bar{\psi}_\downarrow) \otimes (\bar{\psi}_\uparrow\bar{\psi}_\downarrow)$, $(\psi_\downarrow\psi_\uparrow) \otimes (\psi_\downarrow\psi_\uparrow)$, where $\Gamma^{//} := \Gamma(\theta)$, $\Gamma^\perp := \Gamma(\theta + \frac{\pi}{2})$. (Explicit change-of-basis formulae are provided in §3.1 in the case $\theta = 0$, see in particular (3.8) and below). Letting $\mathcal{A}_0^{j\rightarrow}(\Gamma, \Upsilon_{3,diag}) =: a_{diag}^{j\rightarrow} \mathbb{1}$, $\mathcal{A}_0^{j\rightarrow}(\Gamma, \Upsilon_{3,off}) =: -a_{off}^{j\rightarrow} \sigma(\theta)$, one obtains in the $(//, \perp)$ -basis a diagonal matrix $\mathcal{A}_0^{j\rightarrow} = \text{diag}((\mathcal{A}_0^{j\rightarrow})_{//, //}, (\mathcal{A}_0^{j\rightarrow})_{\perp, \perp})$, with

$$(\mathcal{A}_0^{j\rightarrow})_{//, //} = 2(a_{diag}^{j\rightarrow} - a_{off}^{j\rightarrow}), \quad (\mathcal{A}_0^{j\rightarrow})_{\perp, \perp} = 2(a_{diag}^{j\rightarrow} + a_{off}^{j\rightarrow}) \quad (1.64)$$

and $a_{diag}^{j\rightarrow} \approx \frac{m^*}{g} > 0$, $a_{off}^{j\rightarrow} \approx m^* > 0$.

It is useful at this point to introduce the following

Definition 1.2 (pre-gap equation) *Let $\Gamma = \Gamma^{(j'_\phi-1)\rightarrow}$ be the solution of the pre-gap equation,*

$$\lambda(\mathcal{A}_0^{(j'_\phi-1)\rightarrow})_{\perp, \perp}(\Gamma) = 1. \quad (1.65)$$

Because $a_{diag}^{j\rightarrow} \gg a_{off}^{j\rightarrow} > 0$, Γ may also be understood as the solution with largest module of the eigenvalue equation,

$$\left(-\mathbb{1} + \lambda \mathcal{A}_0^{(j'_\phi-1)\rightarrow}(\Gamma, \Upsilon_3) \right) \begin{pmatrix} \Gamma^\perp \\ (\Gamma^\perp)^* \end{pmatrix} = 0. \quad (1.66)$$

The matrix $\mathbb{1} - \lambda \mathcal{A}_0^{(j'_\phi-1)\rightarrow}(\Gamma, \Upsilon_3)$ has eigenvectors $\begin{pmatrix} \Gamma^{//} \\ (\Gamma^{//})^* \end{pmatrix}$, $\begin{pmatrix} \Gamma^\perp \\ (\Gamma^\perp)^* \end{pmatrix}$, with respective eigenvalues $4\lambda a_{off}^{(j'_\phi-1)\rightarrow} \approx g > 0$ and 0. As emphasized in §1.6, this means that *the geometric series of Cooper pair bubble diagrams is **massive** in the parallel direction ($//$), i.e. along $\Gamma(\theta)$, whereas it is **non-massive** in the perpendicular direction (\perp), i.e. along $\Gamma(\theta + \frac{\pi}{2})$* , corresponding to the longitudinal direction along the circle $|\Gamma| = \text{Cst}$, in line with Goldstone's insight. Compare with Definition 1.9. As shown in §1.7 for a corrected version of the gap equation including the Bethe-Salpeter kernel $\bar{\Pi}_0$, this equation has a solution $\approx \hbar\omega_D e^{-\pi/g}$, as expected. Computations in 1.7 reduce to the results of §1.6 if one sets $\bar{\Pi}_0 \equiv \lambda \text{Id}$. The pre-gap equation is corrected in the bosonic regime, see Definition 3.3, leading to a sequence $\Gamma^{j_+\rightarrow}$, $j_+ = j'_\phi, j'_\phi + 1, \dots$ converging when $j_+ \rightarrow \infty$ to the correct value of Γ_ϕ .

1.6 The pre-Goldstone boson propagator

The pre-Goldstone boson propagator is directly related to the second derivatives of $\mathcal{A}_q^{j\rightarrow}(\Gamma, \Upsilon_{3,diag})$ and $\mathcal{A}_q^{j\rightarrow}(\Gamma, \Upsilon_{3,off})$ w.r. to q around $q = 0$. A general argument, relying on the fact that

$$\mathcal{A}_0^{j\rightarrow}(\Gamma, \Upsilon_{3,diag}) = \int d\xi' |C_{diag}^{j\rightarrow}(\xi-\xi')|^2 \geq \int d\xi' e^{-i(q,\xi-\xi')} |C_{diag}^{j\rightarrow}(\xi-\xi')|^2 = \mathcal{A}_q^{j\rightarrow}(\Gamma, \Upsilon_{3,diag}) \quad (1.67)$$

and

$$-\mathcal{A}_0^{j\rightarrow}(\Gamma, \Upsilon_{3,off}) = \int d\xi' |C_{off}^{j\rightarrow}(\xi-\xi')|^2 \geq \int d\xi' e^{-i(q,\xi-\xi')} |C_{off}^{j\rightarrow}(\xi-\xi')|^2 = -\mathcal{A}_q^{j\rightarrow}(\Gamma, \Upsilon_{3,off}) \quad (1.68)$$

implies that $\nabla^2 \mathcal{A}_q^{j\rightarrow}(\Gamma, \Upsilon_{3,diag}) \Big|_{q=0} \leq 0$, resp. $\nabla^2 (-\mathcal{A}_q^{j\rightarrow}(\Gamma, \Upsilon_{3,off})) \Big|_{q=0} \leq 0$. By symmetry, $\partial_{q^0} \mathcal{A}_q(\Gamma, \Upsilon_{3,\varepsilon}) \Big|_{q=0} = 0$, $\nabla \mathcal{A}_q(\Gamma, \Upsilon_{3,\varepsilon}) \Big|_{q=0} = 0$, $\partial_{q^0} \nabla \mathcal{A}_q(\Gamma, \Upsilon_{3,\varepsilon}) \Big|_{q=0} = 0$ and $\nabla^2 \mathcal{A}_q(\Gamma, \Upsilon_{3,\varepsilon}) \Big|_{q=0}$ is a scalar matrix, where $\varepsilon = \text{diag, off}$.

Lemma 1.3

$$\partial_{q^0}^2 \mathcal{A}_q(\Gamma^{(j'_\phi-1)\rightarrow}, \Upsilon_{3,diag}) \Big|_{q=0} =: -\frac{1}{g_{\phi,diag}^0}, \quad \partial_{q^0}^2 \mathcal{A}_q(\Gamma^{(j'_\phi-1)\rightarrow}, \Upsilon_{3,off}) \Big|_{q=0} = \frac{1}{g_{\phi,off}^0} \quad (1.69)$$

$$\nabla^2 \mathcal{A}_q(\Gamma^{(j'_\phi-1)\rightarrow}, \Upsilon_{3,diag}) \Big|_{q=0} =: -\frac{(v_{\phi,diag}^0)^2}{g_{\phi,diag}^0} \text{Id}, \quad \nabla^2 \mathcal{A}_q(\Gamma^{(j'_\phi-1)\rightarrow}, \Upsilon_{3,off}) \Big|_{q=0} =: \frac{(v_{\phi,off}^0)^2}{g_{\phi,off}^0} \text{Id} \quad (1.70)$$

where

$$g_{\phi,diag}^0, g_{\phi,off}^0 \approx \frac{\Gamma_\phi^2}{m^*} \quad (1.71)$$

have the dimension of an energy, and

$$v_{\phi,diag}^0, v_{\phi,off}^0 \approx \frac{p_F^*}{m^*} \quad (1.72)$$

are velocities.

The proof is given in Appendix.

Definition 1.4 (Goldstone pre-boson coupling constant and velocity) *Let*

$$g_\phi^0 := \frac{g_{\phi,diag}^0 g_{\phi,off}^0}{g_{\phi,diag}^0 + g_{\phi,off}^0}, \quad v_\phi^0 := \sqrt{\frac{g_{\phi,off}^0 (v_{\phi,diag}^0)^2 + g_{\phi,diag}^0 (v_{\phi,off}^0)^2}{g_{\phi,diag}^0 + g_{\phi,off}^0}}. \quad (1.73)$$

The Goldstone pre-boson coupling constant g_ϕ^0 and velocity v_ϕ^0 are obtained by inverting $F(q) := \left(\mathcal{A}_q(\Gamma^{(j'_\phi-1)\rightarrow}, \Upsilon_{3,diag}) - \mathcal{A}_0(\Gamma^{(j'_\phi-1)\rightarrow}, \Upsilon_{3,diag}) \right) - \left(\mathcal{A}_q(\Gamma^{(j'_\phi-1)\rightarrow}, \Upsilon_{3,off}) - \mathcal{A}_0(\Gamma^{(j'_\phi-1)\rightarrow}, \Upsilon_{3,diag}) \right)$ for $q \rightarrow 0$, namely,

$$\frac{1}{F(q)} \sim_{q \rightarrow 0} \left(\sum_{\varepsilon=\text{diag,off}} \frac{1}{g_{\phi,\varepsilon}^0} (q^0)^2 + \frac{(v_{\phi,\varepsilon}^0)^2}{g_{\phi,\varepsilon}^0} |\mathbf{q}|^2 \right)^{-1} = \frac{g_\phi^0}{(|q|_+^0)^2} \quad (1.74)$$

where

$$|q|_+^0 := \sqrt{(q^0)^2 + (v_\phi^0 |\mathbf{q}|)^2} \quad (1.75)$$

similarly to (0.68).

The meaning of Definition 1.4 is explained in the next subsection.

Summing the geometric series of Cooper pair bubble diagrams, one gets a 2×2 matrix kernel, called **pre-Goldstone boson propagator** or simply **pre-kernel**,

$$\boxed{\text{Pre}\Sigma(q) := \lambda \sum_{n=0}^{+\infty} \left\{ \lambda \mathcal{A}_q^{(j'_\phi-1)\rightarrow}(\Gamma^{(j'_\phi-1)\rightarrow}, \Upsilon_3) \right\}^n = \frac{\lambda}{\mathbb{1} - \lambda \mathcal{A}_q^{(j'_\phi-1)\rightarrow}(\Gamma^{(j'_\phi-1)\rightarrow}, \Upsilon_3)}} \quad (1.76)$$

with (choosing a basis)

$$\mathcal{A}_q^{(j'_\phi-1)\rightarrow}(\Gamma^{(j'_\phi-1)\rightarrow}, \Upsilon_3) := \begin{array}{cc} & \psi_\downarrow \psi_\uparrow \\ & \bar{\psi}_\uparrow \bar{\psi}_\downarrow \\ \begin{array}{c} \bar{\psi}_\uparrow \bar{\psi}_\downarrow \\ \psi_\downarrow \psi_\uparrow \end{array} & \left(\begin{array}{cc} \mathcal{A}_q^{(j'_\phi-1)\rightarrow}(\Gamma^{(j'_\phi-1)\rightarrow}, \Upsilon_{3,diag}) & \mathcal{A}_q^{(j'_\phi-1)\rightarrow}(\Gamma^{(j'_\phi-1)\rightarrow}, \Upsilon_{3,off}) \\ \mathcal{A}_q^{(j'_\phi-1)\rightarrow}(\Gamma^{(j'_\phi-1)\rightarrow}, \Upsilon_{3,off}) & \mathcal{A}_q^{(j'_\phi-1)\rightarrow}(\Gamma^{(j'_\phi-1)\rightarrow}, \Upsilon_{3,diag}) \end{array} \right) \end{array} \quad (1.77)$$


This kernel is in sandwich between adjoint fermion pairs in Cooper pairings, $\bar{\psi}_\uparrow \bar{\psi}_\downarrow$ or $\psi_\downarrow \psi_\uparrow$. Note that the amplitude $\mathcal{A}_q^{(j'_\phi-1)\rightarrow}(\Gamma^{(j'_\phi-1)\rightarrow}, \Upsilon_3)$ is computed *not* for the exact value Γ_ϕ of Γ , but for $\Gamma = \Gamma^{(j'_\phi-1)\rightarrow}$, in such a way that $\text{Pre}\Sigma(q)$ *diverges* when $q \rightarrow 0$.

As seen in the previous subsection, the above kernel is divergent in the infra-red limit, i.e. when $q \rightarrow 0$, in the (\perp, \perp) -channel. Let us now consider $q \neq 0$ but small. The behavior of $\text{Pre}\Sigma_{\perp, \perp}(q)$ is obtained (see (1.64)) as the inverse of the quadratic form $-\frac{1}{2} \sum_{i,j=0}^3 \partial_{q_i} \partial_{q_j} \left\{ (\mathcal{A}_q(\Upsilon_{3,diag}) + \mathcal{A}_q(\Upsilon_{3,off})) \right\} \Big|_{q=0} q^i q^j$. Lemma 1.3 yields:

$$\boxed{\text{Pre}\Sigma_{\perp, \perp}(q) \sim_{q \rightarrow 0} \frac{1}{2} \frac{g_\phi^0}{(|q|_+^0)^2} (1 + O(g))} \quad (1.78)$$

with the notations of Definition 1.4. On the other hand,

$$\text{Pre}\Sigma_{//, //}(q) \sim_{q \rightarrow 0} \frac{\lambda}{4\lambda a_{off}^{(j'_\phi - 1) \rightarrow}} \approx \frac{1}{m^*}. \quad (1.79)$$

As we shall see in the next subsection, the kernel component $\text{Pre}\Sigma_{\perp, \perp}$ is a good approximation of the (scalar) *Goldstone boson propagator* $\Sigma_{\perp, \perp}$ for large transfer momenta $|q|_+ \gg \Gamma_\phi$. For this reason, and also because it is explicitly produced through the bubble resummations in the fermionic regime, we may consider it as the covariance of fictitious bosonic particles which we call *pre-Goldstone bosons*, whence the name $\text{Pre}\Sigma$; in Feynman diagrams it is represented as a dashed wavy line, . This kernel is dressed by more complicated diagrams, which play an important rôle only in the bosonic regime, but do not modify the general picture described in the previous paragraphs; perturbatively (as shown in (1.141)),

$$\Sigma_{\perp, \perp}(q) \sim_{q \rightarrow 0} \frac{1}{2} \frac{g_\phi}{|q|_+^2} \quad (1.80)$$

where $g_\phi = g_\phi^0(1+O(g))$, $v_\phi = v_\phi^0(1+O(g))$, see (1.135), and $|q|_+ := \sqrt{(q^0)^2 + (v_\phi|\mathbf{q}|)^2}$, see (0.68). The rigorous definition of Σ in section 3 – which relies instead on a somewhat technical multi-scale construction – will be slightly different, but (1.80) will be shown to hold for some modified values of g_ϕ, v_ϕ and up to error terms, for which we only prove a crude bound in $O(g^{1/4})$ (though one should be able to prove that they are $O(g)$ by looking more precisely at lowest-order terms with a small number of vertices).

Let us now describe the (non-rigorous) connection to the effective non-linear sigma model theory described in the Introduction (see Regime II). Let $\Gamma(q) := \int d\xi e^{-i(q, \xi)} (\bar{\Psi} \Gamma^\perp \Psi)(q)$. Bubbles in the channel (\perp, \perp) may be resummed into the following counterterm,

$$\Gamma(-q) \text{Pre}\Sigma_{\perp, \perp}(q) \Gamma(q) \sim_{q \rightarrow 0} \Gamma(-q) \frac{g_\phi^0}{(q^0)^2 + (v_\phi^0)^2 |\mathbf{q}|^2} \Gamma(q) \quad (1.81)$$

implying an effective action, see (0.27), of the form

$$\begin{aligned} & \exp \left(- \int dq \Gamma(-q) \frac{q_0^2 + (v_\phi^0)^2 |\mathbf{q}|^2}{g_\phi^0} \Gamma(q) \right) \\ & \propto \int \mathcal{D}\Gamma \exp - \left(\frac{1}{g_\phi^0} \int d\xi |\nabla \Gamma(\xi)|^2 \right), \end{aligned} \quad (1.82)$$

where by definition

$$\nabla \Gamma(\xi) := \begin{pmatrix} \partial_\tau \Gamma(\xi) \\ v_\phi^0 \nabla \Gamma(\xi) \end{pmatrix}, \quad |\nabla \Gamma(\xi)|^2 := |\partial_\tau \Gamma(\xi)|^2 + (v_\phi^0)^2 |\nabla \Gamma(\xi)|^2. \quad (1.83)$$

Removing the upper 0 indices, we get a similar resummation of the Goldstone *boson*. So g_ϕ plays the *rôle of a coupling constant for the non-linear sigma model* describing the infra-red behavior of the Goldstone boson.

Let us investigate corrections to the leading-order behavior of $\text{Pre}\Sigma_{\perp,\perp}(q)$ when $|q|_+ \rightarrow 0$ (as we shall see in §3, the same estimates hold for $\Sigma_{\perp,\perp}(q)$, up to the replacement of g_ϕ^0, v_ϕ^0 by their counterparts g_ϕ, v_ϕ). Corrections involve fourth-order derivatives of $\mathcal{A}_q(\Upsilon_3)$,

$$\text{Pre}\Sigma_{\perp,\perp}(q) = \frac{g_\phi}{q_0^2 + v_\phi^2 |\mathbf{q}|^2 + O(|q|_+^4/\Gamma_\phi^2)} = \frac{g_\phi}{q_0^2 + v_\phi^2 |\mathbf{q}|^2} + O(|q|_+^2/\Gamma_\phi^2) \quad (1.84)$$

Let

$$|\xi|_+ := \sqrt{\tau^2 + (|\mathbf{x}|/v_\phi)^2} \quad (1.85)$$

(see Notations in the introduction), $|\xi|_+ \approx |\xi|$. An inverse Fourier transform yields

$$\text{Pre}\Sigma_{\perp,\perp}(\xi) := (2\pi)^{-3} \int dq e^{i(q,\xi)} \text{Pre}\Sigma(q) \sim_{|\xi|_+ \rightarrow \infty} \frac{1}{4\pi} \frac{g_\phi/v_\phi}{\sqrt{|\mathbf{x}|^2 + v_\phi^2 \tau^2}} = \frac{1}{4\pi} \frac{g_\phi/v_\phi^2}{|\xi|_+}. \quad (1.86)$$

Error terms can be bounded, yielding

$$\text{Pre}\Sigma_{\perp,\perp}(\xi) \sim_{|\xi|_+ \rightarrow \infty} \frac{1}{4\pi} \frac{g_\phi/v_\phi^2}{|\xi|_+} (1 + O(\frac{1}{\Gamma_\phi |\xi|_+})). \quad (1.87)$$

as proved in the Appendix.

Finally, let us bound the infra-red cut-off matrix kernel $\text{Pre}\Sigma^{j \rightarrow}(\xi)$ with $j_\phi - j \gg 1$. For that, we need further estimates on the Fourier transformed kernel $\text{Pre}\Sigma^{j \rightarrow}(q)$. Consider first the case when $|q|_+ \gtrsim 2^{-j}\mu$. We deduce from the computations of §1.4 that $|\text{Pre}\Sigma^{j \rightarrow}(q)| \lesssim |\frac{\lambda}{1-\lambda \mathcal{A}^{j \rightarrow}(q)}| \approx \frac{1}{m^* \log(|q|_+/\Gamma_\phi)}$. Then, as proved in the Appendix, if $|\kappa| \geq 1$,

$$|\nabla_q^\kappa \text{Pre}\Sigma(q)| \lesssim \frac{1}{m^* |q|_+^{|\kappa|}} \frac{1}{\log^2(|q|_+/\Gamma_\phi)} \quad (1.88)$$

where $\nabla_q^\kappa := (\nabla_{q^0})^{\kappa^0} (\frac{\mu}{p_F^*} \nabla_{q^1})^{\kappa^1} (\frac{\mu}{p_F^*} \nabla_{q^2})^{\kappa^2}$. The other case, namely when $|q|_+ \lesssim 2^{-j}\mu$, is easier. As already observed in §1.4 $\mathcal{A}_q^{j \rightarrow}(\Upsilon_{3,diag}) \sim \mathcal{A}_0^{j \rightarrow}(\Upsilon_{3,diag})$, and similarly,

$$|\nabla_q^\kappa \mathcal{A}_q^{j \rightarrow}(\Upsilon_{3,diag})| \lesssim m^* \int_{2^{-j}\mu}^{2^{-j}D\mu} \frac{\rho d\rho}{\rho^{\kappa+2}} \approx \frac{m^*}{(2^{-j}\mu)^\kappa} \quad (|\kappa| \geq 1), \quad (1.89)$$

so that $1 - \lambda \mathcal{A}_q^{j \rightarrow}(\Upsilon_{3,diag}) \approx m^* \lambda (j_\phi - j)$, and finally, by an elementary computation,

$$|\nabla_q^\kappa \text{Pre}\Sigma(q)| \lesssim \frac{1}{m^* (2^{-j}\mu)^{|\kappa|}} \frac{1}{(j_\phi - j)^2}. \quad (1.90)$$

Introduce a reduced partition of unity for transfer momenta, fix $\chi_+ \equiv \chi$, and let $\chi_+^{j+}(\cdot) := \chi_+(2^{j+}\cdot)$ ($j_+ < j$), $\chi_+^j(\cdot) := \sum_{j_+=-\infty}^j \chi_+(2^{j_+}\cdot)$. Then

$$\begin{aligned}
m^* |\text{Pre}\Sigma^{j\rightarrow}(\xi)| &= m^* \left| \sum_{k=j_D}^j \int dq \chi_+^k(q) e^{i(q,\xi)} \Sigma^{j\rightarrow}(q) \right| \\
&\lesssim \left\{ \sum_{j_+=j_D}^j \frac{1}{(j_\phi - j_+)^2} \text{Vol}(\text{supp}(\chi_+^{j_+})) \left(1 + 2^{-j_+} |\xi|\right)^{-n} \right\} \\
&+ \frac{1}{j_\phi - j_D} \text{Vol}(\text{supp}(\chi_+^{j_D})) \left(1 + 2^{-j_D} |\xi|\right)^{-n} + \frac{1}{j_\phi - j} \text{Vol}(\text{supp}(\chi_+^j)) \left(1 + 2^{-j} |\xi|\right)^{-n}
\end{aligned} \tag{1.91}$$

for every $n \geq 1$, as shown by successive integrations by parts. Whence, in particular,

$$\begin{aligned}
m^* \int d\xi |\text{Pre}\Sigma^{j\rightarrow}(\xi)| &\lesssim \left\{ \sum_{k=j_D}^j \frac{1}{(j_\phi - k)^2} \right\} + \frac{1}{j_\phi - j_D} + \frac{1}{j_\phi - j} \\
&\lesssim \frac{1}{j_\phi - j}, \quad j_\phi - j \gg 1.
\end{aligned} \tag{1.92}$$

When $j \ll j_\phi$, a good approximation for $\text{Pre}\Sigma^{j\rightarrow}(\xi)$ is simply its leading order, which is the $(\bar{\Psi}\Psi)^2$ -vertex $\lambda\delta(\xi)$. The bound (1.92) is coherent with the value of the integrated kernel $\int d\xi \lambda\delta(\xi) = \lambda$, since $\frac{1}{j_\phi} \approx g \approx \lambda m^*$.

On the other hand, the kernel $\text{Pre}\Sigma_{///}^{(j'_\phi-1)\rightarrow}(\xi)$, which is the Fourier transform of the massive kernel

$$\text{Pre}\Sigma_{///}^{(j'_\phi-1)\rightarrow}(q) \approx \frac{1}{m^*} \approx \frac{1}{m^*} \frac{\Gamma_\phi^2}{|q|_+^2 + \Gamma_\phi^2} \quad (|q|_+ \lesssim \Gamma_\phi), \tag{1.93}$$

has a quasi-exponential decay at distances $\gg 1/\Gamma_\phi$,

$$|\text{Pre}\Sigma_{///}^{(j'_\phi-1)\rightarrow}(\xi)| \leq C_n \frac{1}{m^*} \text{Vol}(\text{supp}(\chi_+^{j'_\phi})) (1 + 2^{-j'_\phi} |\xi|)^{-n} \approx C_n \frac{\Gamma_\phi^3}{\mu} (1 + 2^{-j'_\phi} |\xi|)^{-n}, \quad |\xi| \gtrsim \Gamma_\phi^{-1} \tag{1.94}$$

see (2.17), as can be shown in a standard way by repeated integrations by parts.

1.7 Energy gap and Goldstone boson

The above Cooper pair bubble diagrams $\Upsilon_{3,\varepsilon}$, $\varepsilon = \text{diag, off}$, may be composed an arbitrary number of times, yielding λ times the geometric series of bubbles, see Fig. 1.5.1 with transfer momentum q , evaluated as $\frac{\lambda}{1 - \lambda \mathcal{A}_q(\Upsilon_3)}$. A quick but not rigorous computation, taking into account only these diagrams, yields an approximate value for

Γ_ϕ , based on the requirement that *the denominator of the series of bubbles vanishes for $q = 0$* , see **Gap equation** in Definition 1.9 below, namely (considering only the $\Upsilon_{3,diag}$ -diagram, and summarizing briefly the findings of the two previous subsections)

$$\lambda \mathcal{A}_0(\Upsilon_{3,diag}) \sim 1 \quad (1.95)$$

from which

$$\Gamma_\phi \approx \hbar \omega_D e^{-\pi/g} \quad (1.96)$$

and

$$\frac{\lambda}{1 - \lambda \mathcal{A}_q(\Upsilon_{3,diag})} \approx \frac{g_\phi}{|q|_+^2}. \quad (1.97)$$

As explained in the Introduction to this section, what we really need in section 3 is the *effective contribution $\Sigma_{\perp,\perp}$ to the Cooper pair bound state (Goldstone boson) propagator of fermionic four-point functions*. We need some preliminary explanations before we give a closed formula for this quantity, but let us mention already at this stage that the approximation (1.96) gives a correct order of magnitude for Γ_ϕ – as shall be checked self-consistently –, and that the value obtained for the bubble series (1.97) for small q is a good approximation for $\Sigma(q)$ – except that the latter is a two-by-two matrix.

First, a Feynman diagram with Cooper pair external structure

$$\begin{aligned} (\bar{\psi}_\uparrow \bar{\psi}_\downarrow) \otimes (\psi_\downarrow \psi_\uparrow) &= \left(\bar{\psi}_\uparrow(\xi_1) \bar{\psi}_\downarrow(\xi_2) \right) \left(\psi_\downarrow(\xi_3) \psi_\uparrow(\xi_4) \right), \\ (\psi_\downarrow \psi_\uparrow) \otimes (\bar{\psi}_\uparrow \bar{\psi}_\downarrow) &= \left(\psi_\downarrow(\xi_1) \psi_\uparrow(\xi_2) \right) \left(\bar{\psi}_\uparrow(\xi_3) \bar{\psi}_\downarrow(\xi_4) \right) \end{aligned} \quad (1.98)$$

(*non-mixing case*), or

$$\begin{aligned} (\bar{\psi}_\uparrow \bar{\psi}_\downarrow) \otimes (\bar{\psi}_\uparrow \bar{\psi}_\downarrow) &= \left(\bar{\psi}_\uparrow(\xi_1) \bar{\psi}_\downarrow(\xi_2) \right) \left(\bar{\psi}_\uparrow(\xi_3) \bar{\psi}_\downarrow(\xi_4) \right), \\ (\psi_\downarrow \psi_\uparrow) \otimes (\psi_\downarrow \psi_\uparrow) &= \left(\psi_\downarrow(\xi_1) \psi_\uparrow(\xi_2) \right) \left(\psi_\downarrow(\xi_3) \psi_\uparrow(\xi_4) \right) \end{aligned} \quad (1.99)$$

(*mixing case*), is called *two-particle irreducible* if *the compound made up of vertices $\{\xi_1, \xi_2\}$ is connected to the compound made up of vertices $\{\xi_3, \xi_4\}$* . Note that two-particle reducible diagrams may be generated from the partition function by a double Legendre transform, see e.g. [59], eq. (10.132). We could, but have chosen not to, use this nice trick. As detailed in §2.1, external legs possibly have indices – scale j and momentum angular indices α for *sectors* $\mathcal{S}^{j,\alpha}$ with $j < j'_\phi$, scale j'_ϕ , momentum angular indices α and an extra integer index k for *micro-sectors* $\mathcal{S}^{j,\alpha,k}$ –, numbered as the corresponding vertex locations, e.g. $(\bar{\psi}_\uparrow^{j_1,\alpha_1} \bar{\psi}_\uparrow^{j_2,\alpha_2}) \otimes (\psi_\downarrow^{j_3,\alpha_3} \psi_\uparrow^{j_4,\alpha_4}) = \left((\bar{\psi}_\uparrow^{j_1,\alpha_1}(\xi_1) \bar{\psi}_\uparrow^{j_2,\alpha_2}(\xi_2)) \right) \left((\psi_\downarrow^{j_3,\alpha_3}(\xi_3) \psi_\uparrow^{j_4,\alpha_4}(\xi_4)) \right)$. As explained later on in §2.3, only $\tilde{\Pi}$ -kernels with external scales $j_1 = j_2 = j_3 = j_4 = j'_\phi$ need be considered; their external

momenta are very close to, but not on, the Fermi circle. Triples (j'_ϕ, α, k) index regions $\mathcal{S}^{j'_\phi, \alpha, k}$ of the momentum space of dimensions scaling like $2^{-j_+} \times 2^{-j_+} \times 2^{-j_+}$, so that, denoting by $p^{j'_\phi, \alpha, k}$ the center of $\mathcal{S}^{j'_\phi, \alpha, k}$, $|p - p^{j'_\phi, \alpha, k}|_+ \lesssim 2^{-j_+} \mu$ for p lying inside $\mathcal{S}^{j'_\phi, \alpha, k}$. None of this is really required to read the present subsection, which remains at a descriptive level based on finite number of graphs produced by perturbation.

We let $\tilde{\Pi}(\xi_1, \xi_2; \xi_3, \xi_4)$ be the sum of all two-particle irreducible, four-point Feynman diagrams with fixed external structure; it may be represented as a two-by-two matrix, with *non-mixing coefficients* on the diagonal, and *mixing coefficients* off-diagonal,

$$\tilde{\Pi} := \begin{array}{c} \bar{\psi}_\uparrow \bar{\psi}_\downarrow \\ \psi_\downarrow \psi_\uparrow \end{array} \begin{array}{cc} \psi_\downarrow \psi_\uparrow & \bar{\psi}_\uparrow \bar{\psi}_\downarrow \\ \left(\begin{array}{cc} \Pi_{\bar{\psi}_\uparrow \bar{\psi}_\downarrow, \psi_\downarrow \psi_\uparrow} & \Pi_{\bar{\psi}_\uparrow \bar{\psi}_\downarrow, \bar{\psi}_\uparrow \bar{\psi}_\downarrow} \\ \Pi_{\psi_\downarrow \psi_\uparrow, \psi_\downarrow \psi_\uparrow} & \Pi_{\psi_\downarrow \psi_\uparrow, \bar{\psi}_\uparrow \bar{\psi}_\downarrow} \end{array} \right) \equiv \left(\begin{array}{cc} \tilde{\Pi}_{diag} & (\tilde{\Pi}_{off})^\dagger \\ \tilde{\Pi}_{off} & \tilde{\Pi}_{diag} \end{array} \right), \end{array} \quad (1.100)$$

compare with (1.77). Lowest-order terms are

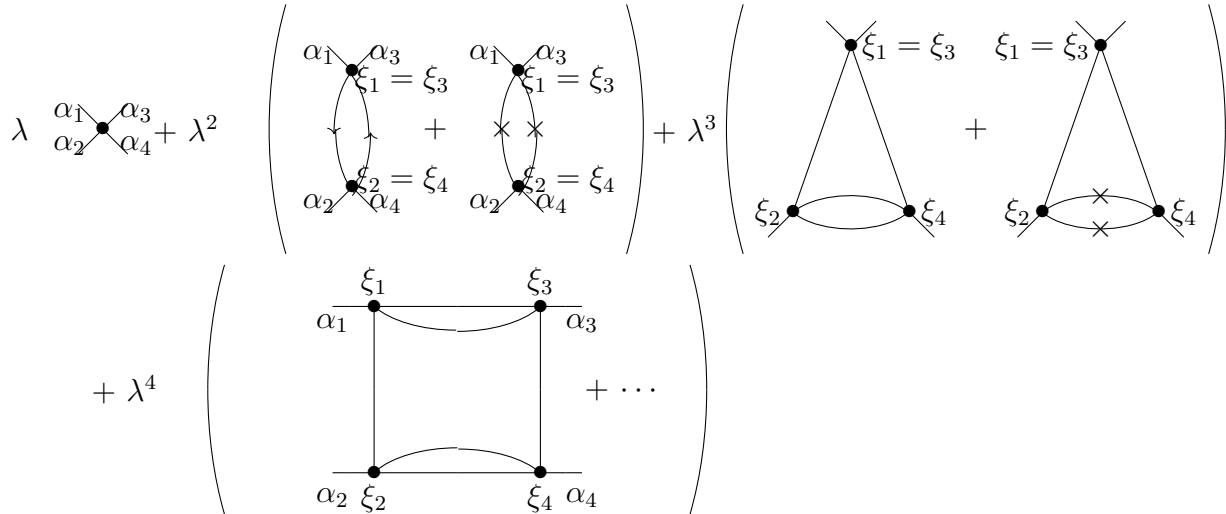

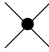


Fig. 1.7.1. Lowest-order terms of the Bethe-Salpeter kernel.

Note that the $O(\lambda^3)$ triangle diagram, Fig. 0.1, is a two-particle *reducible* diagram

obtained by composing  and 

On the other hand, the $O(\lambda^3)$ diagrams on the first line of Fig. 1.7.1 (obtained by tilting the triangle diagram) are two-particle irreducible – but note that by cutting the two long slanted lines, vertices $\{\xi_1, \xi_3\}$ are cut off from the other two, $\{\xi_2, \xi_4\}$.

The first diagram is the vertex, simply evaluated as the coupling constant λ . The second and third diagrams look superficially like bubble diagrams tilted to the side, but the impression is wrong because the momentum circulating inside the "tilded

bubble” diagrams $\tilde{\Upsilon}_1, \tilde{\Upsilon}'_1, \tilde{\Upsilon}_{3,off}$, named with a tilde by reference to the original bubble diagrams of the previous subsection,

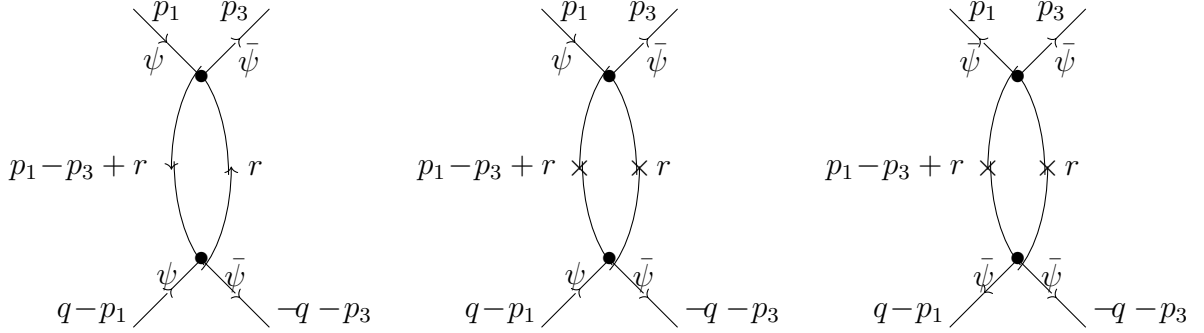


Fig. 1.7.2. "Tilted bubble" diagrams $\tilde{\Upsilon}_1, \tilde{\Upsilon}'_1, \tilde{\Upsilon}_{3,off}$ (from left to right).

isn't q as in the $\tilde{\Upsilon}_1$ -diagram, see Fig. 1.4.1, but $p_1 - p_3$, therefore, generically a *large* momentum. Note incidentally that the third diagram of Fig. 1.7.1 decomposes as the sum of two diagrams, $\tilde{\Upsilon}'_1$ and $\tilde{\Upsilon}_{3,off}$.

The first three diagrams, namely, the vertex, $\tilde{\Upsilon}_1$ and $\tilde{\Upsilon}'_1$, are of non-mixing type. The fourth one, $\tilde{\Upsilon}_{3,off}$, is mixing, proportional (when considered together with the conjugate diagram as entries of a matrix) to the off-diagonal matrix $\begin{pmatrix} 0 & \Gamma^2 \\ (\Gamma^*)^2 & 0 \end{pmatrix}$.

Finally, the last ones (the terms in $O(\lambda^3)$ and $O(\lambda^4)$ in Fig. 1.7.1), can be either of non-mixing or mixing type, see the figure below for the mixing version of the $O(\lambda^4)$ -diagram.

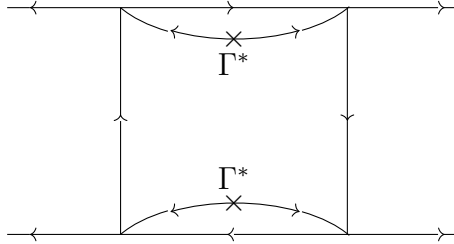


Fig. 1.7.3. Mixing diagram $\tilde{\Upsilon}_{4,off}$.

Consider a general (mixing or non-mixing) diagram with an arbitrary number of Γ - or Γ^* -insertions. Cutting the symmetry-broken propagators in their middle, thus leaving only neutral vertices, i.e. four-leg vertices $(\bar{\psi}_\uparrow \bar{\psi}_\downarrow)(\psi_\downarrow \psi_\uparrow)$ with the same number of entering and exiting lines, one finds: $\#$ entering lines = $\#$ exiting lines, whence (considering the whole diagram): $\# \Gamma - \# \Gamma^* = 2$, resp. 0, resp. -2 depending on whether the external structure is of the type $(\psi_\downarrow \psi_\uparrow) \otimes (\psi_\downarrow \psi_\uparrow)$, resp. $(\psi_\downarrow \psi_\uparrow) \otimes (\bar{\psi}_\uparrow \bar{\psi}_\downarrow)$ or $(\bar{\psi}_\uparrow \bar{\psi}_\downarrow) \otimes (\psi_\downarrow \psi_\uparrow)$, resp. $(\bar{\psi}_\uparrow \bar{\psi}_\downarrow) \otimes (\bar{\psi}_\uparrow \bar{\psi}_\downarrow)$. If $\Gamma = |\Gamma_\phi| e^{i\theta}$, then the corresponding two-by-two symmetrized matrix $\frac{1}{2} \left\{ \tilde{\Pi}(\xi_1, \xi_2; \xi_3, \xi_4) + \tilde{\Pi}(\xi_2, \xi_1; \xi_4, \xi_3) \right\}$ is therefore of the form $\begin{pmatrix} c_{1,1} & c_{1,2} e^{-2i\theta} \\ c_{1,2} e^{2i\theta} & c_{2,2} \end{pmatrix}$, where $c_{1,1}, c_{1,2}, c_{2,2}$ are *real-valued* functions.

Define now $\tilde{\Sigma}(\xi_1, \xi_3)$ to be $\frac{1}{\lambda}$ times the sum of all connected but not necessarily two-particle irreducible Feynman diagrams with external structure as in (1.98,1.99), but with $\xi_1 = \xi_2$, $\xi_3 = \xi_4$:

$$\begin{aligned} \tilde{\Sigma}(\xi_1, \xi_3) = & \delta(\xi_1 - \xi_3) + \lambda \left\{ \left(\begin{array}{c} \xi_1 \quad \xi_3 \quad \xi_1 \quad \xi_3 \\ \bullet \quad \bullet \quad \times \quad \bullet \quad \times \quad \bullet \\ \bullet \quad \bullet \quad \times \quad \bullet \quad \times \quad \bullet \end{array} \right) + \begin{array}{c} \xi'_1 \quad \xi'_3 \\ \bullet \quad \bullet \\ \xi_1 \quad \xi_3 \\ \bullet \quad \bullet \\ \xi'_2 \quad \xi'_4 \end{array} \tilde{\Pi}(\xi'_1, \xi'_2; \xi'_3, \xi'_4) \right. \\ & + \begin{array}{c} \xi'_1 \\ \bullet \\ \xi_1 \\ \bullet \\ \xi'_2 \end{array} \tilde{\Pi}(\xi'_1, \xi'_2; \xi'_3, \xi'_4) \left(\begin{array}{c} \xi'_3 \quad \xi''_1 \quad \xi'_3 \quad \xi''_1 \\ \bullet \quad \bullet \quad \times \quad \bullet \\ \bullet \quad \bullet \quad \times \quad \bullet \\ \xi'_4 \quad \xi''_2 \quad \xi'_4 \quad \xi''_2 \end{array} \right) \\ & \left. + \dots \right\} \begin{array}{c} \xi''_3 \\ \bullet \\ \xi_3 \\ \bullet \\ \xi''_4 \end{array} \tilde{\Pi}(\xi''_1, \xi''_2; \xi''_3, \xi''_4) \end{aligned}$$

Fig. 1.7.4. Formal expansion of the two-particle propagator in terms of two-particle irreducible diagrams.

and let $\tilde{\Sigma}(q)$ be its Fourier transform, with transfer momentum q entering the chain of diagrams at the left end ξ_1 , and exiting at the right end ξ_3 . Note that connecting pairs of propagators preserve momenta, so that corresponding pairs of external momenta for neighboring pairs of $\tilde{\Pi}$ -kernels are equal, e.g. $p'_3 = p''_1, p'_4 = p''_2$.

Let us now introduce the following *projection procedure*, a simplified procedure giving the order of magnitude of the main contributions to the Bethe-Salpeter kernel near the infra-red singularity, i.e. for a transfer momentum $q \rightarrow 0$ (of which a corrected version, called *averaging procedure*, is presented in §3.3 D. (ii)).

Definition 1.5 (Fermi surface projection of 2 P.I. diagrams) For any two-particle irreducible, four-point diagram $\tilde{\Upsilon}$ with Cooper pair external structure, we denote by $\tilde{\mathcal{A}}_q(\tilde{\Upsilon})$ the averaged evaluation of $\tilde{\Upsilon}$ on the Fermi circle, namely,

$$\tilde{\mathcal{A}}_q(\tilde{\Upsilon}) := \frac{1}{(\text{Vol}(\Sigma_F^*))^2} \int_{\Sigma_F^* \times \Sigma_F^*} dp_1 dp_3 \mathcal{A}(p_1, -p_1 + q; p_3, -p_3 - q). \quad (1.101)$$

Lemma 1.6

$$|\tilde{\mathcal{A}}_q(\tilde{\Upsilon}_1)| \lesssim m^* \quad (1.102)$$

$$|\mathcal{A}_q(\tilde{\Upsilon}'_1)|, |\tilde{\mathcal{A}}_q(\tilde{\Upsilon}_{3,off})| \lesssim m^*/N_{j_\phi} \quad (1.103)$$

$$|\tilde{\mathcal{A}}_q(\tilde{\Upsilon}_{4,diag})| \lesssim m^*, |\tilde{\mathcal{A}}_q(\tilde{\Upsilon}_{4,off})| \lesssim m^*/N_{j_\phi} \quad (1.104)$$

$$\left| \frac{d}{d\Gamma_\phi} \tilde{\mathcal{A}}_q(\tilde{\Upsilon}_1) \right|, \left| \frac{d}{d\Gamma_\phi} \tilde{\mathcal{A}}_q(\tilde{\Upsilon}'_1) \right|, \left| \frac{d}{d\Gamma_\phi} \tilde{\mathcal{A}}_q(\tilde{\Upsilon}_{3,off}) \right| \lesssim \frac{m^*}{\mu} \quad (1.105)$$

where $N_{j_\phi} := 2^{-j_\phi}$, see §2.1.

Proof. The bound on $\tilde{\mathcal{A}}_q(\tilde{\Upsilon}_1)$ derives by simple averaging from the bound in $O(m^*)$ showed for $\mathcal{A}_{p_1-p_3}(\Upsilon_1)$. Consider now the r -momentum scale j contribution to $\tilde{\mathcal{A}}_q(\tilde{\Upsilon}'_1)$ or $\tilde{\mathcal{A}}_q(\tilde{\Upsilon}_{3,off})$: one finds Γ^2 or $|\Gamma|^2$ times

$$I^j := \frac{1}{\text{Vol}(\Sigma_F^*)^2} \int_{\Sigma_F^* \times \Sigma_F^*} dp_1 dp_3 \int dr \chi^j(r) \frac{1}{(p_1^0 - p_3^0 + r^0)^2 + (e_{|\Gamma|}^*(\mathbf{p}_1 - \mathbf{p}_3 + \mathbf{r}))^2} \frac{1}{(r^0)^2 + (e_{|\Gamma|}^*(\mathbf{r}))^2} \quad (1.106)$$

Briefly said, both propagators have a scale j_ϕ infra-red cut-off; main contribution comes a priori from the region

$$|r|, |p_1 - p_3 + r| \approx \Gamma, \quad (1.107)$$

in which the product of the two propagators by the integration volume $\int dr \chi^j(r) \approx m^* \Gamma^2$ yields $O(\frac{m^*}{|\Gamma|^2})$. Taking into account the prefactor Γ^2 or $|\Gamma|^2$, the missing prefactor $N_{j_\phi} = 2^{-j_\phi}$ comes from the constraint (1.107) on p_3 . For a more precise computation, one notes that the sector $\alpha \in \mathbb{Z}/2^j\mathbb{Z}$ of \mathbf{r} is fixed by the sectors $\alpha_1, \alpha_3 \in \mathbb{Z}/2^j\mathbb{Z}$ of $\mathbf{p}_1, \mathbf{p}_3$. Hence

$$\begin{aligned} \sum_{j \leq j_\phi} I^j &\lesssim \sum_{j \leq j_\phi} \left(2^{-2j} \sum_{\alpha_1, \alpha_3 \in \mathbb{Z}/2^j\mathbb{Z}} \right) (2^{-3j} \mu^2 m^*) (2^{-j} \mu)^{-4} \\ &\lesssim \sum_{j \leq j_\phi} 2^j \mu^{-2} m^* \lesssim 2^{j_\phi} \mu^{-2} m^* \approx m^* / (N_{j_\phi} |\Gamma|^2). \end{aligned} \quad (1.108)$$

The bounds for $\tilde{\mathcal{A}}_q(\tilde{\Upsilon}_{4,\varepsilon})$, $\varepsilon = \text{diag, off}$, follow from similar bounds for the quantities $\mathcal{A}_{\tilde{\Upsilon}_\varepsilon}(p_1, -p_q; p_3, -p_3 - q)$, themselves consequences of the general bounds of section 2, in particular of the subsection (§3.2) on the complementary $1/N$ -expansion. As in the case of $\tilde{\Upsilon}'_1$ or $\tilde{\Upsilon}_{3,off}$, in the case of scale j inner momenta, one gets compared to the naive power-counting estimates in $O(m^*)$ two supplementary small prefactors, (i) one in $O(1/N_j)$, $N_j := 2^{-j}$; (ii) and one in $O(2^{-(j_\phi-j)})$ for each symmetry-broken propagator since $\frac{|\Gamma|}{(p^0)^2 + (e_{|\Gamma|}^*(\mathbf{p}))^2} \approx \frac{|\Gamma|}{|p|} \cdot \frac{1}{|p|}$. Multi-scale diagrams with inner momenta of scales varying between j_{min} and j_{max} , $j_D \leq j_{min} < j_{max} \leq j_\phi$ enjoy a supplementary "spring factor" $O(2^{-(j_{max}-j_{min})})$, allowing a multi-scale generalization of the previous argument.

Finally, the bound for $\frac{d}{d\Gamma_\phi} \tilde{\mathcal{A}}_q(\tilde{\Upsilon}_1)$, say, may be obtained along the same line by noting that $\Gamma_\phi \left| \frac{d}{d\Gamma_\phi} C_{diag}^*(p) \right| \approx \Gamma_\phi \left| \frac{d}{d\Gamma_\phi} \left(\frac{1}{-ip^0 + e_{|\Gamma|}^*(\mathbf{p})} \right) \right| \lesssim \frac{\Gamma_\phi}{|p|^2 + \Gamma^2}$ is bounded by a symmetry-broken propagator. Thus, using similar arguments as for $\mathcal{A}_q(\tilde{\Upsilon}'_1)$, one obtains a bound

in $O(\frac{1}{\Gamma_\phi} \cdot (m^*/N_{j_\phi})) \approx \frac{m^*}{\mu}$. The bound for $\frac{d}{d\Gamma}\tilde{\mathcal{A}}_q(\tilde{\Upsilon}'_1)$ and $\frac{d}{d\Gamma}\tilde{\mathcal{A}}_q(\tilde{\Upsilon}_{3,off})$ follows more directly from the inequality $|\frac{d}{d\Gamma}C_{diag}^*(p)| \lesssim \frac{C_{diag}^*(p)}{|\Gamma|}$ by noting that $N_{j_\phi}\Gamma \approx \mu$. \square

In order to get the leading behavior of $\tilde{\Sigma}$ in the infra-red limit ($q \rightarrow 0$), we first want to **displace the lower external legs**, namely, those on the second line, $\xi'_4, \xi''_2, \xi''_4, \xi''_2, \dots$ of Fig. 1.7.4, to the corresponding locations on the first line $\xi'_3, \xi''_1, \xi''_3, \xi''_1, \dots$, so that intermediate ladders form *bubbles* inserted between $\tilde{\Pi}$ -kernels, see Fig. 1.7.5 below. To this end, we need to specify both the scales j'_i, j''_i, \dots and the angular sector indices $\alpha'_i, \alpha''_i, \dots, i = 2, 4$, of the *lower* momenta entering and exiting the $\tilde{\Pi}$ -kernels, see (1.33); the Bethe-Salpeter kernel is then obtained by summing over indices of all lower momenta. Next, we rewrite *lower* external propagators of, say, $\tilde{\Pi}(\xi'_1, \xi'_2; \xi'_3, \xi'_4)$

$$C^{j'_2, \alpha'_2}(\xi_4 - \xi'_2) C^{j'_4, \alpha'_4}(\xi'_4 - \xi''_2) \quad (1.109)$$

as convolutional squares,

$$\left(\int dy'_2 \sqrt{C^{j'_2, \alpha'_2}(\xi_4 - y'_2)} \sqrt{C^{j'_2, \alpha'_2}(y'_2 - \xi'_2)} \right) \left(\int dy'_4 \sqrt{C^{j'_4, \alpha'_4}(\xi'_4 - y'_4)} \sqrt{C^{j'_4, \alpha'_4}(y'_4 - \xi''_2)} \right). \quad (1.110)$$

Then we displace lower external legs ξ'_2, ξ'_4 to the corresponding upper locations ξ'_1, ξ'_3 , while taking into account the oscillations. The simplest **displacement procedure**, independent – contrary to the one used for renormalization in §2.2, see e.g. (2.55) – of a choice of angular sector momenta $p^{k, \alpha}$, is done in Fourier coordinates. Namely, fix the momenta $p'_1, p'_2 = -p'_1 + q, p'_3, p'_4 = -p'_3 - q$ of the upper external propagators $C^{j'_1, \alpha'_1}(p'_1), C^{j'_3, \alpha'_3}(p'_3)$, and of the lower external propagators,

$$\int dy'_4 e^{-i(p'_2, y'_4)} \sqrt{C^{j'_2, \alpha'_2}(y'_4 - \xi'_2)}, \int dy'_2 e^{i(p'_4, y'_2)} \sqrt{C^{j'_4, \alpha'_4}(\xi'_4 - y'_2)}. \quad (1.111)$$

We may restrict to $p'_i \in \mathcal{S}^{j_i, \alpha_i}, i = 1, \dots, 4$ (otherwise $C^{j'_i, \alpha'_i}(p'_i) = 0$ by construction, see Definition 2.1). Then we change integration variables in (1.111), $y'_4 \rightarrow y'_4 + (\xi'_1 - \xi'_2), y'_2 \rightarrow y'_2 + (\xi'_3 - \xi'_4)$, so that $\sqrt{C^{j'_2, \alpha'_2}(y'_4 - \xi'_2)} \rightarrow \sqrt{C^{j'_2, \alpha'_2}(y'_4 - \xi'_1)}, \sqrt{C^{j'_4, \alpha'_4}(\xi'_4 - y'_2)} \rightarrow \sqrt{C^{j'_4, \alpha'_4}(\xi'_3 - y'_2)}$ are now attached to the $\tilde{\Pi}$ -kernel at the locations of the *upper* vertices ξ'_1, ξ'_3 . Next, we *replace* the resulting extra oscillations $e^{i(p'_2, \xi'_2 - \xi'_1)}, e^{-i(p'_4, \xi'_4 - \xi'_3)}$ by 1, and rewrite $\int dy'_4 e^{-i(p'_2, y'_4)} \sqrt{C^{j'_2, \alpha'_2}(y'_4 - \xi'_1)}$, resp. $\int dy'_2 e^{i(p'_4, y'_2)} \sqrt{C^{j'_4, \alpha'_4}(\xi'_3 - y'_2)}$, as $e^{i(p'_2, \xi'_1)} \sqrt{C^{j'_2, \alpha'_2}(p'_2)}$, resp. $e^{-i(p'_4, \xi'_2)} \sqrt{C^{j'_4, \alpha'_4}(p'_4)}$. The remaining oscillations $e^{i(p'_2, \xi'_1)}, e^{-i(p'_4, \xi'_2)}$ may now be attached to the partially Fourier transformed kernel

$$\tilde{\Pi}_q^{disp}(p'_1, p'_3; \xi'_1, \xi'_3) := e^{i(-p'_1 + q, \xi'_1)} \Pi(\xi'_1, -p'_1 + q; \xi'_3, -p'_3 - q) e^{i(p'_3 + q, \xi'_3)}.$$

By momentum conservation, the above kernel depends only on $\xi'_1 - \xi'_3$, so its integral

$$\boxed{\tilde{\Pi}_q^{disp}(p'_1, p'_3) := \int d\xi'_3 e^{i(-p'_1 + q, \xi'_1)} \Pi(\xi'_1, -p'_1 + q; \xi'_3, -p'_3 - q) e^{i(p'_3 + q, \xi'_3)}} \quad (1.112)$$

is independent of ξ'_1 . We call it the **displaced kernel**. *Error terms* due to extra oscillations $e^{i(p'_2, \xi'_2 - \xi'_1)}$, $e^{-i(p'_4, \xi'_4 - \xi'_3)}$ involve quantities

$$\approx \delta\xi' \cdot \nabla_{\xi'}(e^{-i(p', \xi')} \sqrt{C^{j, \alpha'}}(\xi' - y')) \sim \delta\xi' \cdot (\nabla_{\xi'} - ip^{\alpha'}) \sqrt{C^{j, \alpha'}}(\xi' - y') \quad (1.113)$$

or conjugate, with $\delta\xi' = \xi'_1 - \xi'_2$, $y' = y'_2$, $\xi' = \xi'_2$, resp. $\delta\xi' = \xi'_3 - \xi'_4$, $y' = y'_4$, $\xi' = \xi'_4$. The derivative $\nabla_{\xi'} - ip^{\alpha'}$ acting on a sector covariance $C^{j, \alpha'}$ or a micro-sector covariance $C^{j, \alpha', k}$ generates (see (2.11), (2.12) or (2.15)) a small prefactor $2^{-j_{ext}}$ proportional to the diameter of the (micro-)sector, where $j_{ext} = j$ or (in the case of a micro-sector) 2^{-j+} , while the displacement distance $\delta\xi'$, associated with the decay factors of the two-particle irreducible diagram, produces a factor $\lesssim 2^{j_{int}}$, where j_{int} is the lowest internal scale of the diagram, all together an *extra small prefactor*

$$O(2^{-(j_{ext} - j_{int})}) \quad (1.114)$$

playing the rôle of a spring factor in section 3, see in particular 3.2 D.

Note that the \sqrt{C} -kernels are now attached to the *upper* external vertices of $\tilde{\Pi}$. Contracting them with their counterparts yields pairs of C -kernels connecting upper vertices,

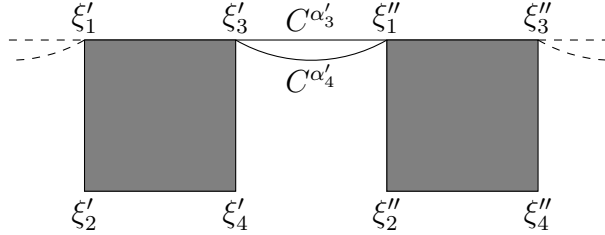


Fig. 1.7.5. Chains contributing to $\tilde{\Sigma}^{disp}$. Gray squares stand for $\tilde{\Pi}^{disp}$ -kernels.

This procedure leads to a kernel $\tilde{\Sigma}^{disp}$ made up of kernels $\tilde{\Pi}_q^{disp}(p_1, p_3) \equiv \tilde{\Pi}^{disp}(p_1, -p_1 + q; p_3, -p_3 - q)$, alternating with pairs of propagators $C_\theta^*(p'_3)C_\theta^*(q - p'_3)$, $C_\theta^*(p''_3)C_\theta^*(q - p''_3), \dots$, which may be arrayed into the Hermitian matrix

$$\mathcal{A}_q(p_3) := \begin{pmatrix} \mathcal{A}_q(\Upsilon_{3,diag}; p_3) & \mathcal{A}_q(\Upsilon_{3,off}; p_3) \\ \mathcal{A}_q^*(\Upsilon_{3,off}; p_3) & \mathcal{A}_q(\Upsilon_{3,diag}; p_3) \end{pmatrix}, \quad p_3 = p'_3, p''_3, \dots$$

Note that p_3 -momenta *cannot* be integrated over in $\mathcal{A}_q(p_3)$ since the $\tilde{\Pi}^{disp}$ -kernels also depend on them, *except* for the leading-order contribution to $\tilde{\Sigma}^{disp}$, which is proportional to the Hermitian bubble matrix $\mathcal{A}_q(\Upsilon_3)$ of eq. (1.77).

Definition 1.7 (Σ -kernel, preliminary version) *Let*

$$\begin{aligned}
\tilde{\Sigma}^{disp}(q) &:= \lambda \mathbb{1} + \lambda^2 \left\{ \mathcal{A}_q(\Upsilon_3) + \int dp'_1 \int dp'_3 \mathcal{A}_q(p'_1) \tilde{\Pi}_q^{disp}(p'_1, p'_3) \mathcal{A}_q(p'_3) \right. \\
&\quad \left. + \int dp'_1 \int dp'_3 \int dp''_1 \int dp''_3 \delta(p''_1 - p'_3) \mathcal{A}_q(p'_1) \left(\tilde{\Pi}_q^{disp}(p'_1, p'_3) \mathcal{A}_q(p''_1) \right) \left(\tilde{\Pi}_q^{disp}(p''_1, p''_3) \mathcal{A}_q(p''_3) \right) \right. \\
&\quad \left. + \cdots + \left\{ \prod_{i=1}^n \int dp_{i,1} \int dp_{i,3} \right\} \left(\prod_{i=1}^{n-1} \delta(p_{i,3} - p_{i+3,1}) \right) \mathcal{A}_q(p_{1,1}) \left\{ \prod_{i=1}^n \left(\tilde{\Pi}_q^{disp}(p_{i,1}, p_{i,3}) \mathcal{A}_q(p_{i,3}) \right) \right\} \right. \\
&\quad \left. + \cdots \right\}
\end{aligned} \tag{1.115}$$

As stated below (1.113), the above displacement procedure neglects error terms smaller by a prefactor $O(2^{-(j_{ext}-j_{int})})$ that goes to 0 with q . This requires however angular (micro-)sectors whose thickness in all directions is comparable to q ; this is explained in details in section 3.

The Fermi and s -wave projections. The above description of the $\tilde{\Sigma}^{disp}$ makes it plain that the two-particle irreducible contributions $\tilde{\Pi}_{disp}$ are not factorized from the bubbles, making the above expressions intractable and not ready for use in the gap equation. In order to obtain a factorization, while keeping the leading-order contribution when $q \rightarrow 0$, we take two further steps.

- (i) **(Fermi projection)** We replace external momenta $p'_1, p'_3, p''_1, p''_3, \dots$ by their orthogonal projection $p'_{1,F} = (0, \mathbf{p}'_{1,F}), p'_{3,F} = (0, \mathbf{p}'_{3,F}), p''_{1,F} = (0, \mathbf{p}''_{1,F}), p''_{3,F} = (0, \mathbf{p}''_{3,F}), \dots$ onto the Fermi circle Σ_F^* . This defines the Fermi projected kernel $\tilde{\Pi}^{proj}$,

$$\tilde{\Pi}_q^{proj}(p_1, p_3) := \tilde{\Pi}_q^{disp}(p_{1,F}, p_{3,F}). \tag{1.116}$$

As mentioned before, the correct procedure, described in section 3, is rather an averaging procedure in the neighborhood of the Fermi circle, but it does not matter at this stage.

- (ii) **(s -wave projection)** If $q = 0$, momenta $(\mathbf{p}_3, \mathbf{p}_4) = (\mathbf{p}_3, -\mathbf{p}_3)$ are obtained from $(\mathbf{p}_1, \mathbf{p}_2) = (\mathbf{p}_1, -\mathbf{p}_1)$ by a rotation of angle θ ; the kernel $\tilde{\Pi}_0^{proj}(p_1, p_3)$ depends only on $|\mathbf{p}_1|, |\mathbf{p}_3|$ and θ , not separately on the angular directions of \mathbf{p}_1 and \mathbf{p}_3 . (For $q \neq 0$ but close to 0, this is only approximately true.) Let $\theta'_1, \theta''_1 = \theta'_3, \theta''_3 = \theta''_3, \dots$ be the angles of $\mathbf{p}'_1, \mathbf{p}''_1 = \mathbf{p}'_3, \mathbf{p}''_3 = \mathbf{p}''_3, \dots$ w.r. to a fixed direction \mathbf{e}_1 , and $\theta := \theta'_1 - \theta''_1 = \theta'_1 - \theta'_3; \theta' := \theta''_1 - \theta''_3 = \theta''_1 - \theta''_3, \dots$ (The definition makes sense also for $q \neq 0$.) Assume first that $q = 0$. Bubble diagrams have by construction $\theta = 0$. Hence – taking a Fourier transform – the convolution of kernels turns into a geometric series which may be resummed for each individual Fourier mode $k \in \mathbb{Z}$, different Fourier modes being prevented from interacting by


orthogonality. From the arguments in the Introduction, it may be conjectured that only the mode $k = 0$ (or s -wave) diverges in the infra-red limit, which is itself a consequence that the interaction vertex itself is in the s -wave. Thus the kernel $\tilde{\Pi}_0^{proj}(p_{1,F}, p_{3,F})$ reduces in the end to the averaged 2×2 matrix $\bar{\Pi}_0 = \frac{1}{(\text{Vol}(\Sigma_F^*))^2} \int_{\Sigma_F^* \times \Sigma_F^*} dp_1 dp_3 \Pi_0(p_1, p_3)$. When $q \neq 0$, we introduce similarly the averaged 2×2 matrix

$$\bar{\Pi}(q) \equiv \bar{\Pi}_q := \frac{1}{(\text{Vol}(\Sigma_F^*))^2} \int_{\Sigma_F^* \times \Sigma_F^*} dp_1 dp_3 \tilde{\Pi}_q^{proj}(p_1, p_3). \quad (1.117)$$

Now, bubbles may be factorized, yielding

Definition 1.8 (Σ -kernel, or Goldstone boson propagator) *Let*

$$\Sigma(q) := \lambda \mathbb{1} + \lambda^2 \left\{ \mathcal{A}(q) + \mathcal{A}(q) \bar{\Pi}(q) \mathcal{A}(q) + \mathcal{A}(q) \bar{\Pi}(q) \mathcal{A}(q) \bar{\Pi}(q) \mathcal{A}(q) + \dots \right\}. \quad (1.118)$$

where $\mathcal{A}(q) = \mathcal{A}_q(\Upsilon_3)$ is the Hermitian bubble matrix of (1.77), which we represent for simplicity as a bubble  : graphically (compare to Fig. 1.7.5)

$$\Sigma(q) = \lambda \mathbb{1} + \lambda^2 \left\{ \text{bubble} + \text{bubble} \bar{\Pi} \text{bubble} + \dots \right\}(q)$$

Let us consider specifically the case of *zero transfer momentum* ($q = 0$). Then, replacing $\tilde{\Pi}_q^{disp}(p_1, p_3)$ by $\tilde{\Pi}_q^{proj}(p_1, p_3)$ in (1.115), the s -wave projection is exact, and defines

$$\Sigma(0) = \lambda \mathbb{1} + \lambda^2 \left\{ \mathcal{A}_0 + \mathcal{A}_0 \bar{\Pi}_0 \mathcal{A}_0 + \dots \right\} = \lambda \text{Id} + \frac{\lambda^2 \mathcal{A}_0}{\text{Id} - \bar{\Pi}_0 \mathcal{A}_0}, \quad (1.119)$$

where $\mathcal{A}_0 = \mathcal{A}_0(\Gamma, \Upsilon_3)$ and

$$\bar{\Pi}_0 = \bar{\Pi}_0(\Gamma) := \frac{1}{(\text{Vol}(\Sigma_F^*))^2} \int \int_{\Sigma_F^* \times \Sigma_F^*} dp_1 dp_3 \tilde{\Pi}_0^{disp}(p_1, p_3). \quad (1.120)$$

First-order terms are

$$\begin{aligned} & \lambda \mathbb{1} + \lambda^2 \left(\text{bubble} \right) + \lambda^3 \left(\text{two bubbles} \right) + \lambda^4 \left(\text{three bubbles} + \text{bubble with internal bubble} \right) \\ & + \lambda^5 \left(\text{four bubbles} + \text{bubble with two internal bubbles} + \text{bubble with one internal bubble and one vertex} + \text{bubble with two vertices} \right) \end{aligned}$$

where propagators are either diagonal or off-diagonal.

The one-point counterterm coefficient $\Gamma \in \mathbb{C}$ is chosen to be *the solution with largest module* of the

Definition 1.9 (gap equation)

$$\boxed{\left(-\mathbb{1} + \bar{\Pi}_0(\Gamma)\mathcal{A}_0(\Gamma)\right) \begin{pmatrix} \Gamma^\perp \\ (\Gamma^\perp)^* \end{pmatrix} = 0,} \quad (1.121)$$

i.e. $\begin{pmatrix} \Gamma^\perp \\ (\Gamma^\perp)^* \end{pmatrix}$ is a null eigenvector of the matrix $-\mathbb{1} + \bar{\Pi}_0\mathcal{A}_0$. Recall $\Gamma^\perp := \Gamma(\theta + \frac{\pi}{2})$. Graphically,

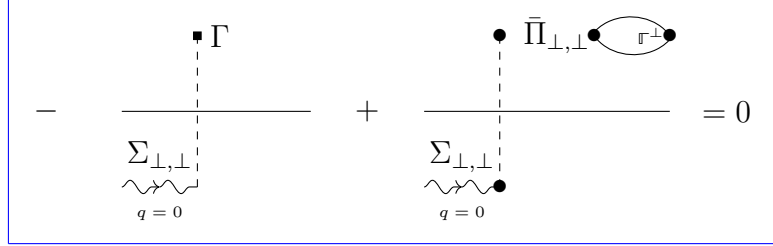


Fig. 1.7.6. Gap equation.

By the arguments below Fig. 1.7.3, the matrix $\bar{\Pi}_0\mathcal{A}_0$ is of the form $\begin{pmatrix} a & -b\omega \\ -b\omega^{-1} & a \end{pmatrix}$ with $\omega := e^{-2i\theta}$ if $\Gamma = |\Gamma|e^{i\theta}$. Hence the matrix $\bar{\Pi}_0\mathcal{A}_0$ can be made *real* by the conjugation

$$\bar{\Pi}_0\mathcal{A}_0 \mapsto \begin{pmatrix} e^{i\theta} & \\ & e^{i\theta} \end{pmatrix} \bar{\Pi}_0\mathcal{A}_0 \begin{pmatrix} e^{i\theta} & \\ & e^{-i\theta} \end{pmatrix}, \quad (1.122)$$

a condition which fixes $\theta \bmod \pi/2$. Then eigenvectors $\begin{pmatrix} |\Gamma|e^{i(\theta+\frac{\pi}{2})} \\ |\Gamma|e^{-i(\theta+\frac{\pi}{2})} \end{pmatrix}$, resp. $\begin{pmatrix} |\Gamma|e^{i\theta} \\ |\Gamma|e^{-i\theta} \end{pmatrix}$ are eigenvalues for two different values, $\Gamma_\phi^+ := \Gamma_\phi^+$ and Γ_ϕ^- , of $|\Gamma|$ obtained by solving the equations $a - 1 = \mp b$, or equivalently (conjugating as in (1.122) to reduce to the case $\theta = 0$)

$$f_\pm(g, \Gamma) := \frac{1}{g} \left\{ \left(\bar{\Pi}_0\mathcal{A}_0 - \mathbb{1} \right)_{diag} \mp \left(\bar{\Pi}_0\mathcal{A}_0 \right)_{off} \right\} \equiv 0 \quad (1.123)$$

for $\Gamma > 0$, yielding *two* solutions, Γ_ϕ^\pm . Using previous computations, see (1.56), (1.53), one obtains leading-order terms as functions of the non-dimensional variables $g, \tilde{\Gamma} := \frac{\Gamma}{\hbar\omega_D}$:

$$\begin{aligned} \mathcal{A}_0(\Gamma) &= \mathcal{A}_0(\Gamma; \Upsilon_3) - \mathcal{A}_0(\Gamma; \Upsilon_{3,off})\sigma(\theta) \\ &= \frac{m^*}{\pi} \left(-\log \tilde{\Gamma} + c_0 + O(\tilde{\Gamma}) \right) \mathbb{1} + mb_2(\tilde{\Gamma})\sigma(\theta) \end{aligned} \quad (1.124)$$

with

$$b_2(\tilde{\Gamma}) := -\frac{1}{m}\mathcal{A}_0(\Gamma; \Upsilon_{3,off}) = b_2 + O(\tilde{\Gamma}) = O(1) \quad (b_2 > 0); \quad (1.125)$$

$$\bar{\Pi}_{diag}(0) = \frac{g}{m}(1 + a_2(\tilde{\Gamma})g + O(g^2)) \mathbb{1}, \quad \bar{\Pi}_{off}(0) = \frac{g^2}{m}O(\tilde{\Gamma}), \quad (1.126)$$

see Lemma 1.6, with $a_2(\tilde{\Gamma}) := \tilde{\mathcal{A}}_0(\Gamma; \tilde{\Upsilon}_1) = a_2 + O(\tilde{\Gamma})$. The coefficients c_0, b_2, a_2 that we introduced – and the coefficients that we introduce below – are $O(1)$. Finally, $m^* = m(1 + m_1(\tilde{\Gamma})g^2 + O(g^3))$. The dependence on $\tilde{\Gamma}$ of a_2, b_2 and m_1 is secondary since $\tilde{\Gamma} = O(e^{-\pi/g})$ vanishes to all orders at $g = 0$, implying in particular that $\bar{\Pi}_0$ is essentially *diagonal*. The change of variable $\tilde{\Gamma} \mapsto \gamma := \tilde{\Gamma}e^{\pi/g}$ allows one to rewrite the function $(\mathcal{A}_0)_{diag}$ as

$$(\mathcal{A}_0)_{diag}(\gamma) = \frac{m^*}{\pi} \left(\frac{\pi}{g} - \log \gamma + c_0 + O(\tilde{\Gamma}) \right) \mathbb{1}, \quad (1.127)$$

whence

$$\begin{aligned} \left(\bar{\Pi}_0 \mathcal{A}_0 - \mathbb{1} \right)_{diag} &= \left(\frac{m^*}{m} \left\{ \left(1 - \frac{g}{\pi} \log \gamma + \frac{g}{\pi} c_0 + O(\tilde{\Gamma}) \right) (1 + a_2 g + O(g^2)) \right\} - 1 \right) \mathbb{1} \\ &= \left(g \left(-\frac{1}{\pi} \log \gamma + m_1 + a_2 + \frac{c_0}{\pi} \right) + O(g^2) \right) \mathbb{1} \end{aligned} \quad (1.128)$$

$$- \left(\bar{\Pi}_0 \mathcal{A}_0 \right)_{off} = \left(b_2 g + O(g^2) \right) \sigma(\theta) \sim b_2 g \sigma(\theta) \quad (1.129)$$

with $b_2 > 0$ provided g is small enough. Thus, by the implicit function theorem,

$$\boxed{\Gamma_\phi^\pm \sim_{g \rightarrow 0} \hbar \omega_D e^{-\pi/g} e^{\pi(m_1 + a_2 + \frac{c_0}{\pi}) + O(g) \pm \delta}} \quad (1.130)$$

with

$$\delta := \pi b_2 + O(g). \quad (1.131)$$

In particular,

$$\boxed{(\mathcal{A}_0)_{diag} = \frac{1}{\lambda} + O(m^*)}. \quad (1.132)$$

We note for further use that, *choosing* $|\Gamma| = \Gamma_\phi^+$, one gets modulo the conjugation (1.122), or for $\theta = 0$,

$$\mathbb{1} - \bar{\Pi}_0 \mathcal{A}_0 = \begin{pmatrix} gb & gb \\ gb & gb \end{pmatrix} \quad (1.133)$$

with $b \sim \pi b_2$, implying a null eigenvector proportional to $\begin{pmatrix} -i \\ i \end{pmatrix}$.

Thus the net effect of diagrams other than the Cooper pair bubble Υ_3 is to change by a finite amount the pre-factor in front of Γ_ϕ and produce a finite multiplicative splitting $e^{\pm\delta}$ between two solutions.

Estimates for $\Sigma(q)$ near $q = 0$. We first need a Taylor expansion of $\mathbb{1} - \Pi(q)\mathcal{A}(q)$ near $q = 0$. Lemma 1.3 and power-counting estimates for $\Pi(q)$ imply that

$$\left(\mathbb{1} - \Pi_{diag}(q)\mathcal{A}_q(\Gamma_\phi^+; \Upsilon_{3,i})\right) = \left(\mathbb{1} - \Pi_{diag}(0)\mathcal{A}_0(\Gamma_\phi^+; \Upsilon_{3,i})\right) + \lambda Q_i(q) + O(|q|_+^4), \quad (1.134)$$

$i=\text{diag,off}$, where $\begin{pmatrix} Q_{diag} \\ Q_{off} \end{pmatrix}$ is a couple of positive-definite quadratic forms, $Q_{diag}(q) = \frac{1}{g_{\phi,diag}}(q^0)^2 + \frac{v_{\phi,i}^2}{g_{\phi,diag}}|\mathbf{q}|^2$, $Q_{off}(q) = -\left(\frac{1}{g_{\phi,off}}(q^0)^2 + \frac{v_{\phi,off}^2}{g_{\phi,off}}|\mathbf{q}|^2\right)$, see Lemma 1.3, with

$$g_{\phi,i} = g_{\phi,i}^0(1 + O(g)), v_{\phi,i} = v_{\phi,i}^0(1 + O(g)). \quad (1.135)$$

Remaining terms involving $\Pi_{off}(q)$ have an extra $1/N_{j_\phi} = 2^{-j_\phi}$ prefactor. Using (1.133), one gets for $\theta = 0$

$$\det(\mathbb{1} - \Pi(q)\mathcal{A}(q)) =: \det M(q) \sim 2b \frac{g^2}{m} Q(q) \quad (1.136)$$

where

$$M(q) := \begin{pmatrix} g\left(b + \frac{1}{m}Q_{diag}(q) + O(|q|_+^4)\right) & g\left(b + \frac{1}{m}Q_{off}(q) + O(|q|_+^4)\right) \\ g\left(b + \frac{1}{m}Q_{off}(q) + O(|q|_+^4)\right) & g\left(b + \frac{1}{m}Q_{diag}(q) + O(|q|_+^4)\right) \end{pmatrix} \quad (1.137)$$

and $Q(q) := Q_{diag}(q) - Q_{off}(q) = \frac{|q|_\pm^2}{g_\phi}$ by Definition 1.4. At this point it is natural to shift to the $(//, \perp)$ -basis (compare with §1.5), in which $M(q) = \text{diag}(M_{//, //}(q), M_{\perp, \perp}(q))$, with

$$M_{//, //}(q) = \sum_{i,i'=1,2} M_{i,i'}(q) \sim_{|q|_+ \rightarrow 0} 4gb, \quad (1.138)$$

$$M_{\perp, \perp}(q) = \left(\sum_{i=i'} - \sum_{i \neq i'}\right) M_{i,i'}(q) \sim_{|q|_+ \rightarrow 0} 2 \frac{g}{m} Q(q) = 2 \frac{g}{m} \frac{|q|_\pm^2}{g_\phi}. \quad (1.139)$$

Multiplying by $\lambda^2(\mathcal{A}_0)_{//, //}$, $\lambda^2(\mathcal{A}_0)_{\perp, \perp} \sim \lambda$ yields (see (1.118), (1.124), (1.132))

$$\Sigma_{//, //}(q) \approx \frac{1}{m^*} \quad (1.140)$$

and

$$\boxed{\Sigma_{\perp, \perp}(q) \sim \frac{1}{2} \frac{g_\phi}{|q|_+^2}}. \quad (1.141)$$

Connection to pre-kernel. Far enough from $q = 0$, it is possible to expand further the denominator: letting $R(q) := \Pi(q) - \lambda = O(\lambda^2 m)$, and representing by \sim the pre-kernel $\frac{\lambda}{1 - \lambda \mathcal{A}(q)}$ as in the previous subsection, we can write down the geometric series

$$\frac{\lambda}{1-\Pi(q)\mathcal{A}(q)} = \text{~~~~~} + \text{~~~~~} \frac{1}{\lambda}\mathcal{A}(q)R(q) \text{~~~~~} + \dots$$

However, the above expansion is faulty for $|q|_+ \lesssim \Gamma_\phi$ (i.e. in our Regime **B.**), since there (replacing ~~~~~ by the kernel $\Sigma_{\perp,\perp}$, of which it is assumed to be an approximation)

$$\Sigma_{\perp,\perp}(q) \cdot \frac{1}{\lambda}\mathcal{A}(q)R(q) \approx \frac{g_\phi}{|q|_+^2} \cdot m \approx \left(\frac{\Gamma_\phi}{|q|_+}\right)^2 \gg 1.$$

2 Fermionic theory

The section is organized as follows. Recall $j'_\phi = j_\phi + O(\ln(1/g))$. We concentrate exclusively on momenta with scales $\leq j'_\phi$.

First (§2.1), we refine the multi-scale analysis of §1.3 by decomposing scale propagators according to *angular sectors* (see Definitions 2.1 and 2.2).

Then (§2.2), we introduce a *dressed action* $\mathcal{L}(\mathbf{t})$, see Definition 2.6, which is the basis of all subsequent computations. This action is dressed by scale dependent \mathbf{t} -parameters which enact the scale decoupling necessary to separate local parts of two-point functions and renormalize. We take the opportunity to give qualitative statements about the renormalization flow of parameters.

With $\mathcal{L}(\mathbf{t})$ at hand, it is possible to present the general cluster expansion scheme (§2.3), involving scale-by-scale *horizontal expansions*, a *bubble resummation*, a vertical *momentum-decoupling expansion*, the *separation of local parts* of divergent diagrams, and a *Mayer expansion*. On the way, we present a preliminary, single-scale version of the bounds for polymers.

Finally, *general bounds for multi-scale fermionic polymers*, based on the preliminary bounds proved in §2.3, and confirming at the same time the predictions of §2.2 about the renormalization flow, are proved in §2.4.

2.1 Angular decompositions

We continue here the analysis of §1.3 by decomposing the j -th momentum shell into 2^j spatial sectors of aperture angle $\approx 2\pi/N_j$, where

$$N_j := 2^j. \tag{2.1}$$

Technically, one uses a smooth partition of unity

$$1 = \sum_{\alpha \in \mathbb{Z}/2^j\mathbb{Z}} \eta^{j,\alpha} \left(\frac{\mathbf{p}}{|\mathbf{p}|} p_F^* \right) \tag{2.2}$$

where the support of $\eta^{j,\alpha}$ intersects the Fermi circle Σ_F^* roughly on the circular arc $\{(p_F^* \cos \theta, p_F^* \sin \theta) \mid 2\pi\alpha 2^{-j} < \theta < 2\pi(\alpha + 1)2^{-j}\}$, in such a way that the distance $\text{dist}(\text{supp}(\eta^{j,\alpha}) \cap \Sigma_F^*, \text{supp}(\eta^{j,\alpha'}) \cap \Sigma_F^*) \approx 2^{-j}|\alpha - \alpha'|$, with $|\alpha - \alpha'| := \min_{k \in \mathbb{Z}} |\alpha - \alpha' + k|$

$\alpha' + 2k\pi$. For definiteness, we choose $\eta^{j,\alpha}$ (defined below, see Definition 2.2) in such a way that $\text{supp}(\chi^{j,\alpha}) \subset \mathcal{S}^{j,\alpha}$, where

Definition 2.1 (angular sectors) (i)

$$\mathcal{S}^j := \left\{ p = (p^0, \mathbf{p}) \mid \frac{1}{2} 2^{-j} \mu < \max(|p^0|, |e(\mathbf{p})|) < \frac{3}{2} 2^{-j} \mu \right\}, \quad j < j'_\phi \quad (2.3)$$

$$\mathcal{S}^{j'_\phi} := \left\{ p = (p^0, \mathbf{p}) \mid \max(|p^0|, |e(\mathbf{p})|) < \frac{3}{2} 2^{-j'_\phi} \mu \right\}; \quad (2.4)$$

$$\mathcal{S}^{j,\alpha} := \left\{ p = (p^0, \mathbf{p}) \in \mathcal{S}^j \mid 2\pi(\alpha-1)2^{-j} < \theta(\mathbf{p}) < 2\pi(\alpha+1)2^{-j} \right\}, \quad \alpha \in \mathbb{Z}/2^j\mathbb{Z}, \quad (2.5)$$

where $(|\mathbf{p}|, \theta(\mathbf{p})) \in \mathbb{R}_+ \times \mathbb{R}/2\pi\mathbb{Z}$ are the polar coordinates of \mathbf{p} , namely, $\frac{\mathbf{p}}{|\mathbf{p}|} = \begin{pmatrix} \cos \theta(\mathbf{p}) \\ \sin \theta(\mathbf{p}) \end{pmatrix}$.

(ii) $\mathcal{S}^j := \{\mathbf{p} \in \mathbb{R}^2 \mid \exists p^0 \in \mathbb{R}, (p^0, \mathbf{p}) \in \mathcal{S}^j\}$ and $\mathcal{S}^{j,\alpha} := \{\mathbf{p} \in \mathbb{R}^2 \mid \exists p^0 \in \mathbb{R}, (p^0, \mathbf{p}) \in \mathcal{S}^{j,\alpha}\}$ are the spatial projections of $\mathcal{S}^j, \mathcal{S}^{j,\alpha}$.

The number N_j of angular sectors is chosen in such a way that sectors are essentially isotropic: they are small deformations of 3-dimensional cubes of side scaling like $O(2^{-j})$. Note that the momentum scale and angular sector of a given spatial momentum \mathbf{p} is defined up to $O(1)$, namely, if $\mathbf{p} \in \mathbb{R}^3$, $2^{-j'_\phi} \mu \lesssim \frac{p_F^*}{m^*} |p_\perp| \lesssim 2^{-j_D} \mu$, then $(\mathbf{p} \in \mathcal{S}^{j,\alpha} \cap \mathcal{S}^{j',\alpha'}) \Rightarrow (|j - j'| = O(1), |\alpha - \alpha'| = O(1))$.

Remark. As discussed in ([25], Lemma 3) in details, see also Proposition 2.5 below, this choice of isotropic sectors is not optimal, and produces spurious (but not really disturbing) $\log N_j \approx j$ prefactors when resumming over angular sectors. However, the choice of curvelet-like anisotropic sectors (see e.g. [10, 11, 69]) with angular width $\approx 2^{-j/2}$ instead of 2^{-j} – taking into account the *curvature* of the Fermi circle – would have led to a tedious wavelet-like phase-space analysis which we want to spare to the reader.

Definition 2.2 Let

$$\chi^{j,\alpha}(p/\mu) := \chi^j(|p|/\mu) \eta^{j,\alpha}\left(\frac{\mathbf{p}}{|\mathbf{p}|} p_F^*\right), \quad j_D \leq j \leq j'_\phi - 1, \quad \alpha \in \mathbb{Z}/2^j\mathbb{Z}, \quad (2.6)$$

$$\chi^{\rightarrow j'_\phi, \alpha}(p/\mu) := \chi^{\rightarrow j'_\phi}(|p|/\mu) \eta^{j'_\phi, \alpha}\left(\frac{\mathbf{p}}{|\mathbf{p}|} p_F^*\right), \quad \alpha \in \mathbb{Z}/2^{j'_\phi}\mathbb{Z}. \quad (2.7)$$

Let us rewrite (1.33), (1.34) for the sake of the reader,

$$\boxed{C_\theta^{j,\alpha}(\xi, \xi') := \int \frac{d^3 p}{(2\pi)^3} \frac{e^{i(p, \xi - \xi')}}{ip^0 - e^*(\mathbf{p})\sigma^3 - \Gamma(\theta)} \chi^{j,\alpha}\left(\frac{p}{\mu}\right), \quad j < j'_\phi} \quad (2.8)$$

$$\boxed{C_\theta^{j'_\phi, \alpha}(\xi, \xi') := \int \frac{d^3 p}{(2\pi)^3} \frac{e^{i(p, \xi - \xi')}}{ip^0 - e^*(\mathbf{p})\sigma^3 - \Gamma(\theta)} \chi^{\rightarrow j'_\phi, \alpha}\left(\frac{p}{\mu}\right)} \quad (2.9)$$

For every (j, α) , one chooses a vector $\mathbf{p}^{j,\alpha} \in \Sigma_F$ lying inside the support of $\eta^{j,\alpha}$, and lets $p^{j,\alpha} = (0, \mathbf{p}^{j,\alpha})$. As explained in §1.3, see discussion in the paragraph between (1.27) and (1.29), all fermions of scale $j_\phi \leq j \leq j'_\phi$ may actually be considered as (non-optimal) decompositions of scale j_ϕ fermions.

Remark. In section 3, we shall need to further decompose scale j'_ϕ sectors $\mathcal{S}^{j'_\phi,\alpha}$, $\alpha \in \mathbb{Z}/2^{j'_\phi}\mathbb{Z}$, into smaller angular sectors of angle aperture $\approx 2\pi/2^{j_+}$, with $j_+ \geq j'_\phi$; we write

$$\chi^{\rightarrow j'_\phi,\alpha}(p/\mu) := \chi^{\rightarrow j'_\phi}(|p|/\mu) \eta^{j_+,\alpha}\left(\frac{\mathbf{p}}{|\mathbf{p}|} p_F^*\right), \quad \alpha \in \mathbb{Z}/2^{j_+}\mathbb{Z}, \quad j_+ \geq j'_\phi \quad (2.10)$$

and define accordingly angular sectors $\mathcal{S}^{j'_\phi,\alpha}$ ($\alpha \in \mathbb{Z}/2^{j_+}\mathbb{Z}$) roughly equal to the support of the cut-off functions $\chi^{\rightarrow j'_\phi,\alpha}(\cdot/\mu)$, and covariance kernels $C^{j'_\phi,\alpha}$, $\alpha \in \mathbb{Z}/2^{j_+}\mathbb{Z}$ as in (2.9). Note that such angular sectors are strongly *anisotropic* if $j_+ \gg j'_\phi$. If necessary, they may be further "chopped" into isotropic "microsectors" $\mathcal{S}^{j'_\phi,\alpha,k}$, $k = 1, 2, \dots, 2^{j_+ - j'_\phi}$ with size $\approx 2^{-j_+}\mu$ in the direction transverse to the Fermi circle. We then let $p^{j'_\phi,\alpha,k} = (0, \mathbf{p}^{j'_\phi,\alpha,k})$ be some momentum lying inside $\mathcal{S}^{j'_\phi,\alpha,k}$, and define covariance kernels $C^{j'_\phi,\alpha,k}$ with characteristic functions $\chi^{\rightarrow j'_\phi,\alpha,k}(\frac{|p|}{\mu})\eta^{j_+,\alpha}\left(\frac{\mathbf{p}}{|\mathbf{p}|} p_F^*\right)$ instead of $\chi^{\rightarrow j'_\phi}(\frac{|p|}{\mu})\eta^{j'_\phi,\alpha}\left(\frac{\mathbf{p}}{|\mathbf{p}|} p_F^*\right)$.

Proposition 2.3 *For every $n > 0$, there exists a constant C_n such that, for every scale $j_D \leq j \leq j'_\phi$, sector $\alpha \in \mathbb{Z}/2^j\mathbb{Z}$ and multi-index $\kappa \geq 0$,*

(i) *if $j \leq j_\phi$,*

$$|(\nabla_\xi - ip^{j,\alpha})^\kappa C_\theta^{j,\alpha}(\xi, \bar{\xi})| \leq C_n 2^{-2j} (2^{-j}\mu)^{\kappa_0} (2^{-j}p_F^*)^{\kappa_1 + \kappa_2} \left(1 + 2^{-j}\mu|\xi - \bar{\xi}|\right)^{-n} (p_F^*)^2; \quad (2.11)$$

(ii) *if $j > j_\phi$,*

$$|(\nabla_\xi - ip^{j,\alpha})^\kappa C_\theta^{j,\alpha}(\xi, \bar{\xi})| \leq C_n 2^{-2j} 2^{-(j-j_\phi)} (2^{-j}\mu)^{\kappa_0} (2^{-j}p_F^*)^{\kappa_1 + \kappa_2} \left(1 + 2^{-j}\mu|\xi - \bar{\xi}|\right)^{-n} (p_F^*)^2. \quad (2.12)$$

Eq. (2.11) is proved in ([25], Lemma 4). If $j \leq j_\phi$ and $\kappa = 0$, then the factor 2^{-2j} is equal to the scaling factor 2^j of $\frac{1}{ip^0 - e_{|\Gamma|}^*(\mathbf{p})\sigma^3 - \Gamma(\theta)}$, times the scaling of the volume of the sector, $2^{-j} \times 2^{-j} \times 2^{-j} = 2^{-3j}$. The supplementary prefactor $(2^{-j}\mu)^{\kappa_0} (2^{-j}p_F^*)^{\kappa_1 + \kappa_2}$ comes from the Fourier multiplier $i(p - p^{j,\alpha})$ associated to the operator $\nabla_\xi - ip^{j,\alpha}$, since $|p - p^{j,\alpha}|$ is bounded over the support of $\chi^{j,\alpha}$ by the diameter of the sector, which is proportional to 2^{-j} . Assume then that $j > j_\phi$, so that $e_{|\Gamma|}^*(\mathbf{p}) \approx \Gamma_\phi$, $\left|\frac{1}{ip^0 - e_{|\Gamma|}^*(\mathbf{p})\sigma^3 - \Gamma(\theta)}\right| \lesssim \Gamma_\phi^{-1} \approx (2^{-j_\phi}\mu)^{-1}$. Hence $|\tilde{C}_\theta^{j,\alpha}(\xi, \bar{\xi})| \lesssim (2^{-j_\phi}\mu)^{-1} \text{Vol}(\mathcal{S}^{j,\alpha}) \approx (2^{-j_\phi}\mu)^{-1} (2^{-j}\mu) (2^{-j}p_F^*)^2$. The summable spring factor $j \mapsto 2^{-(j-j_\phi)}$ shows clearly that this further decomposition would be useless for the free theory. The decay rate is only $2^{-j}\mu$ instead of the

expected fermion mass $2^{-j_\phi}\mu$ because of the scale j cut-offs, which are thus clearly not optimal.

In other words: the average magnitude of $\psi^{j,\alpha}(\xi)$ – defined as the *square-root* of $C_\theta^{j,\alpha}(\xi, \bar{\xi})$ for nearby $\xi, \bar{\xi}$ – is

$$\boxed{\psi^{j,\alpha}(\xi) \sim 2^{-j}p_F^* \quad (j \leq j_\phi), \quad 2^{-(j-j_\phi)/2}2^{-j}p_F^* \quad (j > j_\phi)} \quad (2.13)$$

A similar computation – with a supplementary $O(2^j)$ relative factor coming from integration in Fourier coordinates – holds for the sector-symmetric covariance kernel $C_\theta^j(\xi, \bar{\xi})$, yielding

$$\psi^j(\xi) \sim 2^{-j/2}p_F^* \quad (j \leq j_\phi), \quad 2^{-(j-j_\phi)/2}2^{-j/2}p_F^* \quad (j > j_\phi) \quad (2.14)$$

Remark. The above Proposition generalizes to microsector covariances (see previous Remark),

$$|(\nabla_\xi - ip^{j'_\phi, \alpha, k})^\kappa C_\theta^{j'_\phi, \alpha, k}(\xi, \bar{\xi})| \leq C_n 2^{-2j_+} 2^{-(j_+ - j_\phi)} (2^{-j_+} \mu)^{\kappa_0} (2^{-j_+} p_F^*)^{\kappa_1 + \kappa_2} \left(1 + 2^{-j_+} \mu |\xi - \bar{\xi}|\right)^{-n} (p_F^*)^2 \quad (2.15)$$

if $\alpha \in \mathbb{Z}/2^{j_+}\mathbb{Z}$ ($j_+ \geq j'_\phi$) and $k = 1, 2, \dots, 2^{j_+ - j'_\phi}$. Namely, compared to (2.12), the volume of the microsector scales now like $2^{-j_+} \times 2^{-j_+} \times 2^{-j_+} = 2^{-3j_+}$, and its size along any direction like 2^{-j_+} .

Boxes. For every $j = j_D, \dots, j'_\phi$, we decompose \mathbb{R}^3 into a disjoint union of *scale j boxes* defined as follows.

Definition 2.4 (boxes) A scale j box is a "cube" $\Delta := (k_0 2^j \mu^{-1}, (k_0 + 1) 2^j \mu^{-1}) \times (k_1 2^j (p_F^*)^{-1}, (k_1 + 1) 2^j (p_F^*)^{-1}) \times (k_2 2^j (p_F^*)^{-1}, (k_2 + 1) 2^j (p_F^*)^{-1})$, $k_0, k_1, k_2 \in \mathbb{Z}$. We denote by \mathbb{D}^j the set of scale j boxes, so that (up to a subset of measure zero) \mathbb{D}^j defines a partition of \mathbb{R}^3 . Let finally $\mathbb{D} := \uplus_{j=j_D, \dots, j'_\phi} \mathbb{D}^j$.

In order not to spoil completely momentum preservation at vertices, we further introduce for each $j = j_D, \dots, j'_\phi$ a smoothed partition of unity, $1 = \sum_{\Delta \in \mathbb{D}^j} \chi_\Delta(\xi)$, where each χ_Δ is a smooth, compactly supported function and :

- (scaling property) $\chi_{2^k \Delta^{j_D}}(2^k \xi) = \chi_{\Delta^{j_D}}(\xi)$ if $\Delta^{j_D} \in \mathbb{D}^{j_D}$, $k \geq 0$;
- (translation invariance) if $\mathbf{v} = 2^j \begin{pmatrix} i_0 \mu^{-1} \\ i_1 (p_F^*)^{-1} \\ i_2 (p_F^*)^{-1} \end{pmatrix}$ is a scaled integer translation, then $\chi_{\Delta + \mathbf{v}}(\xi) = \chi_\Delta(\xi - \mathbf{v})$;
- (support) $\chi_\Delta(\xi) \equiv 0$ except if ξ belongs to Δ or its (direct or diagonal) neighbors;
- $\chi_\Delta \equiv 1$ in some neighbourhood of the center ξ_Δ of Δ .

Then (by the scaling and translation invariance properties), for every multi-index $\kappa = (\kappa_0, \boldsymbol{\kappa})$,

$$|\nabla^\kappa \chi_\Delta(\xi)| \leq C_{|\kappa|} (2^{-j} \mu)^{\kappa_0} (2^{-j} p_F^*)^{\kappa_1 + \kappa_2}, \quad \Delta \in \mathbb{D}^j. \quad (2.16)$$

The volume of a scale j box Δ^j is roughly inverse to that of a sector,

$$\text{Vol}(\Delta^j) \approx \text{Vol}(\text{supp}(\chi^{j,\alpha}))^{-1} \approx (2^j \mu^{-1}) (2^j (p_F^*)^{-1})^2 \approx \frac{1}{m^* \mu^2} (2^j)^3. \quad (2.17)$$

The bound (2.16) implies a bound for the Fourier transform with a quasi-exponential decay,

$$|\hat{\chi}_{\Delta^j}(q)| \leq C_n \text{Vol}(\Delta^j) \left(1 + |q|_+ / 2^{-j} \mu\right)^n \quad (2.18)$$

for every $n \geq 0$.

Sector counting. A characteristic feature of dimension 2 is that (*generically*, as we shall see) four spatial momenta $\mathbf{p}_1, \dots, \mathbf{p}_4$ in the immediate neighborhood of the Fermi circle and such that $\mathbf{p}_1 + \mathbf{p}_2 = \mathbf{p}_3 + \mathbf{p}_4 = 0$ are essentially two-by-two equal, namely, $\mathbf{p}_1 \simeq \mathbf{p}_3, \mathbf{p}_2 \simeq \mathbf{p}_4$ or $\mathbf{p}_1 \simeq \mathbf{p}_4, \mathbf{p}_2 \simeq \mathbf{p}_3$, by which we mean (letting $\alpha_i + O(1)$ be the angular sector of \mathbf{p}_i , $i = 1, \dots, 4$) that, to leading order,

$$\left(\alpha_1 = \alpha_3 + O(1), \alpha_2 = \alpha_4 + O(1)\right) \quad \text{or} \quad \left(\alpha_1 = \alpha_4 + O(1), \alpha_2 = \alpha_3 + O(1)\right) \quad (2.19)$$

as illustrated by the following picture

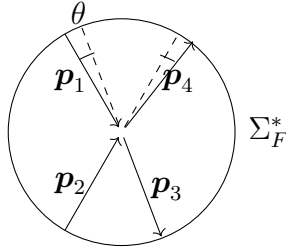


Fig. 2.1.1. Close to the Fermi circle, there are only two free sectors per vertex in dimension 2.

Thus, splitting each of the four fields of a vertex $\int d\xi (\bar{\psi}_\uparrow \bar{\psi}_\downarrow)(\xi) (\psi_\downarrow \psi_\uparrow)(\xi)$ into its (j, α) -components leads for "quasi-scale-diagonal" terms in a near-Cooper pairing,

$$\int d\xi \int d\xi' (\bar{\psi}_\uparrow^{j_1, \alpha_1} \bar{\psi}_\downarrow^{j_3, \alpha_3})(\xi) \delta(\xi - \xi') (\psi_\downarrow^{j_2, \alpha_2} \psi_\uparrow^{j_4, \alpha_4})(\xi') \quad (2.20)$$

with $j_1 \simeq j_2 \simeq j_3 \simeq j_4$, to essentially only *two sums* over angular sectors. More precisely:

Proposition 2.5 (*see [25], Lemma 3*).

(i) Let $\mathcal{S}^{j_i, \alpha_i}$, $i = 1, \dots, 4$ be the spatial projection of four angular sectors of scales $j_1, j_2, j_3, j_4 = j + O(1)$ and $A \geq 1$. Then the set

$$\Omega_4 := \{(\mathbf{p}_1, \dots, \mathbf{p}_4) \in \Sigma^{j_1, \alpha_1} \times \dots \times \Sigma^{j_4, \alpha_4} \mid |\mathbf{p}_1 - \mathbf{p}_3| < |\mathbf{p}_1 + \mathbf{p}_2|, \\ |\mathbf{p}_1 + \mathbf{p}_2 - \mathbf{p}_3 - \mathbf{p}_4| \leq A2^{-j} p_F^*\} \quad (2.21)$$

is empty unless there exists $k \in \{\lfloor \frac{j}{2} \rfloor, \dots, j\}$ such that

$$|\alpha_1 - \alpha_3|, |\alpha_2 - \alpha_4| \lesssim A2^{j-k} \lesssim |\alpha_1 + \alpha_2| \leq CA2^k. \quad (2.22)$$

(ii) (generalization) Let $\mathcal{S}^{j_i, \alpha_i}$, $i = 1, \dots, 2n$ ($2n \geq 6$) be the spatial projection of $2n$ angular sectors of scales $j_1, j_2, \dots, j_{2n} = j + O(1)$. Then the set $\Omega_{2n} := \{(\mathbf{p}_1, \dots, \mathbf{p}_{2n}) \in \Sigma^{j_1, \alpha_1} \times \dots \times \Sigma^{j_{2n}, \alpha_{2n}} \mid |\sum_{i=1}^n \mathbf{p}_i - \sum_{i=n+1}^{2n} \mathbf{p}_i| \leq A2^{-j} p_F^*\}$ has cardinal $O(A^2 2^{(2n-2)j})$.

Sketch of proof for (i) (case of a vertex). The condition $|\mathbf{p}_1 - \mathbf{p}_3| < |\mathbf{p}_1 + \mathbf{p}_2|$ ensures that the aperture angle $\theta := \widehat{(\mathbf{p}_1, \mathbf{p}_3)}$ is smaller than the relative pair angle $\alpha := \widehat{(\mathbf{p}_1, -\mathbf{p}_2)}$. Since $|\mathbf{p}_2 - \mathbf{p}_4| \simeq |\mathbf{p}_1 - \mathbf{p}_3| \approx p_F^* |\sin(\frac{\theta}{2})|$, we deduce that $|\alpha_1 - \alpha_3| \approx |\alpha_2 - \alpha_4| \lesssim |\alpha_1 + \alpha_2| \approx |\alpha_1 + \alpha_4|$. In other words, α_3 is the sector closest to α_1 , and the pair $(\mathbf{p}_2, \mathbf{p}_4)$ is essentially obtained from $(\mathbf{p}_1, \mathbf{p}_3)$ through a rotation of angle α . (Permuting α_3 with α_4 or $-\alpha_2$ yields two equivalent possibilities). Using the approximate equality, $\mathbf{p}_1 + \mathbf{p}_2 \simeq \mathbf{p}_3 + \mathbf{p}_4$, and projecting $\mathbf{p}_2 - \mathbf{p}_4$ onto the axis perpendicular to $\mathbf{p}_1 - \mathbf{p}_3$ yields $|2 \sin(\alpha) \sin(\frac{\theta}{2})| \lesssim A2^{-j}$, whence $|\alpha| |\theta| \lesssim A2^{-j}$. \square

The most important case is $2n = 4$, for the above Proposition gives then the sector counting factor of a vertex: accepting an error $O(A2^{-j} p_F^*)$ on the momentum preservation condition, one has $O(j2^{2j} A^2)$ possibilities for the choices of the sector indices $\alpha_1, \dots, \alpha_4$; namely, for fixed $k = j + \lfloor \log_2 |\alpha_1 - \alpha_3|^{-1} \rfloor$, there are $\approx 2^{j-k}$ choices for α_3 , $\lesssim A2^k$ possibilities for α_2 , and finally, $\lesssim A$ possibilities for α_4 given α_2, α_3 . Summing over $k \in \{\lfloor \frac{j}{2} \rfloor, \dots, j\}$ yields the result. We call **generic** a vertex for which the relative pair angle $\alpha \approx 1$ is large, which implies that the aperture angle θ is small, of order $O(2^{-j})$; diagrams with only generic vertices have the following very important property: *vertices may be cut into two parts in such a way that the transfer momentum between the half-vertices is very small.* In (2.20), half-vertices are $\bar{\psi}_\uparrow^{j_1, \alpha_1} \bar{\psi}_\downarrow^{j_3, \alpha_3}$ and $\psi_\downarrow^{j_2, \alpha_2} \psi_\uparrow^{j_4, \alpha_4}$. Sectors α_1, α_3 are very close. Splitting all vertices in this way yields *fermion loops on which all sectors are very close*, so that there is essentially only *one sum over sectors per loop*. This gives birth to the "1/N" factors. This approach is pursued in a systematic way in §2.3.2. In this ideal case, the 1/N-factor is $1/N_j = 2^{-j}$. Taking into consideration the opposite **degenerate** case when k is closer to $j/2$ than to j , the small factor 2^{-k} is really (at worst) $2^{-j/2}$.

Alternatively, assuming α_1 to be fixed, this leaves only $O(2^j A^2)$ possibilities. Later on, we shall see that (at least perturbatively) sectors are in average shared by two vertices, so fixing one of the sectors is the correct way of counting; thus, for a vertex

($2n = 4$), there is – up to the logarithmic correction – only *one* sum over sectors. Also, as mentioned in the Remark just above Definition 2.2, choosing *anisotropic sectors* with angular width $\approx 2^{-j/2}$ instead, the logarithmic correction disappears, so there is *exactly one sum over sectors*.

An immediate corollary is the following. Let

$$I^j(\Delta^j) := \int d\xi \chi_{\Delta^j}(\xi) \sum_{\alpha_2, \alpha_3, \alpha_4} \left(\bar{\psi}_{\uparrow}^{j, \alpha_1}(\xi) \bar{\psi}_{\downarrow}^{j, \alpha_2}(\xi) \right) \left(\psi_{\downarrow}^{j, \alpha_3}(\xi) \psi_{\uparrow}^{j, \alpha_4}(\xi) \right), \quad (2.23)$$

$\Delta^j \in \mathbb{D}^j$, with α_1 fixed, and χ_{Δ} as above. Then, taking a partial Fourier transform \mathcal{F} w.r. to spatial coordinates, and considering a family of smooth, scaled Fourier cut-offs $\chi_+^k(\mathbf{q})$ such that $\sum_k \chi_+^k \equiv 1$ and $\chi_+^k(\mathbf{q}) \equiv 0$ except if $\sqrt{(q^1)^2 + (q^2)^2} \approx 2^{-k} p_F^*$, so that (in particular) $|\mathcal{F}^{-1}(\chi_+^k)(\mathbf{x})| \leq C_n 2^{-2k} (p_F^*)^2 (1 + 2^{-k} p_F^* |\mathbf{x}|)^{-n}$ for all $n \geq 0$ (compare with the bounds of Proposition 2.3), we get

$$\begin{aligned} I^j(\Delta^j) &= \int d\tau \sum_k \int d\mathbf{q} \hat{\chi}_{\Delta^j}(\tau, \mathbf{q}) \chi_+^k(\mathbf{q}) \sum_{(\alpha_2, \alpha_3, \alpha_4) \in \mathcal{M}_{\alpha_1}^k} \mathcal{F} \left(\bar{\psi}_{\uparrow}^{j, \alpha_1} \bar{\psi}_{\downarrow}^{j, \alpha_2} \psi_{\downarrow}^{j, \alpha_3} \psi_{\uparrow}^{j, \alpha_4} \right) (\tau, \mathbf{q}) \\ &= \sum_k \int d\tau \int d\mathbf{x} (\chi_{\Delta^j}(\tau, \cdot) * \mathcal{F}^{-1}(\chi_+^k))(\mathbf{x}) \sum_{(\alpha_2, \alpha_3, \alpha_4) \in \mathcal{M}_{\alpha_1}^k} \left(\bar{\psi}_{\uparrow}^{j, \alpha_1}(\xi) \bar{\psi}_{\downarrow}^{j, \alpha_2}(\mathbf{x}) \right) \left(\psi_{\downarrow}^{j, \alpha_3}(\mathbf{x}) \psi_{\uparrow}^{j, \alpha_4}(\mathbf{x}) \right). \end{aligned} \quad (2.24)$$

where $\mathcal{M}_{\alpha_1}^k := \{(\alpha_2, \alpha_3, \alpha_4) \mid \exists (\mathbf{p}_1, \dots, \mathbf{p}_4) \in \Sigma^{j, \alpha_1} \times \dots \times \Sigma^{j, \alpha_4}, \mathbf{p}_1 + \mathbf{p}_2 - \mathbf{p}_3 - \mathbf{p}_4 \in \text{supp}(\chi_+^k)\}$ has cardinal $O(j2^j(2^{j-k})^2)$ for $k \leq j$; in practice, we restrict the sum in (2.24) to $k \leq j$ and replace without further mention χ_+^j by $\chi_+^{\rightarrow j} = \sum_{k \geq j} \chi_+^k$. Then

$$\begin{aligned} \int d\tau \int d\mathbf{x} \left| (\chi_{\Delta^j}(\tau, \cdot) * \mathcal{F}^{-1}(\chi_+^k))(\mathbf{x}) \right| &\lesssim \int d\tau \int d\mathbf{x} \left| (\nabla^3 \chi_{\Delta^j}(\tau, \cdot) * \mathcal{F}^{-1}(\mathbf{p} \mapsto |\mathbf{p}|^{-3} \chi_+^k(\mathbf{p}))(\mathbf{x}) \right| \\ &\lesssim (2^{-(j-k)})^3 \text{Vol}(\text{supp}(\chi_{\Delta^j})) \cdot \int d\mathbf{x} |\mathcal{F}^{-1}(\chi_+^k)(\mathbf{x})| \\ &\lesssim (2^{-(j-k)})^3 \cdot \frac{1}{m^* \mu^2} (2^j)^3. \end{aligned} \quad (2.25)$$

Taking into account the $O(2^{-j} p_F^*) = O(2^{-j} \sqrt{m^* \mu})$ scaling of each field, one obtains finally $I^j(\Delta^j) = O(jm^*)$.

In other words: *The vertex, i.e. the quartic term in the interaction, integrated over a scale j box Δ^j , fixing one of the sectors,*

$$\lambda I^j(\Delta^j) = O(j\lambda m^*) = O(jg) \quad (2.26)$$

is small – up to a logarithmic correction –, as follows from our Assumption on the coupling constant g .

We shall see in §2.4 how to get rid of this logarithmic correction in *diagram* bounds. Note that there is no logarithmic correction as soon as $2n \geq 6$.

2.2 Dressed action

The principle of multi-scale expansions is to rewrite the bare action $\mathcal{L}_\theta(\Psi, \bar{\Psi}) \equiv \int_V d\xi \mathcal{L}_\theta(\Psi, \bar{\Psi}; \xi)$ of Definition 1.1 as a sum over $j \geq j_D$ of effective actions $\mathcal{L}_\theta^{\rightarrow j}(\Psi, \bar{\Psi}) \equiv \int_V d\xi \mathcal{L}_\theta^{\rightarrow j}(\Psi, \bar{\Psi}; \xi)$ with highest scale j , and renormalized, scale-dependent coefficients $\lambda^j, \Gamma^j, \mu^j, m^j$.

Field dressing. Recall $\mathbb{D} = \sum_{j=j_D}^{j'_\phi} \mathbb{D}^j$. Given a function $\mathbf{t} : \mathbb{D} \rightarrow [0, 1]$, we let $(T^{\rightarrow j} \Psi)^j(\xi) = \Psi^j(\xi)$,

$$(T^{\rightarrow k} \Psi)^j(\xi) = t_\xi^k t_\xi^{k+1} \dots t_\xi^{j+1} \Psi^j(\xi), \quad k < j \quad (2.27)$$

with

$$t_\xi^k := \sum_{\Delta \in \mathbb{D}^k} \chi_\Delta(\xi) t_\Delta^k \quad (2.28)$$

and

$$(T\Psi)^{\rightarrow k} := \sum_{j \geq k} (T^{\rightarrow k} \Psi)^j. \quad (2.29)$$

The sum in (2.28) contains only at most $6 = O(1)$ terms by the support condition of $(\chi_\Delta)_\Delta$. This definition implies

$$\frac{\partial}{\partial t_\Delta^j} (T\Psi)^{\rightarrow k}(\xi) = t_\xi^k \dots t_\xi^{j+1} \chi_\Delta(\xi) (T\Psi)^{\rightarrow j}(\xi), \quad k < j. \quad (2.30)$$

The above expression vanishes except in some neighborhood of Δ . The adjoint field $\bar{\Psi}$ is dressed similarly.

Let

$$\boxed{\lambda^{j_D} := \lambda, \quad \delta\Gamma^{j_D} := \Gamma_\phi, \quad \delta\mu^{j_D} := \delta\mu = \mu^* - \mu, \quad \delta m^{j_D} := \delta m = \frac{m^*}{m}(m^* - m)}. \quad (2.31)$$

Definition 2.6 (dressed action) *Let*

$$d\mu_{\theta; \lambda}(\mathbf{t}; \Psi, \bar{\Psi}) = \frac{1}{\mathcal{Z}_\lambda^*} e^{-\mathcal{L}_\theta(\mathbf{t}; \Psi, \bar{\Psi})} d\mu_\theta^*(\Psi, \bar{\Psi}), \quad (2.32)$$

where

$$\mathcal{L}_\theta(\mathbf{t}) \equiv \int_V d\xi \mathcal{L}_\theta(\mathbf{t}; \xi), \quad (2.33)$$

$$\mathcal{L}_\theta(\mathbf{t}; \xi) \equiv \sum_{j=j_D}^{j'_\phi} \mathcal{L}^{\rightarrow j}(\mathbf{t}; \xi) \quad (2.34)$$

$$\begin{aligned}
\mathcal{L}_\theta^{\rightarrow j_D}(\mathbf{t}; \xi) &:= \lambda^{j_D} ((T\bar{\Psi})^{\rightarrow j_D} (T\Psi)^{\rightarrow j_D})^2(\xi) \\
&+ (T\bar{\Psi})^{\rightarrow j_D}(\xi) \left(\delta\Gamma^{j_D}(\theta) - \left(\frac{\delta m^{j_D}}{(m^*)^2} \frac{|\nabla|^2}{2} + \delta\mu^{j_D} \right) \sigma^3 \right) (T\Psi)^{\rightarrow j_D}(\xi);
\end{aligned} \tag{2.35}$$

and, for $j = j_D + 1, \dots, j'_\phi$,

$$\begin{aligned}
\mathcal{L}_\theta^{\rightarrow j}(\mathbf{t}; \xi) &:= (1 - (t_\xi^{j-1})^4) \lambda^{j_D} ((T\bar{\Psi})^{\rightarrow j} (T\Psi)^{\rightarrow j})^2(\xi) \\
&+ (1 - (t_\xi^{j-1})^2) (T\bar{\Psi})^{\rightarrow j}(\xi) \left(\delta Z^j \partial_\tau - \left(\frac{\delta m^j}{(m^*)^2} \frac{|\nabla|^2}{2} + \delta\mu^j \right) \sigma^3 + \delta\Gamma^j(\theta) \right) (T\Psi)^{\rightarrow j}(\xi)
\end{aligned} \tag{2.36}$$

where $\nabla = (\partial_{x_1}, \partial_{x_2})$, $|\nabla|^2 := \partial_{x_1}^2 + \partial_{x_2}^2$.

Compare with Definition 1.1. The principle of the dressing is the following:

- If $\mathbf{t} \equiv \mathbf{1}$, then $d\mu_{\theta; \lambda}(\mathbf{t}) \equiv d\mu_{\theta; \lambda}$, i.e. one retrieves the bare theory (see (2.41) below);
- If $t_\Delta = 0$ for all $\Delta \in \mathbb{D}^j$, then $d\mu_{\theta; \lambda}(\mathbf{t}; \Psi, \bar{\Psi}) \propto e^{-\mathcal{L}_\theta(\mathbf{t}^{(j-1)\rightarrow}; \Psi^{j\rightarrow}, \bar{\Psi}^{j\rightarrow})} d\mu_\theta^*(\Psi^{j\rightarrow}, \bar{\Psi}^{j\rightarrow}) \otimes e^{-\mathcal{L}_\theta(\mathbf{t}^{\rightarrow(j+1)}; \Psi^{\rightarrow(j+1)}, \bar{\Psi}^{\rightarrow(j+1)})} d\mu_\theta^*(\Psi^{\rightarrow(j+1)}, \bar{\Psi}^{\rightarrow(j+1)})$ is the tensor product of two *independent* measures, a measure for the *high-momentum fields* $\Psi^{j\rightarrow}, \bar{\Psi}^{j\rightarrow}$, and a measure for the *low-momentum fields* $\Psi^{\rightarrow(j+1)}, \bar{\Psi}^{\rightarrow(j+1)}$. On the other hand, derivatives $\frac{d}{dt_\Delta}$, $\Delta \in \mathbb{D}^j$ acting on $\mathcal{L}_\theta(\mathbf{t}; \Psi, \bar{\Psi})$ produce by construction either (i) *mixed terms* involving both high-momentum fields $(\bar{\Psi})^{j\rightarrow}$ and low-momentum fields $(\bar{\Psi})^{\rightarrow(j+1)}$; or (ii) *subtracted terms* $(\lambda^j - \lambda^{j+1}) ((T\bar{\Psi})^{\rightarrow(j+1)} (T\Psi)^{\rightarrow(j+1)})^2$ or $(T\bar{\Psi})^{\rightarrow(j+1)} \left\{ (\delta Z^j - \delta Z^{j+1}) \partial_\tau - \left((\delta m^j - \delta m^{j+1}) \frac{|\nabla|^2}{2m^2} + (\delta\mu^j - \delta\mu^{j+1}) \right) \sigma^3 + (\delta\Gamma^j(\theta) - \delta\Gamma^{j+1}(\theta)) \right\} (T\Psi)^{\rightarrow(j+1)}$. Subtracted terms (ii) associated with parameter renormalization are there precisely to compensate mixed terms of type (i).

Looking at the theory at scale j , and combining the covariance C_θ^j with the quadratic term in $\mathcal{L}_\theta^{\rightarrow j}$, we obtain an effective fermion covariance

$$\begin{aligned}
&\left(\left\{ i p^0 - \left(\frac{|\mathbf{p}|^2}{2m^*} - \mu^* \right) \sigma^3 - \Gamma(\theta) \right\} + \left\{ i \delta Z^j p^0 - \left(\frac{\delta m^j}{2(m^*)^2} |\mathbf{p}|^2 + \delta\mu^j \right) \sigma^3 + \delta\Gamma^j(\theta) \right\} \right)^{-1} \\
&\equiv (i Z^j p^0 - \left(\frac{|\mathbf{p}|^2}{2m^j} - \mu^j \right) \sigma^3 - \Gamma^j(\theta))^{-1}
\end{aligned} \tag{2.37}$$

where

$$\Gamma^j = \Gamma - \delta\Gamma^j, \tag{2.38}$$

$$m^j = \frac{m^*}{1 + \frac{\delta m^j}{m^*}} = m^* - \delta m^j + O\left(\frac{(\delta m^j)^2}{m^*}\right), \quad (2.39)$$

$$Z^j = 1 + \delta Z^j, \quad \mu^j = \mu^* - \delta \mu^j. \quad (2.40)$$

In particular, when $j = j^D$, one retrieves the bare parameters,

$$\Gamma^{j^D} = \Gamma, \quad m^{j^D} = m, \quad \mu^{j^D} = \mu. \quad (2.41)$$

We determine $\mu^* = \mu^*(\Gamma)$, $m^* = m^*(\Gamma)$, and simultaneously $\Gamma \equiv \Gamma^{(j'_\phi - 1) \rightarrow}$, by a fixed point argument in such a way that

$$\boxed{\delta \mu^{j'_\phi} = 0, \quad \delta m^{j'_\phi} = 0.} \quad (2.42)$$

and the pre-gap equation (see Definition 1.2) holds. As emphasized in the Introduction, this procedure implies that *the effective radius of the Fermi circle is $p_F^* := \sqrt{2m^*\mu^*}$.*

As we shall see (see §2.3.2), the order of divergence $\omega(\Upsilon)$ of a lowest scale j amputated diagram Υ with N_{ext} external fermion legs is $\frac{1}{2}(4 - N_{ext})$ above symmetry-breaking momentum scale j_ϕ , which means that $\mathcal{A}^{j \rightarrow}(\Upsilon)$ scales at most like $O(2^{\frac{j}{2}(4 - N_{ext})})$. Thus diagrams with ≤ 4 external legs must be renormalized. This power-counting estimate is not necessarily true for the amplitude of a polymer, which suffers from non-overlapping constraints; we shall therefore be led to renormalize diagrams with up to 6 external legs, whose local parts may be freed from non-overlapping constraints by the Mayerization procedure described in §2.3.5. In this theory, one renormalizes with external legs on the effective Fermi circle Σ_F^* where the IR singularity lies. By symmetry, non-vanishing N_{ext} -point functions must have $\frac{1}{2}N_{ext}$ external Ψ -fields and $\frac{1}{2}N_{ext}$ external $\bar{\Psi}$ -fields, with N_{ext} even. So we need only discuss two-, four- and six-point functions. *Counterterms* are associated to two-point functions only; they require a precise analysis, which will lead to the renormalization flow.

1. **(two-point functions)** The two external legs $-(\psi, \psi), (\psi, \bar{\psi})$ or $(\bar{\psi}, \bar{\psi})$ are in the vicinity of the Fermi sphere. Let \mathbf{i} be a unit vector, and \mathbf{i}^\perp its image through the rotation of angle $\pi/2$. Expanding with respect to an external momentum $(p^0, \mathbf{p}) = (p^0, (p_F^* + p_\perp)\mathbf{i} + p_{//}\mathbf{i}^\perp)$ in space direction \mathbf{i} , with $|p_\perp|, |p_{//}| \ll 2^{-j}p_F^*$, $|p^0| \ll 2^{-j}\mu$, and using $p_\perp \sim \frac{1}{2p_F^*}(|\mathbf{p}|^2 - (p_F^*)^2)$, one gets

$$\begin{aligned} \mathcal{A}_p^{j \rightarrow}(\Upsilon) &= \mathcal{A}_{(0, p_F^* \mathbf{i})}^{j \rightarrow}(\Upsilon) + p^0 \frac{d}{dp^0} \mathcal{A}_p^{j \rightarrow}(\Upsilon) \Big|_{p=(0, p_F^* \mathbf{i})} + p_{//} \frac{d}{dp_{//}} \mathcal{A}_p^{j \rightarrow}(\Upsilon) \Big|_{p=(0, p_F^* \mathbf{i})} \\ &+ \frac{1}{2p_F^*} (|\mathbf{p}|^2 - (p_F^*)^2) \frac{d}{dp_\perp} \mathcal{A}_p^{j \rightarrow}(\Upsilon) \Big|_{p=(0, p_F^* \mathbf{i})} + O(|p|^2 \frac{d^2}{dp^2} \mathcal{A}_p^{j \rightarrow}(\Upsilon)) \end{aligned} \quad (2.43)$$

and similarly (summing over all diagrams with internal legs of momentum scales $\leq j$), letting $G^{j\rightarrow}(p)$ be as in §1.1 the Fourier transform of the two-point function $\langle {}^t\bar{\Psi}^{j\rightarrow}(\cdot)\Psi^{j\rightarrow}(\cdot)\rangle_{\theta;\lambda}$,

$$\begin{aligned} G^{j\rightarrow}(p) &= G^{j\rightarrow}(0, p_F^* \mathbf{i}) + p^0 \frac{d}{dp^0} G^{j\rightarrow}(p) \Big|_{p=(0, p_F^* \mathbf{i})} + p_{//} \frac{d}{dp_{//}} G^{j\rightarrow}(p) \Big|_{p=(0, p_F^* \mathbf{i})} \\ &\quad + \frac{1}{2p_F^*} (|\mathbf{p}|^2 - (p_F^*)^2) \frac{d}{dp_{\perp}} G^{j\rightarrow}(p) \Big|_{p=(0, p_F^* \mathbf{i})} + O(|p|^2 \frac{d^2}{dp^2} G^{j\rightarrow}(p)). \end{aligned} \quad (2.44)$$

The difference $\delta G^j := G^{j\rightarrow} - G^{(j-1)\rightarrow}$ selects the contribution of diagrams of lowest internal scale precisely equal to j . Second-order derivatives need not be renormalized because the effective order of divergence is $\frac{1}{2}(4-2) - 2 < 0$. By rotation invariance, $\frac{d}{dp_{//}} \delta G^j(p) \Big|_{p=(0, p_F^* \mathbf{i})} = 0$.

Let us discuss to begin with *diagonal components* $\delta G_{i,i}^j$, $i = 1, 2$. First, $\delta G_{i,i}^j(0, p_F^* \mathbf{i})$ and $\frac{d}{dp_{\perp}} \delta G_{i,i}^j(p) \Big|_{p=(0, p_F^* \mathbf{i})}$ yield spin-independent counterterms $\delta \mu^{j+1} - \delta \mu^j$ for the chemical potential and $\delta m^{j+1} - \delta m^j$ for the mass. Finally, $\frac{d}{dp^0} \delta G_{i,i}^j(p) \Big|_{p=(0, p_F^* \mathbf{i})}$ yields a Z -counterterm $\delta Z^{j+1} - \delta Z^j$.

The *off-diagonal part* $\delta G_{off}^j = \begin{pmatrix} 0 & \delta G_{1,2}^j \\ \delta G_{2,1}^j & 0 \end{pmatrix}$ of δG^j involves an *odd* number of off-diagonal propagators with matrix coefficient Γ or $\delta \Gamma^k$, $k < j$, whence (as shown by induction on j) one extra prefactor $O(2^{-j\phi}) = O(2^{-j} 2^{-(j\phi-j)})$, thus lowering the effective degree of divergence of diagrams by 1. Consequently, we need only Taylor expand to order 0,

$$G_{off}^{j\rightarrow}(p) = G_{off}^{j\rightarrow}(0, p_F^* \mathbf{i}) + O(|p| \frac{d}{dp} G_{off}^{j\rightarrow}(p)). \quad (2.45)$$

It follows crucially from the fact that the scale j infra-red cut-off theory, see Definition 1.1 (ii), retains the symmetries of the original theory, so that (by (1.10) and (1.11))

$$\delta G_{1,1}^{j\rightarrow}(0, p_F^* \mathbf{i}) = \left(\delta G_{1,1}^{j\rightarrow}(0, p_F^* \mathbf{i}) \right)^* = -\delta G_{2,2}^{j\rightarrow}(0, p_F^* \mathbf{i}); \quad (2.46)$$

$$\frac{d}{dp^0} \delta G_{1,1}^{j\rightarrow} \Big|_{p=(0, p_F^* \mathbf{i})} = \frac{d}{dp^0} \delta G_{2,2}^{j\rightarrow} \Big|_{p=(0, p_F^* \mathbf{i})} = - \left(\frac{d}{dp^0} \delta G_{1,1}^{j\rightarrow} \Big|_{p=(0, p_F^* \mathbf{i})} \right)^* \quad (2.47)$$

$$\frac{d}{dp_{\perp}} \delta G_{1,1}^{j\rightarrow} \Big|_{p=(0, p_F^* \mathbf{i})} = - \frac{d}{dp_{\perp}} \delta G_{2,2}^{j\rightarrow} \Big|_{p=(0, p_F^* \mathbf{i})} = \left(\frac{d}{dp_{\perp}} \delta G_{1,1}^{j\rightarrow} \Big|_{p=(0, p_F^* \mathbf{i})} \right)^* \quad (2.48)$$

$$\delta G_{1,2}^{j \rightarrow}(0, p_F^* \mathbf{i}) = \left(\delta G_{2,1}^{j \rightarrow}(0, p_F^* \mathbf{i}) \right)^* \quad (2.49)$$

Hence: $\delta \mu_1^j = -\delta \mu_2^j =: \delta \mu^j$, $\delta m_1^j = -\delta m_2^j =: \delta m^j$, $\delta Z_1^j = \delta Z_2^j =: \delta Z^j$ and c^j are all *real* parameters, while $\delta G_{\text{off}}^j(0, p_F^* \mathbf{i})$ is a *Hermitian* matrix of the form $\delta \Gamma^{j+1} - \delta \Gamma^j \equiv \begin{pmatrix} 0 & \delta \bar{\Gamma}^{j+1} - \delta \bar{\Gamma}^j \\ \delta \Gamma^{j+1} - \delta \Gamma^j & 0 \end{pmatrix}$, with $\delta \Gamma^{j+1} - \delta \Gamma^j \in \mathbb{C}$.

Remark. Note that diagrams contributing to $\delta \Gamma$ -counterterms are not necessarily in the θ -direction ($//$) because of mixing diagrams. However, the leading-order contribution is a tadpole, see Fig. 2.2.4 (iv), which *is* in the θ -direction. Furthermore, a Ward identity (see §3.3) ensures that the local part of the fermionic two-point function vanishes in the direction perpendicular (\perp) to θ .

Summarizing:

Definition 2.7 (counterterms) *Let $\mathbf{i} \in \mathbb{R}^2$ be a unit vector. The following definitions do not depend on the orientation of \mathbf{i} :*

(i) (chemical potential counterterm) *let*

$$\boxed{\delta \mu^{j+1} - \delta \mu^j := -\delta G_{1,1}^j(0, p_F^* \mathbf{i}) + \frac{p_F^*}{2} \frac{d}{dp_\perp} \Big|_{p_\perp=0} \delta G_{1,1}^j(0, p_F^* \mathbf{i}).} \quad (2.50)$$

(ii) (mass counterterm)

$$\boxed{\delta m^{j+1} - \delta m^j := -\frac{m^2}{p_F^*} \frac{d}{dp_\perp} \Big|_{p_\perp=0} \delta G_{1,1}^j(0, p_F^* \mathbf{i}).} \quad (2.51)$$

(iii) (energy gap counterterm) *let*

$$\boxed{\delta \Gamma^{j+1} - \delta \Gamma^j := \delta G_{2,1}^j(0, p_F^* \mathbf{i}).} \quad (2.52)$$

(iv) (Z counterterm) *let*

$$\boxed{\delta Z^{j+1} - \delta Z^j := -i \frac{d}{dp^0} \Big|_{p^0=0} \delta G_{1,1}^j(p^0, p_F^* \mathbf{i}).} \quad (2.53)$$

Subtracting counterterms is equivalent to subtracting *local parts* of diagrams, which is done as follows. Let

$$\mathcal{A}^{j \rightarrow}(\Upsilon; \xi, \xi') := \int dp e^{i(p, \xi - \xi')} \mathcal{A}_p^{j \rightarrow}(\Upsilon) \quad (2.54)$$

be the amplitude of Υ in direct space. The external leg at ξ' is paired to a field $\Psi^{k,\alpha}(\xi'')$ or $\bar{\Psi}^{k,\alpha}(\xi'')$, with $k \geq j$, giving rise to an external covariance kernel $C^{k,\alpha}(\xi', \xi'')$. The direct space renormalization algorithm proceeds by applying Taylor's formula to the above kernel, so as to displace its attachment point from ξ' to ξ . For diagrams contributing to G_{diag}^j , we need to expand to order 1 so as to lower the order of divergence by two. For diagrams contributing to G_{off}^j , a simple subtraction is enough:

(i) (*off-diagonal diagrams*) Setting apart only the leading-order term, we get

$$\begin{aligned} \int d\xi' \mathcal{A}^{j \rightarrow}(\Upsilon; \xi, \xi') C^{k,\alpha}(\xi', \xi'') &= \int d\xi' \mathcal{A}^{j \rightarrow}(\Upsilon; \xi, \xi') e^{i(p^{k,\alpha}, \xi' - \xi)} C^{k,\alpha}(\xi, \xi'') \\ &+ \int_0^1 dt \int d\xi' \mathcal{A}^{j \rightarrow}(\Upsilon; \xi, \xi') \partial_t \left(e^{i(1-t)(p^{k,\alpha}, \xi' - \xi)} C^{k,\alpha}((1-t)\xi + t\xi', \xi'') \right) \\ &\equiv \mathcal{A}_{p^{k,\alpha}}^{j \rightarrow}(\Upsilon) C^{k,\alpha}(\xi, \xi'') + \mathcal{R} \bar{\mathcal{A}}^{j \rightarrow}(\Upsilon; \xi, \xi''), \end{aligned} \quad (2.55)$$

a sum of a *local part* as in (2.45), and of a renormalized amplitude $\mathcal{R} \bar{\mathcal{A}}^{j \rightarrow}(\Upsilon; \xi, \xi'')$ involving the scalar product $(\xi' - \xi, (\nabla - ip^{k,\alpha}) C^{k,\alpha}(\cdot, \xi''))$ is manifest. Since the lowest internal scale of Υ is j , distances $|\xi' - \xi|$ between vertices contribute a scaling factor $\lesssim 2^j$ to the expected power-counting, as can be shown using part of the decay factors in the covariance (2.11); this is a standard argument, see e.g. [54]. On the other hand, see again (2.11), the gradient operator $\nabla - ip^{k,\alpha}$ produces a small factor $O(2^{-k})$. All together, we have obtained a small spring factor $O(2^{-(k-j)})$, having the effect of lowering the degree of divergence of the diagram from 0 to -1 .

(ii) (*diagonal diagrams*) For such diagrams, we need to set apart the two leading-order terms,

$$\begin{aligned} \int d\xi' \mathcal{A}^{j \rightarrow}(\Upsilon; \xi, \xi') C^{k,\alpha}(\xi', \xi'') &= \int d\xi' \mathcal{A}^{j \rightarrow}(\Upsilon; \xi, \xi') e^{i(p^{k,\alpha}, \xi' - \xi)} C^{k,\alpha}(\xi, \xi'') \\ &+ \int d\xi' \mathcal{A}^{j \rightarrow}(\Upsilon; \xi, \xi') \left(\xi' - \xi, \partial_\xi \left(e^{i(p^{k,\alpha}, \xi' - \xi)} C^{k,\alpha}(\xi, \xi'') \right) \right) \\ &+ \int_0^1 dt \int d\xi' \mathcal{A}^{j \rightarrow}(\Upsilon; \xi, \xi') \partial_t^2 \left(e^{i(1-t)(p^{k,\alpha}, \xi' - \xi)} C^{k,\alpha}((1-t)\xi + t\xi', \xi'') \right) \\ &\equiv \left(\mathcal{A}_{p^{k,\alpha}}^{j \rightarrow}(\Upsilon) + \left(p, \frac{d}{dp} \mathcal{A}_p^{j \rightarrow}(\Upsilon) \Big|_{p=p^{k,\alpha}} \right) \right) C^{k,\alpha}(\xi, \xi'') + \mathcal{R}^2 \bar{\mathcal{A}}^{j \rightarrow}(\Upsilon; \xi, \xi'') \end{aligned} \quad (2.56)$$

where $\mathcal{R}^2(\cdot)$ subtracts the local part of the diagram to order 1. Compared to (i), the renormalized amplitude involves now the square of the scalar product $(\xi' - \xi, (\nabla - ip^{k,\alpha}) C^{k,\alpha}(\cdot, \xi''))$, hence a spring factor $O(2^{-2(k-j)})$, having the effect of lowering the degree of divergence of the diagram from 1 to $1 - 2 = -1$.

2. (N_{ext} -point functions with $4 \leq N_{ext} < N_0$) A simple subtraction (as for off-diagonal two-point diagrams) is required. Fixing one of the external vertices $\xi_{ext,1}$, we rewrite $\left(\prod_{i=2}^{N_{ext}} \int d\xi_{ext,i} \right) \mathcal{A}^{j \rightarrow}(\Upsilon; \xi_{ext}) \prod_{i=2}^{N_{ext}} C^{k_i, \alpha_i}(\xi_{ext,i}, \xi_i'')$ as a local part, $\left\{ \left(\prod_{i=2}^{N_{ext}} \int d\xi_{ext,i} e^{i(p^{k_i, \alpha_i}, \xi_{ext,i} - \xi_{ext,1})} \right) \mathcal{A}^{j \rightarrow}(\Upsilon; \xi_{ext}) \right\} \prod_{i=2}^{N_{ext}} C^{k_i, \alpha_i}(\xi_{ext,1}, \xi_i'')$, plus an error term which may be written in integral form as in (i) above.

Four-point diagrams are in principle logarithmically divergent. However, as we shall prove in §3.2, the *only* logarithmically divergent contributions come from Goldstone boson insertions, which are explicitly resummed into the Σ -kernel. So *no counterterms need to be introduced for four-point functions*: the coupling constant $\lambda = \lambda^{jD}$ keeps its bare value throughout.

Leading-order diagrams in g or g^2 are obtained as follows,

(i)

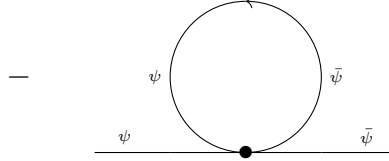


Fig. 2.2.1. Leading contribution to chemical potential renormalization $\delta\mu^{j+1} - \delta\mu^j$.

(ii)

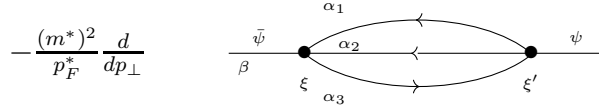


Fig. 2.2.2. Leading contribution to mass renormalization $\delta m^{j+1} - \delta m^j$.

(iii)

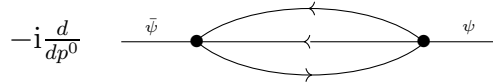


Fig. 2.2.3. Leading contribution to Z renormalization $\delta Z^{j+1} - \delta Z^j$.

(iv)

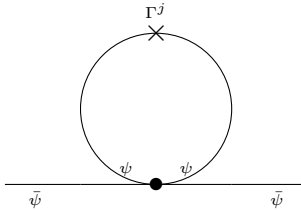


Fig. 2.2.4. Leading contribution to gap renormalization $\delta\Gamma^{j+1} - \delta\Gamma^j$.

We denote by $I_{(i)}$, $I_{(ii)}$, $I_{(iii)}$ and $I_{(iv)}$ their respective values. We can now restate Theorem 1 of the Introduction.

Lemma 2.8 (see Theorem 1) Assume $\Gamma_\phi \approx \hbar\omega_D e^{-\pi/m\lambda} \approx 2^{-j_\phi}\mu$. Then:

1. For $j = j_D, \dots, j_\phi - 1$, the renormalization flow is to leading order

$$\delta\mu^{j+1} - \delta\mu^j = -(\mu^{j+1} - \mu^j) \approx g2^{-2j}\mu \quad (2.57)$$

$$\delta m^{j+1} - \delta m^j \approx -(m^{j+1} - m^j) \approx g^2 2^{-j} m^* \quad (2.58)$$

$$\delta Z^{j+1} - \delta Z^j = Z^{j+1} - Z^j \approx g^2 2^{-j} \quad (2.59)$$

$$\delta\Gamma^{j+1} - \delta\Gamma^j = -(\Gamma^{j+1} - \Gamma^j) \approx -\frac{g}{\pi}(1 + O(g))\Gamma \quad (2.60)$$

For $j = j_\phi, \dots, j'_\phi - 1$, one has instead

$$|\delta m^{j+1} - \delta m^j| \lesssim 2^{-(j-j_\phi)} g^2 2^{-j} m^*, \quad |\delta\mu^{j+1} - \delta\mu^j| \lesssim 2^{-(j-j_\phi)} g 2^{-2j} \mu \quad (2.61)$$

$$|\delta Z^{j+1} - \delta Z^j| \lesssim 2^{-(j-j_\phi)} g^2 2^{-j}, \quad |\delta\Gamma^{j+1} - \delta\Gamma^j| \lesssim 2^{-(j-j_\phi)} g \Gamma_\phi. \quad (2.62)$$

In particular (summing over scales $j = j_D, \dots, j'_\phi - 1$)

$$Z^{j'_\phi} - 1 \approx g^2. \quad (2.63)$$

2. Furthermore, for an adequate choice of m^* , μ^* , $\Gamma = \Gamma^{(j'_\phi-1)\rightarrow}$ such that

$$m^* - m \approx -g^2 m, \quad \mu^* - \mu \approx g\mu, \quad |\Gamma| \approx \hbar\omega_D e^{-\pi/g} \quad (2.64)$$

the scale j'_ϕ mass and chemical potential counterterms vanish, more precisely,

$$\delta m^{j'_\phi} = 0, \quad \delta\mu^{j'_\phi} = 0, \quad (2.65)$$

and the pre-gap equation, see Definition 1.2, holds. Also,

$$\boxed{\delta\Gamma^{j'_\phi} = O(g\Gamma_\phi)}. \quad (2.66)$$

Proof.

1. We shall be content here with computing the values of $I_{(i)}, I_{(ii)}, I_{(iii)}, I_{(iv)}$; the arguments of §1.3 show that more complicated diagrams give contributions which are smaller by a factor $O(g)$. The evaluation of the diagrams of Fig. 2.2.1, 2.2.2, 2.2.3, 2.2.4 (see [25] for details) is based on the decomposition (1.45) of diagonal propagators, implying

$$C_\theta^* \approx \left(\begin{array}{c} \frac{1}{-ip^0 + e^*(\mathbf{p})} \\ \frac{1}{ip^0 + e^*(\mathbf{p})} \end{array} \right) \approx \left(\begin{array}{c} \frac{1}{-ip^0 + p_\perp} \\ \frac{1}{ip^0 + p_\perp} \end{array} \right) \text{ for momenta of scale } j \ll j_\phi.$$

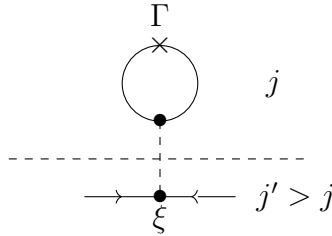
Recall that the integration measure $dp = dp^0 d\mathbf{p}$ averaged over the angular coordinates (i.e. summed over sectors) is $\approx 2\pi p_F dp^0 dp_\perp$. We do the computations for $j \leq j_\phi - 1$; for larger j , one need just remark that the covariance kernel (2.12) has a supplementary $2^{-(j-j_\phi)}$ prefactor.

- (i) (chemical potential) Evaluate the amputated diagram $I_{(i)} := \int \frac{dp}{ip^0 + e^*(\mathbf{p})}$ over momenta $\frac{|p^0|}{\mu}, \frac{|\mathbf{p}|}{p_F} \approx 2^{-j}$. By symmetry, the result is real. Using $e^*(\mathbf{p}) \sim \frac{1}{2m^*} p_\perp (p_\perp + 2p_F^*)$, one gets $I_{(i)} \approx \frac{1}{2m^*} \int dp^0 dp_\perp \frac{p_\perp^2}{(p^0)^2 + (\frac{p_F^*}{m^*})^2 p_\perp^2} \approx 2^{-2j} \mu$. In particular, $I_{(i)} > 0$.

- (ii) (mass) As in §5.4, the best way to get a correct order of magnitude of $I_{(ii)}$ is to choose *anisotropic* sectors $\alpha_1, \alpha_2, \alpha_3$. If $|\xi - \xi'| \gg 2^{j/2} \mu^{-1}$, then the main contribution to the integrand comes from sectors $\alpha_i, i = 1, 2, 3$ roughly parallel to $\xi - \xi'$. Thus: the sum over sectors produces a factor $O(1)$; the product $(C_\theta^*(\xi, \xi'))^3$, a factor $O((2^{-3j/2})^3)$; the derivative ∂_{p_\perp} , a factor $O(2^j)$; the integral over ξ' , a factor $O(2^{5j/2})$, i.e. the volume of an anisotropic box. Whence all together, a contribution $O(2^{-j})$. The integral over $|\xi - \xi'| \lesssim 2^{j/2} \mu^{-1}$ yields a contribution smaller by a factor $O(2^{-3j/2})$, since: each propagator $C_\theta^*(\xi, \xi')$ is a $O(2^{-2j})$ instead of $O(2^{-3j/2})$, see (5.28); the integration volume is $O(2^{2j})$ instead of $O(2^{5j/2})$, while (for β fixed) the sum over sectors $\alpha_i, i = 1, 2, 3$, reduces essentially in fact to a single sum, yields a supplementary factor $O(2^{j/2})$ only (see Proposition 2.5, with logarithmic factor removed for anisotropic sectors, following the Remark just above Definition 2.2).

- (iii) (Z -coefficient) Similar to (ii).

- (iv) (Γ -counterterm renormalization) Main scale j diagram is a tadpole involving the symmetry-broken propagator,



As already noted in §1.5, see Fig. 1.5.1, this diagram involves to leading order the same integral as the Cooper pair bubble diagram $\Upsilon_{3,diag}$, and is evaluated (see (1.56)) as $\sim -\frac{g}{\pi}\Gamma$.

2. (fixed point) Summing over scales $j = j_D, \dots, j'_\phi - 1$, one gets

$$\delta m^{j'_\phi} = \delta m^{j_D} + \sum_{j=j_D}^{j'_\phi-1} (\delta m^{j+1} - \delta m^j) = \frac{m^*}{m} \left\{ (m^* - m) + c_1 g^2 m f_1(m^*, \mu^*, \Gamma_\phi; g) \right\} \quad (2.67)$$

$$\delta \mu^{j'_\phi} = \delta \mu^{j_D} + \sum_{j=j_D}^{j'_\phi-1} (\delta \mu^{j+1} - \delta \mu^j) = (\mu^* - \mu) + c_2 g \mu f_2(m^*, \mu^*, \Gamma_\phi; g) \quad (2.68)$$

$$\delta \Gamma^{j'_\phi} = \delta \Gamma^{j_D} + \sum_{j=j_D}^{j'_\phi-1} (\delta \Gamma^{j+1} - \delta \Gamma^j) = \Gamma \left\{ 1 - \frac{g}{\pi} (j_\phi - j_D) f_3(m^*, \mu^*, \Gamma_\phi; g) \right\} \quad (2.69)$$

(see proof of 1.(iv) for the last equality), where $c_1, c_2 > 0$ are non-dimensional constants, $f_1, f_2, f_3 = 1 + O(g)$, and $\frac{\partial f_i}{\partial g} = O(1)$, $\frac{\partial f_i}{\partial m^*} = O(1/m)$, $\frac{\partial f_i}{\partial \mu^*}, \frac{\partial f_i}{\partial \Gamma_\phi} = O(1/\mu)$ ($i = 1, 2, 3$) for any (m^*, μ^*) such that $m^* - m = o(m), \mu^* - \mu = o(\mu)$. Eq. (2.69), combined with (1.62), imply

$$\delta \Gamma^{j'_\phi} = O(g \Gamma_\phi) \quad (2.70)$$

for such values of m^*, μ^* . Then the implicit function theorem yields for g small enough a unique solution ($m^* = m^*(g), \mu^* = \mu^*(g), \Gamma = \Gamma^{(j'_\phi-1)\rightarrow}$) to the system of equations ($\delta m^{j'_\phi} = 0, \delta \mu^{j'_\phi} = 0$) complemented with the pre-gap equation (1.65). Furthermore, they satisfy (2.64) and (2.66).

2.3 Cluster expansions

The art of cluster expansions for a general renormalizable theory consists in resumming separately the leading contributions of diverging n -point functions, and absorbing them into a *renormalization* of the measure. By "renormalization of the measure", we intend a change of normalization by a constant prefactor (which disappears when one evaluates connected correlations), and a shift of its parameters, here μ, m and Γ . This is done in an organized way by evaluating n -point functions in terms of a *sum over clusters* or *polymers*, which themselves may be expanded perturbatively into an infinite series of diagrams involving only fields located inside the image of the polymer. Clusters are arrays of scaled *boxes* connected by a tree of links – the linking

consisting of propagators $C^j(\xi, \xi')$ between two boxes of \mathbb{D}^j . Polymers are synonymous for clusters, or multi-scale versions of them, involving both *horizontal links* connecting boxes of the same scale, and *vertical links* capturing the interaction between scales through multi-scale vertices. Here is a graphical representation of a multi-scale vertex $(\bar{\Psi}\Psi)^2$, with the four half-propagators connecting it to other vertices; the scale of the vertex is by definition *the scale of the half-propagator with highest momentum*, here j .

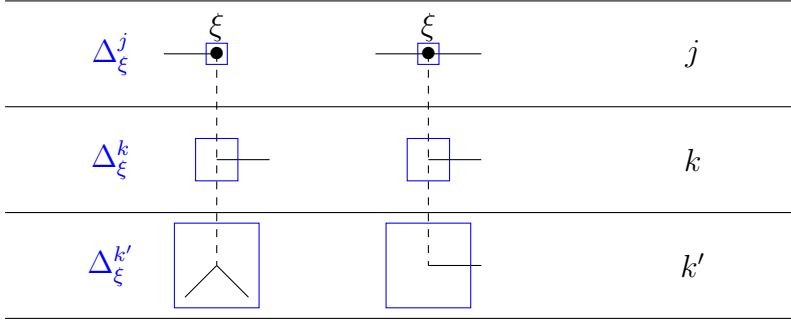


Fig. 2.3.1. Two multi-scale vertices of scale j , from left to right:

$\bar{\Psi}^j(\xi)\bar{\Psi}^k(\xi)(\bar{\Psi}^{k'}\bar{\Psi}^{k'})(\xi)$, and $(\bar{\Psi}^j\bar{\Psi}^j)(\xi)(\bar{\Psi}^k\bar{\Psi}^{k'})(\xi)$. By assumption $j < k \leq k'$.

Horizontal cluster expansions (one per scale) produce horizontal links. *Vertical cluster expansions* produce vertical links, and single out in particular divergent polymers, which are polymers with a small (here ≤ 4) number of external legs. The renormalization step resums the leading term – called *local part* – of divergent polymers into a scale-dependent redefinition of the parameters of the interaction. As a minor correction, a further cluster-like expansion (called *Mayer expansion*) is required to get rid of the non-overlapping conditions between boxes belonging to two different polymers, so as to regain translation invariance for divergent polymers. So far for fundamentals.

We start from scale $j = j_D$ and apply inductively the following **sequence of fermionic expansions**, down to a scale $j'_\phi = j_\phi + o(\ln(1/g))$,

(Horizontal cluster expansion of scale j_D) \longrightarrow (Resummation of (lowest) scale j_D chains of bubbles) \longrightarrow (Momentum-decoupling expansion of scale j_D) \longrightarrow (Displacement of external legs and Mayer expansion of scale j_D) $\longrightarrow \dots$

\longrightarrow (Horizontal cluster expansion of scale j) \longrightarrow (Resummation of lowest scale $(j+1)$ chains of bubbles) \longrightarrow (Momentum-decoupling expansion of scale j) \longrightarrow (Displacement of external legs and Mayer expansion of scale j) $\longrightarrow \dots$

\longrightarrow (Horizontal cluster expansion of scale $(j'_\phi - 1)$) \longrightarrow (Resummation of lowest scale $(j'_\phi - 1)$ chains of bubbles) \longrightarrow (Momentum-decoupling expansion of scale $(j'_\phi - 1)$) \longrightarrow (Displacement of external legs and Mayer expansion of scale $(j'_\phi - 1)$)

Once this program has been completed, we shall be led to apply in the next section (see §3) a sequence of **complementary horizontal** or **bosonic expansions** of *bosonic* scales $j_+ \geq j'_\phi$,

(Horizontal and Complementary horizontal expansions of scale j'_ϕ) \longrightarrow (Complementary horizontal expansion of bosonic scale $j'_\phi + 1$) $\longrightarrow \dots$ (Complementary horizontal expansion of bosonic scale j_+) $\longrightarrow \dots$

with scales ranging from j'_ϕ to $+\infty$. Scale j'_ϕ is very particular, since purely fermionic connectivity issues (see introduction to this subsection) mingle with the necessity of factorizing Goldstone boson propagators to show infra-red summability of the expansion. Therefore the scale j'_ϕ horizontal cluster expansion is postponed to section 3.

Apart from the intertwining sequence of bubble resummations, the sequence of *fermionic expansions* is fairly standard, see e.g. [70] for a review. Through the horizontal and momentum-decoupling expansions, n -point functions are rewritten as sums of products of *polymer*-dependent expressions of the type $F(\mathbb{P})$. A polymer \mathbb{P} is by definition a union of boxes in \mathbb{D} with the following properties:

(i) two boxes $\Delta, \Delta' \in \mathbb{P} \cap \mathbb{D}^j$ may or may not be connected by a *horizontal link* produced by the *scale j horizontal cluster expansion*. The set of all boxes in $\mathbb{P} \cap \mathbb{D}^j$, connected by horizontal links, is a *cluster forest*, i.e. a disjoint union of a finite number of *cluster trees*;

(ii) two boxes $\Delta \in \mathbb{P} \cap \mathbb{D}^j, \Delta' \in \mathbb{P} \cap \mathbb{D}^{j+1}$ such that $\Delta \subset \Delta'$, i.e. Δ' lies just below Δ , may or may not be connected by a *vertical link* produced by the *scale momentum-decoupling* (or *vertical*) *expansion*. The set of all boxes in \mathbb{P} , connected by *cluster links*, i.e. *horizontal and vertical links*, is connected.

The set of all such polymers with lowest scale j_{max} will be denoted by $\mathcal{P}^{j_{max} \rightarrow}$. Furthermore, if $\mathbb{P} \in \mathcal{P}^{j_{max} \rightarrow}$, then

(iii) (*external structure of a polymer*) there exists a subset $\Delta^{j_{max}} = \Delta^{j_{max}}(\mathbb{P}) \subset \mathbb{P} \cap \mathbb{D}^{j_{max}}$ of scale j_{max} boxes vertically connected to the boxes in $\mathbb{D}^{j_{max}+1}$ lying just below them.

The function $F(\mathbb{P}) = F(\mathbb{P}; \Psi^{\rightarrow j_{max}} \Big|_{\Delta^{j_{max}}}, \bar{\Psi}^{\rightarrow j_{max}} \Big|_{\Delta^{j_{max}}})$ is obtained by Gaussian integrations by parts, which produce a number of *vertices*, each lying in one of the boxes contained in \mathbb{P} ; say, $n(\Delta)$ vertices in $\Delta \in \mathbb{P}$. If $\Delta, \Delta' \in \mathbb{P} \cap \mathbb{D}^k$ ($k \leq j_{max}$) are connected, then $F(\mathbb{P})$ contains a propagator $C^{k,\alpha}(\xi, \xi')$, with $\xi \in \Delta, \xi' \in \Delta'$. Furthermore, $F(\mathbb{P})$ contains at least one external field $\Psi^{\rightarrow j_{max}}$ or $\bar{\Psi}^{\rightarrow j_{max}}$ per external box $\Delta \in \Delta^{j_{max}}$, namely, $\left| \frac{\delta F(\mathbb{P}; \Psi^{\rightarrow j_{max}} \Big|_{\Delta^{j_{max}}}, \bar{\Psi}^{\rightarrow j_{max}} \Big|_{\Delta^{j_{max}}})}{\delta \Psi^{\rightarrow j_{max}}(\xi)} \right| + \left| \frac{\delta F(\mathbb{P}; \Psi^{\rightarrow j_{max}} \Big|_{\Delta^{j_{max}}}, \bar{\Psi}^{\rightarrow j_{max}} \Big|_{\Delta^{j_{max}}})}{\delta \bar{\Psi}^{\rightarrow j_{max}}(\xi)} \right| \neq 0$ if $\xi \in \Delta$. The *number of external fields* of \mathbb{P} is denoted by $N_{ext}(\mathbb{P})$.

In principle, the sum over all polymers can be bounded using **perturbative arguments** as follows. First we *fix* the location of one of the lowest-scale boxes, say, $\Delta_0 \in \mathbb{D}^{j_{max}}$, in order to avoid introducing diverging volume factors proportional to $|V|$, and let $\mathcal{P}_{\Delta_0}^{j_{max} \rightarrow}$ be the set of polymers \mathbb{P} in $\mathcal{P}^{j_{max} \rightarrow}$ such that $\Delta_0 \in \mathbb{P}$. In practice, Δ_0 may be seen as the approximate location of one of the external legs of the n -point function. Then the sum $\sum_{\mathbb{P} \in \mathcal{P}_{\Delta_0}^{j_{max} \rightarrow}} F(\mathbb{P})$ is controlled by two types of factors,

– *local factors*, $O(\lambda^\kappa)$ ($\kappa > 0$) for each vertex, in particular, for each box;

– *geometric factors* due to the fast-decaying propagators $C^{k,\alpha}(\xi, \xi')$.

Geometric factors make it possible to sum over all possible geometries and vertex number assignments $(n(\Delta))_\Delta$ for a given number of vertices, say, $n = n(\mathbb{P})$. Local factors ensure that the sum over n is bounded by a geometric series of the type $\sum_n (\lambda^\kappa)^n$.

Things are however not so simple. We have overlooked in the above quick overview extra *volume factors* due to the necessity, for $\Delta' \in \mathbb{P} \cap \mathbb{D}^k$ fixed, of summing over all $\Delta \in \mathbb{P} \cap \mathbb{D}^{k-1}$ lying above Δ' ; this necessity comes from the fact that only the locations of the *external legs* of the polymer (or, more or less equivalently, of $\Delta_0 \in \mathbb{D}^{j_{max}}$) are fixed. If there is a vertex in Δ , then this can be remedied by simply replacing λ^κ by a constant times λ^κ . However, it may well be that successive vertical links $\Delta \subset \Delta^{j+1} \subset \dots \subset \Delta^{k-1} \subset \Delta'$ connect $\Delta \in \mathbb{D}^j$ to Δ' through boxes $\Delta^{j+1}, \dots, \Delta^{k-1}$ void of any vertex. The sum over $\Delta^j \in \mathbb{D}^j$ such that $\Delta^j \subset \Delta'$ becomes an arbitrarily large *volume factor* $2^{3(k-j)}$ as the scale difference $k-j$ increases, eventually swallowing up the small factor λ^κ . However, multi-scale diagrams extending over several scales can be shown by simple power-counting arguments to be smaller than expected by some similar, exponential factor $\leq 2^{-c(k-j)}$, where c depends on the number N_{ext} of external legs. This is typically a situation which calls for *renormalization*; if there are enough links between the part of \mathbb{P} lying above Δ and Δ' , then the vertex power-counting beats the volume factor because $c > 3$; in this theory 6 links are a priori enough, but for technical reasons (due to the complexity of the sum over angular sectors of external legs, see §2.4 below), we shall follow the same procedure whenever $N_{ext} < N_0 := 8$. When $N_{ext} < N_0$, the renormalization procedure described in §2.2 should be applied. Subtracting the local part of a polymer is equivalent to *displacing all its external legs* to the location of one of them. Error terms (polymer) - (local part) have the same relative power-counting as if they had $\geq N_0$ external legs, whence they *are indeed* considered as if they did have $\geq N_0$ external legs. On the other hand, local parts are *resummed* by defining scale-dependent constants μ^j, m^j, Γ^j , at the price of some easy partial resummation of the series of polymers, called *Mayer expansion*, which takes into account the non-overlapping constraints between boxes, and whose outcome is a sum over *Mayer polymers*. At this stage, it is enough to know that the Mayerization step involves a "multicolor" version of the theory, with one color per polymer. Then previously developed links connect boxes of the same color, while Mayer polymers are multicolor polymers connected by *overlap links* between different colored versions of the same two boxes. Painting all boxes gray, Mayer polymers are then polymers in the usual sense, with some extra overlap links connecting a box to itself. Summing over Mayer polymers in $\mathcal{P}_0^{j_D} = \{\mathbb{P} \in \mathcal{P}^{j_D} \mid N_{ext}(\mathbb{P}) = 0\}$, one obtains e.g. for the theory restricted to scale j_D

$$\mathcal{Z}_{\lambda, V}^{j_D} = \sum_{N=0}^{\infty} \frac{1}{N!} \sum_{\mathbb{P}_1, \dots, \mathbb{P}_N \in \mathcal{P}_0^{j_D}} \prod_{n=1}^N F(\mathbb{P}_n) \approx_{|V| \rightarrow \infty} e^{|V| f^{j_D}(\lambda)} \quad (2.71)$$

in the sense that $\frac{1}{|V|} \log \mathcal{Z}_{\lambda, V}^{j_D} \rightarrow_{|V| \rightarrow \infty} f^{j_D}(\lambda)$, where (fixing some box $\Delta_0 \in \mathbb{D}^{j_D}$ in

an arbitrary way) $|V|$ is the volume of V , defined as the number of scale j_D boxes lying inside V , and $f^{j_D}(\lambda) = \sum_{\mathbb{P} \in \mathcal{P}_0^{j_D} \mid \Delta_0 \in \mathbb{P}} F(\mathbb{P})$ is interpreted as the *scale j_D free energy density*. Going further down the scales, the general task is to prove that $\mathcal{Z}_{\lambda, V}^{j \rightarrow} \approx_{|V| \rightarrow \infty} \prod_{k=j}^{j_D} e^{|V| f^k(\lambda)}$, where $f^k(\lambda)$ – similarly interpreted as a scale j free energy density – is obtained by summing over Mayer polymers in $\mathcal{P}^{k \rightarrow}$.

In general, the *coupling constant* λ should also be made scale-dependent, following the above local part resummation pattern. However, the specificity of this model (as explained in the Introduction) is that the "local part" of the main diagrams contributing to the renormalization of λ , making up the Bethe-Salpeter kernel, must be resummed **nonperturbatively** as a series. This strongly model-dependent, nonperturbative step is performed separately, by expanding successively Cooper pairs with transfer momentum q of scales $j_+ = j'_\phi, j'_\phi + 1, j'_\phi + 2, \dots$ down to the lowest infra-red scales. It will be described in the section about the bosonic regime (section 3).

Down to scale $j'_\phi - 1$, however, namely, in the present section, much simpler arguments suffice. Namely, one may *systematically expand chains of bubbles*. Looking more specifically e.g. at the first resummation step of the sequence of fermionic expansions, chains of bubbles with scale j_D fermionic propagators are first considered as contracted external legs of scale j_D fermionic diagrams, and resummed systematically before expanding external legs of scale $\geq j_D + 1$; in some sense, this procedure may be seen as an expansion in itself, of scale " $j_D + \frac{1}{2}$ " intermediate between j_D and $j_D + 1$. Similarly, the resummation of lowest scale j chains of bubbles may be considered as an expansion step of scale " $j + \frac{1}{2}$ ".

The reader will have to wait until §2.4 to have a comprehensive image of how polymers of lowest scale $\leq j'_\phi - 1$ are bounded. It is however not straightforward to understand how all arguments fit together. Therefore, we shall first present a single-scale bound for the outcome of the horizontal cluster expansion in §2.3.1. The bounds of §2.4 cover the whole fermionic regime down to scale $j'_\phi - 1$ and take into account bubble resummations.

2.3.1 Horizontal cluster expansion

Let \mathbf{s} be a family of functions $\mathbf{s} := (s^j)_{j=j_D, \dots, j'_\phi}$, with

$$s^j : \{\Delta, \Delta'\} \rightarrow s_{\Delta, \Delta'}^j \in [0, 1] \quad \Delta, \Delta' \in \mathbb{D}^j, \Delta \neq \Delta' \quad (2.72)$$

extended trivially to the diagonal by letting $s_{\Delta, \Delta}^j \equiv 1$ ($\Delta \in \mathbb{D}^j$). (Later on, we shall use slightly generalized functions, defined on pairs of *clusters*, where clusters are unions of boxes of the same scale). As we shall see, the set of coefficients $(s_{\Delta, \Delta'}^j)$ for j fixed, called *scale j weakening coefficients*, defines an interpolation between the initial covariance $C^{j, \alpha}(s^j = 1) \equiv C^{j, \alpha}$ and the box-diagonal covariances $C^{j, \alpha}(s^j = 0)$ for which fields lying in different boxes have been made independent, namely, $C^{j, \alpha}(s^j = 0; \xi, \xi') \equiv 0$ if $\xi \in \Delta, \xi' \in \Delta', \Delta \neq \Delta' \in \mathbb{D}^j$.

Index notations: it is often useful or simply convenient to use different indices for external Ψ - and $\bar{\Psi}$ -fields; thus we shall often index the Ψ -fields and their coordinates ξ by an index i ranging in some abstract set $\subset \{1, \dots, n\} \subset \mathbb{N}$, and the $\bar{\Psi}$ -fields and their coordinates $\bar{\xi}$ by an index \bar{i} ranging in some abstract set $\subset \{\bar{1}, \dots, \bar{n}\} \subset \bar{\mathbb{N}}$, where $\bar{\mathbb{N}}$ is a copy of \mathbb{N} . On the other hand, on other occasions it will be more convenient to use "neutral" notations which do not distinguish between Ψ 's and $\bar{\Psi}$'s; for instance, if $I \equiv J \uplus \bar{J}$, $J \subset \{1, \dots, n\}$, $\bar{J} \subset \{\bar{1}, \dots, \bar{n}\}$, then $\boldsymbol{\xi}_I := (\xi_{ext,i})_{i \in I}$, $\boldsymbol{\Psi}_I := (\Psi_i(\xi_{ext,i}))_{i \in J}, (\bar{\Psi}_{\bar{i}}(\bar{\xi}_{ext,\bar{i}}))_{\bar{i} \in \bar{J}}$.

Horizontal cluster expansion of scale j_D . In order to compute the connected n -point function

$$\begin{aligned}
G_{n,\bar{n}}(\boldsymbol{\xi}_{ext}, \bar{\boldsymbol{\xi}}_{ext}) &\equiv G_{\{1,\dots,n\} \uplus \{\bar{1},\dots,\bar{n}\}}((\xi_{ext,i})_{i=1,\dots,n}, (\bar{\xi}_{ext,\bar{i}})_{\bar{i}=\bar{1},\dots,\bar{n}}) \\
&:= \left\langle \left(\prod_{i=1}^n \Psi_{\sigma_i}(\xi_{ext,i}) \right) \left(\prod_{\bar{i}=\bar{1}}^{\bar{n}} \bar{\Psi}_{\sigma_{\bar{i}}}(\bar{\xi}_{ext,\bar{i}}) \right) \right\rangle_{\theta;\lambda}^c \\
&\equiv \int d\mu_{\theta;\lambda}(\Psi, \bar{\Psi}) \left(\prod_{i=1}^n \Psi_{\sigma_i}(\xi_{ext,i}) \right) \left(\prod_{\bar{i}=\bar{1}}^{\bar{n}} \bar{\Psi}_{\sigma_{\bar{i}}}(\bar{\xi}_{ext,\bar{i}}) \right) \\
&\quad - \sum_{k \geq 2} \sum_{I_1 \uplus \dots \uplus I_k = \{1,\dots,n\} \uplus \{\bar{1},\dots,\bar{n}\}} \prod_{i=1}^k G_{I_i}(\boldsymbol{\xi}_{I_i})
\end{aligned} \tag{2.73}$$

one applies a Brydges-Kennedy-type expansion, see Appendix, §5.2, to the numerator

$$F_{n,\bar{n}}(s^{j_D}; \boldsymbol{\xi}_{ext}, \bar{\boldsymbol{\xi}}_{ext}) := \int d\mu_{\theta}^*(\boldsymbol{s}; \Psi, \bar{\Psi}) e^{-\mathcal{L}_{\theta}(\Psi, \bar{\Psi})} \left(\prod_{i=1}^n \Psi_{\sigma_i}(\xi_{ext,i}) \right) \left(\prod_{\bar{i}=\bar{1}}^{\bar{n}} \bar{\Psi}_{\sigma_{\bar{i}}}(\bar{\xi}_{ext,\bar{i}}) \right), \tag{2.74}$$

where $d\mu_{\theta}^*(s^{j_D}; \cdot)$ is the free Grassmann measure on $V \times V$ with weakened two-by-two matrix covariance kernel

$$C_{\theta}^*(s^{j_D}) \equiv C_{\theta}^{j_D, \alpha}(s^{j_D}) + C_{\theta}^{\rightarrow(j+1)}, \tag{2.75}$$

$$C_{\theta}^{j_D, \alpha}(s^{j_D}; \xi, \xi') := \sum_{\Delta, \Delta' \in \mathbb{D}^{j_D}} \chi_{\Delta}(\xi) \chi_{\Delta'}(\xi') s_{\Delta, \Delta'}^{j_D} C_{\theta}^{j_D, \alpha}(\xi, \xi'), \tag{2.76}$$

where $s^{j_D} : L(\mathbb{D}^{j_D}) \equiv \{\{\Delta, \Delta'\} \in \mathbb{D}^{j_D} \times \mathbb{D}^{j_D} \mid \Delta \neq \Delta'\} \rightarrow [0, 1]$ are sets of *weakening coefficients* which (as their name indicates) weaken the covariance kernels $C_{\theta}^{j_D, \alpha}(\xi, \xi')$ when ξ, ξ' lie in different boxes. The function s^{j_D} is implicitly trivially extended to the diagonal by letting $s_{\Delta, \Delta}^{j_D} \equiv 1$, $\Delta \in \mathbb{D}^{j_D}$. The unnormalized (n, \bar{n}) -point functions $F_{n,\bar{n}}(s^{j_D}; \boldsymbol{\xi}, \bar{\boldsymbol{\xi}})$ interpolate between the original (n, \bar{n}) -point function $F_{n,\bar{n}}(\mathbf{1}; \boldsymbol{\xi}, \bar{\boldsymbol{\xi}}) \propto G_{n,\bar{n}}(\boldsymbol{\xi}, \bar{\boldsymbol{\xi}})$ and the unnormalized (n, \bar{n}) -point function $F_{n,\bar{n}}(\mathbf{0}; \boldsymbol{\xi}, \bar{\boldsymbol{\xi}})$ computed in a totally decoupled theory. The BKAR formula (§5.2, Proposition 5.2)

yields

$$\begin{aligned}
F_{n,\bar{n}}(\boldsymbol{\xi}_{ext}, \bar{\boldsymbol{\xi}}_{ext}) &= \sum_{I^{jD} \subset I} \sum_{\mathbb{F}^{jD} \in \mathcal{F}^{jD}} \left[\prod_{\ell \in L(\mathbb{F}^{jD})} \int_0^1 dw_\ell^{jD} \int_{\Delta_\ell} d\xi_\ell \int_{\Delta'_\ell} d\xi'_\ell \right] \\
&\int d\mu_\theta^*(s^{jD}(\mathbf{w}^{jD}))(\Psi, \bar{\Psi}) \text{Hor}^{jD} \left(\prod_{i \in I^{jD}} \Psi^{jD}(\xi_{ext,i}) \cdot e^{-\mathcal{L}_\theta(\Psi, \bar{\Psi})} \right) \cdot \left(\prod_{i \notin I^{jD}} \Psi^{\rightarrow(jD+1)}(\xi_{ext,i}) \right)
\end{aligned} \tag{2.77}$$

Induction on j . Let $\mathcal{P}_{N_{ext}}^{j \rightarrow}$, resp. $\mathcal{P}_{\geq N_{ext}}^{j \rightarrow}$ be the set of Mayer polymers with lowest scale j and N_{ext} , resp. $\geq N_{ext}$ external fields. We assume by induction on j that $F_{n,\bar{n}}(\boldsymbol{\xi}_{ext}, \bar{\boldsymbol{\xi}}_{ext})$ has been rewritten as

$$\prod_{k=j_D}^{j-1} e^{|V|f^k(\theta;\lambda)} \sum_{I \subset \{1, \dots, n\} \uplus \{\bar{1}, \dots, \bar{n}\}} F_I^{(j-1) \rightarrow}(\boldsymbol{\xi}_{ext}, \bar{\boldsymbol{\xi}}_{ext}), \tag{2.78}$$

where

$$F_I^{(j-1) \rightarrow}(\boldsymbol{\xi}_{ext}, \bar{\boldsymbol{\xi}}_{ext}) = \int d\mu_\theta^*(\Psi^{\rightarrow j}, \bar{\Psi}^{\rightarrow j}) e^{-\mathcal{L}_\theta(\Psi^{\rightarrow j}, \bar{\Psi}^{\rightarrow j})} \left(\prod_{i \notin I} \Psi_{\sigma_i}^{\rightarrow j}(\xi_i) \right) G_I^{(j-1) \rightarrow}(\boldsymbol{\xi}_I), \tag{2.79}$$

and $G_I^{(j-1) \rightarrow}(\cdot)$ is expressed in terms of a sum over Mayer polymers $\mathbb{P}_1, \dots, \mathbb{P}_N$ extending down to scale $j-1$,

$$G_I^{(j-1) \rightarrow}(\boldsymbol{\xi}_I) = \sum_{n=1}^{\infty} \frac{1}{n!} \sum_{\mathbb{P}_1, \dots, \mathbb{P}_n \in \mathcal{P}_{\geq 4}^{(j-1) \rightarrow}} \sum_{I_1, \dots, I_n} \prod_{i=1}^n F^{j-1}(\mathbb{P}_i; \Psi^{\rightarrow j}, \bar{\Psi}^{\rightarrow j}; \boldsymbol{\xi}_{I_i}). \tag{2.80}$$

The expression involves a sum over all possible assignments of the external field indices to the various polymers, so that $I = I_1 \uplus \dots \uplus I_n$; the function $F^{j-1}(\mathbb{P}_i; \Psi^{\rightarrow j}, \bar{\Psi}^{\rightarrow j}; \boldsymbol{\xi}_{I_i})$ is obtained by contracting in a certain way the external fields $\Psi^{(j-1) \rightarrow}(\xi_p)$, $p \in I_i$ with the interaction or between themselves. The function $F^{j-1}(\mathbb{P}_i; \Psi^{\rightarrow j}, \bar{\Psi}^{\rightarrow j}; \boldsymbol{\xi}_{I_i})$ depends (polynomially) on the fields $\Psi^{\rightarrow j}, \bar{\Psi}^{\rightarrow j}$ through the external structure of \mathbb{P}_i . By assumption only Mayer polymers with $N_{ext} \geq 4$ external fields are considered in the sum; the reason is that

(i) *vacuum polymers* (i.e. polymers with $N_{ext} = 0$) have been resummed into the scale free energies;

(ii) *two-point polymers* (i.e. polymers with $N_{ext} = 2$) have been absorbed into the renormalization of the parameters μ, m, Γ ;

We shall *not* decouple boxes $\Delta, \Delta' \in \mathbb{D}^j$ vertically connected to two boxes of scale $j-1$ belonging to the same polymer $\mathbb{P} \in \mathcal{P}^{(j-1) \rightarrow}$, since they are **connected from above**. Identifying all such sets of boxes defines a set of objects \mathcal{O}^j , which are unions

of boxes in \mathbb{D}^j . Thus it is enough to introduce a weakening function $s^j : L(\mathcal{O}^j) \rightarrow [0, 1]$, with $L(\mathcal{O}^j) \equiv \{\{o, o'\} \in \mathcal{O}^j \times \mathcal{O}^j \mid o \neq o'\}$. Replace in (2.79) the integral $\int d\mu_\theta^*(\Psi^{\rightarrow j}, \bar{\Psi}^{\rightarrow j}) e^{-\mathcal{L}_\theta(\Psi^{\rightarrow j}, \bar{\Psi}^{\rightarrow j})}$ with

$$\int d\mu_\theta^*(s^j)((T\Psi)^{\rightarrow j}, (T\bar{\Psi})^{\rightarrow j}) e^{-\mathcal{L}_\theta((T\Psi)^{\rightarrow j}, (T\bar{\Psi})^{\rightarrow j})}. \quad (2.81)$$

Horizontal cluster expansion of scale $j \leq j'_\phi - 1$. Start from the expression (2.81), and proceed as we did at scale j_D :

$$\begin{aligned} F_I^{(j-1)\rightarrow}(\xi_{ext}, \bar{\xi}_{ext}) &= \sum_{I^j \subset I} \sum_{\mathbb{F}^j \in \mathcal{F}^j} \left[\prod_{\ell \in L(\mathbb{F}^j)} \int_0^1 dw_\ell^j \int_{\Delta_\ell} d\xi_\ell \int_{\Delta'_\ell} d\xi'_\ell \right] \cdot \\ &\cdot \int d\mu_\theta^*(s^j(\mathbf{w}^j))(\Psi^{\rightarrow j}, \bar{\Psi}^{\rightarrow j}) \tilde{G}_{I^j}^{(j-1)\rightarrow}(\xi_I), \\ \tilde{G}_{I^j}^{(j-1)\rightarrow}(\xi_I) &:= \text{Hor}^j \left(\prod_{i \in I^j} \Psi^j(\xi_{ext,i}) \cdot e^{-\mathcal{L}_\theta(\Psi^{\rightarrow j}, \bar{\Psi}^{\rightarrow j})} \right) \cdot \left(\prod_{i \notin I^j} \Psi^{\rightarrow(j+1)}(\xi_i) \right) \end{aligned} \quad (2.82)$$

The above scale j horizontal cluster expansion has produced *step j polymers* $\mathbb{P}_1, \dots, \mathbb{P}_n$ in $\mathcal{P}^{j\rightarrow}$, described as follows:

- $\mathbb{P}_i \cap \mathbb{D}^{(j-1)\rightarrow}$ is a union of the polymers in $\mathcal{P}^{(j-1)\rightarrow}$ obtained at the end of the scale $(j-1)$ perturbative expansions;
- $\mathbb{P}_i \cap \mathbb{D}^j, i = 1, \dots, n$ is a union of clusters belonging to \mathcal{O}^j .

More precisely: two step $(j-1)$ polymers $\mathbb{P}_1, \mathbb{P}_2 \in \mathcal{P}^{(j-1)\rightarrow}$ are connected after step j if and only if there exist two horizontally connected boxes $\Delta'_1, \Delta'_2 \in \mathbb{D}^j$ (i.e. boxes belonging to the same step j polymer) and two boxes $\Delta_1 \in \mathbb{P}_1 \cap \mathbb{D}^{j-1}, \Delta_2 \in \mathbb{P}_2 \cap \mathbb{D}^{j-1}$ such that Δ_1 , resp. Δ_2 is vertically connected to Δ'_1 , resp. Δ'_2 ; in other words, if $\mathbb{P}_1, \mathbb{P}_2$ are **connected from below**.

Polymers $\mathbb{P}_1, \dots, \mathbb{P}_n$ with $N_{ext} < N_0 := 8$ external legs have been "mayerized" at scales $\leq j-1$, but not at scale j , which means that they are **non- j -overlapping**: $\mathbb{P}_i \cap \mathbb{D}^{(j-1)\rightarrow}, i = 1, \dots, n$ are free to overlap, but $(\mathbb{P}_i \cap \mathbb{D}^j) \cap (\mathbb{P}_{i'} \cap \mathbb{D}^j) = \emptyset$ if $i \neq i'$.

The final outcome of the set of scale j expansions for a given scale j can be found in §2.3.4, see (2.107).

2.3.2 Single-scale bounds

In this preliminary version of our final bounds, we present a bound for a single-scale *amputated* diagram. It is correct, but not fully conclusive, because it fails to take into account bubbles in an effective way, which will be done only in §2.3.3; as we

shall see, the core principles are left unchanged by bubble resummations, but power-counting estimates are modified in an essential way. Fix $j_D \leq j \leq j'_\phi - 1$, and assume we want to bound some connected, amputated N_{ext} -point function $F^j(\boldsymbol{\xi}_I)$, $\boldsymbol{\xi}_I \equiv (\xi_{ext,1}, \dots, \xi_{ext, \frac{N_{ext}}{2}}, \bar{\xi}_{ext,1}, \dots, \bar{\xi}_{ext, \frac{N_{ext}}{2}})$,

$$F^j(\boldsymbol{\xi}_I) = \left(\prod_{i=1}^{N_{ext}/2} \frac{\delta}{\delta \Phi^j(\xi_i)} \right) \Big|_{\Phi^j=0} \left(\prod_{i=1}^{N_{ext}/2} \frac{\delta}{\delta \bar{\Phi}^j(\xi_i)} \right) \Big|_{\bar{\Phi}^j=0} \log \left(\int d\mu_\theta^*(\Psi^j + \Phi^j, \bar{\Psi}^j + \bar{\Phi}^j) \left(e^{-\mathcal{L}_\theta(\Psi^j + \Phi^j, \bar{\Psi}^j + \bar{\Phi}^j)} \right) \right), \quad (2.83)$$

a sum of connected diagrams. In this subsection, we do not want to distinguish between ξ 's and $\bar{\xi}$'s, and shift consequently to a neutral notation, $\boldsymbol{\xi}_{ext} := (\xi_{ext,1}, \dots, \xi_{ext, N_{ext}})$. Scale j cluster expansions do not produce directly $F^j(\boldsymbol{\xi}_I)$, but a sum $\sum_{\mathbb{P}} \mathcal{A}(\mathbb{P}; \boldsymbol{\xi}_{ext})$ over scale j polymers \mathbb{P} with N_{ext} external fields located in $\xi_{ext,i} \in \Delta_{ext,i}, \Delta_{ext,1}, \dots, \Delta_{ext, N_{ext}} \in \mathbb{D}^j$. Polymers are in principle evaluated by expanding as a sum over Feynman diagrams; however, diagrams differing by merely *exchanging* vertices belonging to the same box should be evaluated together: their sum is much smaller than expected due to sign compensations (see arguments in §5.3 and later explanations). In coherence with the logic of multi-scale cluster expansions, we are really interested in power-counting estimates for the integrated quantities

$$\mathcal{A}(\mathbb{P}; \xi_{ext,1}) := \left(\prod_{i=2}^{N_{ext}} m^* \mu^2 \int_{\Delta_{ext,i}} d\xi_{ext,i} \right) \mathcal{A}(\mathbb{P}; \boldsymbol{\xi}_{ext}). \quad (2.84)$$

The dimensional factors $m^* \mu^2 \approx \frac{1}{\text{Vol}(\Delta^0)}$, $\Delta^0 \in \mathbb{D}^0$ are chosen in such a way that $m^* \mu^2 \int_{\Delta_{ext,i}} d\xi_{ext,i} \approx 2^{3j}$ is a non-dimensional scaling factor, so that $\mathcal{A}(\mathbb{P}; \xi_{ext,1})$ has the same dimensionality as that of an amputated N_{ext} -point function. The fixed vertex location $\xi_{ext,1}$ will be integrated later on at some lower scale (equal to the scale of one of the low-momentum external fields attached at $\xi_{ext,1}$).

Single-scale bounds for a given diagram with fixed sectors. Let us first bound the contribution to $\mathcal{A}(\mathbb{P}; \xi_{ext,1})$ of a *single diagram* $\mathcal{A}^{j,\alpha}(\Upsilon; \xi_1)$, with angular sectors of all internal lines fixed. Because of the sign issue mentioned above (easily solved by summing over permutations of vertices located in the same box), but mainly because the present power-counting principle overlooks the main problem – which consists in summing over the different choices of angular sectors –, this paragraph can only be of pedagogical value, therefore it can be skipped. Here are two examples of polymers with $N_{ext} = 4$ external legs. Black lines are cluster links. We actually selected contributions to the polymers containing only one vertex per box (or cluster),

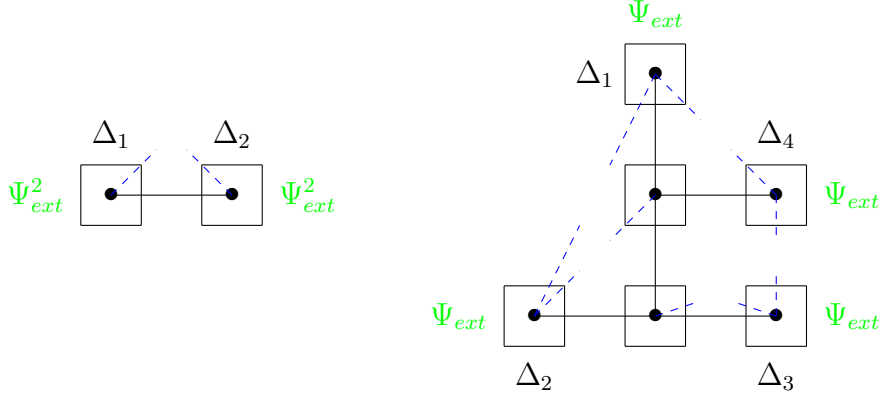


Fig. 2.3.2. Examples of cluster trees for a diagram with four external legs.

with $\xi_{ext,i} \in \Delta_i$, $\Delta_i \in \mathcal{O}^j$. Locations of external fields are indicated by the symbol Ψ_{ext} (in green). Dashed lines (in blue) indicate unpaired fields. In general there may be more than one vertex per box, hence many more unpaired lines than cluster links. Pairing unpaired fields using Wick's theorem, we obtain Feynman diagrams, e.g.

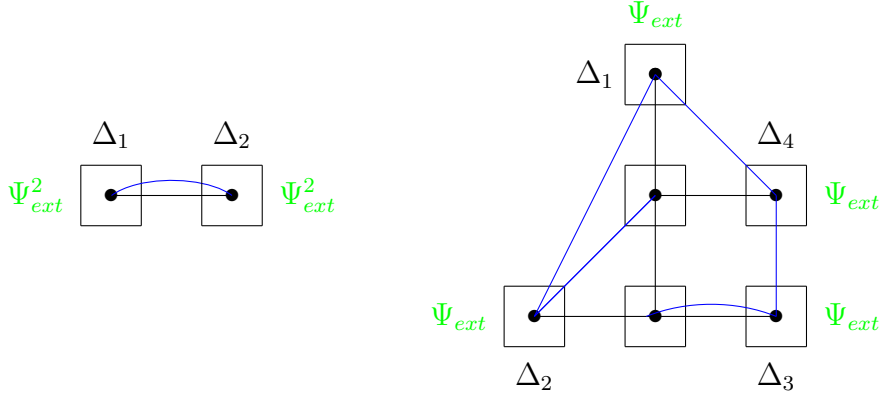


Fig. 2.3.3. For the bubble diagram (left), $N_{ext} = 4$ (in green), $n = 2$, $I_{tree} = 1$ (in black), $L = 1$ (in blue), $I = I_{tree} + L = 2$. Similarly, for the other diagram, $N_{ext} = 4$, $n = 6$, $I_{tree} = 5$, $L = 5$, $I = I_{tree} + L = 10$.

General topological properties of a Feynman graph Υ with n four-valent vertices, L loops, I internal lines ($2I$ internal fields) and N_{ext} external legs imply that

$$L - I + n = 1, \quad N_{ext} = 4n - 2I. \quad (2.85)$$

These relations give a quick power-counting argument for the evaluation of an amputated diagram *with fixed angular sectors*. Choose some spanning tree \mathfrak{t} (which may be e.g. the cluster tree in the above examples, but in general, \mathfrak{t} has much more vertices and edges than \mathbb{T} ; in fact one may take $\mathfrak{t} \supset \mathbb{T}$). Internal lines are split into $I_{tree} = n - 1$ internal lines on the spanning tree (in black) – in this very particular example, cluster links – and $L = I_{tree} - \frac{1}{2}(N_{ext} - 4)$ lines generating the loops (in blue). All together, $I = I_{tree} + L = 2I_{tree} - \frac{1}{2}(N_{ext} - 4)$.

Now, fixing $\xi_{ext,1}$ and integrating the other $\xi_{ext,i}$'s in their respective boxes, one obtains an overall scaling factor

$$(2^{3j})^{n-1}(2^{-2j})^I = (2^{3j})^{I_{tree}}(2^{-2j})^{2I_{tree}-\frac{1}{2}(N_{ext}-4)} = (2^{-j})^L(2^{-j})^{\frac{1}{2}(4-N_{ext})}, \quad (2.86)$$

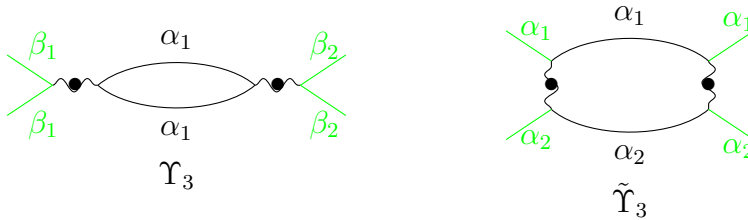
which takes into account the integration of vertices over their respective boxes, and the pre-scaling factor $O(2^{-2j})$ of each propagator $C_\theta^{j,\alpha}$, see Proposition 2.3.

Counting one sum over angular sector assignments per loop yields a *total scaling factor* $(2^{-j})^{\frac{1}{2}(4-N_{ext})}$, characteristic of a just renormalizable theory with four-valent vertices. However, our aim is to prove that diagrams are *smaller* than that by a factor of the type $O(N_j^{-cn})$ for some constant $c > 0$, with $N_j := 2^j$, providing the basis for the $1/N$ -expansion.

Single-scale bounds for a given polymer. We shall actually use a different power-counting argument, not based on general topological properties of a Feynman graph, but on the concept of *total weight per vertex* (see below). Previous considerations – see Proposition 2.5 and the bound just below for the integrated vertex $I^j(\Delta^j)$ – imply that the leading behavior is obtained by assuming that sectors $\alpha_1, \alpha_2, \alpha_3, \alpha_4$ on a given vertex satisfy up to some permutation

$$|\alpha_1 - \alpha_3|, |\alpha_2 - \alpha_4| \approx 2^{j-k} \lesssim |\alpha_1 + \alpha_2| \lesssim 2^k \quad (2.87)$$

for some $k \in \{\lfloor \frac{j}{2} \rfloor, \dots, j\}$. We then *decide* that α_1, α_3 are on the same fermion loop, and similarly for α_2, α_4 . Generically, $k = j$, $|\alpha_1 + \alpha_2| \approx 2^j$, $|\alpha_1 - \alpha_3| \approx 1$ so it makes sense (at least graphically) to assume that the angular sector along a fermion loop is constant. Following loops, one obtains e.g.



for the bubble diagram, and

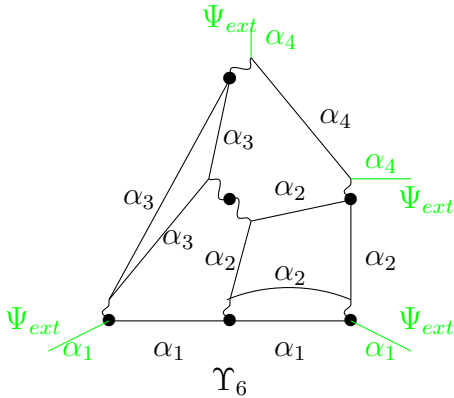


Fig. 2.3.4. Loop decompositions. Loop lengths are $L(\alpha_1) = 2, L(\beta_1) = L(\beta_2) = 0$ (Υ_3), $L(\alpha_1) = L(\alpha_2) = 1$ ($\tilde{\Upsilon}_3$), $L(\alpha_4) = 1, L(\alpha_1) = 2, L(\alpha_3) = 3, L(\alpha_2) = 4$.

for the other diagram. The diagram Υ_3 is the usual Cooper bubble diagram. Define the *length* L of a loop to be the number of internal propagators belonging to it, see Figures above. Considering the generic case, we see that there are e.g. only $L' = 4 < L = 5$ independent sector assignments for Υ_6 . In $\tilde{\Upsilon}_3$, the external sectors β_1, β_2 keep *outside* the diagram; in all other cases, there are *broken loops*, finishing with two external legs, for instance, the loop with sector α_1 in Υ_6 .

Note that, by splitting vertices into half vertices, one has rewritten the original bubble diagram into the sum of two contributions: a *bubble*, Υ_3 , and another diagram, $\tilde{\Upsilon}_3$, which is of a different nature. *Bubbles*, in this sense, are characterized that they make up a *loop of length 2*. *Loops of length 1*, such as α_1, α_2 in $\tilde{\Upsilon}_3$ or α_4 in Υ_6 , are called **incomplete bubbles** because external propagators may contract at some lower scale to form a full, multi-scale bubble, implying the possibility of obtaining chains of multi-scale bubbles of arbitrary lengths,

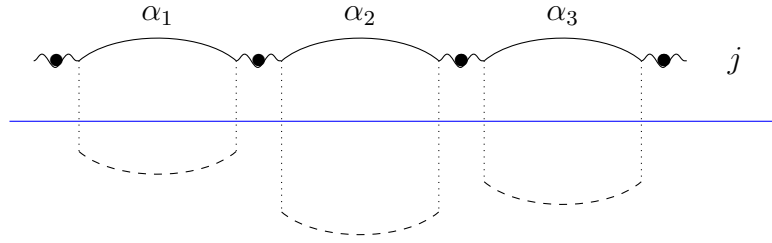


Fig. 2.3.5. A chain of 3 incomplete upper scale j bubbles, possibly completed at lower scales into a chain of multi-scale bubbles.

Let us start with the argument. First of all, single scale polymers must be prepared as in [45], Proposition 5.3, by displacing all fields lying in a scale j box or sub-box to the same location; see Appendix, §5.3 for a description of the procedure. Because of the fermionic nature of the fields $(\Psi^{j,\alpha})_\alpha, (\bar{\Psi}^{j,\alpha})_\alpha$, there remains only contributions with at most *one* field $\Psi^{j,\alpha}$ or $\bar{\Psi}^{j,\alpha}$ per box, and terms featuring gradient fields $(\nabla - ip^\alpha)^\kappa \Psi^{j,\alpha}, (\nabla + ip^\alpha)^\kappa \bar{\Psi}^{j,\alpha}$ integrated over sub-boxes. The net outcome is a sum over Feynman diagrams with supplementary gradients, inducing an overall scaling factor bounded by

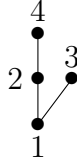
$$C_r^n \prod_{\Delta} \prod_{\alpha} \frac{1}{(n_{\Delta,\alpha})^r (\bar{n}_{\Delta,\alpha})^r} \quad (2.88)$$

for every $r \geq 0$, where $n_{\Delta,\alpha}$, resp. $\bar{n}_{\Delta,\alpha}$ is the number of $\Psi^{j,\alpha}$, resp. $\bar{\Psi}^{j,\alpha}$ -fields in the scale j box Δ .

Choose now a set of (not necessarily distinct) boxes $\mathbf{\Delta} \equiv \{\Delta_1, \dots, \Delta_n\} \subset \mathbb{D}^j$ such that $\Delta_{ext,i} \subset \mathbf{\Delta}$, and some **loop structure** $\gamma \equiv \{\gamma_1, \dots, \gamma_{L'}\}$, namely, an equivalence set of Feynman diagrams with fixed topological structure – allowing the permutation

of vertices located in the same box – and sector assignment compatible with the above set of loops, i.e. satisfying (2.87). We shall compute to begin with an upper bound to the power-counting of the sum of all Feynman diagrams in the equivalence set (Δ, γ) , *including the integration of ξ_1 in its box, the power-counting of external legs, and the sum over external sectors*. The main task consists in summing over angular sector attributions of each vertex. In order not to lose the benefit of (2.88), we *fix* a set of integers $n_{\Delta,i}, \bar{n}_{\Delta,i} \geq 0, i = 1, \dots, 2^j$ and restrict to diagrams such that each list $\{n_{\Delta,\alpha}, \alpha \in \mathbb{Z}/2^j\mathbb{Z}\}$ is some *permutation* of the list $\{n_{\Delta,i}, i = 1, \dots, 2^j\}$. The power-counting proceeds as follows:

(i) First select a "loop spanning tree", i.e. a tree \mathfrak{t}' connecting the loops. This may be done inductively by choosing γ_1 for a root; then connecting γ_1 successively to all loops $\gamma_{i_1}, \dots, \gamma_{i_{n_1}}$ ($1 \neq i_1 < \dots < i_{n_1}$) such that there is a vertex connecting two successive moments along γ_1 to two successive moments along $\gamma_{i_k}, k = 1, \dots, n_1$; then connecting γ_{i_1} successively to all loops $\gamma_{i'_1}, \dots, \gamma_{i'_{n_{i_1}}}$ *other than those previously chosen* such that there is a vertex connecting two successive moments along γ_{i_1} to two successive moments along $\gamma_{i'_k}, k = 1, \dots, n_{i_1}$; and so on, until all loops have been exhausted. For instance, choosing γ_1 to be the loop with sector α_1 in Υ_6 , the loop



spanning tree associated to Υ_6 is

(ii) Reorder loops by using depth-first search algorithm on \mathfrak{t}' . In the case of Υ_6 , the algorithm visits successively vertices 1, 2, 4 and 3, so loops are reordered by permuting indices 3 and 4.

(iii) Order the vertices $v_{i,p}, p = 1, \dots, n_i$ along γ_i in such a way that vertices connecting γ_i to its *descendant loops* on the loop spanning tree (e.g. γ_1 to γ_2, γ_4 for \mathfrak{t}' , with its loop reindexing defined in (ii)) are $v_{i,1}, \dots, v_{i,n'_i}$. Then choose some propagator along γ_i , denote by $\alpha_{i,1}$ its sector, go around the loop in some arbitrary direction starting from $\alpha_{i,1}$, and index the successive sectors by $\alpha_{i,1}, \dots, \alpha_{i,n_i}$. Write $k_v = k$ if v is a vertex along γ_i connecting the momentum in the sector $\alpha_{i,p}$ to the momentum in the sector $\alpha_{i,p+1}$, and $\lfloor \log_2 \left(1 + |\alpha_{i,p} - \alpha_{i,p+1}| \right) \rfloor = j - k, k \in \{\lfloor \frac{j}{2} \rfloor, \dots, j\}$. This means the following: *there are $O(2^{j-k})$ possibilities for $\alpha_{i,p+1}$ for $\alpha_{i,p}$ fixed*.

(iv) Let $\delta_j := \begin{cases} 0 & (j \leq j_\phi) \\ j - j_\phi & (j > j_\phi) \end{cases}$. The power-counting associated to a vertex v with its 4 legs (see (2.13)) is $O(\lambda \times \frac{1}{m^* \mu^2} 2^{3j} \times (2^{-j} 2^{-\delta_j/2} p_F^*)^4) = O(g 2^{-j} 2^{-2\delta_j})$ (hence roughly a factor $O(2^{-j})$ per vertex or per loop, compare with (2.86)), *times* 2^{j-k_v} , all together $O(g \times 2^{-k_v})$, that is, a $(\frac{1}{N})$ -*type* factor, generically but not always $O(N_j) = O(2^{-j})$.

(v) (*overall rotation factor $O(2^j)$*) Consider one of the connecting vertices $v = v_{i,1}, \dots, v_{i,n'_i}$ along γ_i , see (iii). Denote by $(\alpha_1, \alpha_3) = (\alpha_{i,p}, \alpha_{i,p+1}), (\alpha_2, \alpha_4) = (\alpha_{i',p'}, \alpha_{i',p'+1})$ ($i < i'$) its two halves, one on γ_i , the other on $\gamma_{i'}$. Summing over α_2 for α_1 fixed (see

(2.87)) yields a factor $O(2^{k_v})$ compensating the factor $O(2^{-k_v})$ in (iv). Now *local rotation invariance* has almost been fixed: choose some sector along γ_1 (2^j possibilities), then the factors $O(2^{k_v})$ associated to connecting vertices fix one sector on every other loop.

(vi) (*total weight associated to a connecting vertex*) Let $v = v_{i,p}$, $p \leq n'_i$ be a connecting vertex. Given (iv), (v), there remains only a small factor $O(g)$, and a sum over all possible values of k_v in $\{\lfloor \frac{j}{2} \rfloor, \dots, j\}$, all together a factor $O(gj2^{-2\delta j}) = O(1)$ if $j \leq j_\phi \approx g^{-1}$. If $j > j_\phi$ then $O(gj2^{-2\delta j})$ is small, but this is actually very deceptive because of bubble resummations (see §2.3.3). The power-counting for connecting vertices *associated to bubbles* is better than that and computed in (viii) below.

(vii) (*total weight associated to a non-connecting vertex*) Let $v = v_{i,n}$, $n > n'_i$ be a non-connecting vertex. Given (iv), its total weight is $\leq \sum_{k_v} g2^{-k_v}2^{-2\delta j} \lesssim g2^{-j/2}2^{-2\delta j}$, featuring a $O(\frac{1}{\sqrt{N_j}})$ -prefactor.

(viii) (*subcase of (vi): bubbles*) A loop γ_i is called a **bubble** when $n_i = 2$, $n'_i = 1$. As explained above, it can be *complete* or *incomplete*, depending on whether $L(\gamma_i) = 2$ or 1. Then the outgoing transfer momentum is equal to the ingoing transfer momentum, so that in (vi) no sum over k_v is required. Hence the total weight associated to the connecting vertex $v_{i,1}$ is $O(g2^{-2\delta j})$ instead of $O(1)$. Call **strongly connecting vertex** a connecting vertex which is *not* originated from a bubble as just described. Note that a vertex which is *not* a strongly connecting vertex (see cases (vii) and (viii)) has a *small weight* $\lesssim g2^{-2\delta j}$ attached to it. On the other hand, strongly connecting vertices have a weight $O(1)$.

Assume for simplicity that $j \leq j_\phi$. Let $n' \leq n$ be the number of strongly connecting vertices, and $n'' := n - n'$. The total weight obtained by multiplying all the above factors is $O((g2^{-2\delta j})^{n''}2^j)$. Let B be the number of bubbles (in the sense defined in (viii)). Using the equality $n' + B + 1 = L'$ (number of loops) – which is modified into $n' + B = L'$ in the case of diagrams containing only bubbles, e.g. $\Upsilon_3, \tilde{\Upsilon}_3$ – and the bound $L' - B \leq \frac{2}{3}(n - B)$ (expressing the fact that each loop γ_i different from a bubble has at least three half-vertices attached to it), one obtains

$$(g2^{-2\delta j})^{n''} = (g2^{-2\delta j})^{n-n'} \leq (g2^{-2\delta j})^{\frac{n}{3} + \frac{2}{3}B+1} \leq (g2^{-2\delta j})^{\frac{n}{3}+1}, \quad (2.89)$$

or $(g2^{-2\delta j})^{n/3}$ in the case of diagrams containing only bubbles. For instance, $n' = 0, n = n'' = 2$ and $L' = B = 1$, resp. 2 for Υ_3 , resp. $\tilde{\Upsilon}_3$; and $L' = 4, n = 6$ and (depending on how the bubble tree is generated) $n' = n'' = 3, B = 0$ or $n' = 2, n'' = 4, B = 1$ for Υ_6 .

The lowest possible value of n'' for small diagrams with $N_{ext} \geq 4$ which are *not only made up of bubbles* is $n'' = 3$. Namely, such diagrams have at least *two* loops α_1, α_2 and *two external vertices*. One (connecting) vertex is needed to connect α_1 and α_2 , while another, non-connecting one is needed to assure that these do not make a chain of two bubbles. At least two other non-connecting vertices are needed to connect α_1, α_2 either to other loops or to external legs. Therefore (disregarding diagrams containing only

bubbles), one may replace the exponent $\frac{n}{3} + 1$ by $\max(3, \frac{n}{3} + 1) = 2 + \max(1, \frac{n}{3} - 1)$, so that, improving on (2.89),

$$(g2^{-2\delta j})^{n''} \leq (g2^{-2\delta j})^{2+\max(1, \frac{n}{3}-1)}, \quad (2.90)$$

Individual pre-factors $g2^{-2\delta j}$, which can be interpreted as the weight of *bare vertices*, compare with (2.23), are modified in multi-scale bounds because effective vertices are scale-dependent, but the exponent $2 + \max(1, \frac{n}{3} - 1)$ remains the same, and is essential for polymer bounds.

One also gets a product of " $1/N$ "-factors, $O(2^{-j/2})$ per *non-connecting vertex*, see (vii), which however is simply 1 for diagrams consisting only of bubbles (chains of bubbles); this feature will however be exploited only later on, once chains of bubbles will have been resummed, see §2.3.3. *The overall scaling factor must however be corrected*: first, the location of ξ_1 is fixed, leading to a correcting factor $\frac{1}{\text{Vol}(\Delta_{ext,1})} = O(m^* \mu^2 2^{-3j})$. Second, the above weight mistakenly includes the power-counting of external fields Ψ_{ext}^j together with their sectors, see (2.14), which leads to a correcting factor $O((2^{\frac{j}{2}}(p_F^*)^{-1})^{N_{ext}})$. Finally, assuming the underlying cluster tree is \mathbb{T} , the above may be multiplied by the decay factor $C_p^n \prod_{\ell \in L(\mathbb{T})} \left(1 + 2^{-j} \frac{|\xi_{\Delta_\ell} - \xi_{\Delta'_\ell}|}{\mu}\right)^{-p}$ for every $p \geq 0$.

All together, we have proved the following bound for a single-scale diagram Υ not made up only of bubbles, with underlying cluster tree \mathbb{T} and angular sector distribution $\{n_{\Delta,i}\} \uplus \{\bar{n}_{\Delta,i}\}$:

$$|\mathcal{A}(\Upsilon; \xi_1)| \leq \left\{ C_{p,r}^n \prod_{\Delta} \prod_{i=1}^{2^j} \frac{1}{(n_{\Delta,i}!)^r (\bar{n}_{\Delta,i}!)^r} \prod_{\ell \in L(\mathbb{T})} \left(1 + 2^{-j} \frac{|\xi_{\Delta_\ell} - \xi_{\Delta'_\ell}|}{\mu}\right)^{-p} \right\} \\ (g2^{-2\delta j})^{2+\max(1, \frac{n}{3}-1)} (2^{-j})^{\frac{1}{2}(4-N_{ext})} (p_F^*)^{-N_{ext}}, \quad (2.91)$$

where $\xi_{\Delta_\ell}, \xi_{\Delta'_\ell}$ are the centers of the boxes $\Delta_\ell, \Delta'_\ell$. *Diagrams made up only of bubbles feature a small factor $(g2^{-2\delta j})^{n/3}$ instead.*

Sum over trees. This is a standard argument in statistical mechanics and constructive field theory; see e.g. [54], Corollary 5.3. Recall that there is no sum over permutations of vertices. So all trees may be generated by the following algorithm. (All boxes in the argument are in \mathbb{D}^j). Fix a box Δ_1 . Sum at step 1 over all possible boxes $\Delta'_1 \in \mathbb{D}^j$ (including Δ_1), and add a link between Δ_1 and Δ'_1 , i.e. a pairing $\langle \Psi^{j,\alpha}(\xi_1) \bar{\Psi}^{j,\alpha}(\xi'_1) \rangle$ or $\langle \bar{\Psi}^{j,\alpha}(\xi_1) \Psi^{j,\alpha}(\xi'_1) \rangle$ between fields located at $\xi_1 \in \Delta_1, \xi'_1 \in \Delta'_1$. The corresponding multiplicative spatial decrease factor is $C := \sum_{\Delta'_1} \left(1 + d^j(\Delta_1, \Delta'_1)\right)^{-p}$, where

$$d^j(\Delta, \Delta') := \sup_{\xi \in \Delta, \xi' \in \Delta'} 2^{-j} |\xi - \xi'| \quad (2.92)$$

is a scaled distance between two scale j boxes. Ordering boxes by their distance to Δ_1 , one obtains

$$C \lesssim \sum_{i \geq 1} i^{2-p} < \infty \quad (2.93)$$

provided $p \geq 4$. Continue by picking a second link) between Δ_1 and a box Δ_1'' , and so on, until all pairings between fields in Δ_1 and fields either in Δ_1 or in any other box have been exhausted. There are local factorials involved, since fields located inside Δ_1 may be permuted, but inverse local factorials $\frac{1}{(n_{\Delta_1, i'})^r (\bar{n}_{\Delta_1, i'})^r}$ beat them for $r > 1$; a precise argument may be found in [54], Corollary (5.3) 2., where inverse local factorials are deduced from the quasi-exponential decay of propagators, and not from the fermionic nature of the theory (see discussion in §2.4). Then, at step 2, one looks for all possible pairings between a field located in Δ_2 defined as Δ'_i , where $i := \min\{i' \geq 1 \mid \Delta'_i \neq \Delta_1\}$, and a field located in $\Delta'_2 \neq \Delta_1$, and so on. Once all vertices of the tree have been explored, the procedure stops. In the end, one finds for the sum over all scale j polymers \mathbb{P} with fixed number n of vertices:

$$\sum_{\mathbb{P} \mid |\mathbb{P}|=n} |\mathcal{A}(\mathbb{P}; \xi_{ext,1})| \lesssim (Cg2^{-2\delta j})^{2+\max(1, \frac{n}{3}-1)} (2^{-j})^{\frac{1}{2}(4-N_{ext})} (p_F^*)^{-N_{ext}}, \quad (2.94)$$

which is the general term of a converging series for λ small enough. Hence, finally,

$$\left| \sum_{\mathbb{P}} \mathcal{A}(\mathbb{P}; \xi_{ext,1}) \right| \leq \sum_n \sum_{\mathbb{P} \mid |\mathbb{P}|=n} |\mathcal{A}(\mathbb{P}; \xi_1)| \lesssim (2^{-j})^{\frac{1}{2}(4-N_{ext})} (p_F^*)^{-N_{ext}}. \quad (2.95)$$

2.3.3 Bubble resummations

Let $j_+ \leq j'_\phi - 1$. We shall now detail the resummation of chains of bubbles with lowest fermionic scale j_+ , also called " $j_+ + \frac{1}{2}$ "-scale expansion. The notation " j_+ " for a *fermionic* scale seemingly contradicts the principles laid out in the "Important notations" section of the Introduction. However, as emphasized in §1.4, see (1.58), the kernel $\text{Pre}\Sigma^{j_+ \rightarrow}(q)$ has an effective infra-red cut-off for $|q|_+ \leq 2^{-j_+ \mu}$. Therefore it makes sense in this context to identify the lowest *fermionic* scale with a *bosonic* cut-off scale.

This step proceeds "by inspection", namely, it requires no supplementary expansion, rather an explicit resummation by hand of *structures* found in the sum of perturbative diagrams.

The structures we want to single out are chains of bubbles made up of pairs of propagators with lowest scale k , see Fig. 1.4.5. The lowest-order term, λId , connecting the two halves of any vertex,

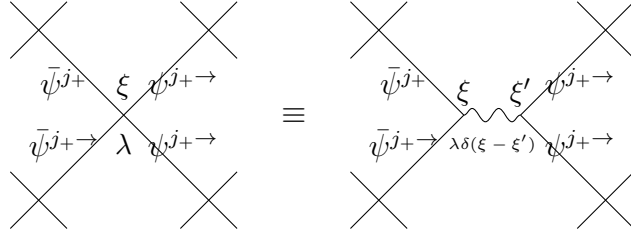


Fig. 2.3.6. Two equivalent ways a representing a local vertex.

is complemented by a sum of terms involving ≥ 1 bubbles forming a ladder diagram,

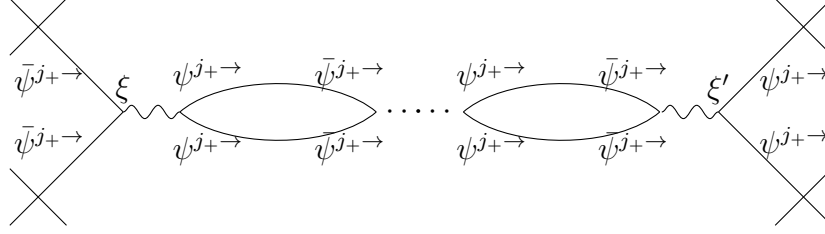


Fig. 2.3.7. Bubble resummation. At least one of the fields $\psi^{j_+ \rightarrow}$ or $\bar{\psi}^{j_+ \rightarrow}$ is assumed to be of scale j_+ .

Resumming the above series yields – up to the discrepancy between the current value $\Gamma^{(j'_\phi-1)\rightarrow}$ and the asymptotic infra-red value Γ_ϕ of the energy gap – the kernel $\text{Pre}\Sigma^{j_+ \rightarrow}(\xi - \xi') - \text{Pre}\Sigma^{(j_+-1)\rightarrow}(\xi - \xi')$. The error term due to the difference $\Gamma_\phi - \Gamma^{(j'_\phi-1)\rightarrow}$ will be bounded only in section 3, following the arguments of §3.4 C., 2. and 3. Now internal vertices of the chain may in turn be replaced by chains of bubbles with lowest momentum of scale $\leq j_+ - 1$, yielding all together $\text{Pre}\Sigma^{j_+ \rightarrow}(\xi, \xi')$.

This has the following consequence; see the preliminary bounds of §2.3.2 for notations. All loops γ_i have at least 3 vertices along them ($n_i \geq 3$), so case (viii) is absent. On the other hand, half-vertices are now possibly connected by $\text{Pre}\Sigma^{j_+ \rightarrow}$ -kernels with $j_+ \geq j$, which is materialized by the substitution of **delocalized vertices** to the original, local vertices,

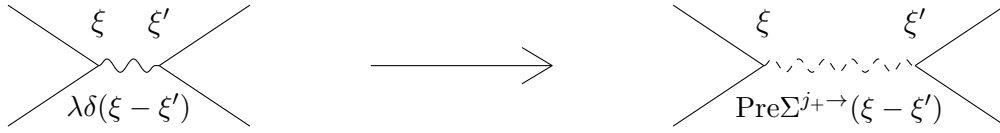


Fig. 2.3.8. Local vertices (on the left), substituted by delocalized vertices (on the right).

Let Δ^{j_+} be a scale j_+ box, and $\text{Vol}(\Delta^{j_+}) \approx \frac{1}{m^* \mu^2} 2^{3j_+}$ its volume. Assume first that $j_+ < j_\phi$. Then the integrated vertex $m^* \int d\xi' |\text{Pre}\Sigma^{j_+ \rightarrow}(\xi - \xi')|$ is $O(\frac{1}{j_\phi - j_+})$, see (1.92), a bound substituting itself to the bound obtained by considering only the lowest-order term in $O(\lambda)$ in the Goldstone boson propagator, $m^* \int d\xi' \lambda\delta(\xi - \xi') = O(g)$. For the highest scales, say $j_+ < j_\phi - c(j_\phi - j_D)$, $0 < c < 1$, the integrated vertex is $O(g)$ since $j_\phi - j_D \approx g^{-1}$. However, for larger scale indices j_+ , that is, close to the transition scale, the bound is only $O(1)$. For $j_\phi \leq j_+ \leq j'_\phi - 1$, the bounds of §1.6 yield instead a large bound $O(2^{2(j_+ - j_\phi)})$. Recapitulating, one may define an equivalent **scale j_+ coupling constant g^{j_+}** replacing the bare constant g :

Definition 2.9 (scale j_+ coupling constant g^{j_+}) Let $g^{j_+} := m^* \int d\xi' |\text{Pre}\Sigma^{j_+ \rightarrow}(\xi - \xi')|$ ($j_+ \leq j'_\phi - 1$).

Previous computations show that

$$g^{j_+} \lesssim \begin{cases} \frac{1}{j_\phi - j_+} & (j_+ < j_\phi) \\ 2^{2(j_+ - j_\phi)} & (j_\phi \leq j_+ \leq j'_\phi - 1) \end{cases} \quad (2.96)$$

Thus the **weight** $g^{j_+} 2^{-2\delta j}$ of a vertex other than strongly connecting *including its four half-propagators* (called **effective vertex** in the literature), compare with §2.3.2 (viii), is $\lesssim \mathcal{W}^{j,j_+}$ ($j_D \leq j \leq j_+ \leq j'_\phi - 1$), where one has set

Definition 2.10 (scale (j, j_+) effective vertex) *Let*

$$\mathcal{W}^{j,j_+} := \begin{cases} \frac{1}{j_\phi - j_+} & (j \leq j_+ < j_\phi) \\ 2^{2(j_+ - j)} & (j_\phi \leq j \leq j_+ \leq j'_\phi - 1) \\ 2^{2(j_+ - j_\phi)} & (j \leq j_\phi \leq j_+ \leq j'_\phi - 1) \end{cases} \quad (2.97)$$

and

$$\mathcal{W}^j := \max_{j \leq j_+ \leq j'_\phi - 1} \mathcal{W}^{j,j_+} = \begin{cases} 2^{2(j'_\phi - j)} & (j_\phi \leq j \leq j'_\phi) \\ 2^{2(j'_\phi - j_\phi)} & (j \leq j_\phi) \end{cases} \quad (2.98)$$

Strongly connecting vertices, see §2.3.2 (vi) and (viii), have an extra logarithmic prefactor $O(j)$.

Above the transition scale, i.e. if $j, j_+ \leq j_\phi$, \mathcal{W}^{j,j_+} grows *logarithmically* in terms of j_+ from the UV cut-off scale j_D to the transition scale j_ϕ . *Below transition scale*, i.e. if $j_\phi \leq j_+ \leq j'_\phi - 1$, \mathcal{W}^{j,j_+} is the *inverse of a spring factor* between scales $\max(j_\phi, j)$ and j'_ϕ . This shows clearly why other arguments (namely, Ward identities, developed in section 3) are required to bound polymers with $j_+ \gg j_\phi$. However, keeping $j'_\phi - j_\phi = o(\ln(1/g))$, in line with (0.35), ensures that large factors \mathcal{W}^{j,j_+} , $j \ll j_+ \leq j'_\phi$, bounded by $\mathcal{W}^j \leq 2^{2(j'_\phi - j_\phi)}$, may be absorbed by putting aside some power of g , say,

$$\mathcal{W}^{j,j_+} g^{1/2} = O(1) \quad (2.99)$$

for all $j \leq j_+ \leq j'_\phi - 1$ provided $j'_\phi - j_\phi \leq \frac{1}{4} \ln(1/g)$. *For definiteness, we choose*

Definition 2.11 (choice of j'_ϕ)

$$j'_\phi := j_\phi + \lfloor \frac{1}{4} \ln(1/g) \rfloor. \quad (2.100)$$

Hence the total weight of \mathcal{W}^{j,j_+} for a diagram with n vertices is $\lesssim g^{-n/2}$. For single-scale diagrams, or multi-scale diagrams with no external legs in Cooper pair configuration, later to form a pre-Goldstone boson, only *small* weights $\mathcal{W}^{j,j} = \begin{cases} \frac{1}{j_\phi - j} & (j \leq j_\phi) \\ 1 & (j_\phi \leq j \leq j'_\phi - 1) \end{cases}$ show up. The problem of potentially large \mathcal{W}^{j,j_+} weights is therefore raised up again only in §2.4.

Summarizing, and referring to the details of the computations in §2.3.2, the small factor $g^{2+\max(1, \frac{n}{3}-1)}$ in (2.91) undergoes the following transformations:

(vi) \rightarrow (vi)' (*total weight associated to a connecting vertex*) $O(gj2^{-2\delta j}) \rightarrow O(\mathcal{W}^{j,j}j)$, featuring now a (probably spurious but not very disturbing) logarithmic factor j ;

(vii) \rightarrow (vii)' (*total weight associated to a non-connecting vertex*)

$$O(g2^{-j/2}2^{-2\delta j}) \rightarrow O(\mathcal{W}^{j,j}2^{-j/2}) \lesssim O(\mathcal{W}^{j,j}2^{-j/2}) = O\left(\frac{\mathcal{W}^{j,j}}{\sqrt{N_j}}\right), \quad (2.101)$$

featuring a "1/N"-type factor $N_j = 2^j$.

Most importantly, we note here that – *after* bubble chains have been resummed – *connecting* or *strongly connecting* vertices are now the same. Hence the number of factors $\mathcal{W}^{j,j}j$ in (vi) is $n' = n - n'' \leq 2n/3 \leq 2\left(2 + \max(1, \frac{n}{3} - 1)\right)$ (since $n'' = n - n' \geq 2 + \max(1, \frac{n}{3} - 1) \geq n/3$). Combining these with the n'' factors $O\left(\frac{\mathcal{W}^{j,j}}{\sqrt{N_j}}\right)$ coming from (vii), we finally get instead of (2.91)

$$|\mathcal{A}(\Upsilon; \xi_{ext,1})| \leq \left\{ (C_{p,r} \mathcal{W}^{j,j})^n \prod_{\Delta} \prod_{i=1}^{2^j} \frac{1}{(n_{\Delta,i}!)^r (\bar{n}_{\Delta,i}!)^r} \prod_{\ell \in L(\mathbb{T})} \left(1 + 2^{-j} \frac{|\xi_{\Delta_\ell} - \xi_{\Delta'_\ell}|}{\mu}\right)^{-p} \right\} \\ (j^2 2^{-j/2})^{2+\max(1, \frac{n}{3}-1)} (2^{-j})^{\frac{1}{2}(4-N_{ext})} (p_F^*)^{-N_{ext}}. \quad (2.102)$$

By the same argument as in §2.3.2, one may sum over diagrams. This may be done in two stages; first one sums over all diagrams spanning a given polymer \mathbb{P}^j of scale j , yielding

$$|\mathcal{A}(\mathbb{P}^j; \xi_{ext,1})| \lesssim \left\{ (C_p \mathcal{W}^{j,j})^{n(\mathbb{P}^j)} \prod_{\ell \in L(\mathbb{T})} \left(1 + 2^{-j} \frac{|\xi_{\Delta_\ell} - \xi_{\Delta'_\ell}|}{\mu}\right)^{-p} \right\} \\ (j^2 2^{-j/2})^{2+\max(1, \frac{n(\mathbb{P}^j)}{3}-1)} (2^{-j})^{\frac{1}{2}(4-N_{ext})} (p_F^*)^{-N_{ext}} \quad (2.103)$$

where \mathbb{T} is a cluster tree spanning \mathbb{P}^j , and $n(\mathbb{P}^j)$ is the number of boxes of \mathbb{P}^j . Then the sum over polymers may be bounded using space-time decay, so that

$$\sum_{\mathbb{P}^j \in \mathcal{P}_{N_{ext}}^j \mid n(\mathbb{P}^j)=n} |\mathcal{A}(\mathbb{P}^j; \xi_{ext,1})| \lesssim (C_p \mathcal{W}^{j,j})^n (j^2 2^{-j/2})^{2+\max(1, \frac{n}{3}-1)} (2^{-j})^{\frac{1}{2}(4-N_{ext})} (p_F^*)^{-N_{ext}} \quad (2.104)$$

and finally, summing over all polymers of scale j with one external leg located at $\xi_{ext,1}$

$$\left| \sum_{\mathbb{P} \in \mathcal{P}_{N_{ext}}^j} \mathcal{A}(\mathbb{P}; \xi_{ext,1}) \right| \lesssim (j^2 2^{-j/2})^{N_{ext}/9} (j^2 2^{-j})^{\frac{1}{2}(4-N_{ext})} (p_F^*)^{-N_{ext}} \quad (2.105)$$

since (considering the worst case, for which external momenta are grouped 3 by 3, see Figure below) $n(\mathbb{P}^j) \geq \frac{1}{3}N_{ext}(\mathbb{P}^j) = \frac{1}{3}N_{ext}$.

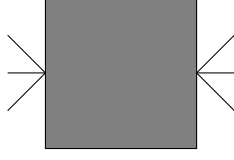


Fig. 2.3.9. One example of external momentum configuration for a polymer with $N_{ext} = 6$. The minimal number of vertices is 2.

2.3.4 Momentum-decoupling expansion and displacement of external legs

One must now *test* how step j polymers $\mathbb{P}_1, \dots, \mathbb{P}_n$ are connected from below to boxes in \mathbb{D}^{j+1} . To this end, we apply to each polymer \mathbb{P} in $\mathcal{P}^{j \rightarrow}$ the following expansion operator

$$\text{Vert}^j(\mathbb{P}) = \prod_{\Delta \in \mathbb{P} \cap \mathbb{D}^j} \left(\sum_{\mu_\Delta=0}^{N_0-1} \frac{1}{\mu_\Delta!} \partial_{t_\Delta}^{\mu_\Delta} \Big|_{t_\Delta=0} + \int_0^1 dt_\Delta \frac{(1-t_\Delta)^{N_0-1}}{(N_0-1)!} \partial_{t_\Delta}^{N_0} \right). \quad (2.106)$$

Expanding the product yields a sum of terms with μ_Δ , $\Delta \in \mathbb{P} \cap \mathbb{D}^j$, ranging in $\{0, \dots, N_0\}$, N_0 coding for the integral remainder term. Let $N_{ext}(\mathbb{P}) := \sum_{\Delta \in \mathbb{P} \cap \mathbb{D}^j} \mu_\Delta$, and denote by $\mathbf{\Delta}_{ext}(\mathbb{P}) \equiv \{\Delta_1, \Delta_2, \dots\}$ the boxes in $\mathbb{P} \cap \mathbb{D}^j$ containing the external fields. If $N_{ext}(\mathbb{P}) < N_0$, then all $\mu_\Delta, \Delta \in \mathbb{P} \cap \mathbb{D}^j$ are $< N_0$, so $N_{ext}(\mathbb{P})$ is equal to the number of external fields. If $N_{ext}(\mathbb{P}) \geq N_0$ then (i) either all μ_Δ are $< N_0$ and the same conclusion holds; or (ii) some $\mu(\Delta)$ is equal to N_0 , which means that $t_\Delta > 0$: when this happens, we decide somewhat arbitrarily that the polymer has exactly N_0 vertical links connecting Δ to the box below it in \mathbb{D}^{j+1} . As we shall see, polymers with $N_{ext} < N_0$ will undergo a further treatment.

The final outcome of the horizontal and momentum-decoupling expansion may be written as

$$F_I(\boldsymbol{\xi}_{ext}, \bar{\boldsymbol{\xi}}_{ext}) = \sum_{\mathbb{F}^j \subset \mathcal{F}^j} \prod_i \text{Vert}^j(\mathbb{P}_i) \left(\int d\mathbf{w} \int d\mu_\theta^*(s^j(\mathbf{w}); \Psi^{\rightarrow j}, \bar{\Psi}^{\rightarrow j}) \tilde{G}_I^{(j-1)\rightarrow}(\boldsymbol{\xi}_I) \right), \quad (2.107)$$

where:

- \mathbb{F}^j ranges over the set \mathcal{F}^j of scale j cluster forests;
- $\mathbb{P}_1, \dots, \mathbb{P}_n \in \mathcal{P}^{j \rightarrow}$ are the non- j -overlapping polymers introduced at the end of the last subsection;
- and $\tilde{G}_I^{(j-1)\rightarrow}(\cdot)$ is as in (2.82).

Instead of summing over cluster forests, it is equivalent, but more convenient, to sum over non- j -overlapping polymers, so that

$$\sum_{\mathbb{F}} \prod_i \text{Vert}^j(\mathbb{P}_i)(\dots) \longrightarrow \sum_n \sum_{\mathbb{P}_1, \dots, \mathbb{P}_n \text{ non-}j\text{-overlapping}} \prod_i \sum_{\mathbb{T}_i} \text{Vert}^j(\mathbb{P}_i)(\dots) \quad (2.108)$$

in (2.107), where \mathbb{T}_i , $i = 1, \dots, n$ are cluster trees compatible with the choice of non- j -overlapping polymers $\mathbb{P}_1, \dots, \mathbb{P}_n \in \mathcal{P}^{j \rightarrow}$, namely: \mathbb{T}_i , $i = 1, \dots, n$ are the connected components of \mathbb{F} , and $\mathbb{T}_i = \mathbb{P}_i \cap \mathbb{D}^j$. It is in this form that we shall be using (2.107). Thus:

$$F_I(\boldsymbol{\xi}_{ext}, \bar{\boldsymbol{\xi}}_{ext}) = \sum_n \sum_{\mathbb{P}_1, \dots, \mathbb{P}_n \text{ non-}j\text{-overlapping}} \prod_{i=1}^n F^{HV}(\mathbb{P}_i). \quad (2.109)$$

Displacement of external legs. Let us discuss the smallest values for $N_{ext}(\mathbb{P})$:

- (i) if $N_{ext}(\mathbb{P}) = 0$, then \mathbb{P} has no external field, so \mathbb{P} is a vacuum polymer;
- (ii) if $N_{ext}(\mathbb{P}) = 2$, then \mathbb{P} is a two-point polymer, with corresponding contribution

$$\begin{aligned} & \int d\xi_1 \chi_{\Delta_1}(\xi_1) \int d\xi_2 \chi_{\Delta_2}(\xi_2) \mathcal{A}^j(\mathbb{P}; \xi_1, \xi_2) \Psi^{\rightarrow(j+1)}(\xi_1) \bar{\Psi}^{\rightarrow(j+1)}(\xi_2) \\ &= F_{local}^j(\mathbb{P}; \Psi^{\rightarrow(j+1)}, \bar{\Psi}^{\rightarrow(j+1)}) + \delta F^j(\delta\mathbb{P}; \Psi^{\rightarrow(j+1)}, \bar{\Psi}^{\rightarrow(j+1)}) \end{aligned} \quad (2.110)$$

where

$$\begin{aligned} & F_{local}^j(\mathbb{P}; \Psi^{\rightarrow(j+1)}, \bar{\Psi}^{\rightarrow(j+1)}) := \\ & \sum_{k_1, k_2 \geq j+1} \sum_{\alpha_1 \in \mathbb{Z}/2^{k_1}\mathbb{Z}, \alpha_2 \in \mathbb{Z}/2^{k_2}\mathbb{Z}} \int d\xi_1 \chi_{\Delta_1}(\xi_1) \int d\xi_2 \chi_{\Delta_2}(\xi_2) \mathcal{A}^j(\mathbb{P}; \Psi^{\rightarrow(j+1)}, \bar{\Psi}^{\rightarrow(j+1)}; \xi_1, \xi_2) \cdot \\ & \cdot \frac{1}{2} \left[\Psi^{k_1, \alpha_1}(\xi_1) \left(\bar{\Psi}^{k_2, \alpha_2}(\xi_1) + \left(\xi_2 - \xi_1, \partial_{\xi_1} \left(e^{i(p^{k_2, \alpha_2}, \xi_2 - \xi_1)} \Psi^{k_2, \alpha_2}(\xi_1) \right) \right) \right) \right. \\ & \left. + \bar{\Psi}^{k_2, \alpha_2}(\xi_2) \left(\Psi^{k_1, \alpha_1}(\xi_2) + \left(\xi_1 - \xi_2, \partial_{\xi_2} \left(e^{i(p^{k_1, \alpha_1}, \xi_1 - \xi_2)} \Psi^{k_1, \alpha_1}(\xi_2) \right) \right) \right) \right], \end{aligned} \quad (2.111)$$

see (2.56), is the local part of the polymer, obtained by *displacing* symmetrically *one of the external fields to the location of the other*. The error term $\delta F^j(\cdot)$, once its external legs are contracted (at some later stage, namely, at scales k_1 and k_2), may be rewritten as a Taylor remainder as in (2.56), and comes with an extra spring factor $O(2^{-2(\min(k_1, k_2) - j)})$. Since two-point functions are *linearly divergent*, subtracting local part to order 1 makes the remainder convergent. Referring to the logarithmically divergent, four-point bubble diagram, and to the power-counting of a contracted pair $C^j(\cdot, \cdot) = \langle \Psi^j(\cdot) \Psi^j(\cdot) \rangle = O(2^{-j})$, \mathbb{P} may be thought of as having 6 external legs; however, for pure book-keeping reasons, we shall consider it as a polymer with $N_0 = 8$ external legs – which simply means that it is convergent enough for our purposes. For future use we indeed replace \mathbb{P} with a polymer $\delta\mathbb{P}$ which is identical to \mathbb{P} , except that

it has N_0 external legs in the box where the external fields have been displaced to, Δ_1 , resp. Δ_2 , and *none* in the other box, Δ_2 , resp. Δ_1 .

(iii) if $4 \leq N_{ext}(\mathbb{P}) < N_0 = 8$, then we proceed as in (2.111), Taylor expanding to order 2 symmetrically in the neighborhood of each external vertex location $\xi_1, \dots, \xi_{N_{ext}}$. All such diagrams – recall Cooper pair bubble diagrams have already been resummed by hand – are already convergent *before* displacing external legs. However (see §2.4), the above operation will help us sum over external angular sectors in the multi-scale bounds. Local contributions $F_{local}^j(\mathbb{P}; \Psi^{\rightarrow(j+1)}, \bar{\Psi}^{\rightarrow(j+1)})$ are *translation invariant* polymers with $N_{ext}(\mathbb{P})$ external legs; the error term $\delta F_{local}^j(\delta\mathbb{P}; \Psi^{\rightarrow(j+1)}, \bar{\Psi}^{\rightarrow(j+1)})$, on the other hand, is considered as a polymer $\delta\mathbb{P}$ with N_0 external legs.

2.3.5 Mayer expansion

We shall now apply the *restricted cluster expansion*, see Proposition 5.4, to the result of our expansion. Cluster expansions have allowed us to rewrite Green functions as sums over non- j -overlapping polymers denoted by $\mathbb{P}_1, \dots, \mathbb{P}_n$. The *objects* are now polymers \mathbb{P} in $\mathcal{O} = \{\mathbb{P}_1, \dots, \mathbb{P}_n\} \subset \mathcal{P}^{j \rightarrow}$; a link $\ell \in L(\mathcal{O})$ is a pair of polymers $\{\mathbb{P}_i, \mathbb{P}_{i'}\}$, $i \neq i'$. Objects of type 2 are polymers with $\geq N_0$ external legs, whose non-overlap conditions we shall not remove. Then objects of type 1 are polymers with $< N_0$ external legs. Due to the displacement of external legs operated in §2.3.4, all external legs are located in the *same* scale j box.

Implicit in the outcome of the cluster expansions is the **non-overlapping condition**,

$$\begin{aligned} \text{NonOverlap}(\mathbb{P}_1, \dots, \mathbb{P}_n) &:= \prod_{(\mathbb{P}_i, \mathbb{P}_{i'})} \mathbf{1}_{\mathbb{P}_i, \mathbb{P}_{i'} \text{ non-}j\text{-overlapping}} \\ &= \prod_{(\mathbb{P}_i, \mathbb{P}_{i'})} \prod_{\Delta \in \Delta^j(\mathbb{P}_i), \Delta' \in \Delta^j(\mathbb{P}_{i'})} (1 + (\mathbf{1}_{\Delta \neq \Delta'} - 1)) \end{aligned} \quad (2.112)$$

stating that a scale j box Δ belonging to \mathbb{P}_i and a scale j box Δ' belonging to $\mathbb{P}_{i'}$ are necessarily distinct. Similarly to what we did during the horizontal cluster expansion, we choose some polymer with $< N_0$ external legs, say \mathbb{P}_1 , and weaken the non-overlap condition between \mathbb{P}_1 and all the other polymers $\mathbb{P}_{i'}, i' \neq 1$ by introducing a parameter S_1 ,

$$\begin{aligned} &\text{NonOverlap}(\mathbb{P}_1, \dots, \mathbb{P}_n)(S_1) \\ &= \left(\prod_{\{\mathbb{P}_i, \mathbb{P}_{i'}\}_{i, i' \neq 1}} \prod_{\Delta \in \Delta^j(\mathbb{P}_i), \Delta' \in \Delta^j(\mathbb{P}_{i'})} \mathbf{1}_{\Delta \neq \Delta'} \right) \left(\prod_{(\Delta, \Delta') \in \Delta_{ext}(\mathbb{P}_1) \times \Delta_{ext}(\mathbb{P}_{i'})} \mathbf{1}_{\Delta \neq \Delta'} \right) \cdot \\ &\quad \prod_{(\Delta, \Delta') \in \Delta^j(\mathbb{P}_1) \times \Delta^j(\mathbb{P}_{i'}) \setminus \Delta_{ext}(\mathbb{P}_1) \times \Delta_{ext}(\mathbb{P}_{i'})} (1 + S_1 (\mathbf{1}_{\Delta \neq \Delta'} - 1)), \end{aligned} \quad (2.113)$$

$$(2.114)$$

where $\Delta_{ext}(\mathbb{P}) \subset \Delta^j(\mathbb{P})$ is the subset of boxes Δ with external legs - i.e. that have been differentiated with respect to t_Δ^j -, and Taylor expand in S_1 to order 1; each factor

$$\mathbf{1}_{\Delta \neq \Delta'} - 1 = -\mathbf{1}_{\Delta = \Delta'} \quad (2.115)$$

produced by differentiation is a **Mayer link** between \mathbb{P}_1 and some $\mathbb{P}_{i'}, i' \neq 1$, or more precisely, some box $\Delta \in \Delta(\mathbb{P}_1)$ and some box $\Delta' \in \Delta(\mathbb{P}_{i'})$, implying an explicit overlap between \mathbb{P}_1 and $\mathbb{P}_{i'}$, and adding a link to the forest \mathbb{F}^j . Iterating the procedure and applying Proposition 5.4 to the weakened non-overlap condition

$$\begin{aligned} \text{NonOverlap}(\mathbb{P}_1, \dots, \mathbb{P}_n)(\mathbf{S}) &:= \prod_{\{\mathbb{P}_i, \mathbb{P}_{i'}\}} \prod_{\Delta \in \Delta_{ext}(\mathbb{P}_i), \Delta' \in \Delta_{ext}(\mathbb{P}_{i'})} \mathbf{1}_{\Delta \neq \Delta'} \cdot \\ &\prod_{(\Delta, \Delta') \in \Delta^j(\mathbb{P}_i) \times \Delta^j(\mathbb{P}_{i'}) \setminus \Delta_{ext}(\mathbb{P}_i) \times \Delta_{ext}(\mathbb{P}_{i'})} (1 + S_{i, i'} (\mathbf{1}_{\Delta \neq \Delta'} - 1)), \end{aligned} \quad (2.116)$$

The outcome is a sum

$$\begin{aligned} \sum_{\mathbb{G} \in \mathcal{F}_{res}(\mathcal{O})} \left(\prod_{\ell \in L(\mathbb{G})} \int_0^1 dW_\ell \right) \text{Mayer}(\mathbf{S}(\mathbf{W})), \\ \text{Mayer}(\mathbf{S}(\mathbf{W})) := \left[\left(\prod_{\ell \in L(\mathbb{G})} \frac{\partial}{\partial S_\ell} \right) \text{NonOverlap}(\mathbb{P}_1, \dots, \mathbb{P}_n) \right](\mathbf{S}(\mathbf{W})) \end{aligned} \quad (2.117)$$

Links $\ell = \ell_{\mathbb{P}_i, \mathbb{P}_{i'}} \in L(\mathbb{G})$ are obtained as links between *polymers*, however the corresponding differentiation $\frac{\partial}{\partial S_\ell}$ is immediately rewritten as a sum over pairs of boxes $(\Delta, \Delta') \in \Delta^j(\mathbb{P}_i) \times \Delta^j(\mathbb{P}_{i'})$. Thus we see Mayer links as *links between boxes*. As such they add up to the set of links $L(\mathbb{F}^j)$ produced by the horizontal cluster expansion, producing a forest $\bar{\mathbb{F}}^j$ with same vertices as \mathbb{F}^j but larger set of links $L(\bar{\mathbb{F}}^j) \equiv L(\mathbb{F}^j) \uplus L_{\text{Mayer}}$, where L_{Mayer} (in bijection with $L(\mathbb{G})$) is the set of Mayer links. Since a forest is characterized by its set of links, we rewrite in practice (2.117) as

$$\begin{aligned} \sum_{L_{\text{Mayer}}} \left(\prod_{\ell \in L_{\text{Mayer}}} \int_0^1 dW_\ell \right) \text{Mayer}(\mathbf{S}(\mathbf{W})), \\ \text{Mayer}(\mathbf{S}(\mathbf{W})) := \left[\left(\prod_{\ell \in L_{\text{Mayer}}} \frac{\partial}{\partial S_\ell} \right) \text{NonOverlap}(\mathbb{P}_1, \dots, \mathbb{P}_n) \right](\mathbf{S}(\mathbf{W})) \end{aligned} \quad (2.118)$$

The number of external legs of a set of polymers connected by Mayer links is the sum of the number of external legs of each of the polymers. In particular,

- (i) new vacuum polymers without any non-overlap conditions have been produced; they are resummed into the *scale j free energy function* $f^j(\lambda)$;

- (ii) two-point polymers have been *dressed by a cloud* of vacuum polymers; they can now be resummed into a *renormalization of the two-point function*;
- (iii) links from polymers of type 1 to polymers of type 2 produce new polymers with $\geq N_0$ external legs, whose overlap conditions have not been removed.

Other possibilities include e.g. polymers with 4, 6, 8, \dots external legs without any non-overlap condition, produced by Mayer-linking 2, 3, 4, \dots two-point polymers.

Let us now give some necessary precisions. Since the Mayer expansion is really applied to the non-overlap function `NonOverlap` and *not* to the outcome of the expansion, one must still extend the outcome of the expansion to the case when the \mathbb{P}_i , $i = 1, \dots, n$ have some overlap. The natural way to do this is to assume that the fields $(\Psi^{j,\alpha}|_{\mathbb{P}_i}, \bar{\Psi}^{j,\alpha}|_{\mathbb{P}_i})_{i=1,\dots,n}$ remain independent even when they overlap. This may be understood in the following way. Choose a different color for each polymer $\mathbb{P}_i = \mathbb{P}_1, \dots, \mathbb{P}_n$, and paint with that color *all* boxes $\Delta \in \mathbb{P}_i \cap \mathbb{D}^j$. If $\Delta \in \Delta_{ext}(\mathbb{P}_i)$, then its external vertical links to \mathbb{D}^{j+1} are left in black. The previous discussion implies that boxes with different colors may superpose; on the other hand, *external inclusion links* may *not*, so that *low-momentum fields* $\Psi^{\rightarrow(j+1)}, \bar{\Psi}^{\rightarrow(j+1)}$ do not superpose and may be left in black.

Hence one must see $\Psi, \bar{\Psi}$ as living on a two-dimensional set, $\mathbb{D}^j \times \{\text{colors}\}$, so that copies of $\Psi, \bar{\Psi}$ with different colors are independent of each other. This defines new, *extended* fields $\Psi, \bar{\Psi} : \mathbb{R}_x \mathbb{R}^2 \times \{\text{colors}\} \rightarrow \mathbb{R}$, and *Mayer-extended polymers*. By abuse of notation, we shall skip the tilde in the sequel, and always implicitly extend the fields and the measures by taking into account colors.

As a general principle (see [9] for a single-scale version, or [54] for the general, multi-scale version), sums over Mayer-extended polymers are bounded exactly as sums over *non-Mayer-extended* polymers, $\sum_n \sum_{\mathbb{P} \in \mathcal{P}^j \rightarrow \mid_{|\mathbb{P}|=n}} (C_p)^n g^{n/3}$, see (2.103), (2.123), with the constant C_p of non-Mayer-extended polymers replaced by eC_p .

2.4 Multi-scale bounds and fermionic fixed-point

Our starting point is the single-scale bound

$$|\mathcal{A}(\mathbb{P}^j; \xi_{ext,1})| \lesssim \left\{ (C_p \mathcal{W}^{j,j})^{n(\mathbb{P}^j)} \prod_{\ell \in L(\mathbb{T})} \left(1 + 2^{-j} \frac{|\xi_{\Delta_\ell} - \xi_{\Delta'_\ell}|}{\mu} \right)^{-p} \right\} \\ (j^2 2^{-j/2})^{2+\max(1, \frac{n(\mathbb{P}^j)}{3}-1)} (2^{-j})^{\frac{1}{2}(4-N_{ext})} (p_F^*)^{-N_{ext}}$$

see (2.103), complemented by multi-scale bounds for the effective vertex, (2.104) and (2.105), and Definition 2.10, which imply a total supplementary weight $\leq (2^{2(j'_\phi - j_\phi)})^{n(\mathbb{P}^j)}$

in a multi-scale setting. Recall $\mathcal{W}^{j,j} = \begin{cases} \frac{1}{j_\phi - j} & (j \leq j_\phi) \\ 1 & (j_\phi \leq j \leq j'_\phi - 1) \end{cases}$. We shall now

prove by scale induction the following *multi-scale bound*. Fix $N_0 := 8$ and consider a polymer $\mathbb{P} \in \mathcal{P}^{k \rightarrow}$ with external legs $\Psi^{k_{ext,1}, \alpha_{ext,1}}, \dots, \Psi^{k_{ext,N_{ext}}, \alpha_{ext,N_{ext}}}$, $k \leq k_{ext,1}, \dots, k_{ext,N_{ext}}$. Let $k_{ext} := \min(k_{ext,1}, \dots, k_{ext,N_{ext}})$ be the highest external momentum scale, considered as the external scale of \mathbb{P} . The procedure considered in §2.3.4 has produced three types of polymers:

- (i) local parts of polymers with $4 \leq N_{ext} < N_0$ external legs;
- (ii) polymers with $\geq N_0$ external legs; and
- (ii') error terms $\delta F^k(\delta \mathbb{P}; \Psi^{\rightarrow(k+1)}, \bar{\Psi}^{\rightarrow(k+1)})$ associated with polymers $\delta \mathbb{P}$ with $2 \leq N_{ext} < N_0$ external legs, which have a spring factor $2^{-2(k_{ext}-k)}$, and have been considered as polymers with N_0 external legs in the above book-keeping.

As we shall see, the power-counting associated to external leg angular sectors is more favorable for translation-invariant polymers (case (i)), for which Proposition 2.5 holds. On the other hand, polymer contributions of type (ii), (ii') enjoy (though for different reasons) a spring factor $2^{-2(k_{ext}-k)}$, making it possible to control them in a similar way.

Note that, for every $c > 0$,

$$\frac{1}{j_\phi - j} 2^{-cj} \lesssim \frac{1}{j_\phi} \approx g, \quad j 2^{-cj} \lesssim 1 \quad (2.119)$$

and (by (2.100)) $2^{2(j'_\phi - j_\phi)} = O(g^{-1/2})$, hence

$$(\mathcal{W}^{j,j} 2^{2(j'_\phi - j_\phi)})^{n(\mathbb{P}^j)} (j^2 2^{-j/2})^{2 + \max(1, \frac{n(\mathbb{P}^j)}{3} - 1)} \lesssim g^{n(\mathbb{P}^j)/2} 2^{j(-3/2 + o(1))}. \quad (2.120)$$

For multi-scale polymers of lowest internal scale k and highest external scale j , the factor $2^{-3k/2}$ in (2.120) is multiplied by the spring factor $2^{-(j-k)\frac{N_{ext}-4}{2}}$. For $N_{ext} = 6$, the sum

$$\sum_{k < j} 2^{-(j-k)\frac{N_{ext}-4}{2}} 2^{-3k/2} \quad (2.121)$$

is only $O(2^{-j})$, thus one expects the decay exponent $3j/2$ to be lowered to j at most. With a decay $O(2^{-k})$ however, the sum (2.121) yields $O(2^{-j})$ but with a logarithmic correction. Hence it is safer to say that a lower decay exponent holds, say, $(\frac{1}{2} - o(1))j$ only, compare with the exponent in (2.120).

Our claims are therefore the following. (2.103), (2.104), (2.105) and (2.120) ensure that they hold for a single-scale polymer. Let $N_0 := 8$ and

$$(N_{ext} - N_0)_+ := \begin{cases} 1 & (N_{ext} \geq N_0) \\ 0 & (N_{ext} < N_0) \end{cases}. \quad (2.122)$$

General fermionic multi-scale bound. Let $\mathbb{P}^{j\rightarrow} \in \mathcal{P}^{j\rightarrow}$ not made up only of bubbles, then

$$\boxed{|\mathcal{A}(\mathbb{P}^{j\rightarrow}; \xi_{ext,1})| \lesssim g^{n(\mathbb{P}^{j\rightarrow})/2} 2^{j(-\frac{1}{2}+o(1))} 2^{-j(N_{ext}-N_0)_+} (2^j)^{\frac{1}{2}(N_{ext}-4)} (p_F^*)^{-N_{ext}}} \quad (2.123)$$

Furthermore, if $\mathbb{P}^{j\rightarrow}$ ranges in the set of polymers in $\mathcal{P}^{j\rightarrow}$ with $n \geq 1$ vertices,

$$\boxed{\sum_{\mathbb{P}^{j\rightarrow} \in \mathcal{P}^{j\rightarrow} \mid n(\mathbb{P}^{j\rightarrow})=n} |\mathcal{A}(\mathbb{P}^{j\rightarrow}; \xi_{ext,1})| \lesssim g^{n/2} 2^{-j/2} (2^j)^{\frac{1}{2}(N_{ext}-4)} (p_F^*)^{-N_{ext}}} \quad (2.124)$$

from which, finally, summing over all polymers in $\mathbb{P}^{j\rightarrow}$ with one external vertex located in $\xi_{ext,1}$,

$$\sum_{\mathbb{P}^{j\rightarrow} \in \mathcal{P}^{j\rightarrow}} |\mathcal{A}(\mathbb{P}^{j\rightarrow}; \xi_{ext,1})| \lesssim g^{N_{ext}/6} 2^{-j/2} (2^j)^{\frac{1}{2}(N_{ext}-4)} (p_F^*)^{-N_{ext}}, \quad (2.125)$$

compare with the discussion above Fig. 2.3.9. The single remaining factor $2^{-j/2}$, coming originally from the $1/N$ -expansion, is sufficient to perform the sum over scales, as we shall see.

We now consider p polymers $\mathbb{P}_1 \in \mathcal{P}^{k_1\rightarrow}, \dots, \mathbb{P}_p \in \mathcal{P}^{k_p\rightarrow}$ ($k_1, \dots, k_p < j$) with n_1, \dots, n_p vertices, forming at scale j a polymer $\mathbb{P}^{j\rightarrow}$ through pairings of (some of) their external legs between themselves or with scale j propagators expanded at scale j .

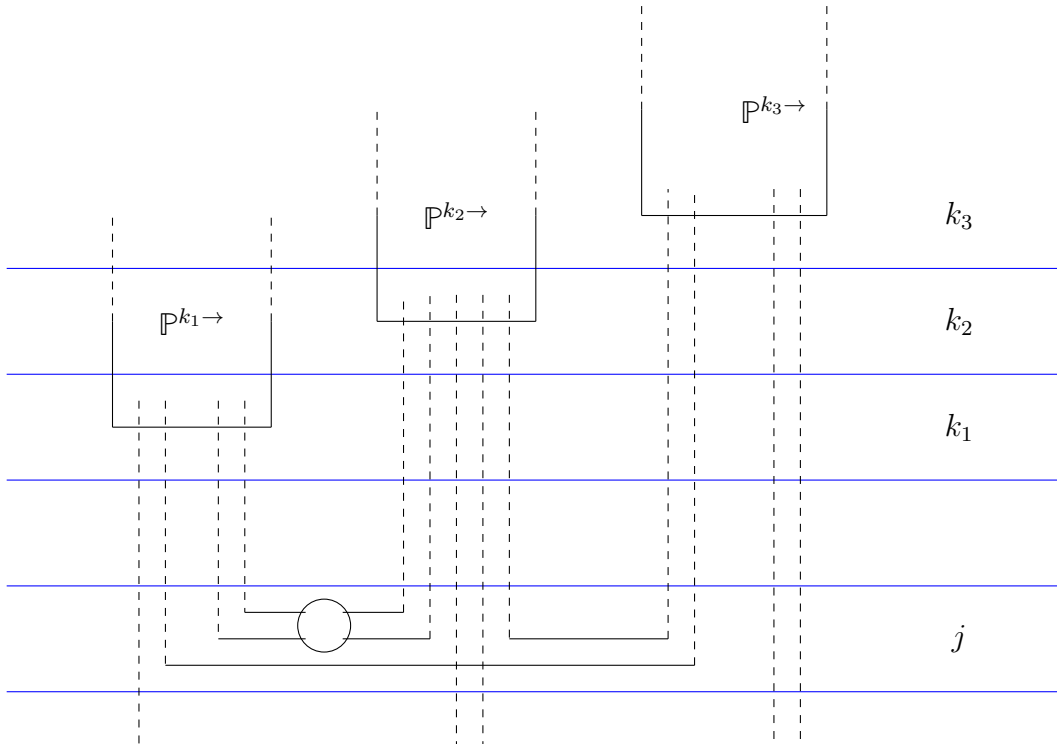


Fig. 2.4.1. Multi-scale polymer $\mathbb{P}^{j \rightarrow}$ with lowest scale j and $N_{ext} = 5$, obtained by contracting $\mathbb{P}_i \in \mathcal{P}^{k_i \rightarrow}$, $i = 1, 2, 3$, with $N_{ext,1} = 4$, resp. $N_{ext,2} = 5$, $N_{ext,3} = 4$ external legs. The blob represents a polymer expanded at scale j and connecting the scale j external legs of $\mathbb{P}^{k_1 \rightarrow}$ and $\mathbb{P}^{k_2 \rightarrow}$.

Assuming (2.123) holds for the connected components $\mathbb{P}_1, \dots, \mathbb{P}_p$ of $\mathbb{P}^{j \rightarrow} \cap \mathbb{D}^{(j-1) \rightarrow}$, we want to show that it also holds for $\mathbb{P}^{j \rightarrow}$. For that, we must take into account several factors related to the scale j integrations. The following discussion is relative to a polymer $\mathbb{P} \in \mathcal{P}^{k \rightarrow}$ with external scale k_{ext} , which is one of the \mathbb{P}_i 's. By assumption $k < k_{ext} \leq j$. For simplicity, we remove all dimensional constants $(\mu, p_F^*, m^* \dots)$ from our estimates.

Volume factors. External legs of \mathbb{P} which are contracted at scale j are integrated in a box Δ^j of scale j . This implies an absolute volume factor $O(2^{3j})$.

Field scaling factors. Each external field Ψ^{j, α_i} , $j = k_{ext, i}$ of \mathbb{P} which is contracted at scale j comes with a supplementary absolute prefactor 2^{-j} .

Taking into account volume and field scaling factors yields the general bound

$$\begin{aligned}
|\mathcal{A}(\mathbb{P}; \xi_{ext,1})| &\lesssim 2^{jN_{ext}} 2^{-3j} \prod_{i=1}^p \left\{ |\mathcal{A}(\mathbb{P}_i; \cdot)| 2^{-jN_{ext,i}} 2^{3j} \right\} \times \mathcal{N}_{sec} \\
&\lesssim 2^{jN_{ext}} 2^{-3j} \prod_{i=1}^p \left\{ g^{n_i/2} 2^{-k_i/2} 2^{-k_i(N_{ext,i} - N_0)_+} + 2^{\frac{k_i}{2}(N_{ext,i} - 4)} 2^{-jN_{ext,i}} 2^{3j} \right\} \times \mathcal{N}_{sec} \\
&= 2^{j(N_{ext} - 3)} \prod_{i=1}^p \left\{ g^{n_i/2} 2^{-(j - k_i) \frac{N_{ext,i} - 4}{2}} 2^{-k_i/2} 2^{-k_i(N_{ext,i} - N_0)_+} + 2^{-j \frac{N_{ext,i} - 2}{2}} \right\} \times \mathcal{N}_{sec},
\end{aligned} \tag{2.126}$$

where \mathcal{N}_{sec} is a bound on the sum over all possible sector assignments of external legs of polymers contracted at scale j . The $2^{jN_{ext}} 2^{-3j}$ prefactor comes from an over-counting: the number of scale j contracted external fields is not $\sum_i N_{ext,i}$, but $\left\{ \sum_i N_{ext,i} \right\} - N_{ext}$, which changes the overall field scaling factor; and the overall volume factor $(2^{3j})^n$ is corrected by a factor 2^{-3j} , since amputated diagrams are evaluated by definition with one vertex location fixed. *Polymers with 4 external legs may be considered as four-valent vertex insertions in a scale j diagram.* From the diagrammatic analysis of §2.3.2 and §2.3.3, it follows in particular that *a compound polymer obtained by contracting only polymers with 4 external legs* has at least one extra non-connecting vertex, which produces an extra factor $\lesssim 2^{-j}$, see (2.120), w.r. to the bound (2.126).

Sector assignment factors. We rewrite the overall sector assignment factor \mathcal{N}_{sec} as $\mathcal{N}'_{sec} \times \mathcal{N}''_{sec}$, where $\mathcal{N}'_{sec} := \prod_{i=1}^p \mathcal{N}'_{sec,i}$, and

$$\mathcal{N}'_{sec,i} = (2^{j/2})^{N_{ext,i} - 2} \overline{\mathcal{N}}_{sec,i}, \tag{2.127}$$

and

$$\mathcal{N}''_{sec} := (2^{j/2})^{-N_{ext} + 2} \overline{\mathcal{N}}''_{sec}. \tag{2.128}$$

Factors $\mathcal{N}'_{sec,i}$, \mathcal{N}''_{sec} combine nicely with the factors between brackets $\{ \cdot \}$ in (2.126): $2^{j(N_{ext}-3)} \times \mathcal{N}''_{sec} = (2^j)^{\frac{1}{2}(N_{ext}-4)}$, while $\left\{ \prod_{i=1}^p 2^{-j \frac{N_{ext,i}-2}{2}} \right\} \times \mathcal{N}'_{sec} = \prod_{i=1}^p \overline{\mathcal{N}}_{sec,i}$. Thus

$$|\mathcal{A}(\mathbb{P}; \xi_{ext,1})| \lesssim \prod_{i=1}^p \left\{ g^{n_i/2} 2^{-(j-k_i) \frac{N_{ext,i}-4}{2}} 2^{-k_i/2} 2^{-k_i(N_{ext,i}-N_0)_+} \overline{\mathcal{N}}_{sec,i} \right\} \times (2^j)^{\frac{1}{2}(N_{ext}-4)}. \quad (2.129)$$

The value of the *correcting factors* $\overline{\mathcal{N}}_{sec,i}$ and $\overline{\mathcal{N}}''_{sec}$ will be presently computed. The induction is successful provided we manage to prove that

$$\prod_{i=1}^p \left\{ \sum_{k_i < j} 2^{-(j-k_i) \frac{N_{ext,i}-4}{2}} 2^{-k_i/2} 2^{-k_i(N_{ext,i}-N_0)_+} \overline{\mathcal{N}}_{sec,i} \right\} \stackrel{?}{\lesssim} 2^{-j/2} 2^{-j(N_{ext}-N_0)_+} \quad (2.130)$$

if $\max_{i=1,\dots,p} N_{ext,i} > 4$, or

$$\prod_{i=1}^p \left\{ \sum_{k_i < j} 2^{-(j-k_i) \frac{N_{ext,i}-4}{2}} 2^{-k_i/2} 2^{-k_i(N_{ext,i}-N_0)_+} \overline{\mathcal{N}}_{sec,i} \right\} \stackrel{?}{\lesssim} 2^{-j(N_{ext}-N_0)_+} \quad (2.131)$$

in the specific case when $N_{ext,i} = 4$ for all $i = 1, \dots, p$. Sums $\sum_{k_i < j}$ take care of all possible choices for scales k_1, \dots, k_p .

Scale j momentum conservation for local parts of polymers with $6 \leq N_{ext} (< N_0)$. Local parts may be seen as sums of Fourier diagrams with external momenta $p_{ext,1}, \dots, p_{ext,N_{ext}}$, all coming from the same external vertex. Consider a local part whose external momenta are all contracted at scale j . Let $\alpha_1, \dots, \alpha_{N_{ext,i}} \in \mathbb{Z}/2^j\mathbb{Z}$ be their angular sectors. Since (by momentum conservation) $\sum_{i=1}^{N_{ext}} p_{ext,i} = 0$, from which $\left| \sum_{i=1}^{N_{ext}} p^{j,\alpha_i} \right| \lesssim 2^{-j} p_F^*$, and sectors of contracted legs $\langle \Psi^{j,\alpha}(\xi_{ext}) \bar{\Psi}^{j,\alpha}(\xi'_{ext}) \rangle \equiv C_\theta^{j,\alpha}(\xi_{ext}, \xi'_{ext})$ are **shared** between the two contracted fields, Proposition 2.5 gives an external sector assignment $\lesssim \mathcal{N}'_{sec,i} := (2^j)^{\frac{N_{ext,i}-2}{2}}$. Thus one sets $\overline{\mathcal{N}}_{sec,i} = 1$ for such polymers. Then

$$\sum_{k_i < j} 2^{-(j-k_i) \frac{N_{ext,i}-4}{2}} 2^{-k_i/2} \leq \sum_{k_i < j} 2^{-(j-k_i)} 2^{-k_i/2} \leq 2^{-j/2} \sum_{k_i < j} 2^{-(j-k_i)/2} = O(2^{-j/2}). \quad (2.132)$$

Polymers with $N_{ext} \geq N_0$ external legs. For polymers of type (ii) or (ii'), momentum conservation does not hold in general, so that (disregarding the sharing issue) the number of scale k_i external sector assignments is $O(2^{k_i N_{ext,i}})$. The factor $2^{-k_i(N_{ext,i}-N_0)_+} = 2^{-k_i}$ in the term between brackets $\{ \cdot \}$ in (2.130) can however be put to good use, enhancing the factor $O(2^{k_i N_{ext,i}})$ to $O(2^{k_i(N_{ext,i}-2)})$, with the same exponent $N_{ext,i} - 2$ as for local parts of polymers.

Next, each possible scale k_i sector assignment for each of the $N_{ext,i}$ external legs must be redivided into $O(2^{j-k_i})$ scale j subsectors. Assume once again that all external

momenta are contracted at scale j . Compared to the external sector assignment factor for local parts (see previous paragraph), the outcome is that *polymers of type (ii)* have an extra (shared) relative factor $O(2^{j-k_i})$. For polymers of type (ii'), this factor is compensated by the spring factor $2^{-2(j-k_i)}$, so one may set $\overline{\mathcal{N}}_{sec,i} = 1$ as for polymers of type (i). So let us concentrate on the case of polymers of type (ii), for which $\overline{\mathcal{N}}_{sec,i} = 2^{j-k_i}$ is precisely this extra relative factor. The factor 2^{j-k_i} is then compensated by the factor $2^{-(j-k_i)\frac{N_{ext,i}-4}{2}}2^{-3k_i/2}$ found in the terms between brackets $\{ \cdot \}$ in (2.126) or (2.130): namely,

$$2^{-(j-k_i)\frac{N_{ext,i}-4}{2}}2^{-3k_i/2} \cdot 2^{j-k_i} = 2^{-3k_i/2}(2^{-\frac{1}{2}(j-k_i)})^{N_{ext,i}-6} \leq 2^{-\frac{1}{2}(j-k_i)} 2^{-j} \quad (2.133)$$

if $N_{ext,i} \geq N_0$. The relative factor $2^{-\frac{1}{2}(j-k_i)}$ makes it possible to sum over scales $k_i < j$. The extra remaining factor, 2^{-j} per polymer with $N_{ext} \geq N_0$ external legs, may be used to produce the required overall $2^{-j/2}$ factor in (2.123), except, of course, if *all* polymers are local parts.

Scale j external legs. The above arguments double-count the external sector assignment for legs which are *not* contracted at scale j , and therefore remain external legs of the polymer $\mathbb{P}^{j \rightarrow}$. Removing this double-counting produces an extra sector assignment factor $\leq (2^{j/2})^{-N_{ext}} = 2^{-j} \mathcal{N}_{sec}''$ when scale j momentum conservation does not hold globally, i.e. when there is at least one polymer with $\geq N_0$ external legs. On the other hand, if *all* polymers \mathbb{P}_i are local parts, then momentum conservation for each of them implies momentum conservation for \mathbb{P} , hence the extra sector assignment factor is $\leq (2^{j/2})^{-N_{ext}+2} = \mathcal{N}_{sec}''$. Thus $\overline{\mathcal{N}}_{sec}'' = 2^{-j}$ in the first case, 1 in the second case.

Case when all polymers are local parts. In that case, all correcting factors $\overline{\mathcal{N}}_{sec,i}$ are equal to 1, so (2.131) holds when all $N_{ext,i} = 4$. Otherwise, assuming e.g. that $N_{ext,1} \geq 6$, one has $2^{-(j-k_1)\frac{N_{ext,1}-4}{2}}2^{-k_1/2} \leq 2^{-\frac{1}{2}(j-k_i)} 2^{-j/2}$, whence (2.130) holds.

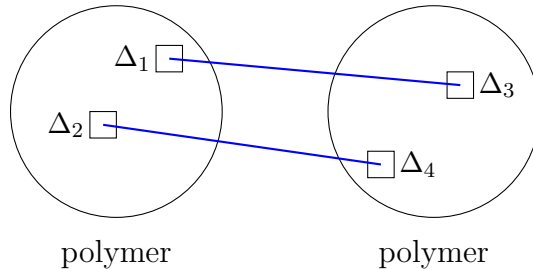
Combinatorial factors. Compared to *single-scale* trees, *multi-scale* trees involve supplementary combinatorial factors. This is a well-known problem in constructive field theory, which has been e.g. exposed in details and some generality for *bosonic theories* in [54]. The fact that the present model is *fermionic*, hence obeys Pauli's principle, leads to substantial simplifications.

Accumulation of low-momentum fields (see [54], Remark below Definition 2.9). Let $\Delta^k \in \mathbb{D}^k$, $j_D \leq k \leq j'_\phi - 1$, and $\Delta_1^j, \dots, \Delta_n^j$, $n = 2^{3(k-j)}$, be the boxes of given scale $j \leq k$ included in Δ^k . The scale j t -derivatives may have produced up to $O(1)$ low-momentum fields $\Psi^{\rightarrow(j-1)}$ or $\bar{\Psi}^{\rightarrow(j-1)}$ in each box Δ_i^j . Decomposing $\Psi^{\rightarrow(j-1)}$, $\bar{\Psi}^{\rightarrow(j-1)}$ into scales, this means that there are for each sector $\alpha \in \mathbb{Z}/2^k\mathbb{Z}$ up to $N = O(n)$ fermion fields $\Psi^{k,\alpha}$, $\bar{\Psi}^{k,\alpha}$ located in a single box Δ^k . The inverse local factorial factor $\prod_\alpha \frac{1}{(n_{\Delta,\alpha}!)^r (\bar{n}_{\Delta,\alpha}!)^r}$ of (2.105) makes it possible to sum over all pairing possibilities.

3 Low-energy theory for Cooper pairs

The picture emerging after the expansions of section 2 is that of *fermionic polymers* connected by chains of bubbles evaluated as $\text{Pre}\Sigma$ -kernels. The infra-red cut-off at scale $j'_\phi - 1$ keeps away infra-red singularities, and the $1/N$ expansions ensures that the series of perturbations converges. This is still clearly one step behind the conjectured, divergent infra-red behavior in $O(1/|q|^2)$ of the Goldstone boson propagator (or $\Sigma_{\perp,\perp}$ -kernel), found in principle by means of the gap equation as in §1.7.

We need in the first place a proper definition of the Goldstone boson propagator that goes beyond perturbation theory. Instead of developing blindly an infinite sum of individual four-point diagrams, and selecting those which are two-particle irreducible by checking all possible ways of cutting it into two pieces, we implement a decision rule relying only on the number of links explicitly constructed by hand between pairs of polymers seen as small, almost pointwise vertex insertions. This is the object of the **complementary cluster expansions** of §3.2. Those are horizontal cluster expansions, between scale j'_ϕ fermions only, obtained by expanding links *to third order* between boxes of pairs of polymers. The idea is that we exhaust explicitly in this way *all possible* configurations of the type



where two polymers are connected by exactly two links; displacing one of the blue fermion links so as to form a bubble as in Fig. 1.7.5, one obtains eventually a rung connecting Bethe-Salpeter kernels. Such configurations contribute to the infra-red divergence of the Goldstone boson propagator, therefore the two polymers are not *sufficiently* connected to be able to sum over the location of one of them w.r. to that of the other. On the other hand, *three* links suffice to ensure **strong connectivity** between these. Building upon this concept of strong connectivity, we develop multi-scale trees whose vertices are polymers, and edges – three-fold links. Because polymers with ≥ 6 external legs are not diverging, emphasis is laid on four-point polymers. Those are considered to have a bosonic scale $j_+ \geq j'_\phi$ given by the scale of their transfer momentum q , which may be determined to some precision by refining the sector decomposition of the fermions.

The outcome of these complementary expansions is an expression of the kernel $\Pi(q)$ for $|q| \approx 2^{-j+\mu}$ in terms of a sum over polymer configurations, n -point functions are then

rewritten in terms of sums over simplified trees called **bosonic trees**, whose vertices are still polymers, but edges are now **single-scale Goldstone boson propagators** (not yet Goldstone boson propagators, see below) of given scales, see Fig. 3.2.14.

However, even at this stage, we are not able to prove that n -point functions are infra-red summable, because the theory is a priori plagued with infra-red divergences coming from Goldstone boson propagators with low transfer momentum, connecting arbitrarily far-away fermionic polymers. This problem is solved in §3.3 using *Ward identities* similar to those used to solve the problem of "soft photons" (infra-red photons) in QED. First of all, multi-scale *two-point functions* of Cooper pairs, inductively extracted from bosonic trees (see Fig. 3.2.14), have no associated Ward identity, hence must be resummed by hand. This is a simple geometric series, whose sum gives at last the **Goldstone boson propagator** we were looking for. As a consequence of these partial resummations, previous bosonic trees are replaced by very similar bosonic trees with the same type of vertices, but whose edges are Goldstone boson propagators, and that furthermore have no internal two-point functions. We may now solve the gap equation by an easy fixed-point argument, and verify the predictions of §1.7 concerning the infra-red behavior of the geometric series Σ .

In the large-scale limit, i.e. at space-time scales much larger than $1/\Gamma_\phi$, polymers of bosonic trees appear in our multi-scale picture as tiny islands giving subleading contributions to n -point functions. This makes plausible the general structure of the formula of Theorem 2,

$$\left\langle \prod_{i=1}^{2n} : (\bar{\Psi} \Gamma^\perp \Psi)(\eta^{-1} \xi_i) : \right\rangle_{\theta; \lambda} \sim_{\eta \rightarrow 0} \lambda^{-2n} \sum_{(i_1, i_2), \dots, (i_{2n-1}, i_{2n})} \prod_{k=1}^n \left({}^t \Gamma^\perp \Sigma \Gamma^\perp \right) (\eta^{-1} (\xi_{i_{2k-1}} - \xi_{i_{2k}})). \quad (3.1)$$

As apparent in (3.1), the effective theory is roughly that of a *free bosonic particle* – the *Goldstone boson* – with covariance kernel Σ . This Theorem is proved in §3.5.

Let us now turn to another question. The effective potential approach described in the Introduction (Regime II) suggested that the *field* $\Gamma(\xi)$ conjugate to Cooper pairs should behave like a non-linear sigma-model valued in the immediate neighborhood of the circle of radius Γ_ϕ . Thus, it is in principle possible to distinguish *transverse* (i.e. orthogonal to the circle) fluctuations – "slow" degrees of freedom – from *tangential* fluctuations – "fast" degrees of freedom.

Here, by comparison, a preferential direction θ has been fixed by the symmetry-breaking term. Thus all there remains to be done is to check that with high probability, the Cooper-pair field is to a good approximation aligned with this direction, and has a modulus fixed by the gap equation. This is the content of Theorems 4 and 5 in the Introduction, proved resp. in §3.7 and §3.8.

The introductory, heuristic subsection §3.1, recapitulates the main findings of mean-field theory concerning the infra-red behavior of the theory. Classical results presented there without proof are only half-quantitative since the Goldstone boson propagator has been replaced by its leading order obtained by resumming Cooper pair bubbles, but notations introduced there are important for the subsection on Ward identities.

3.1 A heuristic introduction

We present in this subsection a heuristic derivation of the large-scale behavior of the theory in the Cooper channel, based on elementary considerations, and the fundamental assumption that asymptotics may be obtained by considering only chains of Cooper pair bubble diagrams. Notations introduced here are fundamental for §3.3 where Ward identities will be proved, justifying the present heuristics beyond its pedagogical value.

Let us first write down the various quadratic fields built out of one $\bar{\Psi}$ and one Ψ :

- *Cooper pairs:*

$$\bar{\Psi}\Gamma(\theta)\Psi = \Gamma_\phi \bar{\Psi} \begin{pmatrix} 0 & e^{-i\theta} \\ e^{i\theta} & 0 \end{pmatrix} \Psi = \Gamma_\phi \left(e^{-i\theta} \bar{\psi}_\uparrow \bar{\psi}_\downarrow + e^{i\theta} \psi_\downarrow \psi_\uparrow \right); \quad (3.2)$$

dividing by Γ_ϕ , we get a different possible normalization, $\bar{\Psi}\sigma(\theta)\Psi = \bar{\Psi} \begin{pmatrix} 0 & e^{-i\theta} \\ e^{i\theta} & 0 \end{pmatrix} \Psi$, where

$$\sigma(\theta) \equiv \frac{1}{\Gamma_\phi} \Gamma(\theta) = \cos \theta \sigma^1 + \sin \theta \sigma^2. \quad (3.3)$$

- *normal pairs:*

$$\bar{\Psi}\sigma^3\Psi = \bar{\psi}_\uparrow\psi_\uparrow + \bar{\psi}_\downarrow\psi_\downarrow; \quad (3.4)$$

- *identity pairings:*

$$\bar{\Psi}\mathbb{1}\Psi = \bar{\psi}_\uparrow\psi_\uparrow - \bar{\psi}_\downarrow\psi_\downarrow. \quad (3.5)$$

Let us now translate expressions (1.78,1.79) for $\text{Pre}\Sigma(q)$ in a new base: denoting by $//$ the direction parallel to θ , and \perp the direction rotated by an angle $\pi/2$, so that

$$\Gamma// \equiv \Gamma//(\theta) = \Gamma(\theta), \quad \Gamma^\perp \equiv \Gamma^\perp(\theta) = \Gamma\left(\theta + \frac{\pi}{2}\right), \quad (3.6)$$

we consider the $\text{Pre}\Sigma$ -kernel in the $(//, \perp)$ basis:

$$\begin{pmatrix} \text{Pre}\Sigma_{//, //} & \text{Pre}\Sigma_{//, \perp} \\ \text{Pre}\Sigma_{\perp, //} & \text{Pre}\Sigma_{\perp, \perp} \end{pmatrix}. \quad (3.7)$$

When $\theta = 0$, one gets $\bar{\Psi}\Gamma^{//}\Psi = \Gamma_\phi(\bar{\psi}_\uparrow\bar{\psi}_\downarrow + \psi_\downarrow\psi_\uparrow)$, $\bar{\Psi}\Gamma^\perp\Psi = -i\Gamma_\phi(\bar{\psi}_\uparrow\bar{\psi}_\downarrow - \psi_\downarrow\psi_\uparrow)$ and

$$\begin{aligned} \text{Pre}\Sigma_{//, //} &= \text{Pre}\Sigma_{(\bar{\psi}_\uparrow\bar{\psi}_\downarrow + \psi_\downarrow\psi_\uparrow) \otimes (\bar{\psi}_\uparrow\bar{\psi}_\downarrow + \psi_\downarrow\psi_\uparrow)} \\ &:= \text{Pre}\Sigma_{\bar{\psi}_\uparrow\bar{\psi}_\downarrow, \bar{\psi}_\uparrow\bar{\psi}_\downarrow} + \text{Pre}\Sigma_{\bar{\psi}_\uparrow\bar{\psi}_\downarrow, \psi_\downarrow\psi_\uparrow} + \text{Pre}\Sigma_{\psi_\downarrow\psi_\uparrow, \bar{\psi}_\uparrow\bar{\psi}_\downarrow} + \text{Pre}\Sigma_{\psi_\downarrow\psi_\uparrow, \psi_\downarrow\psi_\uparrow} \end{aligned} \quad (3.8)$$

and similarly

$$\text{Pre}\Sigma_{//, \perp} = -i\text{Pre}\Sigma_{(\bar{\psi}_\uparrow\bar{\psi}_\downarrow + \psi_\downarrow\psi_\uparrow) \otimes (\bar{\psi}_\uparrow\bar{\psi}_\downarrow - \psi_\downarrow\psi_\uparrow)}, \quad \text{Pre}\Sigma_{\perp, //} = -i\text{Pre}\Sigma_{(\bar{\psi}_\uparrow\bar{\psi}_\downarrow - \psi_\downarrow\psi_\uparrow) \otimes (\bar{\psi}_\uparrow\bar{\psi}_\downarrow + \psi_\downarrow\psi_\uparrow)} \quad (3.9)$$

$$\text{Pre}\Sigma_{\perp, \perp} = -\text{Pre}\Sigma_{(\bar{\psi}_\uparrow\bar{\psi}_\downarrow - \psi_\downarrow\psi_\uparrow) \otimes (\bar{\psi}_\uparrow\bar{\psi}_\downarrow - \psi_\downarrow\psi_\uparrow)}. \quad (3.10)$$

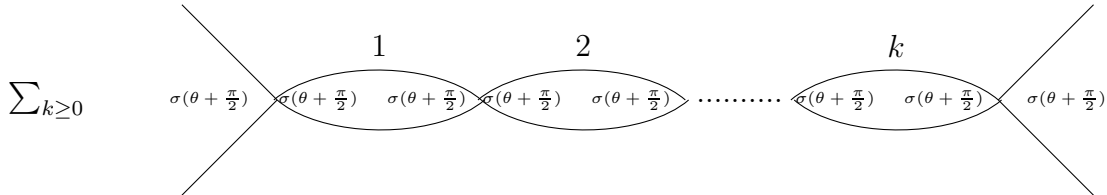
Using rotation equivariance, it is easy to prove that

$$\begin{aligned} {}^t\mathbf{\Gamma}^{//}\text{Pre}\Sigma\mathbf{\Gamma}^{//} &= \Gamma_\phi^2\text{Pre}\Sigma_{//, //}, \quad {}^t\mathbf{\Gamma}^{//}\text{Pre}\Sigma\mathbf{\Gamma}^\perp = \Gamma_\phi^2\text{Pre}\Sigma_{//, \perp}, \\ {}^t\mathbf{\Gamma}^\perp\text{Pre}\Sigma\mathbf{\Gamma}^{//} &= \Gamma_\phi^2\text{Pre}\Sigma_{\perp, //}, \quad {}^t\mathbf{\Gamma}^\perp\text{Pre}\Sigma\mathbf{\Gamma}^\perp = \Gamma_\phi^2\text{Pre}\Sigma_{\perp, \perp}. \end{aligned} \quad (3.11)$$

Hermitian symmetry implies that $\text{Pre}\Sigma$ is diagonal in the $(//, \perp)$ -basis. Now, (1.79,1.78) implies that

$$\text{Pre}\Sigma_{\perp, \perp}(q) \sim \frac{g_\phi^0}{(|q|_+^0)^2}, \quad \text{Pre}\Sigma_{//, //}(q) \approx \frac{1}{m^*}. \quad (3.12)$$

The kernel $\text{Pre}\Sigma_{//, //}(q) \approx \frac{1}{m^*} \approx \frac{1}{m^*} \frac{\Gamma_\phi^2}{|q|_+^2 + \Gamma_\phi^2} \approx \frac{g_\phi^0}{|q|_+^2 + \Gamma_\phi^2}$ has a characteristic massive decay for $|q|_+ \lesssim \Gamma_\phi$, with mass $\approx \Gamma_\phi$. Hence the main term in the large-scale behavior of N -point functions of Cooper pairs is obtained by considering only bound states $\bar{\Psi}\Gamma^\perp\Psi$ propagating through space-time through chains of Cooper space bubble diagrams



3.1.1. Bound state propagation.

which is simply the $\text{Pre}\Sigma$ -kernel $\text{Pre}\Sigma_{\perp, \perp}$ in the perpendicular direction.

If $\theta', \theta'' \neq \theta$, the leading-order term of the function

$$\left\langle : (\bar{\Psi}\Gamma(\theta')\Psi)(\xi) : : (\bar{\Psi}\Gamma(\theta'')\Psi)(\xi') : \right\rangle_{\theta, \lambda}$$

is (letting $\sigma^\perp := \sigma(\theta + \frac{\pi}{2})$)

$$\Gamma(\theta') \begin{array}{c} \text{---} \\ \text{---} \\ \text{---} \end{array} \Gamma(\theta'') + \sum_{k \geq 0} \Gamma(\theta') \begin{array}{c} \text{---} \\ \text{---} \\ \text{---} \end{array} \begin{array}{c} 1 \\ \sigma^\perp \quad \sigma^\perp \end{array} \begin{array}{c} \text{---} \\ \text{---} \\ \text{---} \end{array} \begin{array}{c} 2 \\ \sigma^\perp \quad \sigma^\perp \end{array} \dots \begin{array}{c} \text{---} \\ \text{---} \\ \text{---} \end{array} \begin{array}{c} k \\ \sigma^\perp \quad \sigma^\perp \end{array} \Gamma(\theta'')$$

Fig. 3.1.2. Two-point function.

evaluated as the inverse Fourier transform of

$$\begin{aligned} q \mapsto & \text{Tr}(\Gamma(\theta')\sigma(\theta)\Gamma(\theta''))(\mathcal{A}_q)_{//, //} + \text{Tr}(\Gamma(\theta')\sigma(\theta + \frac{\pi}{2})\Gamma(\theta''))(\mathcal{A}_q)_{\perp, \perp} \\ & + \text{Tr}(\Gamma(\theta')\sigma^\perp)\text{Tr}(\sigma^\perp\Gamma(\theta''))(\mathcal{A}_q)_{\perp, \perp} \text{Pre}\Sigma(q)(\mathcal{A}_q)_{\perp, \perp} \\ \sim & \left\{ \text{Tr}(\Gamma(\theta')\Gamma(\theta'')) - \text{Tr}(\Gamma(\theta')\sigma^\perp) - \text{Tr}(\Gamma(\theta')\sigma^\perp)\text{Tr}(\sigma^\perp\Gamma(\theta'')) \right\} (\mathcal{A}_q)_{\perp, \perp} \\ & + \text{Tr}(\Gamma(\theta')\sigma^\perp)\text{Tr}(\sigma^\perp\Gamma(\theta''))(\mathcal{A}_q)_{\perp, \perp} \left(1 + \text{Pre}\Sigma(q)(\mathcal{A}_q)_{\perp, \perp} \right) \\ = & \left\{ \text{Tr}(\Gamma(\theta')\Gamma(\theta'')) - \text{Tr}(\Gamma(\theta')\sigma^\perp)\text{Tr}(\sigma^\perp\Gamma(\theta'')) \right\} (\mathcal{A}_q)_{\perp, \perp} \\ & + \frac{1}{\lambda} \text{Tr}(\Gamma(\theta')\sigma^\perp)\text{Tr}(\sigma^\perp\Gamma(\theta''))(\mathcal{A}_q)_{\perp, \perp} \text{Pre}\Sigma(q). \end{aligned} \tag{3.13}$$

where one has neglected the difference $(\mathcal{A}_q)_{//, //} - (\mathcal{A}_q)_{\perp, \perp}$ in the term without $\text{Pre}\Sigma$ kernel. Since $(\mathcal{A}_q)_{//, //}, (\mathcal{A}_q)_{\perp, \perp} \sim_{q \rightarrow 0} \frac{1}{\lambda}$ are not singular in the infra-red limit, this gives to leading order in g if $\theta', \theta'' \neq \theta$

$$\left\langle : (\bar{\Psi}\Gamma(\theta')\Psi)(\xi) : : (\bar{\Psi}\Gamma(\theta'')\Psi)(\xi') : \right\rangle_{\theta; \lambda} \approx_{|\xi - \xi'| \rightarrow \infty} \text{Tr}(\Gamma(\theta')\sigma^\perp) \text{Tr}(\sigma^\perp\Gamma(\theta'')) \frac{1}{\lambda^2} \text{Pre}\Sigma(\xi - \xi'). \tag{3.14}$$

Graphically,

$$\left\langle : (\bar{\Psi}\Gamma(\theta')\Psi)(\xi) : : (\bar{\Psi}\Gamma(\theta'')\Psi)(\xi') : \right\rangle_{\theta; \lambda} \approx \xi \begin{array}{c} \frac{\Gamma}{\lambda} \\ \bullet \\ \text{---} \\ \bullet \\ \frac{\Gamma}{\lambda} \end{array} \xi'$$

Generalizing, one obtains a semi-perturbative version of Theorem 2: the leading term of $\left\langle \prod_{i=1}^{2n} : (\bar{\Psi}\Gamma^\perp\Psi)(\xi_i) : \right\rangle_{\theta; \lambda}$ for widely separated points ξ_1, \dots, ξ_{2n} is graphically (taking e.g. $n = 3$)

$$\begin{array}{c} \xi_1 \begin{array}{c} \frac{\Gamma}{\lambda} \\ \bullet \\ \text{---} \\ \bullet \\ \frac{\Gamma}{\lambda} \end{array} \xi_4 \\ \\ \xi_2 \begin{array}{c} \frac{\Gamma}{\lambda} \\ \bullet \\ \text{---} \\ \bullet \\ \frac{\Gamma}{\lambda} \end{array} \xi_5 \quad + \text{perm.} \\ \\ \xi_3 \begin{array}{c} \frac{\Gamma}{\lambda} \\ \bullet \\ \text{---} \\ \bullet \\ \frac{\Gamma}{\lambda} \end{array} \xi_6 \end{array}$$

Fig. 3.1.2. 6-point function of Cooper pairs.

where "perm." indicates the sum over all possible pairings.

Let us now consider the one-point function in the parallel direction ($//$). Main term is

$$\langle\langle\bar{\Psi}\sigma(\theta)\Psi\rangle\rangle_{\theta;\lambda}(\xi) = \text{Tr}((\sigma(\theta))^2) \bullet \text{---} \Gamma \approx 2\frac{\Gamma_\phi}{\lambda}$$

where the coefficient 2 comes from the trace $\text{Tr}((\sigma(\theta))^2)$. The gap equation, see Fig. 1.7.6, implies that the correction due to the Goldstone boson

$$\xi \bullet \text{---} \left(- \Gamma \quad + \quad \text{---} \right)$$

vanishes identically.

Let us finally mention another identity,

$$\boxed{\langle\langle\bar{\Psi}\mathbb{1}\Psi\rangle\rangle_{\theta;\lambda}(\xi) = 0,} \tag{3.15}$$

obvious by the symmetry exchanging \uparrow - and \downarrow -states.

3.2 Complementary expansion

After these heuristics and general power-counting considerations, let us now come back to where we left the story. At the end of section 2, the situation was as follows: n -point functions have been rewritten as a sum over polymers $\mathbb{P}_1, \dots, \mathbb{P}_p \in \mathcal{P}^{\rightarrow(j'_\phi-1)}$ with lowest scale $\leq j'_\phi - 1$. Because two-point functions have been renormalized at scale $j'_\phi - 1$, and vacuum polymers have been divided out using Mayer's expansion, there remain only polymers with 4 external legs, and polymers with ≥ 6 (not fully produced) external legs. Since there is only one scale left, all external legs are of scale j'_ϕ . The measure has retained an exponential weight $e^{-\sum_\Delta \int d\xi \chi_\Delta(\xi) \mathcal{L}_\theta^{j'_\phi}(\xi)}$, where $\Delta \in \mathbb{D}^{j'_\phi}$ ranges over the set of scale j'_ϕ boxes – thereafter called **isolated boxes** – that are not connected by a vertical link to boxes of higher scale $\leq j'_\phi - 1$, and

$$\mathcal{L}_\theta^{j'_\phi}(\xi) := \mathcal{L}_\theta^{\rightarrow j'_\phi}(\mathbf{t} = 0; \xi) = \lambda(\bar{\Psi}^{j'_\phi}\Psi^{j'_\phi})^2(\xi) + \bar{\Psi}^{j'_\phi}(\xi) (\delta Z^{j'_\phi}\partial_\tau + \delta\Gamma^{j'_\phi}) \Psi^{j'_\phi}(\xi), \tag{3.16}$$

compare with (2.36) and (2.66), since by hypothesis $\delta\mu^{j'_\phi} = 0, \delta m^{j'_\phi} = 0$. Recall that $\delta\Gamma^{j'_\phi} = O(g\Gamma_\phi)$ has an extra $O(g)$ pre-factor. As apparent from §1.7, a particular rôle will be played by what are called **polymers of type 2** in the following

Definition 3.1 (polymers of type 1 and type 2) *Let $\mathbb{P} \in \mathcal{P}^{(j'_\phi-1)\rightarrow}$ be a four-point polymer with scale j'_ϕ external legs in angular sectors $\alpha_1, \dots, \alpha_4 \in \mathbb{Z}/2^{j'_\phi}\mathbb{Z}$. Then \mathbb{P} is said to be of **type 2** if all the following conditions are satisfied:*

(i) $N_{ext} = 4$;

(ii) $|\alpha_1 + \alpha_2|, |\alpha_3 + \alpha_4| \leq 1$.

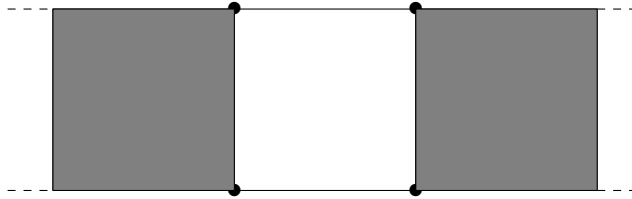
Its external structure is either non-mixing, $(\bar{\psi}_{\uparrow}^{j',\alpha_1} \bar{\psi}_{\downarrow}^{j',\alpha_2}) \otimes (\psi_{\downarrow}^{j',\alpha_3} \psi_{\uparrow}^{j',\alpha_4})$, or mixing, $(\bar{\psi}_{\uparrow}^{j',\alpha_1} \bar{\psi}_{\downarrow}^{j',\alpha_2}) \otimes (\bar{\psi}_{\uparrow}^{j',\alpha_3} \bar{\psi}_{\downarrow}^{j',\alpha_4})$ or $(\psi_{\downarrow}^{j',\alpha_1} \psi_{\uparrow}^{j',\alpha_2}) \otimes (\psi_{\downarrow}^{j',\alpha_3} \psi_{\uparrow}^{j',\alpha_4})$. Furthermore, if the polymer is mixing, we require that

(iii) $|\alpha_1 + \alpha_4|, |\alpha_2 + \alpha_3| > 1$.

All other polymers \mathbb{P} in $\mathcal{P}^{(j'_\phi-1)\rightarrow}$, and also isolated scale j'_ϕ boxes, are said to be of **type 1**.

Polymers of type 2 are exactly those which make part of the Bethe-Salpeter kernel, accounting for the large-scale behavior of the theory. Roughly speaking: \mathbb{P} is a polymer of type 2 if it is a four-point polymer with transfer momentum $q = p_1 + p_2 = p_3 + p_4$ such that $|q| \lesssim 2^{-j'_\phi} \mu$. Note that conditions (ii), (iii) have some degree of arbitrariness. For instance, because angular sectors do not have sharp cut-offs, one may have $|\alpha_1 + \alpha_2| \leq 1$ but $|\alpha_3 + \alpha_4| > 1$, or vice-versa. Also, in the case of a mixing diagram, say with external structure $(\bar{\psi}_{\uparrow}^{j',\alpha_1} \bar{\psi}_{\downarrow}^{j',\alpha_2}) \otimes (\bar{\psi}_{\uparrow}^{j',\alpha_3} \bar{\psi}_{\downarrow}^{j',\alpha_4})$, one may exchange α_2 and α_4 . Condition (iii) ensures that our criterion is unambiguous: there can be only *one* numbering of external legs such that \mathbb{P} is of type 2. As we shall see later on, such subtleties are irrelevant in the infra-red limit.

A. General introduction. The general philosophy in this subsection is to perform a partial, carefully devised separation of *fermionic* degrees of freedom from *bosonic* degrees of freedom. In theory, this means the following. Imagine the interaction $e^{-\mathcal{L}_\theta}$ has been wholly expanded into series, after which Wick's formula has turned an n -point function into an (infinite) sum of diagrams. Then sequences



see Fig. 1.7.4, of two-particle irreducible, four-point diagrams with Cooper pair external structure connected by two fermionic lines, should be resummed into a Goldstone boson propagator, plus error terms due to displacements and projections, as in §1.7. Then diagrams would be bound as in §2.3 by following fermionic loops.

Things are however not so simple, because of the well-known problem of accumulation of low-momentum fields characteristic of non-massive bosonic theories (see e.g. [54]).

Let us give a sketchy description of this problem, assuming for simplicity that $j'_\phi = j_\phi$. Suppose that one has produced one Cooper pair with transfer momentum $|q| \approx 2^{-j_+ \mu}$ ($j_+ > j_\phi$) per scale j_ϕ box Δ included in a large scale j_+ box Δ^{j_+} ; in total, $n = 2^{3(j_+ - j_\phi)}$ fields Cooper pairs. Then the (supposedly asymptotically Gaussian) contribution of all possible Σ -pairings of Cooper pairs through Wick's formula would lead to a combinatorial factor $\approx \Gamma(n/2)$, in other words, $O((2^{j_+ - j_\phi})^{3/2})$ per Cooper pair. This is more than can be compensated by the weight due to the products of the Σ -kernels, which is (leaving out dimensional constants) roughly $(\Sigma(|\xi - \xi'| \approx 2^{-j_+ \mu})^{n/2} \approx (g_\phi/|\xi - \xi'|_+)^{n/2} \approx 2^{-j_\phi n/2} (2^{-\frac{1}{2}(j_+ - j_\phi)})^n$. Taking further into account small factors due to Ward identities, see §3.3, would contribute in the best case $O(2^{-(j_+ - j_\phi)})$ per Cooper pair: a global $O(1)$ counting, not sufficient though to sum over all scales $j_+ > j_\phi$.

Strategies often developed to deal with this problem in equilibrium statistical physics, relying mainly on large-deviation estimates (see [54]), are difficult to implement here because the Goldstone boson has not been introduced in the first place. Instead we choose to expand *some* and not *all* Goldstone boson propagators, in such a way as to form a multi-scale forest, where scales refer to the bosonic scales of transfer momenta. As briefly mentioned in the introduction to §2.3, we develop links between *objects*, which are polymers $\mathbb{P}_1, \dots, \mathbb{P}_n$ of lowest fermionic scale $\leq j'_\phi$, *with external legs of scale* j'_ϕ . Fix some bosonic scale $j_+ \geq j'_\phi$. At that scale, we must still deal with potentially diverging four-point functions with transfer momentum of scale j_+ . In order to read easily the transfer momentum of a Cooper pair $\bar{\psi}_\uparrow^{j'_\phi} \bar{\psi}_\downarrow^{j'_\phi}$ or $\psi_\downarrow^{j'_\phi} \psi_\uparrow^{j'_\phi}$, we decompose $\psi_\uparrow^{j'_\phi}, \bar{\psi}_\uparrow^{j'_\phi}$ into 2^{j_+} angular sectors $\mathcal{S}^\alpha \equiv \mathcal{S}^{j'_\phi, \alpha}$, following (2.10), $\psi_\uparrow^{j'_\phi} \equiv \sum_{\alpha \in \mathbb{Z}/2^{j_+} \mathbb{Z}} \psi_\uparrow^{j'_\phi, \alpha}$, $\bar{\psi}_\uparrow^{j'_\phi} \equiv \sum_{\alpha \in \mathbb{Z}/2^{j_+} \mathbb{Z}} \bar{\psi}_\uparrow^{j'_\phi, \alpha}$. Then the total momentum of a pair $\bar{\psi}_\uparrow^{j'_\phi, \alpha_1} \bar{\psi}_\downarrow^{j'_\phi, \alpha_2}$ or $\psi_\downarrow^{j'_\phi, \alpha_1} \psi_\uparrow^{j'_\phi, \alpha_2}$ is $\lesssim 2^{-j_+ \mu}$ if and only if $|\alpha_1 + \alpha_2| \lesssim 1$. Apart if $j_+ = j'_\phi$ (in which case we also want to deal with the remaining interaction $\mathcal{L}_\theta^{j'_\phi}$), we mainly want to understand how polymers of type 2 are connected at scale j_+ . Compared to the fermionic cluster expansion of §2.3, things are more involved, because expansion rules are strongly dependent on the scales of transfer momenta. Furthermore, we shall also need to resum (by inspection) two-particle irreducible four-point diagrams with Cooper pair external structure, so as to produce the Goldstone boson propagator Σ .

Extending Definition 3.1, we may say that a four-point polymer with external structure

$$(\bar{\psi}_\uparrow^{j'_\phi, \alpha_1} \bar{\psi}_\downarrow^{j'_\phi, \alpha_2}) \otimes (\psi_\downarrow^{j'_\phi, \alpha_3} \psi_\uparrow^{j'_\phi, \alpha_4}), (\bar{\psi}_\uparrow^{j'_\phi, \alpha_1} \bar{\psi}_\downarrow^{j'_\phi, \alpha_2}) \otimes (\bar{\psi}_\uparrow^{j'_\phi, \alpha_3} \bar{\psi}_\downarrow^{j'_\phi, \alpha_4}) \text{ or } (\psi_\downarrow^{j'_\phi, \alpha_1} \psi_\uparrow^{j'_\phi, \alpha_2}) \otimes (\psi_\downarrow^{j'_\phi, \alpha_3} \psi_\uparrow^{j'_\phi, \alpha_4}) \quad (3.17)$$

$(\alpha_1, \dots, \alpha_4 \in \mathbb{Z}/2^{j_+} \mathbb{Z})$ is a *scale j_+ polymer of type 2* provided $|\alpha_1 + \alpha_2|, |\alpha_3 + \alpha_4| \leq 1$, and (if the polymer is mixing) $|\alpha_1 + \alpha_4|, |\alpha_2 + \alpha_3| > 1$, so that, in particular, the transfer momentum has scale $\geq j_+$. However, as we shall see, this notion is essentially redundant as soon as $j_+ > j'_\phi$, because four-point polymers not satisfying these conditions have already been taken care of at some higher scale $< j_+$.

As a general principle, polymers will be of two types:

- **scale j_+ four-point polymers** ($j_+ \geq j'_\phi$), generically called **low transfer momentum four-point polymers**, whose transfer momentum is $|q| \approx 2^{-j_+\mu}$;
- and **”scale-neutral” polymers** – that is, all other types of polymers –, whose external leg transfer momenta we do not need to determine, because they cannot by themselves produce divergences in the infra-red limit.

Particularizing, we have **irreducible polymers**,

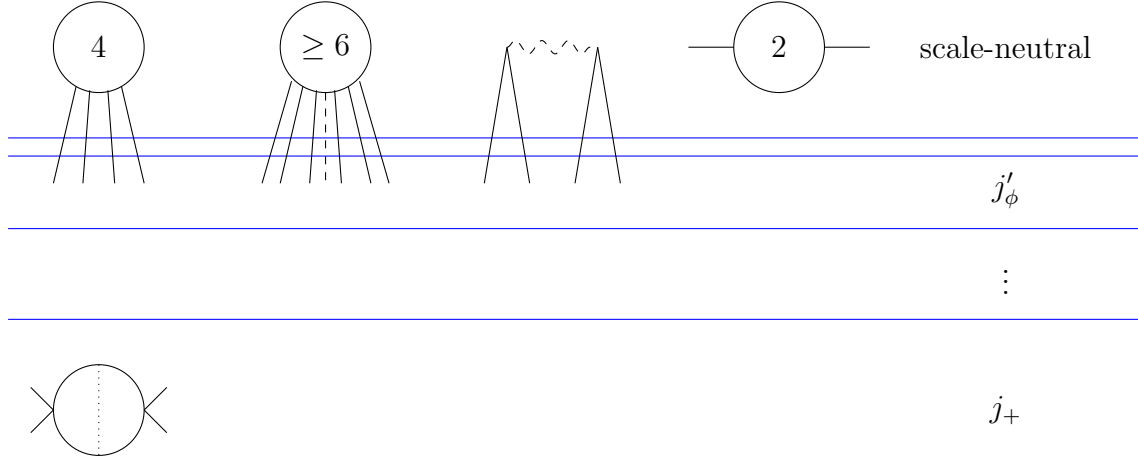


Fig. 3.2.1. Irreducible polymers.

Polymers are represented by *blobs*.

Figures at the center of *scale-neutral polymers* indicate the number of external legs. Polymers with 2 scale j'_ϕ external legs contribute to an inessential renormalization of the two-point function (whereas two-point polymers with higher momentum external legs have already been resummed in section 2). Scale-neutral four-point polymers are four-point polymers with a large transfer momentum $\gtrsim 2^{-j'_\phi\mu}$. Six-point polymers are convergent, whence one does not need to investigate the scale of transfer momenta of external leg pairs. The same holds for lonely Goldstone pre-boson propagators coming from ”half-integer” fermionic scales, which have not become part of a fermionic polymer: they may couple to scale j_+ four-point polymers because their transfer momentum may be arbitrarily small; however, due to their scale $j'_\phi - 1$ infra-red cut-off, such propagators have quasi-exponential decay at distances larger than Γ_ϕ^{-1} , hence they may be considered at lower energies as irreducible.

The dotted line at the center of a *scale j_+ four-point polymer* separates external legs with index 1,2 from external legs with index 3,4, in such a way that the transfer momentum flowing from either side is $\approx 2^{-j_+\mu}$.

Assembling irreducible polymers yields irreducible and **reducible polymers**. There are no scale-neutral reducible polymers; contracting scale-neutral polymers simply gives a new scale-neutral polymer, whose number of external legs is at least equal to the sum of external legs of each constituent polymer, minus twice the number of

pairings ("at least" because pairings of not fully expanded polymers may yield new vertices instead of contracting previously developed external legs),

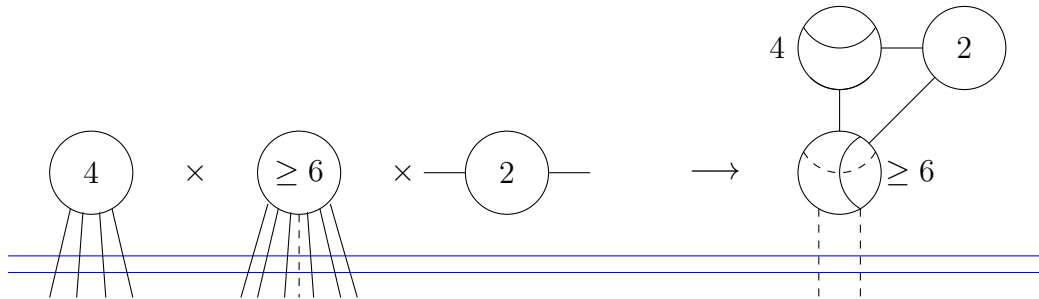


Fig. 3.2.2. Assembly rules of scale-neutral polymers: an example.

Scale j_+ reducible polymers are made up of scale j_+ four-point polymers and possibly scale-neutral polymers, interspersed with bubbles: pure scale j_+ polymers generalizing chains of bubbles,

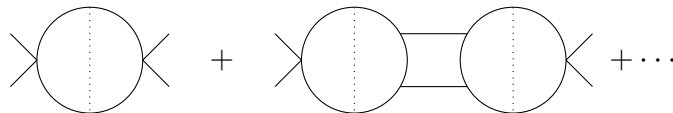


Fig. 3.2.3. Generalized chains of bubbles.

and chains including one or more contribution from scale-neutral polymers with ≥ 4 external legs,

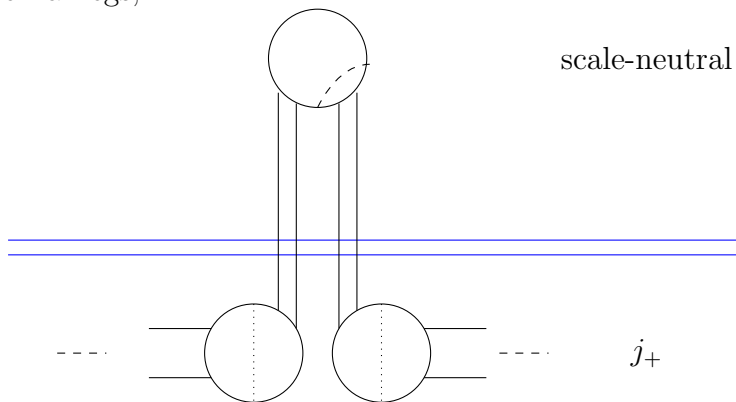


Fig. 3.2.4. Insertion of scale-neutral polymers into chains of bubbles.

Double lines are Cooper bubbles with dressed propagators obtained by resumming scale-neutral two-point polymers. Fig. 3.2.3 may be seen as the leading term of Fig. 3.2.4, the scale-neutral polymer being just a four-point vertex with a λ coefficient. After a Mayer expansion and an s -wave projection (see **D.** below for the detailed procedure), all these chains are resummed to form so-called **single-scale Goldstone boson propagators** with transfer momentum $|q| \approx 2^{-j_+} \mu$, denoted by a dotted

wiggling line $\sim\sim\sim\sim\sim\sim$ (not to be confused with the previous Pre- Σ kernel *dashed* wiggling lines). A final resummation procedure produces at last our *Goldstone boson propagator* Σ , which contain internal single-scale Goldstone boson propagators with transfer momentum with higher scales $\leq j_+$.

There is a slight inaccuracy in Fig. 3.2.1 and Fig. 3.2.2, in that the scales $j_{+,1}, j_{+,2}$ of the low transfer momentum polymers need not be exactly the same; because momentum cut-offs are not sharp, one has instead $|j_{+,1} - j_{+,2}| \lesssim 1$. Note also that a Mayer resummation is necessary to have momentum conservation.

If the inserted scale-neutral polymer has exactly 4 external legs, then this configuration forms a chain. If, however, it has ≥ 6 external legs, then its supplementary legs may also contract to an arbitrary number $n \geq 3$ of low transfer momentum four-point polymers according to the following pattern (where one has chosen $n = 3$),

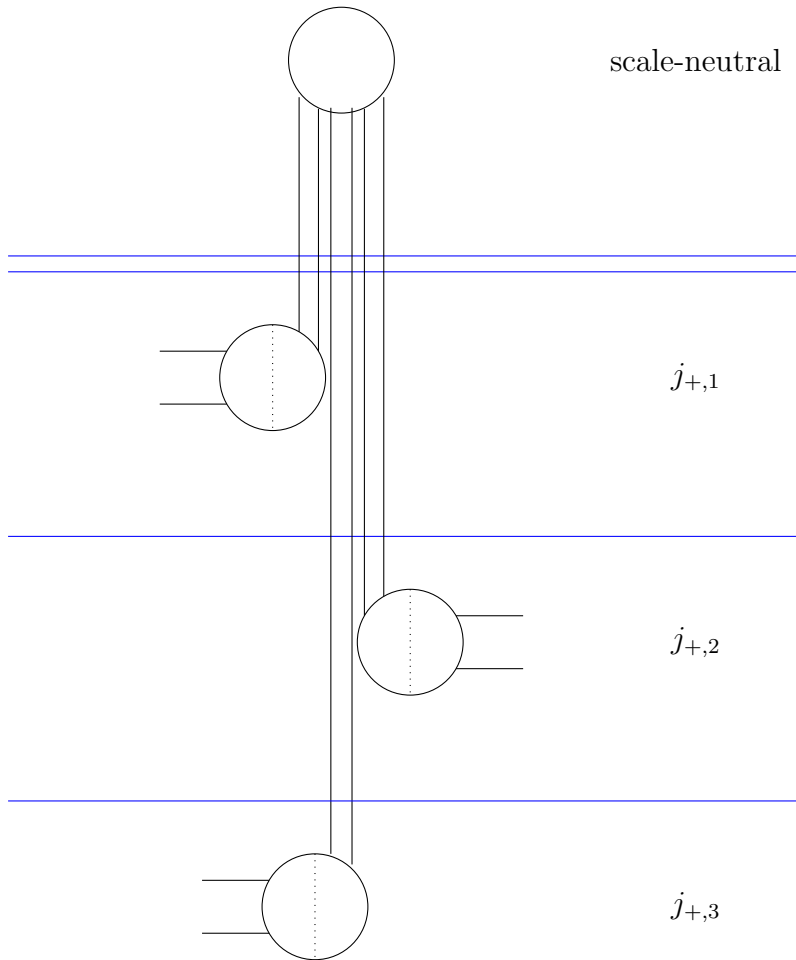


Fig. 3.2.5 (same as Fig. 3.2.6).

Scale-neutral polymers can also appear at either end of a chain.

Since external legs of a scale-neutral polymer \mathbb{P} with ≥ 6 external legs – which is virtually connected to an infinite number of polymers, since the scale j'_ϕ interaction

$\mathcal{L}^{j'_\phi}$ has not been expanded inside \mathbb{P} – can be paired with an arbitrary number of low transfer momentum four-point polymers with arbitrary scales, it is only at the very end of the expansion – i.e., once *all* low transfer momentum four-point polymers have been connected – that the general connectivity structure of \mathbb{P} emerges. Then the scale-neutral polymer of Fig. 3.2.5 will be interpreted as a vertex of the multi-scale bosonic cluster tree,

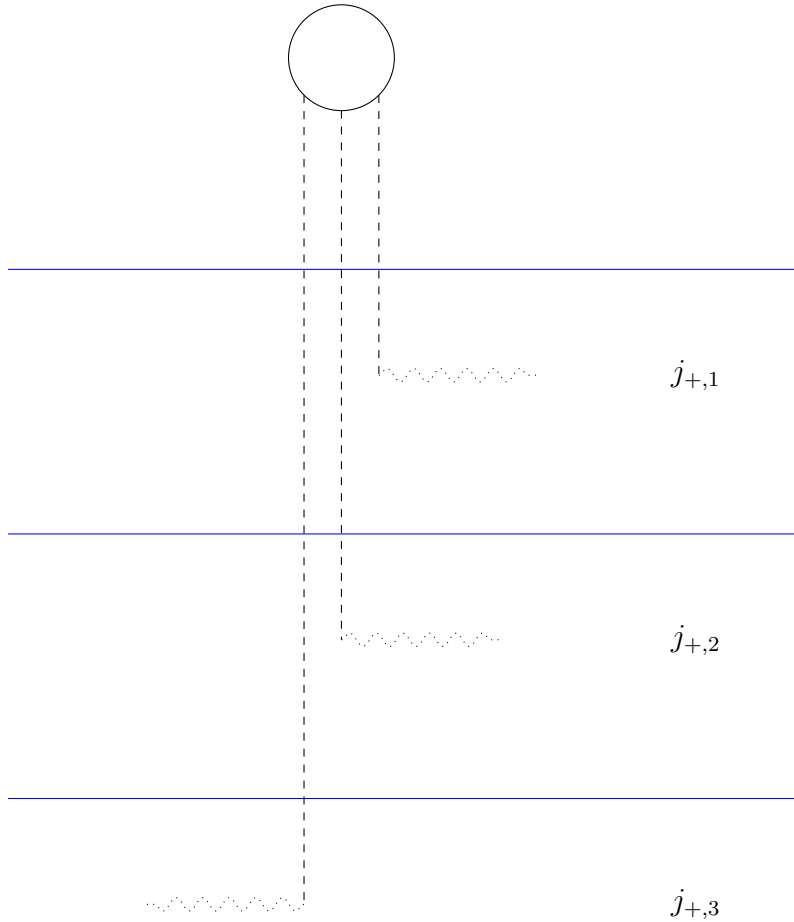


Fig. 3.2.6. A vertex of the multi-scale bosonic cluster tree (same as Fig. 3.2.5).

Finally (see next Figure) a low transfer momentum four-point polymer may contract one of its two Cooper pairs to two *different* (scale neutral or low transfer momentum) polymers (left part of the figure), in which case the three polymers may be considered as a single, compound scale-neutral polymer (blue rectangle on the right part of the figure).

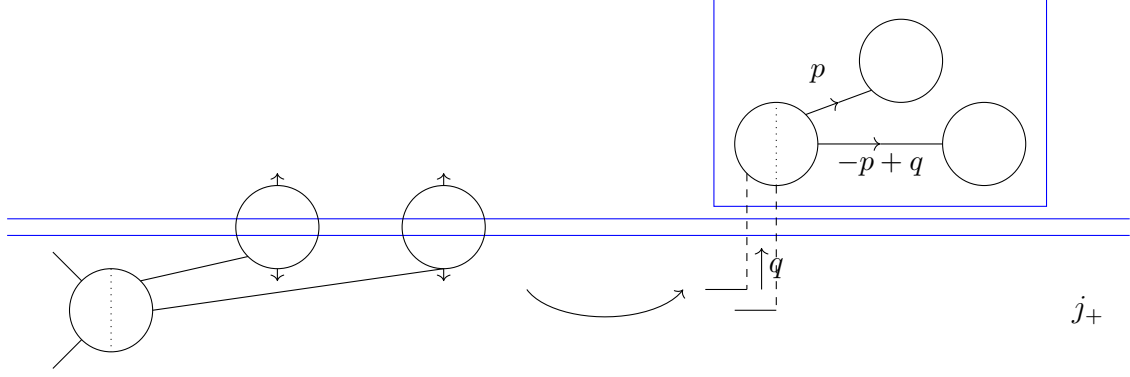


Fig. 3.2.7. One scale-neutral Cooper pair contraction. Blobs with ascending/descending arrows \uparrow, \downarrow are located above (\uparrow), resp. below (\downarrow) the double line, and represent scale-neutral, resp. low transfer momentum four-point polymers.

The remaining Cooper pair may contract to a single scale j_+ four-point polymer, yielding the first bricks of a scale j_+ Goldstone boson attached to a scale-neutral polymer; otherwise it does not show up any more as a Cooper pair, and becomes part of a scale-neutral polymer.

Let us start with a precise typology of irreducible diagrams, depending on the scale:

– at scale j'_ϕ , there are polymers in $\mathcal{P}^{(j'_\phi-1)\rightarrow}$ with ≥ 6 external legs, four-point polymers of type 1, and four-point polymers of type 2. Four-point polymers of type 1 are not divergent in the infra-red limit. Four-point polymers of type 2 are further split (see below) into four-point polymers of type 2 with transfer momentum of scale j'_ϕ – whose connections are closely examined through the scale j'_ϕ cluster expansion – and four-point polymers of type 2 with *low transfer momentum* of scale $> j'_\phi$. The latter ones are left for further investigation at scale $j'_\phi + 1$. As for four-point polymers of type 2 with transfer momentum of scale j'_ϕ , they are assembled together in a line into a single-scale Goldstone boson propagator with transfer momentum of scale j'_ϕ . The two ends of each scale j'_ϕ Goldstone boson propagator are either connected to one (or several) of the external legs $\xi_{ext,1}, \dots, \xi_{ext,N_{ext}}$; or connected to diagrams with ≥ 6 external legs, whose links with four-point polymers of type 2 with low transfer momentum have not been clarified at this stage. As mentioned earlier, scale j'_ϕ Goldstone boson propagators may also be connected to Goldstone boson propagators of lower scale $> j'_\phi$ because momentum cut-offs are not sharp;

– the final diagrammatical outcome of the scale j'_ϕ cluster expansion is:

- (i) a new set of polymers in $\mathcal{P}^{j'_\phi\rightarrow}$ with ≥ 6 external legs;
- (ii) the left-over set of four-point polymers of type 2 with low transfer momentum;
- (iii) newly developed vacuum polymers (which must be divided out by a Mayer expansion), and **two-point polymers**, which contribute to a small, finite *dressing* of

fermion propagators (therefore requiring no mass or chemical potential renormalization), resulting in the replacement of $C_\theta^{j'_\phi}$ by the **dressed propagator** $C_{dressed}$;

– at scale $j'_\phi + 1$, as discussed in the two previous paragraphs, all scale j'_ϕ four-point polymers of type 2 with transfer momentum $|q| \approx 2^{-j'_\phi} \mu$ have been resummed and integrated into larger polymers. Therefore there remain only four-point polymers with transfer momentum scale $\geq j'_\phi + 1$: all four-point polymers (save for inessential cut-off effects) are already of type 2 for the scale $j'_\phi + 1$. After performing (as at scale j'_ϕ) a splitting according to whether the transfer momentum is of scale $j'_\phi + 1$ or higher, and leaving the latter case for further investigation at scale $j'_\phi + 2$, we are left with an assembly composed of *scale $(j'_\phi + 1)$ four-point polymers, and scale-neutral two-point polymers and polymers with ≥ 6 external legs.*

By convention, scale-neutral polymers (i.e. two-point polymers, polymers with ≥ 6 external legs, and and scale j'_ϕ four-point polymers of type 1) are drawn on multi-scale figures in a separate upper line (above the double blue line).

– the above description of the final diagrammatical outcome of the scale j'_ϕ cluster expansion, and of the scale $(j'_\phi + 1)$ -cluster expansion, extends to lower scales without modification.

Let us first describe diagrammatically the various expansions that shall be needed. We add some short comments and refer to **B.** and **C.** below for detailed explanations.

Preliminary second-order expansion in isolated boxes (step #0) at scale j'_ϕ .

$$\begin{aligned}
 \blacksquare &= 1 + \square_{\text{1 vertex}} + \square_{\text{2 vertices}} \\
 &= 1 + \text{circle}_{\text{1 vertex}} + \text{circle}_{\geq 6}
 \end{aligned}$$

Fig. 3.2.8. Preliminary second-order expansion in isolated boxes.

Expanding the interaction $\mathcal{L}_\theta^{j'_\phi}$ to order 2 in each isolated box $\Delta \in \mathbb{D}^{j'_\phi}$ yields 1, plus a term with one vertex – interpreted as a scale j'_ϕ polymer with 4 external legs, on equal footing with four-point polymers in $\mathcal{P}^{(j'_\phi-1) \rightarrow -}$, plus a term with ≥ 2 vertices – interpreted as a scale j'_ϕ polymer with $\geq 8 \geq 6$ external legs –. This is done only once – as a preliminary step to scale j'_ϕ cluster expansion.

Scale j_+ splitting phase for four-point polymers of type 2.

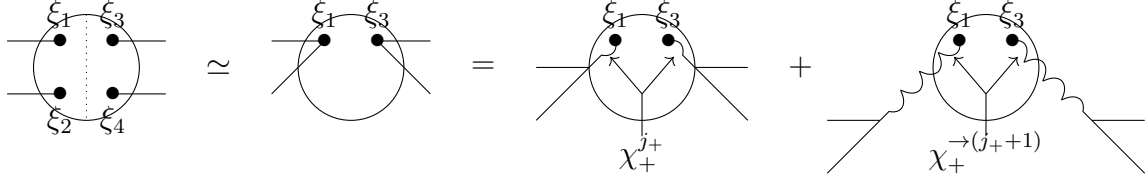
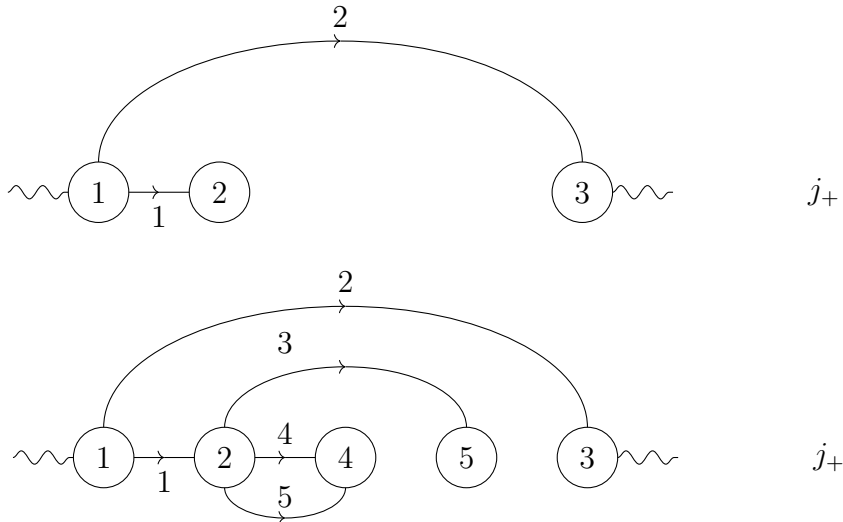


Fig. 3.2.9. Scale j_+ splitting phase for four-point polymers.

Consider a four-point polymer of type 2 with external legs located at $\xi_1, \xi_2, \xi_3, \xi_4$ which have not been contracted at scales $< j_+$. Displace external legs as in §1.7, $\xi_2 \rightarrow \xi_1$ and $\xi_4 \rightarrow \xi_3$. Then insert characteristic functions $\chi_+^{j_+}$ at ξ_1, ξ_3 singling out the case when the transfer momentum is of scale j_+ . Since the polymer is of type 2, the remainder (last diagram on the right) involves only *low transfer momenta* of scale $> j_+$. Low transfer momentum four-point diagrams are left for future investigation at scale $j_+ + 1$.

A single-scale diagram with trivial strongly connected components. Specifically at scale $j_+ = j'_\phi$, we develop links between scale j'_ϕ isolated boxes and fermionic polymers in $\mathcal{P}^{(j'_\phi-1)\rightarrow}$, except four-point polymers with low transfer momentum, $|q| \ll 2^{-j'_\phi}\mu$. The algorithm is as follows. Choose some arbitrary ordering of the set of polymers (four-point polymers with low transfer momentum excluded), $\mathbb{P}_1, \dots, \mathbb{P}_p$. Start from \mathbb{P}_1 and try to develop ≥ 3 links between \mathbb{P}_1 and \mathbb{P}_2 . Say that \mathbb{P}_1 and \mathbb{P}_2 are *strongly connected* if there exist ≥ 3 such links. In the example below – where all polymers are four-point polymers with scale j_+ transfer momenta, represented by numbered blobs – no pair of polymers is strongly connected. The general algorithm is simple: expand all links between \mathbb{P}_1 and $\mathbb{P}_2, \mathbb{P}_3, \mathbb{P}_4, \mathbb{P}_5, \dots$ (first figure). Then expand all links between \mathbb{P}_2 and $\mathbb{P}_3, \mathbb{P}_4, \mathbb{P}_5, \dots$ (second figure), and so on, until one has obtained a new polymer which is isolated at scale j'_ϕ . The figures below present the successive stages of the expansion. Arrows point successively from $\mathbb{P}_i, i = 1, 2, 3, 4$, uncovering links between \mathbb{P}_i and new polymers $\mathbb{P}_{i+1}, \dots, \mathbb{P}_5$.



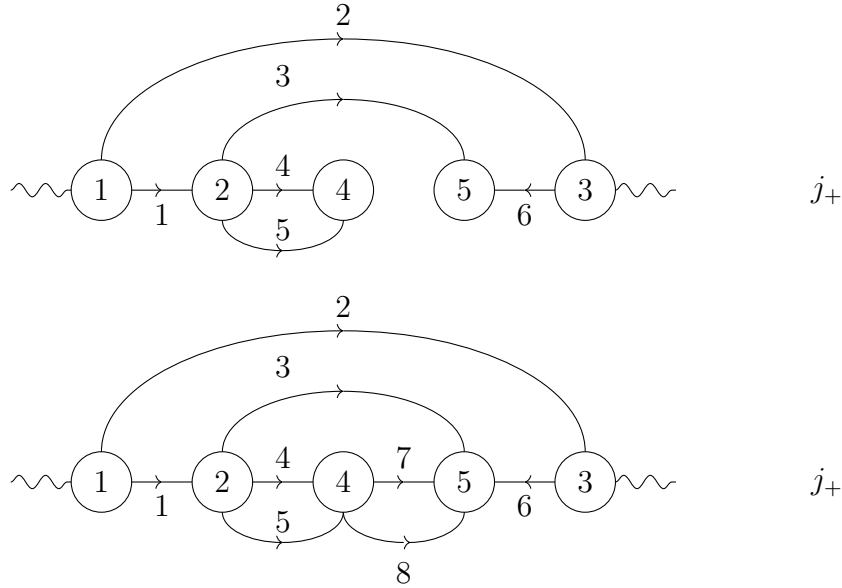


Fig. 3.2.10. Dressed propagator, dressed bubble. Wiggling lines at the two ends stand for low transfer momentum Cooper pairs.

This diagram is actually a "dressed" bubble, involving one bare propagator (the one with index 2), and a dressed propagator from blob number 1 to blob number 3, involving blobs 2, 4 and 5.

The above algorithm also produces non-trivial strongly connected clusters of polymers, discussed in the next two examples.

A single-scale diagram with a single, non-trivial strongly connected component.

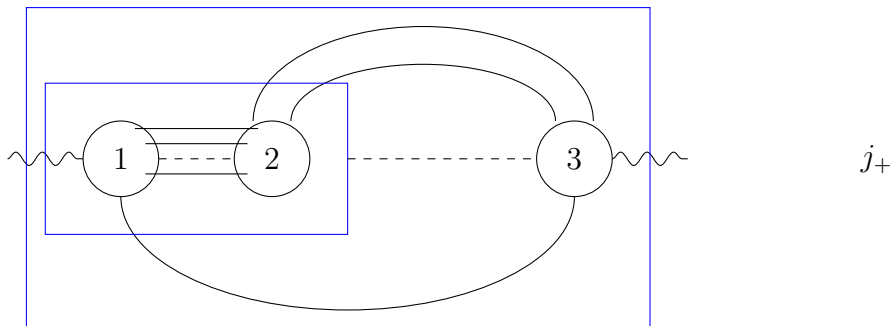


Fig. 3.2.11. One contribution to the Π -kernel.

Blob 1 has ≥ 3 links to blob 2. Hence blobs 1 and 2 are assembled into a single cluster $\{12\}$. Then cluster $\{12\}$ has ≥ 3 links to blob 3, thereby forming a new cluster $\{123\}$. This four-point irreducible polymer contributes to the Π -kernel.

Other contributions to the dressed propagators. This dressed bubble diagram involves strongly connected two-point polymers.

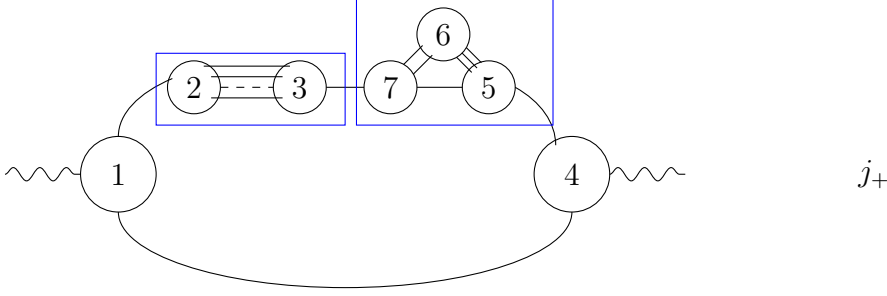


Fig. 3.2.12. Dressed propagators.

At scales $j_+ > j'_\phi$, we keep the idea of a third-order cluster expansion, but explore only links starting from four-point polymers with low transfer momentum of scale j_+ , and connecting them to arbitrary polymers, *except* four-point polymers with transfer momenta of higher scale $> j_+$.

B. Scale j'_ϕ complementary expansion.

The scale j'_ϕ horizontal cluster expansion.

We resume from expression (2.107) for $F_I(\xi_{ext}, \bar{\xi}_{ext})$.

Step #0. Preliminary second-order expansion in isolated boxes (see Fig. 3.2.8). Let $\Delta \in \mathbb{D}^{j'_\phi}$. Expand $e^{-\int d\xi \chi_\Delta(\xi) \mathcal{L}_\theta^{j'_\phi}(\xi)}$, see (3.16), into

$$\begin{aligned} & 1 - \int d\xi \chi_\Delta(\xi) \mathcal{L}_\theta^{j'_\phi}(\xi) + \left(\int d\xi \chi_\Delta(\xi) \mathcal{L}_\theta^{j'_\phi}(\xi) \right)^2 \int_0^1 dt (1-t) e^{-t \int d\xi \chi_\Delta(\xi) \mathcal{L}_\theta^{j'_\phi}(\xi)} \\ & = 1 - \lambda \int d\xi \chi_\Delta(\xi) (\bar{\Psi}^{j'_\phi} \Psi^{j'_\phi})^2(\xi) + \dots \end{aligned} \quad (3.18)$$

The first non-trivial term is seen as a four-point polymer. Neglected terms (\dots) involve at least 8 fields in Δ , hence are considered as polymers with ≥ 6 external legs.

Step #1. Splitting phase for four-point polymers of type 2

 (see Fig. 3.2.9).

Let \mathbb{P} be a four-point polymer of type 2, with external structure $(\bar{\Psi}_1 \Psi_2) \otimes (\bar{\Psi}_3 \Psi_4)$ as in (3.17), with external sectors $\alpha_1, \dots, \alpha_4 \in \mathbb{Z}/2^{j'_\phi} \mathbb{Z}$. By definition, $|\alpha_1 + \alpha_2|, |\alpha_3 + \alpha_4| \leq 1$. The argument below can be repeated without any modification at scale j_+ with $\alpha_1, \dots, \alpha_4 \in \mathbb{Z}/2^{j_+} \mathbb{Z}$, so we state the general version. Consider first the *left part* of \mathbb{P} . Take the Fourier transform,

$$F(\xi_1, \xi_2) := \bar{\psi}_{\uparrow,1}^{j'_\phi, \alpha_1}(\xi_1) \bar{\psi}_{\downarrow}^{j'_\phi, \alpha_2}(\xi_2) = (2\pi)^{-6} \int dp_1 \int dp_2 e^{i \sum_{i=1}^2 (p_i, \xi_i)} \bar{\psi}_{\uparrow}^{j'_\phi, \alpha_1}(p_1) \bar{\psi}_{\downarrow}^{j'_\phi, \alpha_2}(p_2) \quad (3.19)$$

or conjugate. Insert inside the last expression the kernel $1 = \chi_+^{j_+ \rightarrow}(p_1 + p_2) + (1 - \chi_+^{j_+ \rightarrow})(p_1 + p_2)$. Because $|\alpha_1 + \alpha_2| = O(1)$, there are two cases: (i) either the transfer

momentum $q := p_1 + p_2$ has bosonic scale $\simeq j_+$, and $\chi_+^{j_+ \rightarrow}(p_1 + p_2) > 0$; or (ii) $|q|_+ \ll 2^{-j_+} \mu$, and $\chi_+^{j_+ \rightarrow}(p_1 + p_2) = 0$. Hence

$$(\chi_+^{j_+ \rightarrow} F)(\xi_1, \xi_2) = \int d\zeta \chi_+^{j_+ \rightarrow}(\zeta) F(\zeta + \xi_1, \zeta + \xi_2) \quad (3.20)$$

with a convolution kernel $\chi_+^{j_+ \rightarrow}(\cdot)$ essentially supported on $\{|\zeta|_+ \lesssim 2^{j_+} \mu\}$.

As a result, \mathbb{P} has been rewritten as the sum of two terms interpreted as follows:

(i) a polymer with **upper transfer momentum scale** j_+ (term with $\chi_+^{j_+ \rightarrow}$ in factor);

(ii) a polymer with **lower transfer momentum scale** $> j_+$ (term with $1 - \chi_+^{j_+ \rightarrow}$ in factor).

Step #2. External leg displacement for four-point polymers of type 2 with upper transfer momentum scale (see Fig. 3.2.9).

Consider four-point polymers obtained in (i) just above. Displace the fields Ψ_2 , resp. Ψ_4 on the lower line to the location of the fields $\bar{\Psi}_1$, resp. $\bar{\Psi}_3$ on the upper line, see Fig. 1.7.5 and eq. (1.112), namely, replace $\Psi^{j'_\phi, \alpha_2}(\xi_2)$ by $e^{ip^{\alpha_2} \cdot (\xi_2 - \xi_1)} \Psi^{j'_\phi, \alpha_2}(\xi_1)$ and similarly for $\Psi(\xi_4)$.

Step #3. Scale j'_ϕ expansion.

One step of expansion. Fermionic expansions have produced scale j'_ϕ clusters, as described in §2.3.1. Consider two scale j'_ϕ clusters, $\Delta_1 \in \mathbb{P}_1$, and $\Delta \equiv \Delta_2 \in \mathbb{P}_2$, where $\mathbb{P}_1, \mathbb{P}_2$ are arbitrary polymers, *except* four-point polymers with low transfer momentum scale $> j'_\phi$. Introduce an *interpolation coefficient* $s_{\Delta_1, \Delta_2}^\alpha$ between Δ_1 and Δ_2 , namely, multiply $\chi_{\Delta_1}(\xi) \chi_{\Delta_2}(\xi') C_\theta^{j'_\phi, \alpha}(\xi, \xi')$ by $s_{\Delta_1, \Delta_2}^\alpha$ ($\alpha \in \mathbb{Z}/2^{j'_\phi} \mathbb{Z}$); and differentiate $F_I(\bar{\xi}_{ext}, \xi_{ext})$ in (2.107) w.r. to $s_{\Delta_1, \Delta_2}^\alpha$. The connecting operator associated to the cluster link $\ell = (\Delta_1, \Delta_2)$ as in Proposition 5.2,

$$D_\ell^\alpha := \int_{\Delta_1} d\xi_\ell \int_{\Delta_2} d\xi'_\ell C^{j'_\phi, \alpha}(\xi_\ell, \xi'_\ell) \frac{\delta^2}{\delta \Psi^{j'_\phi, \alpha}(\xi_\ell) \delta \bar{\Psi}^{j'_\phi, \alpha}(\xi'_\ell)}, \quad (3.21)$$

either (i) transforms a pair of dangling fields into a cluster link, or produces (ii) one or (iii) two extra vertices, one in Δ_1 , one in Δ_2 . The procedure may be iterated an arbitrary number of terms by differentiating $F_I(\bar{\xi}_{ext}, \xi_{ext})$ w.r. to $s_{\Delta_1, \Delta_2}^{\alpha_1}, s_{\Delta_1, \Delta_2}^{\alpha_2}, \dots$. We shall actually do so at most 3 times per pair of boxes (see below).

We say that Δ_1 and Δ_2 are *strongly connected at scale j'_ϕ* if there exist at least 3 cluster or complementary cluster links $C^{j'_\phi, \alpha}(\xi_1, \xi_2), C^{j'_\phi, \alpha'}(\xi'_1, \xi'_2), C^{j'_\phi, \alpha''}(\xi''_1, \xi''_2)$ between Δ_1 and Δ_2 .

We now introduce a linking number $LN(\Delta_1, \Delta_2)$, which is initially zero, and is incremented as links are added. If there is *one* link between Δ_1 and Δ_2 , we set $LN(\Delta_1, \Delta_2) := 1$. If there are *two* links, set $LN(\cdot, \cdot) = 2$.

We repeat the above procedure until $LN(\Delta_1, \Delta_2)=3$, so that Δ_1 and Δ_2 are strongly connected. By choosing one of the terms in the cluster expansion in which an interpolation coefficient has been set to 0, one also gets *factorized expressions* of the form $G(\Delta_1, \Delta_2)$, times a quantity averaged w.r. to a measure $d\mu_\theta^*(s; \cdot)$, with $s_{\Delta_1, \Delta_2} = 0$, for which fields in Δ_1 and Δ_2 are independent one from the other. The quantity $G(\Delta_1, \Delta_2)$ is either 1 (in which case Δ_1 and Δ_2 are totally factorized), a single propagator, or a product of two propagators. In the latter case, we consider that we have *one external Cooper pair propagator* connecting Δ_1 to Δ_2 .

After completing the cluster expansion between Δ_1 and Δ_2 , we define a new set of objects as follows. First of all, we are not really interested in the linking number between two boxes belonging to two given polymers $\mathbb{P}_1, \mathbb{P}_2$, but rather in the *total number of links connecting \mathbb{P}_1 and \mathbb{P}_2* (see Figure in the introduction to section 3), which is defined as

$$LN(\mathbb{P}_1, \mathbb{P}_2) := \sum_{\Delta_1 \in \mathbb{P}_1} \sum_{\Delta_2 \in \mathbb{P}_2} LN(\Delta_1, \Delta_2). \quad (3.22)$$

Then we stop the cluster expansion between \mathbb{P}_1 and \mathbb{P}_2 as soon as $LN(\mathbb{P}_1, \mathbb{P}_2) \geq 3$. This mutualized stopping rule is more economical, sufficient for our purposes and consistent with the general organization of the expansion in terms of polymers.

Let us come back to the outcome of the first step of expansion. As in §2.3.1, we describe (super)-clusters, called *objects*, produced by connecting clusters. Scale j'_ϕ clusters $\neq \Delta_1, \Delta_2$ are objects. If $LN(\Delta_1, \Delta_2) \leq 2$, then clusters Δ_1, Δ_2 are also objects; otherwise a new object $o_1 := \{\Delta_1, \Delta_2\}$ has been formed. The expansion goes on by considering links between the object containing Δ_1 and clusters $\Delta \neq \Delta_1, \Delta_2$. Explore in this way all clusters $\Delta \neq \Delta_1$. In the end, one has an object o_1 containing Δ_1 , and a set of clusters which are not strongly connected to o_1 . Then one starts from a new box $\Delta_2 \notin o_1$ and explores in the same manner its links to clusters $\neq \Delta_2, o_1$, and so on. Here is one example.

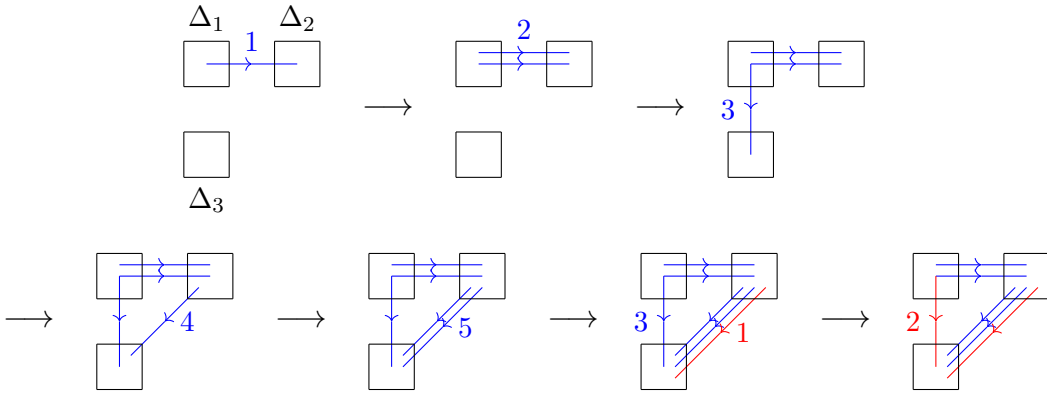


Fig. 3.2.13. Third order cluster graph.

Blue lines are cluster links. Because we expand to third order, we obtain in general a graph, not a tree. However, it is easy to extract a tree out of this graph (in red on the figure). Decide that every third link between two objects is a tree link (red link number 1). It may happen that, upon introducing a third link (here between Δ_2 and Δ_3), and forming the corresponding cluster (here $o_1 = \{\Delta_2, \Delta_3\}$), previously non strongly-connected objects become strongly connected, here Δ_1 and o_1 . One then adds a tree link, here between Δ_1 and o_1 ; for the sake of clarity, it is convenient to represent it as a link between Δ_1 and one of the boxes of o_1 , here (but it is an arbitrary choice) Δ_3 . Thus a new cluster $o_2 = \{\Delta_1, \Delta_2, \Delta_3\}$ is formed, and so on. These rules generate a tree.

C. Complementary expansions of scales $j_+ \geq j'_\phi + 1$. The series of steps Step #1 \rightarrow Step #2 \rightarrow Step #3 may be repeated at scale $j_+ = j'_\phi + 1, j'_\phi + 2, \dots$ until all Cooper pairs of all scales have been connected. Note that the preliminary second-order expansion in isolated boxes (Step #0) is performed only once, at the beginning of the scale j'_ϕ complementary expansion. As discussed above, Step #1 (splitting phase for low transfer momentum for four-point polymers) is applied to Cooper pairs belonging to four-point polymers of type 2 (in the sense of Definition 3.1) which already have $1 - \chi^{(j_+ - 1) \rightarrow (p_1 + p_2)}$ in factor, therefore there is no need to add a further type specification at scales $j_+ > j'_\phi$. Step #3 is somewhat simplified w.r. to the case $j_+ = j'_\phi$, since (as explained above) there is no need to test pairings between scale-neutral polymers any more; so the exploration process starts exclusively from scale j_+ four-point polymers, whose sectors α range not in $\mathbb{Z}/2^{j'_\phi}\mathbb{Z}$, but in $\mathbb{Z}/2^{j_+}\mathbb{Z}$. Generally speaking, the scale j_+ complementary expansion inserts scale j_+ Cooper pairs and the four-point polymers they belong to inside a multi-scale tree (see Fig. 3.2.6). Also, newly developed Goldstone boson propagators of scales $\geq j'_\phi$ produce inductively scale $j'_\phi, j'_\phi + 1, \dots$ contributions to the two-point function, e.g.

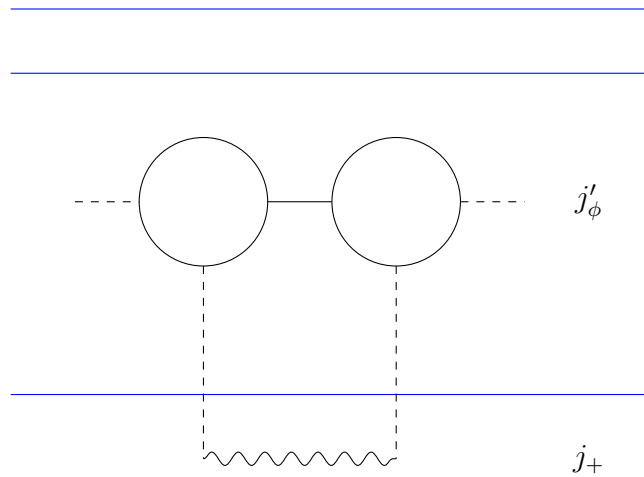


Fig. 3.2.14. Scale j_+ dressing of the fermion propagator by internal Goldstone boson propagators.

yielding in the end of the story the dressed fermion propagator $C_{dressed}$.

D. Resummation of Goldstone boson propagators. Once all Cooper pairs of all scales have been connected, the remains at each scale $j_+ \geq j'_\phi$ a sum of structures as in Fig. 3.2.3 or 3.2.4. However, it isn't yet in the form of a geometric series; rather of a non-factorized expression of the form

$$\begin{aligned} \tilde{\Sigma}_{disp}(q) &:= \lambda \mathbb{1} + \lambda^2 \left\{ \mathcal{A}_q(\Upsilon_3) + \int dp'_1 \int dp'_3 \mathcal{A}_q(p'_1) \tilde{\Pi}_q^{disp}(p'_1, p'_3) \mathcal{A}_q(p'_3) \right. \\ &+ \cdots + \left\{ \prod_{i=1}^n \int dp_{i,1} \int dp_{i,3} \right\} \left(\prod_{i=1}^{n-1} \delta(p_{i,3} - p_{i+3,1}) \right) \mathcal{A}_q(p_{1,1}) \left\{ \prod_{i=1}^n \left(\tilde{\Pi}_q^{disp}(p_{i,1}, p_{i,3}) \mathcal{A}_q(p_{i,3}) \right) \right\} \\ &+ \cdots \end{aligned} \quad (3.23)$$

as in Definition 1.7 (and §1.7 for notations), *except* that $\mathcal{A}_q(p_{i,3})$ is now computed as a product of two *dressed* propagators, $C_{dressed}(p_{i,3})C_{dressed}(-p_{i,3} + q)$. The displacement procedure of §1.7, see eq. (1.112), is defined in terms of isotropic "micro-sectors" $\mathcal{S}^{\alpha,k} \equiv \mathcal{S}^{j'_\phi, \alpha, k}$ obtained by chopping the angular sectors $\mathcal{S}^\alpha := \mathcal{S}^{j'_\phi, \alpha}$ as in the Remark following Definition 2.2. Error terms have by (1.114) a supplementary $O(2^{-(j_+ - j'_\phi)})$ small pre-factor corresponding to the difference of scales between the external legs, and the internal fermions, which are of scale $\leq j'_\phi$. One must first

- (i) resum over the locations of all intermediate scale-neutral polymers $\mathbb{P}_1, \dots, \mathbb{P}_n$, implying in particular the possibility of overlaps between polymers. This is a standard problem, solved by means of a Mayer expansion as in §2.3.5.

Once this is settled, one must still take into account the dependence of $\tilde{\Pi}_q^{disp}(p_{i,1}, p_{i,3})$ in $p_{i,1}$ and $p_{i,3}$. In order to extract factorized contributions, we mimic the procedure sketched in a perturbative context in §1.7 under the name of *Fermi and s-wave projections*. As suggested in Definition 1.5, it is rather an **averaging procedure**, a double one in fact. we must get rid of the dependence on the norms $|p_{i,1}|, |p_{i,3}|$, and (if $q = 0$) on the angles $\theta_{i,1} - \theta_{i,3} := \widehat{\mathbf{p}_1, \mathbf{p}_3}$. (If $q \neq 0$ then $\tilde{\Pi}_q^{disp}(p_{i,1}, p_{i,3})$ depends separately on $\theta_{i,1}$ and $\theta_{i,3}$). Let $\mathcal{A}_{\mathcal{S}^\alpha}(p) := \chi^{j'_\phi, \alpha}(p)C_{dressed}(p)C_{dressed}(q - p)$.

- (ii) (*norm averaging procedure*) The kernel $\tilde{\Pi}_q^{disp}(p_{i,1}, p_{i,3})$ has a support $\mathcal{S}^{\alpha_{i,1}} \times \mathcal{S}^{\alpha_{i,3}}$ centered on $p^{\alpha_{i,1}}$, resp. $p^{\alpha_{i,3}}$. We absorb the intermediate $\mathcal{A}_{\mathcal{S}^\alpha}$ -functions by rewriting products

$$\begin{aligned} \int_{\mathcal{S}^{\alpha_1}} dp_1 \cdots \int_{\mathcal{S}^{\alpha_n}} dp_n \mathcal{A}_{\mathcal{S}^{\alpha_1}}(p_1) \tilde{\Pi}^{disp}(p_1, p_2) \mathcal{A}_{\mathcal{S}^{\alpha_2}}(p_2) \\ \tilde{\Pi}^{disp}(p_2, p_3) \mathcal{A}_{\mathcal{S}^{\alpha_3}}(p_3) \cdots \tilde{\Pi}^{disp}(p_{n-1}, p_n) \mathcal{A}_{\mathcal{S}^{\alpha_n}}(p_n) \end{aligned} \quad (3.24)$$

as

$$\begin{aligned} \left\{ \prod_{i=1}^n \int dp_i \right\} (\mathcal{A}_{\mathcal{S}^{\alpha_1}}(p_1))^{1/2} K^{\alpha_1, \alpha_2}(p_1, p_2) \\ K^{\alpha_2, \alpha_3}(p_2, p_3) \cdots K^{\alpha_{n-1}, \alpha_n}(p_{n-1}, p_n) (\mathcal{A}_{\mathcal{S}^{\alpha_n}}(p_n))^{1/2}, \end{aligned} \quad (3.25)$$

where

$$K^{\alpha_{i,1}, \alpha_{i,3}}(p_{i,1}, p_{i,3}) := (\mathcal{A}_{\mathcal{S}^{\alpha_{i,1}}}(p_{i,1}))^{1/2} \tilde{\Pi}^{disp}(p_{i,1}, p_{i,3}) (\mathcal{A}_{\mathcal{S}^{\alpha_{i,3}}}(p_{i,3}))^{1/2}. \quad (3.26)$$

Define P^α , $\alpha = \alpha_{i,1}, \alpha_{i,3}$ to be the projection on the function $(\mathcal{A}_{\mathcal{S}^\alpha})^{-1/2}$ w.r. to the L^2 -norm $(f, g)_{L^2(\mathcal{A}_{\mathcal{S}^\alpha}(p)dp)} := \int dp \mathcal{A}_{\mathcal{S}^\alpha}(p) f(p) g^*(p)$ in momentum space,

$$P^\alpha(f)(p) := \frac{\int dp' f(p') (\mathcal{A}_{\mathcal{S}^\alpha}(p'))^{1/2}}{\text{Vol}(\mathcal{S}^\alpha)} (\mathcal{A}_{\mathcal{S}^\alpha}(p))^{-1/2}, \quad \text{supp}(f) \subset \mathcal{S}^\alpha \quad (3.27)$$

Let $\text{Vol}(\mathcal{S})$ be the volume of \mathcal{S}^α for any sector α . Then a short-hand for (3.24) is simply

$$\left(\frac{(\mathcal{A}_{\mathcal{S}^{\alpha_1}})^{-1/2}}{\text{Vol}(\mathcal{S})} \otimes \frac{(\mathcal{A}_{\mathcal{S}^{\alpha_n}})^{-1/2}}{\text{Vol}(\mathcal{S})}, K^{\alpha_1, \alpha_2} \dots K^{\alpha_{n-1}, \alpha_n} \right)_{L^2(\mathcal{A}_{\mathcal{S}^{\alpha_1}}(p)dp) \otimes L^2(\mathcal{A}_{\mathcal{S}^{\alpha_n}}(p)dp)}. \quad (3.28)$$

Define

$$\begin{aligned} K_{0|0}^{\alpha_{i,1}, \alpha_{i,3}}(p_1, p_3) &:= (P^{\alpha_{i,1}} \otimes P^{\alpha_{i,3}})(K)(p_1, p_3) \\ &= \frac{\int_{\mathcal{S}^{\alpha_{i,1}}} dp'_1 \int_{\mathcal{S}^{\alpha_{i,3}}} dp'_3 K(p'_1, p'_3) (\mathcal{A}_{\mathcal{S}^{\alpha_{i,1}}}(p'_1))^{1/2} (\mathcal{A}_{\mathcal{S}^{\alpha_{i,3}}}(p'_3))^{1/2}}{(\text{Vol}(\mathcal{S}))^2} \times \\ &\quad \times (\mathcal{A}_{\mathcal{S}^{\alpha_{i,1}}}(p_1))^{-1/2} (\mathcal{A}_{\mathcal{S}^{\alpha_{i,3}}}(p_3))^{-1/2} \end{aligned} \quad (3.29)$$

$(p_1 \in \mathcal{S}^{\alpha_{i,1}}, p_3 \in \mathcal{S}^{\alpha_{i,3}})$;

$$\begin{aligned} K_{1|0}^{\alpha_{i,1}, \alpha_{i,3}}(p_1, p_3) &:= \left((1 - P^{\alpha_{i,1}} \otimes P^{\alpha_{i,3}}) \right) (K)(p_1, p_3) \\ &\frac{\int_{\mathcal{S}^{\alpha_{i,1}}} dp'_1 \int_{\mathcal{S}^{\alpha_{i,3}}} dp'_3 \left\{ K(p_1, p'_3) (\mathcal{A}_{\mathcal{S}^{\alpha_{i,1}}}(p'_3))^{-1/2} - K(p'_1, p_3) (\mathcal{A}_{\mathcal{S}^{\alpha_{i,1}}}(p_1))^{-1/2} \right\}}{(\text{Vol}(\mathcal{S}))^2} \times \\ &\quad (\mathcal{A}_{\mathcal{S}^{\alpha_{i,3}}}(p_3))^{-1/2} \end{aligned} \quad (3.30)$$

and a similar formula by symmetry for $K_{0|1}^{\alpha_{i,1}, \alpha_{i,3}}(p_1, p_3) := \left(P^{\alpha_{i,1}} \otimes (1 - P^{\alpha_{i,3}}) \right) (K)(p_1, p_3)$; and finally,

$$\begin{aligned} K_{1|1}^{\alpha_{i,1}, \alpha_{i,3}}(p_1, p_3) &:= \left((1 - P^{\alpha_{i,1}}) \otimes (1 - P^{\alpha_{i,3}}) \right) (K)(p_1, p_3) \\ &= \frac{1}{(\text{Vol}(\mathcal{S}))^2} \int_{\mathcal{S}^{\alpha_{i,1}}} dp'_1 \int_{\mathcal{S}^{\alpha_{i,3}}} dp'_3 \\ &\quad \left\{ \left((K(p_1, p_3) (\mathcal{A}_{\mathcal{S}^{\alpha_{i,1}}}(p'_1))^{-1/2} - K(p'_1, p_3) (\mathcal{A}_{\mathcal{S}^{\alpha_{i,1}}}(p_1))^{-1/2}) (\mathcal{A}_{\mathcal{S}^{\alpha_{i,3}}}(p'_3))^{-1/2} \right. \right. \\ &\quad \left. \left. - \left((K(p_1, p'_3) (\mathcal{A}_{\mathcal{S}^{\alpha_{i,1}}}(p'_1))^{-1/2} - K(p'_1, p_3) (\mathcal{A}_{\mathcal{S}^{\alpha_{i,1}}}(p_1))^{-1/2}) (\mathcal{A}_{\mathcal{S}^{\alpha_{i,3}}}(p_3))^{-1/2} \right) \right\}. \end{aligned} \quad (3.31)$$

By L^2 -orthogonality, (3.28) reduces to a sum over chains $0 = \varepsilon_1 \rightarrow \varepsilon_2 \rightarrow \varepsilon_{n-1} \rightarrow \varepsilon_n = 0$ of intermediate $0 - 1$ states,

$$\sum_{\varepsilon_2, \dots, \varepsilon_{n-1}=0,1} \left(\frac{(\mathcal{A}_{\mathcal{S}^{\alpha_1}})^{-1/2}}{\text{Vol}(\mathcal{S})} \otimes \frac{(\mathcal{A}_{\mathcal{S}^{\alpha_n}})^{-1/2}}{\text{Vol}(\mathcal{S})}, \right. \\ \left. K_{0|\varepsilon_2}^{\alpha_1, \alpha_2} K_{\varepsilon_2|\varepsilon_3}^{\alpha_2, \alpha_3} \dots K_{\varepsilon_{n-2}|\varepsilon_{n-1}}^{\alpha_{n-2}, \alpha_{n-1}} K_{\varepsilon_{n-1}|0}^{\alpha_{n-1}, \alpha_n} \right)_{L^2(\mathcal{A}_{\mathcal{S}^{\alpha_1}}(p)dp) \otimes L^2(\mathcal{A}_{\mathcal{S}^{\alpha_n}}(p)dp)}. \quad (3.32)$$

Also – and this is the crucial point –, the covariance kernels are nearly constant,

$$\frac{1}{ip^0 - e^*(p) - \mathbb{F}} = -\frac{1}{\mathbb{F}}(1 + O(2^{-(j'_\phi - j_\phi)})), \quad (3.33)$$

hence all kernels except $K_{0|0}$ have a small prefactor, namely, $O(2^{-(j'_\phi - j_\phi)})$ for $K_{1|0}, K_{0|1}$, and $O(2^{-2(j'_\phi - j_\phi)})$ for $K_{1|1}$. We may therefore *resum all contributions* corresponding to chains $0 = \varepsilon_1 \rightarrow 1 \rightarrow 1 \dots \rightarrow 1 \rightarrow \varepsilon_n = 0$ of length $n \geq 3$, i.e. including at least one intermediate state 1, and reconsider them as *scale-neutral four-point polymers with a small factor*

$$g' := 2^{-2(j'_\phi - j_\phi)}. \quad (3.34)$$

Thus we are left (up to a redefinition of $K_{0|0}^{\alpha_1, \alpha_2}$ including these chains, for which we choose not to introduce a new notation) with purely $0 \rightarrow 0 \dots \rightarrow 0$ chains: *there is no norm dependence any more.*

- (iii) (*angle averaging procedure*) One must still a priori sum over intermediate sector variables $\alpha_2, \dots, \alpha_{n-1}$. Assume first that $q = 0$. Then $K_{0|0}^{\alpha_i, \alpha_{i+1}} = K_{0|0}^{\beta_i}$, $\beta_i := \alpha_i - \alpha_{i+1}$ depends only (by global rotation invariance) on angle differences. Using a discrete Fourier transform, $f(\beta) = \sum_{k=0}^{2^{j^+}-1} \hat{f}(k) e^{-2ik\beta/2^{j^+}}$, so that

$$\sum_{\alpha_2, \dots, \alpha_n} K_{0|0}^{\alpha_1, \alpha_2} \dots K_{0|0}^{\alpha_{n-1}, \alpha_n} = \sum_{k_1, \dots, k_{n-1}} \hat{K}_{0|0}^{k_1} \dots \hat{K}_{0|0}^{k_{n-1}}, \quad (3.35)$$

we immediately see by standard orthogonality properties of Fourier series that only *diagonal terms* $k = k_1 = \dots = k_{n-1}$ contribute. The terms $k = 0, 1, 2, \dots$ are called resp. *s-, p-, d-wave* contributions, following the standard chemists' notation for angular momentum. Dominant contributions here are due to bubbles, which are in the *s-wave* because the interaction $\int (\bar{\psi}_\uparrow \psi_\uparrow)(\bar{\psi}_\downarrow \psi_\downarrow)$ itself is. Hence the sum of all contributions other than that in the *s-wave* has a supplementary factor $O(g)$, and may be reconsidered as in (ii) as *scale-neutral four-point polymers with a small factor* $O(g)$. Thus there remains only the *s-wave* contribution.

One then obtains a geometric series $\mathcal{A} + \mathcal{A}\bar{\Pi}\mathcal{A} + \mathcal{A}\bar{\Pi}\mathcal{A}\bar{\Pi}\mathcal{A} + \dots$ resummed as the *single-scale Goldstone boson propagator*.

An easy supplementary step consists in

- (iv) resumming single-scale Goldstone boson propagators connecting a polymer to itself. Namely, these tadpole like bosonic insertions are convergent.
- (v) The last step consists in resumming by scale induction two-point functions of single-scale Goldstone boson propagators. For instance, the following scale $j_{+,3}$ two-point function may be built out of the bosonic tree of Fig. 3.2.6 "glued" with its mirror image,

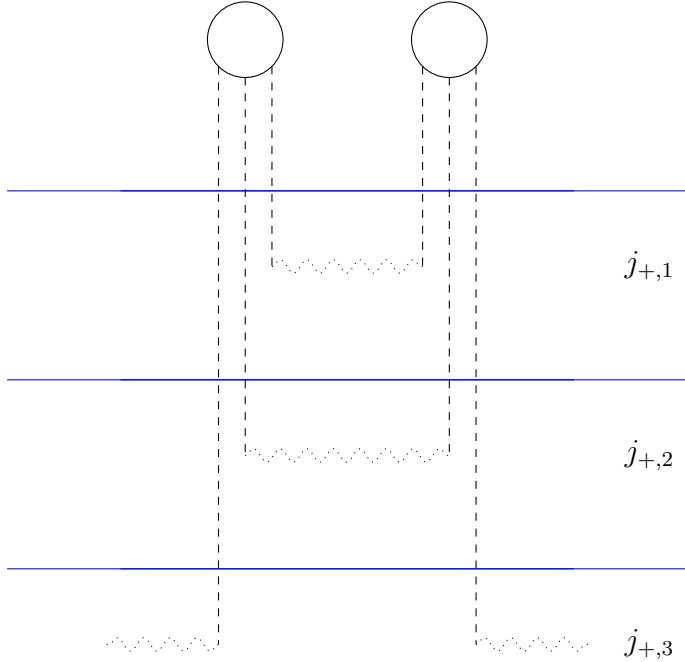


Fig. 3.2.15. Two-point function of the single-scale Goldstone boson propagator.

Resumming the geometric series of such diagrams with lowest transfer momentum scale $< j_{+,3}$ yields the Goldstone boson propagator, denoted by a wiggling line $\sim\sim\sim\sim\sim$

The final outcome of this series of expansion is a multi-scale tree \mathbb{T} , with *scale-neutral polymers* as vertices, and *Goldstone boson propagators* as edges. Vertices have an arbitrary coordination number $n \geq 3$. The case $n = 1$ is excluded by the gap equation; the case $n = 2$ is excluded since polymers in sandwich between two Goldstone boson propagators have already been included in the geometric series. The only cases when $n = 1$ or 2 are allowed is when external legs – either isolated fermions $\Psi_{ext} = \Psi(\xi_{ext})$ or Cooper pairs $(\bar{\Psi}\Gamma\Psi)_{ext} = (\bar{\Psi}\Gamma\Psi)(\xi_{ext})$ – are connected to the polymer. See Figure below.

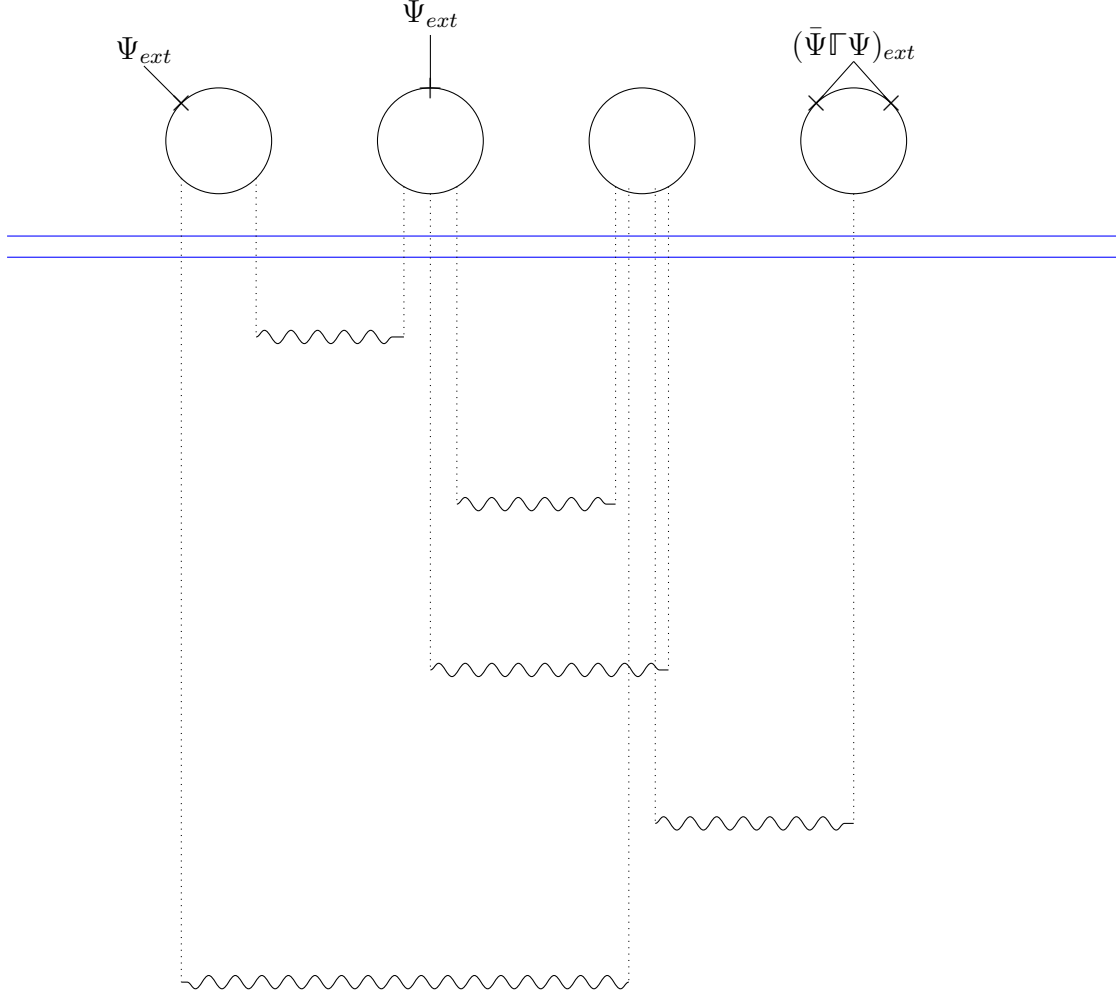


Fig. 3.2.16. Final bosonic multi-scale tree.

E. General principle of the bounds.

The next lines are concerned with the power-counting of a polymer $\mathbb{P}_i^{j_+ \rightarrow}$ with Cooper pair external structure

$$\prod_{i=1}^{N_{ext}} \int d\zeta_i \chi_+^{k_+,i}(\zeta_i) \bar{\Psi}^{j_\phi, \alpha_{i,1}}(\zeta_i + \xi_i) \Gamma_i \Psi^{j_\phi, \alpha_{i,2}}(\zeta_i + \xi_i), \quad (3.36)$$

with $k_{+,1}, \dots, k_{+,N_{ext}} > j_+$, $\alpha_{i,1}, \alpha_{i,2} \in \mathbb{Z}/2^{k_+,i}\mathbb{Z}$, see splitting phase, step #1 (3.20). As in the fermionic scales, see §2.3, one is led to separate the *absolute power-counting*, obtained by assuming that $k_{+,1} = \dots = k_{+,N_{ext}} = j_+ + 1$, from the *relative power-counting*, i.e. the power of the prefactor in $2^{-(k_+,min-j_+)}$, where $k_+,min := \min(k_+,i, i = 1, \dots, N_{ext})$ is the highest external scale.

It is instructive at this point to redo the power-counting of §2.3.2 for a connected fermion diagram with $N_{ext,+}$ external Cooper pair legs located at $\xi_1, \dots, \xi_{N_{ext,+}}$, and with scales $k_{+,1}, \dots, k_{+,N_{ext,+}}$, i.e. (considering the Fourier transformed graph) such that transfer momenta $|q_i|_+ \approx \mu 2^{-j_{+,i}}$. The worst case is when Cooper pairs are connected by Goldstone boson propagators $\Sigma(\xi - \xi') \approx \frac{g_\phi/v_\phi^2}{|\xi - \xi'|_+}$, scaling like $(\Gamma_\phi 2^{-j_{+}/2})^2$. Hence the power-counting of a Cooper pair $\int d\zeta \chi_+^{k_+}(\zeta) \bar{\Psi}^{j'_\phi, \alpha_1}(\zeta + \xi) \Gamma \Psi^{j'_\phi, \alpha_2}(\zeta + \xi) = \sum_{\alpha_1, \alpha_2 \in \mathbb{Z}/2^{k_+} \mathbb{Z}} \int d\zeta_i \chi_+^{k_+}(\zeta) \bar{\Psi}^{j'_\phi, \alpha_1}(\zeta + \xi) \Gamma \Psi^{j'_\phi, \alpha_2}(\zeta + \xi)$, see (3.36), summed over all possible sectors scales, like $O(\Gamma_\phi 2^{-j_{+}/2})$; note that this contrasts with the naive scaling (2.13) for the product of two fermions, $\sum_{\alpha \in \mathbb{Z}/2^{j_+} \mathbb{Z}} \bar{\Psi}^{j_+, \alpha}(\xi) \Psi^{j_+, \alpha}(\xi) \approx 2^{-3j_+/2}$. If $j_+ \gg j'_\phi$, then the ξ -integration in a box $\Delta \in \mathbb{D}_+^{k_+}$ costs a volume factor $O(2^{3k_+})$. Thus, the *relative power-counting* for a polymer in $\mathcal{P}^{j_+ \rightarrow}$ with highest external scale $k_+ > j_+$ is

$$O((2^{k_+ - j_+})^{\omega(N_{ext,+})}), \quad \omega(N_{ext}) := \frac{1}{2}(6 - N_{ext,+}), \quad (3.37)$$

$\omega(\cdot)$ =relative degree of divergence, which implies that *only diagrams with ≤ 6 external Cooper pair legs are potentially divergent when $k_+ - j_+ \rightarrow \infty$ with j_+ fixed.*

Let us now bound instead the *absolute* power-counting of *non-amputated polymers* (i.e. including external bosonic legs) for $k_+ - j_+ = O(1)$ is fixed; the total power-counting of the full diagram for $k_+ > j_+$ arbitrary is by construction the *product* of the relative power-counting (3.37) by the absolute power-counting which we shall presently bound.

We restrict here to the case of a *fermionic polymer* in $\mathcal{P}^{j \rightarrow}$ with $N_{ext,+}$ external bosonic legs, hence $N_{ext} = 2N_{ext,+}$ external fermionic legs. The corresponding amputated power-counting (as shown in (2.123)) is $\lesssim (2^{j/2})^{2N_{ext,+} - 4} = 2^{j(N_{ext,+} - 2)}$. Polymers in $\mathcal{P}^{j \rightarrow}$, $j < j'_\phi - 1$ with $N_{ext} = 2$ have been resummed into the fermionic two-point function, hence we may assume that either $j = j'_\phi - 1$ or $N_{ext,+} \geq 2$; thus, $2^{j(N_{ext,+} - 2)} \leq 2^{j'_\phi(N_{ext,+} - 2)}$, and the worst bound is obtained when $j_+ = k_+ = j'_\phi$, which we now assume. The power-counting of the corresponding *full* diagram is obtained by multiplying by the weight of the external bosonic legs, and by the volume of a scale j'_ϕ box, all together (taking into account that $\Gamma_\phi \approx 2^{-j_\phi \mu}$) at most:

$$2^{j'_\phi(N_{ext,+} - 2)} \times (2^{-j_\phi} 2^{-j'_\phi/2})^{N_{ext,+}} \times 2^{3j'_\phi} \leq (2^{j'_\phi})^{-\frac{N_{ext,+}}{2} + 1}. \quad (3.38)$$

For $N_{ext,+} \geq 3$ (excluding the case of a Goldstone boson one-point function, or of a Goldstone boson propagator, for which $N_{ext,+} = 2$) this is small.

Ward identities – proved in §3.3 – will show that Goldstone boson one-point function vanish, and that diagrams with $N_{ext,+} \leq 6$ are actually $O(1)$. They will also allow to compute the absolute power-counting of non-amputated polymers in $\mathcal{P}^{j_+ \rightarrow}$ including scale j'_ϕ fermions.

3.3 Ward identities

The general purpose of this subsection is to obtain supplementary spring factors $O(2^{-(k_+-j_+)})$ for external Cooper pair legs of $N_{ext,+}$ -point functions or bosonic polymers with lowest internal scale j_+ and highest external scale k_+ . As is apparent from the previous discussion in §3.2 E., only a small (actually *two*, as we shall see), finite number of spring factors is really required to show that polymers converge. In this subsection, we shall be uniquely concerned with *showing that the naive relative degree of divergence* $\omega(\mathbb{P}) = \frac{1}{2}(6 - N_{ext,+}(\mathbb{P}))$, $\mathbb{P} \in \mathcal{P}^{j_+ \rightarrow}$ of (3.37) can be enhanced to $\tilde{\omega}(\mathbb{P}) = \omega(\mathbb{P}) - \delta\omega(\mathbb{P})$, with $\delta\omega(\mathbb{P})$ (called: relative gain) large enough so that $\tilde{\omega}(\mathbb{P}) < 0$.

In guise of introduction: gauge symmetries. The Grassmann measure is invariant under $U(1)$ number symmetry,

$$(\bar{\psi}, \psi)(\xi) \longrightarrow (\bar{\psi} e^{-i\alpha}, e^{i\alpha} \psi)(\xi) \quad (3.39)$$

or equivalently

$$(\bar{\Psi}, \Psi)(\xi) \longrightarrow (\bar{\Psi} e^{-i\alpha\sigma^3}, e^{i\alpha\sigma^3} \Psi)(\xi) \quad (3.40)$$

if $\alpha \in \mathbb{R}$ is a constant. Furthermore, the interaction $\lambda(\bar{\Psi}\Psi)^2(\xi)$ is invariant under $U(1)$ gauge transformations

$$(\bar{\Psi}, \Psi)(\xi) \longrightarrow (\bar{\Psi} e^{-i\alpha(\xi)\sigma^3}, e^{i\alpha(\xi)\sigma^3} \Psi)(\xi) \quad (3.41)$$

where now $\alpha = \alpha(\xi)$ is allowed to depend on space-time.

Multiplying α by ε and letting $\varepsilon \rightarrow 0$, we obtain an infinitesimal transformation δ_α such that

$$\delta_\alpha(\bar{\Psi}\Psi)^2(\xi) = 0 \quad (3.42)$$

$$\begin{aligned} \delta_\alpha \left(\int dp \bar{\Psi}(-p) \left(ip^0 - e^*(\mathbf{p})\sigma^3 - \Gamma(\theta) \right) \Psi(p) \right) \\ = \int d\xi \alpha(\xi) \bar{\Psi}(\xi) \left\{ 2\alpha(\xi)\Gamma^\perp(\theta) - \left(\partial_\tau \alpha(\xi) \sigma^3 + \frac{1}{m^*} (\nabla \alpha(\xi) \cdot \nabla) \mathbf{1} \right) \right\} \Psi(\xi) \end{aligned} \quad (3.43)$$

where $\mathbf{\Gamma}^\perp(\theta) := \begin{pmatrix} -\Gamma_2(\theta) \\ \Gamma_1(\theta) \end{pmatrix}$ is the image of the vector $\mathbf{\Gamma}(\theta) \equiv \mathbf{\Gamma}^{//}(\theta)$ by a rotation of angle $\pi/2$, and $\mathbb{\Gamma}^\perp(\theta)$ the associated off-diagonal Hermitian matrix. The inserted kernel $ip^0 - e^*(\mathbf{p})\sigma^3 - \Gamma(\theta)$ is essentially the inverse of the fermion covariance kernel. This is true up to the ultra-violet cut-off $\chi^{-j_D}(|p|/\mu)$, however. *If α is constant*, then the multiplication by $e^{\pm i\alpha(\xi)\sigma^3}$ commutes with Fourier cut-offs; however, this is not true for non-constant gauge transformations. This generates *error terms* denoted by "err." in the expressions below, which will be shown in §5.5 to be of the same order or smaller than the terms in (3.43). Exponentiating the infinitesimal transformation $\mathbb{\Gamma}(\theta) \mapsto$

$\mathbb{F}(\theta) + 2\varepsilon\alpha(\xi)\mathbb{F}^\perp(\theta)$, one obtains a *rotated order parameter*, $\mathbb{F}(\theta + 2\alpha(\xi))$; equivalently (see (0.65)), gauge transformations locally rotate Γ -vectors, $\Gamma(\theta) \mapsto \Gamma(\theta + \alpha(\xi))$.

Applying gauge transformations specifically to products of Cooper pair fields $\prod_{i=1}^n \bar{\Psi}(\xi_i)\mathbb{F}(\theta_i)\Psi(\xi_i)$ yields up to error terms, denoted by "err.",

$$\begin{aligned}
& \left\langle \delta_\alpha \left(\prod_{i=1}^n (\bar{\Psi}\mathbb{F}(\theta_i)\Psi)(\xi_i) \right) \right\rangle_{\theta;\lambda}^{connected} \\
&= 2 \sum_{i=1}^n \alpha(\xi_i) \left(\prod_{i' \neq i} (\bar{\Psi}\mathbb{F}(\theta_{i'})\Psi)(\xi_{i'}) \right) (\bar{\Psi}\mathbb{F}(\theta_i)\Psi)(\xi_i) \\
&= \int d\xi \left\langle \left(\prod_{i=1}^n (\bar{\Psi}\mathbb{F}(\theta_i)\Psi)(\xi_i) \right) \cdot \right. \\
&\quad \left. \bar{\Psi}(\xi) \left\{ -2\alpha(\xi)\mathbb{F}^\perp(\theta) + \left(\partial_\tau \alpha(\xi)\sigma^3 + \frac{1}{m^*} (\nabla\alpha(\xi) \cdot \nabla)\mathbb{1} \right) \right\} \Psi(\xi) \right\rangle_{\theta;\lambda}^{connected} + \text{err.},
\end{aligned} \tag{3.44}$$

where δ_α acts as $i\varepsilon\alpha(\xi_i)\sigma^3$ on $\Psi(\xi_i)$, and as $-i\varepsilon\alpha(\bar{\xi}_i)\sigma^3$ on $\bar{\Psi}(\bar{\xi}_i)$.

We are however interested in *infra-red cut-off* quantities obtained by integrating Goldstone boson propagators Σ^{k+} with scales $k_+ \leq j_+$, and leaving out Σ^{k+} -kernels with scales $k_+ > j_+$. This introduces further error terms due to the infra-red cut-off on the Σ -kernel this time. Otherwise (3.44) still holds true with $\langle \cdot \rangle_{\theta;\lambda}^{connected}$ replaced by $\langle \cdot \rangle_{\theta;\lambda,j_+ \rightarrow}^{connected}$.

We choose to apply Ward identities to *amputated bosonic n-point functions* $f_n^{j_+ \rightarrow}(\theta_1, \dots, \theta_n; \xi_1, \dots, \xi_n)$. By definition, compare with (2.83) and (3.20),

$$\begin{aligned}
& f_n^{j_+ \rightarrow}(\theta_1, \dots, \theta_n; \xi_1, \dots, \xi_n) := \\
& \left(\prod_{i=1}^n \int d\bar{\xi}_i \int d\zeta_i \chi_+^{j_+ \rightarrow}(\zeta_i) \right) \left(\prod_{i=1}^n \frac{\delta}{\delta\Phi(\zeta_i + \xi_i)} \sigma(\theta_i) \frac{\delta}{\delta\bar{\Phi}(\zeta_i + \bar{\xi}_i)} \right) \Big|_{\Phi, \bar{\Phi}=0} \log(\mathcal{Z}_\lambda^{j_+ \rightarrow}(\Phi, \bar{\Phi})),
\end{aligned} \tag{3.45}$$

where $\log \mathcal{Z}_\lambda^{j_+ \rightarrow}(\Phi, \bar{\Phi})$ is the generating function of connected diagrams excluding four-point diagrams with transfer momentum scale $> j_+$, and additive sources, $\Psi \rightarrow \Psi + \Phi$, $\bar{\Psi} \rightarrow \bar{\Psi} + \bar{\Phi}$. The multi-scale cluster expansions of §3.2 down to scale j_+ typically produce – after displacing the $\bar{\Psi}$ -legs of each external Cooper pair – polymers with low-momentum external $\Sigma_{\perp,\perp}$ -kernels, summed as

$$F_n^{j_+ \rightarrow}(\theta + \frac{\pi}{2}, \dots, \theta + \frac{\pi}{2}; \xi_1, \dots, \xi_n) := \left(\prod_{i=1}^n \Sigma_{\perp,\perp}^{k_+,i}(\xi_{\text{ext},i}, \xi_i) \right) f_n^{j_+ \rightarrow}(\theta + \frac{\pi}{2}, \dots, \theta + \frac{\pi}{2}; \xi_1, \dots, \xi_n) \tag{3.46}$$

However, there is the possibility that some of the Cooper pairs are in the ($//, //$)-channel, or that the two fermions composing the Cooper pair connect to two different polymers. These "massive" cases are treated in **C.** below. Using linear combinations, one may restrict to $\theta_i \in \theta + \frac{\pi}{2}\mathbb{Z}$ or even to $\theta_i \in \{\theta, \theta + \frac{\pi}{2}\}$.

A. One-point functions and gap equation. Let us for a start consider the amputated one-point function $f_1^{j+\rightarrow}(\theta')$, $\theta' = \theta$ or $\theta + \frac{\pi}{2}$. The latter function is conveniently rewritten as

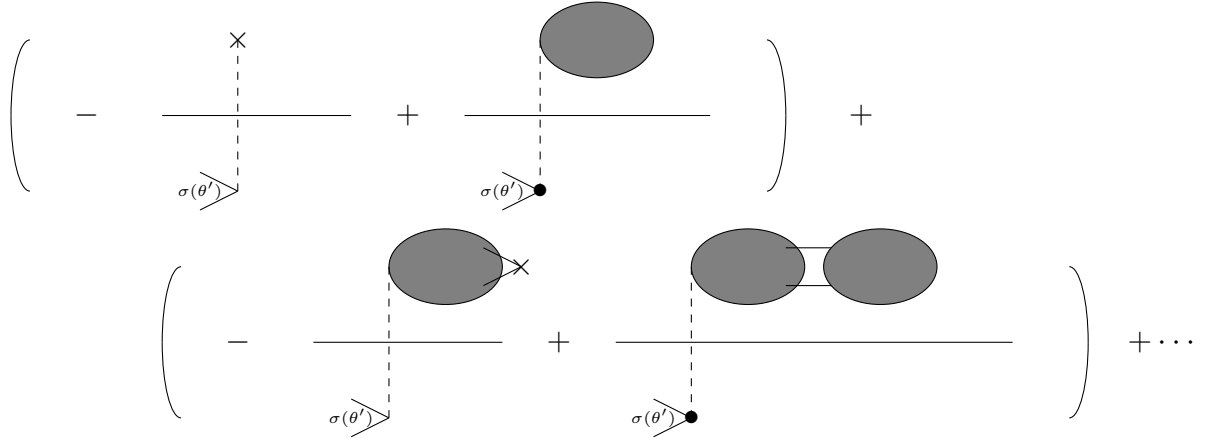



Fig. 3.3.1. Amputated one-point function.

where gray blobs  denote strongly connected (see 3.2), bosonic one-point functions, excluding four-point subdiagrams with transfer momentum scale $> j_+$; and \times are two-point vertex insertions coming from off-diagonal propagators computed in the $\sigma(\theta')$ -channel and with the Γ -coefficient computed at scale j_+ , therefore evaluated as $\Gamma^{j+\rightarrow}$ when $\theta' = \theta$, resp. 0 when $\theta' = \theta + \frac{\pi}{2}$.

Consider to begin with the one-point function in the parallel ($//$) direction $\theta' = \theta$. Setting to zero the first line of Figure 3.3.1

$$\left(-\Gamma^{j+\rightarrow} + \begin{array}{c} \text{gray oval blob} \\ \vdots \\ \text{horizontal line} \\ \vdots \\ \text{dashed vertical line} \\ \vdots \\ \text{bracketed arrow } \sigma(\theta) \text{ ending in a dot} \end{array} \right) = 0$$

Fig. 3.3.2 Gap equation, one-point version.

yields an implicit equation for $\Gamma^{j+\rightarrow}$,

Definition 3.2 (gap equation, one-point version)

$$-\Gamma^{j+\rightarrow} + I_{s.c.,//}^{j+\rightarrow} = 0, \quad (3.47)$$

$I_{s.c.,//}^{j+\rightarrow}$ being the sum of strongly connected (s.c.), bosonic one-point function diagrams (drawn above as a gray blob), which is – as we shall presently prove, using a Ward identity – exactly equivalent in the infra-red limit to its *two-point* version (a refined version of Definition 1.9) stating that the Goldstone boson propagator has a pole in the transverse (\perp) direction. Let us note that, provided the above gap equation is verified, *all lines* in Fig 3.3.1 vanish *up to error terms due to external leg displacements* which are at most of order $2^{-(j_+ - j'_\phi)}$, hence vanish in the infra-red limit ($j_+ \rightarrow +\infty$), e.g.

$$\left(- \text{diagram 1} + \text{diagram 2} \right) = 0.$$

Next, we apply to the one-point function in the parallel direction, see Fig. 3.3.2, the global (constant) Ward identity associated to $\alpha \equiv 1$. We immediately obtain

$$\text{diagram} = 0,$$

in other words,

$$\boxed{f_1^{j+\rightarrow}(\theta + \frac{\pi}{2}) = 0 :} \quad (3.48)$$

the one-point function in the perpendicular (\perp) direction vanishes.

Finally, we consider the sum $I_{s.c.,\perp}^{j+\rightarrow}$ of strongly connected (s.c.) contributions to the one-point function $f_1^{j+\rightarrow}(\theta + \frac{\pi}{2})$ in the perpendicular direction (\perp). Applying to it likewise the global (constant) Ward identity associated to $\alpha \equiv 1$, we get

$$\left(- \text{diagram 1} + \int d\xi \text{diagram 2} \right) = 0$$

Fig. 3.3.3. Ward identity connecting one- and two-point functions of the Goldstone boson.

The left term is immediately seen to be $I_{s.c.,//}^{j+\rightarrow}$, which is equal to $\Gamma^{j+\rightarrow}$ by Definition 3.2. On the other hand, the gray blob in the right term is now a strongly connected *four-point* diagram. Displacing its external leg ξ_4 to ξ_3 following the displacement procedure of the previous subsection yields a product of a $\bar{\Pi}$ -kernel by a bubble in the (\perp, \perp) -channel. The error term due to the displacement procedure has by symmetry an extra spring factor $2^{-2(j_+-j'_\phi)}$. One has found:

$$\bar{\Pi}_{\perp, \perp}^{j+\rightarrow}(0) \mathcal{A}(\Gamma^{j+\rightarrow}, \Upsilon_3)_{\perp, \perp}(0) = O(g^2 2^{-2(j_+-j'_\phi)}). \quad (3.49)$$

As asserted above, this is – up to error terms in $O(q^2)$ – equivalent to the gap equation of §1.7. For convenience, *we shall define $\Gamma^{j+\rightarrow}$ in §2.4 – see Definition 3.3 – in such a way that the infra-red cut-off Goldstone boson propagator in the (\perp, \perp) -channel, $\Sigma^{j+\rightarrow}(q)$, has a pole precisely at $q = 0$.* This implies in turn that the one-point function version of the gap equation, see Definition 3.2, is satisfied up to error terms,

$$-\Gamma^{j+\rightarrow} + I_{s.c.,//}^{j+\rightarrow} = O(g^2 2^{-2(j_+-j'_\phi)}). \quad (3.50)$$

B. Local Ward identities. Let $n \geq 2$. We shall now apply to

$$I_{(0,n)}^{j+\rightarrow}(\xi_1, \dots, \xi_n) := f^{j+\rightarrow}(\theta + \frac{\pi}{2}, \dots, \theta + \frac{\pi}{2}; \xi_1, \dots, \xi_n) \quad (3.51)$$

a general gauge transformation along α . Note that we do *not* restrict to strongly connected diagrams any more. At this point it is useful to introduce the following general notation,

$$I_n^{j+\rightarrow} \left(\begin{array}{ccc} \varepsilon_1 & \cdots & \varepsilon_n \\ \xi_1 & \cdots & \xi_n \end{array} \right) := \left(\prod_{i=1}^n \int d\bar{\xi}_i \int d\zeta_i \chi_+^{j+\rightarrow}(\zeta_i) \right) \left(\prod_{i=1}^n \frac{\delta}{\delta\Phi(\zeta_i + \xi_i)} \varepsilon_i \frac{\delta}{\delta\bar{\Phi}(\zeta_i + \bar{\xi}_i)} \right) \Big|_{\Phi, \bar{\Phi}=0} \log(\mathcal{Z}_\lambda^{j+\rightarrow}(\Phi, \bar{\Phi})) \quad (3.52)$$

generalizing (3.45), where ε_i are general Hermitian (not even necessarily off-diagonal)

two-by-two matrices. Gauge transformations rotate the matrix ε_i to $\hat{\varepsilon}_i := \begin{cases} \mathbb{F}^\perp, & \varepsilon_i = \mathbb{F}^{//} \\ -\mathbb{F}^{//}, & \varepsilon_i = \mathbb{F}^\perp \\ 0, & \varepsilon_i = \mathbb{1}, \sigma^3 \end{cases}$.

The lower pair of indices $(0, n)$ points to the fact that all angles θ_i , $i = 1, \dots, n$ are in the perpendicular (\perp) direction.

Then – generalizing Fig. 3.3.3 – we obtain the following order 1 **local Ward iden-**

tities,

$$\begin{aligned}
0 &= \delta_\alpha I_{(0,n-1)}^{j+\rightarrow}(\xi_1, \dots, \xi_{n-1}) = 2 \sum_{i=1}^{n-1} \alpha(\xi_i) I_{n-1}^{j+\rightarrow} \left(\begin{array}{cccccc} \mathbb{F}^\perp & \dots & \mathbb{F}^\perp & -\mathbb{F} // & \mathbb{F}^\perp & \dots & \mathbb{F}^\perp \\ \xi_1 & \dots & \xi_{i-1} & \xi_i & \xi_{i+1} & \dots & \xi_{n-1} \end{array} \right) \\
&+ 2 \int d\xi_n \alpha(\xi_n) I_{(0,n)}^{j+\rightarrow}(\xi_1, \dots, \xi_n) \\
&- \int d\xi_n \partial_\tau \alpha(\xi_n) I_n^{j+\rightarrow} \left(\begin{array}{cccc} \mathbb{F}^\perp & \dots & \mathbb{F}^\perp & \sigma^3 \\ \xi_1 & \dots & \xi_{n-1} & \xi_n \end{array} \right) \\
&- \int d\xi_n \left\{ \frac{1}{m^*} \nabla \alpha(\xi_n) \cdot \nabla_{\xi_n} \right\} I_n^{j+\rightarrow} \left(\begin{array}{cccc} \mathbb{F}^\perp & \dots & \mathbb{F}^\perp & \mathbb{1} \\ \xi_1 & \dots & \xi_{n-1} & \xi_n \end{array} \right) + \text{err.}
\end{aligned} \tag{3.53}$$

Take α such that $\alpha(\xi_i) = 0$, $i = 1, \dots, n-1$. Then the first term on the r.-h.s. of (3.53) vanishes, so that

$$\begin{aligned}
&\int d\xi_n \alpha(\xi_n) I_{(0,n)}^{j+\rightarrow}(\xi_1, \dots, \xi_n) \\
&= \frac{1}{2} \int d\xi_n \partial_\tau \alpha(\xi_n) I_n^{j+\rightarrow} \left(\begin{array}{cccc} \mathbb{F}^\perp & \dots & \mathbb{F}^\perp & \sigma^3 \\ \xi_1 & \dots & \xi_{n-1} & \xi_n \end{array} \right) \\
&+ \int d\xi_n \left\{ \frac{1}{2m^*} \nabla \alpha(\xi_n) \cdot \nabla_{\xi_n} \right\} I_n^{j+\rightarrow} \left(\begin{array}{cccc} \mathbb{F}^\perp & \dots & \mathbb{F}^\perp & \mathbb{1} \\ \xi_1 & \dots & \xi_{n-1} & \xi_n \end{array} \right) + \text{err.}
\end{aligned} \tag{3.54}$$

Let us now take the functional derivative $\frac{\delta}{\delta \alpha(\xi_n)}(\cdot)$ of (3.54) w.r. to α :

$$\begin{aligned}
I_{(0,n)}^{j+\rightarrow}(\xi_1, \dots, \xi_n) &= \frac{1}{2} \partial_{\tau_n} I_n^{j+\rightarrow} \left(\begin{array}{cccc} \mathbb{F}^\perp & \dots & \mathbb{F}^\perp & \sigma^3 \\ \xi_1 & \dots & \xi_{n-1} & \xi_n \end{array} \right) \\
&+ \frac{1}{2m^*} \nabla_{\xi_n}^2 I_n^{j+\rightarrow} \left(\begin{array}{cccc} \mathbb{F}^\perp & \dots & \mathbb{F}^\perp & \mathbb{1} \\ \xi_1 & \dots & \xi_{n-1} & \xi_n \end{array} \right) + \text{err.}
\end{aligned} \tag{3.55}$$

Finally, integrating w.r. to the external legs except ξ_1 , one finds in particular by integrations by parts,

$$\begin{aligned}
F_n^{j+\rightarrow}(\theta + \frac{\pi}{2}, \dots, \theta + \frac{\pi}{2}; \xi_1) &= \frac{1}{2} \left(\prod_{i=2}^{n-1} \int d\xi_i \Sigma^{k_+, i}(\xi_{ext, i}, \xi_i) \right) \int d\xi_n \\
&\left\{ I_n^{j+\rightarrow} \left(\begin{array}{cccc} \mathbb{F}^\perp & \dots & \mathbb{F}^\perp & \Gamma_\phi \sigma^3 \\ \xi_1 & \dots & \xi_{n-1} & \xi_n \end{array} \right) \left(\frac{1}{\Gamma_\phi} \frac{\partial}{\partial \tau_n} \right) \Sigma^{k_+, n}(\xi_{ext, n}, \xi_n) \right. \\
&+ \left. I_n^{j+\rightarrow} \left(\begin{array}{cccc} \mathbb{F}^\perp & \dots & \mathbb{F}^\perp & \Gamma_\phi \mathbb{1} \\ \xi_1 & \dots & \xi_{n-1} & \xi_n \end{array} \right) \left(\frac{1}{2m^* \Gamma_\phi} \nabla_{\xi_n}^2 \right) \Sigma^{k_+, n}(\xi_{ext, n}, \xi_n) \right\} \\
&+ \text{err.}
\end{aligned} \tag{3.56}$$

The second-order operator $\frac{1}{2m^*\Gamma_\phi}\nabla_{\xi_n}^2$ contributes a factor of order $2^{j+2-2k_+} \leq 2^{-2(k_+-j_+)}$, a squared spring factor; on the other hand, the first-order operator $\frac{1}{\Gamma_\phi}\frac{\partial}{\partial\tau_n}$ contributes a single spring factor $O(2^{-(k_+-j_+)})$, which is not enough for our purposes. Fortunately, the whole procedure may be iterated twice, using successively two derivatives $\delta_\alpha, \delta_\beta$, with $\alpha(\xi_i) = 0, i \neq n-1$ and $\beta(\xi_i) = 0, i \neq n$, and taking the functional derivative $\frac{\delta^2}{\delta\alpha(\xi_{n-1})\delta\beta(\xi_n)}$. Considering only time-derivatives, one has schematically

$$0 = \delta_\alpha I_{(0,n-1)}^{j+\rightarrow} \longrightarrow I_{(0,n)}^{j+\rightarrow} \equiv \partial_\tau I_n^{j+\rightarrow} (\mathbb{F}^\perp \dots \mathbb{F}^\perp \sigma^3) \quad (3.57)$$

$$\begin{aligned} 0 &= \delta_\beta I_{n-1}^{j+\rightarrow} (\mathbb{F}^\perp \dots \mathbb{F}^\perp \sigma^3) \\ &\longrightarrow I_n^{j+\rightarrow} (\mathbb{F}^\perp \dots \mathbb{F}^\perp \sigma^3) \equiv \partial_\tau I_n^{j+\rightarrow} (\mathbb{F}^\perp \dots \mathbb{F}^\perp \sigma^3 \sigma^3) \end{aligned} \quad (3.58)$$

Thus $F_n^{j+\rightarrow}(\theta + \frac{\pi}{2}, \dots, \theta + \frac{\pi}{2}; \xi_1)$, $n \geq 3$ has been rewritten as a sum of four terms involving $I_n^{j+\rightarrow}(\mathbb{F}^\perp \dots \mathbb{F}^\perp * *)$ with $*$ = $\mathbb{1}, \sigma^3$, and product differential operators of the type $(\frac{1}{\Gamma_\phi}\frac{\partial}{\partial\tau_{n-1}}, \frac{1}{2m^*\Gamma_\phi}\nabla_{\xi_{n-1}}^2) \times (\frac{1}{\Gamma_\phi}\frac{\partial}{\partial\tau_{n-1}}, \frac{1}{2m^*\Gamma_\phi}\nabla_{\xi_{n-1}}^2)$, therefore of order ≥ 2 . Thus one has decreased the relative degree of divergence $\omega_n = \frac{1}{2}(6-n)$ of the original n -point function by at least two units. This is sufficient to show the convergence of amputated n -point functions $I_{(0,n)}^{j+\rightarrow}$ provided $n \geq 3$, since then the corrected degree of divergence is $\tilde{\omega}_n := \frac{1}{2}(6-n) - 2 < 0$.

C. Massive configurations. We have not considered in previous computations the following two cases:

(i) n -point functions of the type

$$I_{(k_{//}, k_\perp)}^{j+\rightarrow}(\xi_1, \dots, \xi_n) := I_n^{j+\rightarrow} \left(\begin{array}{cccccc} \mathbb{F}^{//} & \dots & \mathbb{F}^{//} & \mathbb{F}^\perp & \dots & \mathbb{F}^\perp \\ \xi_1 & \dots & \xi_{k_{//}} & \xi_{k_{//}+1} & \dots & \xi_n \end{array} \right) \quad (3.59)$$

with $k_\perp = n - k_{//}$, $k_{//} \geq 1$;

(ii) n -point functions $I_{(0,n)}^{j+\rightarrow}(\dots)$ such that at least one of the external Cooper pairs connects to two different polymers, as in Fig. 3.2.7.

Both cases are *massive*, featuring at least one external fermionic propagator with quasi-exponential decay at distances $\gg \Gamma_\phi^{-1}$, implying that the corresponding polymers are convergent, and furthermore, their contribution decreases exponentially as $j_+ \rightarrow \infty$. More precisely:

(i) external Cooper pairs along the parallel ($//$) direction form a $\Sigma_{//, //}^{\rightarrow(j_++1)}$ -kernel which is bounded as in (1.94).

(ii) Referring to the notations on Fig. 3.3.7, we have the following scaling factors for the compound polymer connected by two fermions (assuming fermion angular sectors are fixed):

- $2^{-3j'_\phi}$ for the integral over p ;
- 2^{-3j_+} for the integral over $p' := -p + q$ constrained by the fact that $p + p' = q$;
- $(2^{j'_\phi})^2$ for the two fermionic propagators;
- a scaled quasi-exponential decay factor of scale j'_ϕ for the propagator with momentum p , resp. j_+ for the propagator with momentum $-p + q$;
- and finally the squared spring factor $(2^{-(j_+ - j'_\phi)})^2$ coming from the Ward identities. The total factor is $2^{-4j'_\phi} 2^{-5(j_+ - j'_\phi)}$, multiplied by the two quasi-exponential decay factors. The first factor $2^{-4j'_\phi} = (2^{-j'_\phi})^4$ is the expected weight for four fermions $(\psi^{j,\alpha})^4$. The bad scale j_+ decay factor for the second propagator yields an extra volume factor $2^{3(j_+ - j'_\phi)}$ compared to the expected volume implied by a scale j'_ϕ decay factor. Decomposing $2^{-5(j_+ - j'_\phi)}$ into $2^{-3(j_+ - j'_\phi)} \times 2^{-2(j_+ - j'_\phi)}$, one sees that the extra volume factor is compensated, and that one has a further spring factor $2^{-2(j_+ - j'_\phi)}$ which makes it possible to sum over the scale j_+ .

3.4 Bosonic fixed-point procedure and low-energy multi-scale bounds

Consider a bosonic multi-scale tree as in Fig. 3.2.15. Bounds for *fermionic* polymers with low-momentum Cooper pair legs in 3.2 **E**. was based on the naive power-counting for a Goldstone boson propagator $\Sigma_{\perp,\perp}(\xi - \xi')$ of scale k_+ ,

$$O((\Gamma_\phi 2^{-k_+/2})^2) = O((2^{-j_\phi} 2^{-k_+/2} \mu)^2), \quad (3.60)$$

therefore, $O(2^{-j_\phi} 2^{-k_+/2} \mu)$ per Cooper pair. Ward identities (see 3.3), as proved just above (see below (3.56)), imply however that one can get one or two supplementary spring factors $O(2^{-(k_+ - j_\phi)})$ per polymer, thus modifying the scaling of the corresponding Cooper pairs,

$$2^{-j'_\phi} 2^{-k_+/2} \mu \longrightarrow 2^{-(k_+ - j_\phi)} \cdot 2^{-j'_\phi} 2^{-k_+/2} \mu = 2^{-3k_+/2} \mu. \quad (3.61)$$

Thus the sum over bosonic multi-scale trees may be bounded as follows. We first need some notations. Let $\mathbb{P}_1^{(j'_\phi - 1) \rightarrow}, \dots, \mathbb{P}_{n_{j'_\phi - 1}}^{(j'_\phi - 1) \rightarrow}$ be the scale-neutral polymers. By assumption, we *fix* the location of *one* of the vertices of $(\mathbb{P}_i^{(j'_\phi - 1) \rightarrow})_{i \leq n_{j'_\phi - 1}}$, so that their power counting is $O(g')$, where $g' = 2^{-2(j'_\phi - j_\phi)}$. The scale j'_ϕ Goldstone boson propagators merge these polymers into **bosonic polymers** $\mathbb{P}_1^{j'_\phi \rightarrow}, \dots, \mathbb{P}_{n_{j'_\phi}}^{j'_\phi \rightarrow}$ with lowest scale $\leq j'_\phi$. The power-counting of each of these is computed with the same convention,

namely, by fixing the location of one of the vertices. Repeating this procedure, we get a sequence of polymers $(\mathbb{P}_i^{j+\rightarrow})_{i \leq n_{j_+}}$, $j_+ \geq j'_\phi$ which becomes stationary when all Goldstone boson propagators have been integrated into polymers.

We proceed as in §1.3 (compare with (2.123), (2.124), (2.125)).

General bosonic multi-scale bound. The actual energy gaps Γ_ϕ , resp. non-linear sigma model coupling constant g_ϕ , resp. velocity v_ϕ are obtained inductively as the limits of the converging series $\Gamma^{j+\rightarrow} + \sum_{j_+=j'_\phi+1}^{+\infty} (\Gamma^{j+\rightarrow} - \Gamma^{(j_+-1)\rightarrow})$, resp. $g_\phi := g_\phi^{j'_\phi\rightarrow} + \sum_{j_+=j'_\phi+1}^{+\infty} (g_\phi^{j+\rightarrow} - g_\phi^{(j_+-1)\rightarrow})$, resp. $v_\phi := v_\phi^{j'_\phi\rightarrow} + \sum_{j_+=j'_\phi+1}^{+\infty} (v_\phi^{j+\rightarrow} - v_\phi^{(j_+-1)\rightarrow})$.

We start in **A.** by stating the *difference estimates*. Such estimates make it possible to solve inductively a sequence of approximate gap equations (see Definition 3.3) yielding a Cauchy sequence $(\Gamma^{j+\rightarrow})_{j_+ \geq j'_\phi}$. As an intermediate step, we first prove in **B.** *polymer bounds* by scale induction. Difference estimates are finally proved in **C.**

A. Statement of difference estimates and gap equations. For each $j_+ \geq j'_\phi$, we search for the solution $\Gamma := \Gamma^{j+\rightarrow}$ of largest module of the

Definition 3.3 (scale j_+ gap equation)

$$\left(-\mathbb{1} + \bar{\Pi}_0^{j+\rightarrow}(\Gamma^{j+\rightarrow}) \mathcal{A}_0(\Gamma^{j+\rightarrow}, \Upsilon_3) \right) \begin{pmatrix} (\Gamma^{j+\rightarrow})^\perp \\ ((\Gamma^{j+\rightarrow})^\perp)^* \end{pmatrix} = 0, \quad (3.62)$$

compare with Definition 1.9 and (1.121). The parameters $g_\phi^{j+\rightarrow}, v_\phi^{j+\rightarrow}$ of the Goldstone boson propagator $\Sigma_{\perp, \perp}^{j+\rightarrow}$ are defined as in Lemma 1.3 and Definition 1.4 by

Definition 3.4 (scale j_+ Goldstone boson propagator parameters) *Let*

$$\partial_{q^0}^2 \left\{ \bar{\Pi}_q^{j+\rightarrow}(\Gamma^{j+\rightarrow}) \mathcal{A}_q(\Gamma^{j+\rightarrow}, \Upsilon_3) \right\} \Big|_{diag, q=0} =: -\frac{1}{g_{\phi, diag}^{j+\rightarrow}} \quad (3.63)$$

$$\partial_{q^0}^2 \left\{ \bar{\Pi}_q^{j+\rightarrow}(\Gamma^{j+\rightarrow}) \mathcal{A}_q(\Gamma^{j+\rightarrow}, \Upsilon_3) \right\} \Big|_{off, q=0} =: -\frac{1}{g_{\phi, off}^{j+\rightarrow}} \quad (3.64)$$

$$\nabla^2 \left\{ \bar{\Pi}_q^{j+\rightarrow}(\Gamma^{j+\rightarrow}) \mathcal{A}_q(\Gamma^{j+\rightarrow}, \Upsilon_3) \right\} \Big|_{diag, q=0} =: -\frac{(v_{\phi, diag}^{j+\rightarrow})^2}{g_{\phi, diag}^{j+\rightarrow}} \text{Id}, \quad (3.65)$$

$$\nabla^2 \left\{ \bar{\Pi}_q^{j+\rightarrow}(\Gamma^{j+\rightarrow}) \mathcal{A}_q(\Gamma^{j+\rightarrow}, \Upsilon_3) \right\} \Big|_{off, q=0} =: -\frac{(v_{\phi, off}^{j+\rightarrow})^2}{g_{\phi, off}^{j+\rightarrow}} \text{Id} \quad (3.66)$$

and

$$\boxed{g_\phi^{j+\rightarrow} := \frac{g_{\phi, diag}^{j+\rightarrow} g_{\phi, off}^{j+\rightarrow}}{g_{\phi, diag}^{j+\rightarrow} + g_{\phi, off}^{j+\rightarrow}}, \quad v_\phi^{j+\rightarrow} := \sqrt{\frac{g_{\phi, off}^{j+\rightarrow} (v_{\phi, diag}^{j+\rightarrow})^2 + g_{\phi, diag}^{j+\rightarrow} (v_{\phi, off}^{j+\rightarrow})^2}{g_{\phi, diag}^{j+\rightarrow} + g_{\phi, off}^{j+\rightarrow}}}.} \quad (3.67)$$

The scale j_+ gap equations are solved by induction on j_+ using *difference bounds* of two types:

(i) (*scale differences*) let Γ such that $|\Gamma| \approx \hbar\omega_D e^{-\pi/g}$, then

$$\left| \bar{\Pi}_0^{j_+ \rightarrow}(\Gamma) - \bar{\Pi}_0^{(j_+-1) \rightarrow}(\Gamma) \right| \lesssim 2^{-2(j_+-j_\phi)} g \quad (3.68)$$

$$|g_\phi^{j_+ \rightarrow} - g_\phi^{(j_+-1) \rightarrow}| \lesssim 2^{-2(j_+-j_\phi)} g_\phi, \quad |v_\phi^{j_+ \rightarrow} - v_\phi^{(j_+-1) \rightarrow}| \lesssim 2^{-2(j_+-j_\phi)} v_\phi \quad (3.69)$$

with $g_\phi \approx \frac{\Gamma_\phi^2}{m^*}$, $v_\phi \approx v_F$;

(ii) (Γ *dependence*) let Γ, Γ' such that $|\Gamma|, |\Gamma'| \approx \hbar\omega_D e^{-\pi/g}$, and $\delta\Gamma := |\Gamma - \Gamma'|$, then

$$\left| \bar{\Pi}_q^{j_+ \rightarrow}(\Gamma) - \bar{\Pi}_q^{j_+ \rightarrow}(\Gamma') \right| \lesssim \frac{\delta\Gamma}{\Gamma_\phi} g \quad (3.70)$$

$$\lambda \left| \mathcal{A}_q(\Gamma) - \mathcal{A}_q(\Gamma') \right| \lesssim \frac{\delta\Gamma}{\Gamma_\phi}. \quad (3.71)$$

If difference bounds hold, then subtracting (3.62)_(j_+-1) from (3.62)_{j_+} and applying the implicit function theorem yields after an elementary computations

$$|\Gamma^{j_+ \rightarrow} - \Gamma^{(j_+-1) \rightarrow}| \lesssim 2^{-2(j_+-j_\phi)} \Gamma_\phi \quad (3.72)$$

where $\Gamma_\phi \approx 2^{-j_\phi} \mu$. In particular, $\Gamma^{j_+ \rightarrow} \rightarrow_{j_+ \rightarrow +\infty} e^{i\theta} \Gamma_\phi$.

Also, by elementary computation, $v_\phi^{j_+ \rightarrow} \rightarrow_{j_+ \rightarrow \infty} v_\phi \approx v_F$, $g_\phi^{j_+ \rightarrow} \rightarrow_{j_+ \rightarrow \infty} g_\phi \approx \frac{\Gamma_\phi^2}{m^*}$, and

$$\Sigma_{\perp, \perp}^{j_+ \rightarrow}(q) \rightarrow_{j_+ \rightarrow \infty} \Sigma(q) = \frac{g_\phi}{(q^0)^2 + v_\phi^2 |\mathbf{q}|^2 + O(|q|_+^4 / \Gamma_\phi^2)}, \quad (3.73)$$

$$\Sigma_{\perp, \perp}^{j_+ \rightarrow}(\xi - \xi') \rightarrow_{j_+ \rightarrow \infty} \Sigma_{\perp, \perp}(\xi - \xi'), \quad (3.74)$$

$$\Sigma_{\perp, \perp}(\xi - \xi') \sim_{|\xi - \xi'| \rightarrow \infty} \frac{g_\phi / 4\pi v_\phi}{\sqrt{|\mathbf{x} - \mathbf{x}'|^2 + v_\phi^2 (\tau - \tau')^2}} \left(1 + O\left(\frac{1}{\Gamma_\phi (|\tau - \tau'| + |\mathbf{x} - \mathbf{x}'| / v_\phi)} \right) \right), \quad (3.75)$$

as stated in Theorem 2.

B. Proof of polymer bounds.

Let $\mathbb{P}^{j_+ \rightarrow} \in \mathcal{P}^{j_+ \rightarrow} \neq \emptyset$, then we want to prove, in analogy with the bounds (2.123), (2.123), (2.125) of section 2 for fermionic polymers in $\mathcal{P}^{j \rightarrow}$, $j \leq j'_\phi - 1$, but now with $j \rightarrow j_+$, $j_+ \geq j'_\phi$, and *bosonic polymers* obtained by merging polymers also including scale j'_ϕ fermions, following the procedure of §3.2:

General bosonic multi-scale bound.

For every $\mathbb{P}^{j+\rightarrow}$ belonging to the set $\mathcal{P}_{N_{ext,+}}^{j+\rightarrow}$ of polymers with lowest scale j_+ and $N_{ext,+}$ external legs,

$$|\mathcal{A}(\mathbb{P}^{j+\rightarrow}; \xi_{ext,1})| \lesssim g^{n(\mathbb{P}^{j+\rightarrow})/4} (2^{-j_\phi/4})^{N_{ext,+}(\mathbb{P}^{j+\rightarrow})-4} (2^{j_+})^{\frac{1}{2}(N_{ext,+}(\mathbb{P}^{j+\rightarrow})-6)} (p_F^*)^{-2N_{ext,+}} \quad (3.76)$$

The exponent of 2^{j_+} has been chosen in such a way that the factor $(2^{j_+})^{\frac{1}{2}(N_{ext,+}-6)}$, times the *weight* $(2^{-j_\phi} 2^{-j_+/2})^{N_{ext,+}} 2^{3j_+}$ of the external structure of a polymer with $N_{ext,+}$ external Cooper pair legs (see below), is scale independent. Then, if $\mathbb{P}^{j+\rightarrow}$ ranges in the set $\mathcal{P}_{N_{ext,+}}^{j+\rightarrow}(n)$ of polymers in $\mathcal{P}_{N_{ext,+}}^{j+\rightarrow}$ with $n \geq 1$ vertices,

$$\sum_{\mathbb{P}^{j+\rightarrow} \in \mathcal{P}_{N_{ext,+}}^{j+\rightarrow}(n)} |\mathcal{A}(\mathbb{P}^{j+\rightarrow}; \xi_{ext,1})| \lesssim g^{n/4} (2^{-j_\phi/4})^{N_{ext,+}(\mathbb{P}^{j+\rightarrow})-4} (2^{j_+})^{\frac{1}{2}(N_{ext,+}(\mathbb{P}^{j+\rightarrow})-6)} (p_F^*)^{-2N_{ext,+}} \quad (3.77)$$

from which, finally, summing over all polymers in $\mathcal{P}_{N_{ext,+}}^{j+\rightarrow}$ with one external leg located at $\xi_{ext,1}$,

$$\sum_{\mathbb{P}^{j+\rightarrow} \in \mathcal{P}_{N_{ext,+}}^{j+\rightarrow}} |\mathcal{A}(\mathbb{P}^{j+\rightarrow}; \xi_{ext,1})| \lesssim g^{N_{ext,+}/4} (2^{-j_\phi/4})^{N_{ext,+}(\mathbb{P}^{j+\rightarrow})-4} (2^{j_+})^{\frac{1}{2}(N_{ext,+}-6)} (p_F^*)^{-2N_{ext,+}} \quad (3.78)$$

The proof of **bosonic polymer bounds** (3.76),(3.77),(3.78) is by induction on j_+ . Note first that (3.76),(3.77),(3.78) follow from the general *fermionic* multi-scale bound (2.123),(2.123),(2.125) if one sets $j_+ = j_\phi$, which means that *all fermionic polymers* (i.e. all polymers having all internal propagators of scales $\leq j'_\phi - 1$) *are assimilated to polymers with lowest scale j_ϕ* ; this is a convenient choice for the induction, since field scaling factors (see below) have a scale-independent prefactor proportional to $\Gamma_\phi \approx 2^{-j_\phi} \mu$. Namely, identifying the $N_{ext,+}$ *bosonic* legs of a *fermionic* polymer $\mathbb{P}^{j'_\phi \rightarrow} \in \mathcal{P}^{j'_\phi \rightarrow}$ with

$$N_{ext} := 2N_{ext,+} \quad (3.79)$$

fermionic legs, we remark that

$$(2^{-j_\phi/4})^{N_{ext,+}-4} (2^{j_+})^{\frac{1}{2}(N_{ext,+}-6)} = (2^{j_\phi})^{\frac{1}{2}(N_{ext}-4)} \quad (3.80)$$

which shows that (3.76) holds with prefactor $g^{n/2}$ instead of $g^{n/4}$ for a fermionic polymer in $\mathcal{P}^{j_\phi \rightarrow}$. Since $N_{ext} \geq 4$, the fermionic bound $j \mapsto (2^j)^{\frac{1}{2}(N_{ext}-4)}$ increases with j , hence (3.76) is all the more true for a fermionic polymer in $\mathcal{P}^{j \rightarrow}$ if $j \leq j_\phi$. Finally, for $j_\phi \leq j \leq j'_\phi$, a correcting factor $\leq (2^{j'_\phi - j_\phi})^{\frac{1}{2}(N_{ext}-4)} = (2^{j'_\phi - j_\phi})^{N_{ext,+} - 2}$ is required to obtain the fermionic bounds $(2^j)^{\frac{1}{2}(N_{ext}-4)}$, which is compensated by $g^{-n/4}$ since $n \geq N_{ext,+}$.

We now suppose as in §2.4 that $\mathbb{P}^{j_+ \rightarrow}$ is obtained by merging at scale j_+ polymers $\mathbb{P}_1, \dots, \mathbb{P}_n$ with lowest bosonic scales $k_{+,1}, \dots, k_{+,n} < j_+$ and $n_i := N_{ext,+}(\mathbb{P}_i)$ external Cooper pair legs.

Ward spring factor. As discussed in the introduction to this subsection, we have an extra spring factor $O(2^{-2(j_+ - k_+)})$ for each polymer \mathbb{P}_i .

Volume factors. External legs of $\mathbb{P}^{j_+ \rightarrow}$ which are contracted at scale j_+ are integrated in a box Δ^{j_+} of scale j_+ . This yields a volume factor $O(2^{3j_+})$.

Field scaling factors. Each external Goldstone boson half-propagator of $\mathbb{P}^{j_+ \rightarrow}$ which is contracted at scale j_+ comes with a supplementary prefactor $2^{-j_\phi} 2^{-j_+/2}$.

The product of the volume factors and of the field scaling factors gives the above mentioned *weight* $(2^{-j_\phi} 2^{-j_+/2})^{N_{ext,+}} 2^{3j_+}$. Taking these into account for the polymers $\mathbb{P}^{k_i}, i = 1, \dots, n$ and (in the denominator, in order to avoid double-counting) for $\mathbb{P}^{j_+ \rightarrow}$, yields the general multi-scale bound (dismissing dimensional factors)

$$|\mathcal{A}(\mathbb{P}^{j_+ \rightarrow}; \xi_{ext,1})| \lesssim g^{n(\mathbb{P}^{j_+ \rightarrow})/2} (2^{j_\phi} 2^{j_+/2})^{N_{ext,+}(\mathbb{P}^{j_+ \rightarrow})} 2^{-3j_+} \prod_{i=1}^n \left\{ a(\mathbb{P}_i; \cdot) 2^{-2(j_+ - k_{+,i})} (2^{-j_\phi} 2^{-j_+/2})^{n_i} 2^{3j_+} \right\}. \quad (3.81)$$

where

$$a(\mathbb{P}_i) := (2^{-j_\phi/4})^{n_i - 4} (2^{k_{+,i}})^{\frac{1}{2}(n_i - 6)} \quad (3.82)$$

is the scale-dependent part of (3.76). We show that this is $\lesssim (2^{-j_\phi/4})^{N_{ext,+} - 4} (2^{j_+})^{\frac{1}{2}(N_{ext,+} - 6)} \prod_{i=1}^n 2^{-\frac{1}{2}(j_+ - k_{+,i})}$, where $N_{ext} := N_{ext}(\mathbb{P}^{j_+ \rightarrow})$. For this we consider separately *scale-independent factors*, *scale j_+ factors*, and *rescaling factors*:

- (i) (*scale-independent factors*) Each polymer is connected at least to one other polymer, hence at least one of the external legs of each polymer \mathbb{P}_i does not belong to the N_{ext} external legs of $\mathbb{P}^{j_+ \rightarrow}$. Thus $\sum_{i=1}^n n_i \geq N_{ext,+} + n$. The total exponent of the scale-independent factor 2^{-j_ϕ} in (3.81) is

$$-N_{ext,+} + \sum_{i=1}^n \left(\frac{5}{4} n_i - 1 \right) \geq \frac{1}{4} (N_{ext,+} - 4). \quad (3.83)$$

- (ii) (*rescaling factors*) rewrite $2^{-2(j_+ - k_{+,i})} (2^{k_{+,i}})^{\frac{1}{2}(n_i - 6)}$ as $(2^{j_+})^{\frac{1}{2}(n_i - 6)}$ times $(2^{-(j_+ - k_{+,i})})^{2 + \frac{1}{2}(n_i - 6)}$. Since by hypothesis $n_i \geq 3$, the exponent $2 + \frac{1}{2}(n_i - 6)$ is $> \frac{1}{2}$. The remaining spring factor $\leq \prod_{i=1}^n (2^{-(j_+ - k_{+,i})})^{1/2}$ makes it possible to sum over all scales $k_{+,1}, \dots, k_{+,n} < j_+$.

- (iii) (*scale j_+ factors*) For each $i = 1, \dots, n$, the left-over factor $(2^{j_+})^{\frac{1}{2}(n_i - 6)}$ in (ii) cancels with the scale-dependent part $(2^{-j_+/2})^{n_i} 2^{3j_+}$ of the weight of \mathbb{P}_i . Therefore, there remains only the required overall prefactor $(2^{j_+})^{\frac{1}{2}(N_{ext,+} - 6)}$.

C. Proof of difference estimates.

1. *Difference estimates for Γ .* The difference $\bar{\Pi}^{j_+ \rightarrow}(\Gamma) - \bar{\Pi}^{(j_+-1) \rightarrow}(\Gamma)$, see (3.68), involves terms of three types which we present by *decreasing* order:

- (i) pure scale j_+ irreducible four-point polymers, like the first term of Fig. §3.2.3. These contain no inner Goldstone boson, hence enjoy by Ward identities a spring factor $O(2^{-2(j_+-j_\phi)})$, multiplied by the scaling (2.123) of an amputated, four-point, fermionic polymer of lowest scale $j \leq j'_\phi$, $O((2^j)^{\frac{1}{2}(N_{ext}-4)}) = O(1)$; all together, one gets the expected factor $2^{-2(j_+-j_\phi)}$.

The two remaining types are *multi-scale* bosonic trees obtained in the last two resummation steps, Step (iv), resp. Step (v) of p. 126, involving at least one Goldstone boson of scale $j_+ - 1$:

- (ii) (internal Goldstone boson propagator)

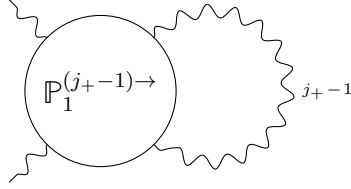


Fig. 3.4.1. Case of a scale $(j_+ - 1)$ internal Goldstone boson propagator.

involving one internal Goldstone boson propagator connecting a polymer $\mathbb{P}_1^{(j_+-1) \rightarrow}$ to itself. Leading terms are as in the above Figure, leading to a contribution larger than in case (i),

$$\left(2^{-j_+}\right) \times \left(2^{-2j_\phi} 2^{-j_+}\right) = 2^{-2j_\phi} 2^{-2j_+}, \quad (3.84)$$

that is, (Amplitude of a polymer with 4 external Cooper pair legs $\mathbb{P}_1^{(j_+-1) \rightarrow}$) \times (Scale j_+ Goldstone boson propagator). See (3.76).

- (iii) (Goldstone boson connecting two different polymers)

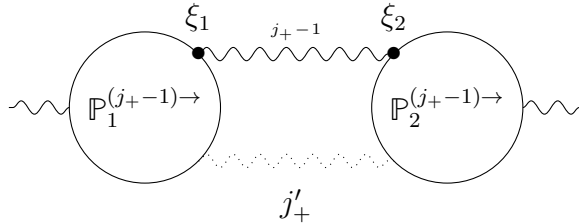


Fig. 3.4.2. Case of a scale j_+ Goldstone boson connecting two different polymers.

involving *two* Goldstone boson propagators connecting the *same two* polymers $\mathbb{P}_1^{(j_+-1)\rightarrow}, \mathbb{P}_2^{(j_+-1)\rightarrow} \in \mathcal{P}^{j_+\rightarrow}$, one of scale $j_+ - 1$, the other of scale $j'_+ \leq j_+ - 1$. Spring factors make it possible to sum over $j'_+ \leq j_+ - 1$ for $j_+ - 1$ fixed, hence we can assume that $j'_+ = j_+ - 1$.

Other more complicated diagrams $\mathbb{P}^{j_+\rightarrow}$ with $N_{ext,+}(\mathbb{P}^{j_+\rightarrow}) = 2$ as in **B.**, connecting $\mathbb{P}_1^{(j_+-1)\rightarrow}, \dots, \mathbb{P}_n^{(j_+-1)\rightarrow}$, with $n \geq 2$ and $\ell \geq 2$ internal Goldstone boson propagators, are possible. The power-counting of such diagrams is as in the General bosonic multi-scale bound, eq. (3.76). Eq. (3.83) and point (i) around it show that the largest power-counting is obtained for $n = \ell = 2$, that is, for the situation depicted in the above Figure, for which one obtains a contribution to $\bar{\Pi}^{j_+\rightarrow}(\Gamma) - \bar{\Pi}^{(j_+-1)\rightarrow}(\Gamma)$ of order at most

$$2^{3j_+} \left(2^{j_\phi/4} 2^{-\frac{3}{2}j_+} \right)^2 \times \left(2^{-2j_\phi} 2^{-j_+} \right)^2 = 2^{-\frac{7}{2}j_\phi} 2^{-2j_+}, \quad (3.85)$$

that is, (Integration volume of ξ_2 w.r. to fixed ξ_1) \times (Product of the amplitudes of the polymers with 3 external Cooper pair legs $\mathbb{P}_1^{(j_+-1)\rightarrow}, \mathbb{P}_2^{(j_+-1)\rightarrow}$) \times (Squared scale j_+ Goldstone boson propagator).

2. *Difference estimates for g_ϕ, v_ϕ .* These are obtained in a straightforward way using (3.63), (3.64), (3.65), (3.66) from $\nabla_q^2 \left\{ (\bar{\Pi}_q^{j_+\rightarrow}(\Gamma) - \bar{\Pi}_q^{(j_+-1)\rightarrow}(\Gamma)) \mathcal{A}_q(\Gamma^{j_+\rightarrow}, \Upsilon_3) \right\} \Big|_{q=0}$. Because the bubble diagram $\mathcal{A}_q(\Gamma^{j_+\rightarrow}, \Upsilon_3)$ is made up of fermion propagators with a scale $\leq j_\phi$ effective infra-red cut-off due to the $|\Gamma|^2$ -term in the denominator of (1.20), operators ∇_q change its scaling by a factor $\lesssim 2^{j_\phi}$. So let us study instead the effect of the action of ∇_q on polymers of the type $\bar{\Pi}_q^{j_+\rightarrow}(\Gamma) - \bar{\Pi}_q^{(j_+-1)\rightarrow}(\Gamma)$ studied in 1. As a general rule, gradients w.r. to the transfer momentum q of a diagram with two external Cooper pairs can be evaluated by choosing a line of propagators connecting the two external vertices ξ_1, ξ_2 ,

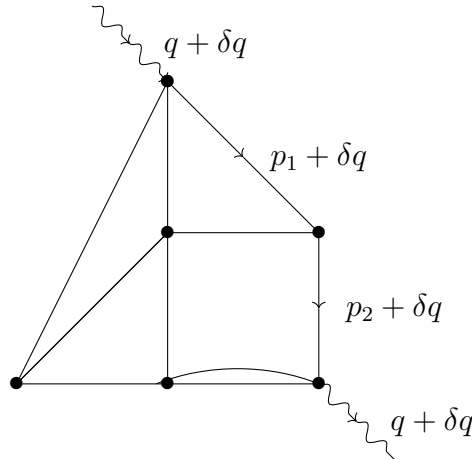


Fig. 3.4.3. Changing the transfer momentum flowing inside a diagram.

see Fig. 2.3.3. Translating q by δq inside the diagram is equivalent to substituting $C_\theta^*(p_1) \cdots C_\theta^*(p_n) \longrightarrow C_\theta^*(p_1 + \delta q) \cdots C_\theta^*(p_n + \delta q)$. Taking two successive derivatives w.r. to q yields sums of terms featuring the product $\{ \prod_{k \neq i, i'} C_\theta^*(p_k) \} \nabla C_\theta^*(p_i) \nabla C_\theta^*(p_{i'})$. In principle, the inverse Fourier transform of a gradient fermion propagator $\nabla C_\theta^{j, \alpha}(p)$, $j \leq j'_\phi$, is $i(x-y)C_\theta^{j, \alpha}(x-y)$, which is bounded as in (2.11), but with a further prefactor scaling at most like $2^{j\phi}$, induced by the scale j quasi-exponential decay. This implies directly for scale j_+ irreducible diagrams $\mathbb{P}_{(i)}$ of type (i) as above a relative scaling of $\nabla_q^2 \mathcal{A}(\mathbb{P}_{(i)}; \xi_{ext,1})$ w.r. to $\mathcal{A}(\mathbb{P}_{(i)}; \xi_{ext,1})$ of order $2^{2j\phi}$ at most. Consider now a diagram \mathbb{P} or type (ii) or (iii), involving a scale $(j_+ - 1)$ Goldstone boson propagator, assume that the line contains a Goldstone boson propagator of scale $k_+ \leq j_+ - 1$. Differentiating $\Sigma_{\perp, \perp}^{k_+}(q + \delta q)$ w.r. to δq yields (by the resolvent identity)

$$\Sigma_{\perp, \perp}^{k_+}(q + \delta q) - \Sigma_{\perp, \perp}^{k_+}(q) \sim_{\delta q \rightarrow 0} \Sigma_{\perp, \perp}^{k_+}(q) \nabla_q (\Pi^{(j_+ - 1) \rightarrow}(\Gamma)) \mathcal{A}(\Gamma, \Upsilon_3) \Sigma_{\perp, \perp}^{k_+}(q) \delta q. \quad (3.86)$$

Proceeding by induction, we see now that $\nabla_q (\Pi^{(j_+ - 1) \rightarrow}(\Gamma))(q)$ involves a supplementary scaling factor $2^{j\phi}$, exactly as $\nabla_q \mathcal{A}_q(\Gamma, \Upsilon_3)$.

Concluding, and letting $\delta g_\phi := g_\phi^{j_+ \rightarrow} - g_\phi^{(j_+ - 1) \rightarrow}$, and similarly $\delta v_\phi := v_\phi^{j_+ \rightarrow} - v_\phi^{(j_+ - 1) \rightarrow}$: $\frac{\delta g_\phi}{g_\phi^2}, \frac{v_\phi}{g_\phi} \delta v_\phi$ (see (3.63), (3.64), (3.65), (3.66)) scale at most like $(2^{j\phi})^2 \times 2^{-2(j_+ - j\phi)}$, namely, (scaling factor due to ∇_q) $^2 \times$ (scaling factor of $\bar{\Pi}^{j_+ \rightarrow}(\Gamma) - \bar{\Pi}^{(j_+ - 1) \rightarrow}(\Gamma)$), whence the estimates (3.69).

3. Γ -dependence. Exactly as for ∇_q , and for the same reasons (see arguments in 2.), the Γ -derivative operator $\frac{\partial}{\partial \Gamma}$ costs a scaling factor $2^{j\phi}$ or (reintroducing dimensional constants) $\frac{1}{\Gamma_\phi}$. Thus

$$\left| (\bar{\Pi}_q^{j'_+ \rightarrow}(\Gamma) - \bar{\Pi}_q^{(j'_+ - 1) \rightarrow}(\Gamma)) - (\bar{\Pi}_q^{j'_+ \rightarrow}(\Gamma') - \bar{\Pi}_q^{(j'_+ - 1) \rightarrow}(\Gamma')) \right| \lesssim 2^{-2(j_+ - j\phi)} \frac{\delta \Gamma}{\Gamma_\phi} g. \quad (3.87)$$

Summing over scales $j'_+ = j'_\phi, \dots, j_+$ yields (3.70). The other estimate (3.71) follows as in 2. from the scale j_ϕ effective cut-off scale $|\Gamma|^2$ in the denominator of (1.20).

Error terms $|\text{Pre}\Sigma(\Gamma^{j_+ \rightarrow}; \xi - \xi') - \text{Pre}\Sigma(\Gamma^{(j_+ - 1) \rightarrow}; \xi - \xi')|$, $j_+ \geq j'_\phi$ (see §2.3.3), modifying the value of the pre-Goldstone boson propagators inserted inside fermionic polymers, are similarly bounded.

Next subsections are dedicated to the proof of Theorems 2–5 giving estimates for various n -point functions. The general scheme of proof is as follows. Define *infra-red*

cut-off n -point functions

$$f^{j_+ \rightarrow}(\boldsymbol{\xi}, \bar{\boldsymbol{\xi}}) := \left\langle \prod_{i=1}^n \Psi(\xi_i) \prod_{i=1}^{\bar{N}} \bar{\Psi}(\bar{\xi}_i) \right\rangle_{\theta; \lambda, j_+ \rightarrow} \quad (3.88)$$

for $j_+ \geq j'_\phi$. When $j_+ = j'_\phi$, $f^{j_+ \rightarrow}(\cdot)$ is the sum of entirely fermionic diagrams obtained by the fermionic expansion of $\left\langle \prod_{i=1}^n \Psi(\xi_i) \prod_{i=1}^{\bar{N}} \bar{\Psi}(\bar{\xi}_i) \right\rangle_{\theta; \lambda}$, i.e. of all fermionic polymer contributions including no Goldstone boson propagator. When $j_+ > j'_\phi$, the sum is rather obtained from the fermionic polymer expansion of $\left\langle \prod_{i=1}^n \Psi(\xi_i) \prod_{i=1}^{\bar{N}} \bar{\Psi}(\bar{\xi}_i) \right\rangle_{\theta; \lambda}$ by substituting $\Sigma^{j_+ \rightarrow}$ to all Goldstone boson propagators Σ .

To go from the purely fermionic contribution $f^{j'_\phi \rightarrow}(\boldsymbol{\xi}, \bar{\boldsymbol{\xi}})$ to the n -point function $\left\langle \prod_{i=1}^n \Psi(\xi_i) \prod_{i=1}^{\bar{N}} \bar{\Psi}(\bar{\xi}_i) \right\rangle_{\theta; \lambda} = \lim_{j_+ \rightarrow +\infty} f^{j_+ \rightarrow}(\boldsymbol{\xi}, \bar{\boldsymbol{\xi}})$, one proceeds by induction, extending downwards the polymers to the bosonic scales. Namely, let $\mathbb{P}_1, \dots, \mathbb{P}_n$ be the fermionic polymers of a given contribution to the n -point function, and decide that \mathbb{P}_i and $\mathbb{P}_{i'}$ are connected at scale j_+ (which we denote by $\mathbb{P}_i \sim^{j_+} \mathbb{P}_{i'}$) if there exists a scale j_+ propagator Σ^{j_+} connecting \mathbb{P}_i to $\mathbb{P}_{i'}$. Then we define

$$\mathbb{P}_i^{j'_\phi \rightarrow} = \mathbb{P}_i, \quad i = 1, \dots, n; \quad (3.89)$$

$$\mathbb{P}_i^{j_+ \rightarrow} = \uplus \{ \mathbb{P}_{i'} \mid \exists k_+ \leq j_+, \mathbb{P}_i \sim^{k_+} \mathbb{P}_{i'} \}, \quad j_+ > j'_\phi, i = 1, \dots, n. \quad (3.90)$$

External legs of a polymer $\mathbb{P}_i^{j_+ \rightarrow}$ are then made up of $N_{ext,+} \equiv N_{ext,+}(\mathbb{P}_i^{j_+ \rightarrow})$ external Σ -propagators with scales $> j_+$. It is important to realize that no supplementary cluster expansion is needed here: going down the scales inductively, polymers $\mathbb{P}_i^{j_+ \rightarrow}$ simply coalesce, until there is only one polymer left at some scale $j_{+,max}$.

3.5 Proof of Theorem 2: Cooper pair n -point functions

In this section we prove Theorem 2. Fix $n \geq 1$ and $\xi_1, \dots, \xi_{2n} \in \mathbb{R} \times \mathbb{R}^2$. The main contribution to

$$F_{2n}(\boldsymbol{\xi}) \equiv F_{2n}(\xi_1, \dots, \xi_{2n}) := \left\langle \prod_{i=1}^{2n} : \left(\bar{\Psi} \Gamma^\perp \Psi \right) (\xi_i) : \right\rangle_{\theta; \lambda} \quad (3.91)$$

is as in Fig. 3.1.2, except that Pre Σ -kernels are replaced by Σ -kernels,

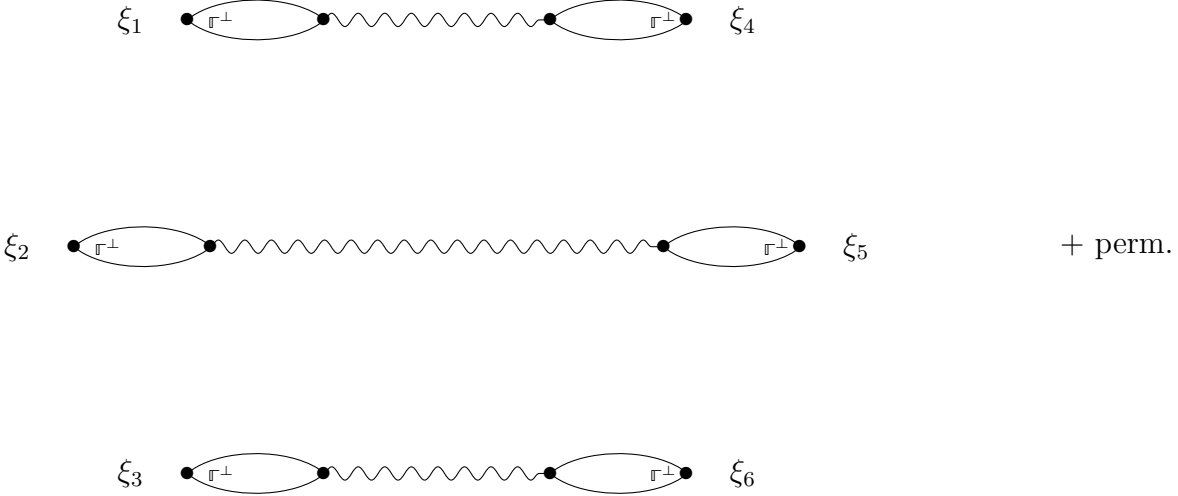


Fig. 3.5.2. 6-point function of Cooper pairs.

where "perm." indicates the sum over all possible pairings. Each bubble diagram is equal to $(1 + O(g')) \frac{1}{\lambda}$ by the gap equation. This yields the leading term in Theorem 2. Corrections are due to more complicated fermionic diagrams than bubble diagrams, possibly containing other Goldstone bosons. They all contain at least one more vertex, implying a further prefactor in $O(g)$.

3.6 Proof of Theorem 3: fermion quasi-exponential decay

Main diagrams contributing to (0.52), resp. (0.53) in Theorem 3 are



Fig. 3.6.1. Two-point functions for isolated fermions.

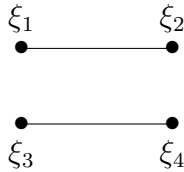


Fig. 3.6.2. Four-point functions for fermions either in non-Cooper pairing, or in parallel (//) Cooper pairing.

in the limit when $\xi_3 = \xi_1, \xi_4 = \xi_2$ and $|\xi - \xi'|$, resp. $|\xi_1 - \xi_2| \rightarrow \infty$.

This, and the quasi-exponential decay of the C^j -kernels (see Proposition 2.3) and of the $\Sigma_{//, //}$ -kernel (see (1.94) and discussion in §3.3 C.), accounts for the quasi-exponential decay of such correlation functions.

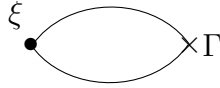
3.7 Proof of Theorem 4: phase transition

In this section we prove Theorem 4. By global rotation invariance, we may assume that $\theta = 0$. We want to prove

$$F_1(\xi) := \langle (\bar{\Psi}\sigma^1\Psi)(\xi) \rangle_{0;\lambda} = 2(1 + O(g')) \frac{\Gamma_\phi}{\lambda}. \quad (3.92)$$

On the other hand, $\langle (\bar{\Psi}\sigma^2\Psi)(\xi) \rangle_{0;\lambda} = 0$, as follows from the vanishing of the bosonic one-point function in the perpendicular direction (see (3.48)), proved using a Ward identity. Note that, for any cut-off scale j_+ , the gray blob in the figure above (3.48) cannot be connected to the external Cooper pair $\bar{\Psi}\sigma^2\Psi$ by a Goldstone boson by momentum conservation, hence the limit $j_+ \rightarrow +\infty$ can be taken; also, error terms in $O(2^{-(j_+-j'_\phi)})$ vanish in that limit. All together, this implies Theorem 4. Clearly (by translation invariance) $F_1(\xi) = F_1$ is a constant.

Main contribution to $\langle (\bar{\Psi}\sigma^1\Psi)(\xi) \rangle_{0;\lambda}$ is the bubble diagram



which is indeed equal to $\text{Tr}((\sigma^1)^2)(1 + O(g'))\Gamma_\phi\mathcal{A}_0(\Upsilon_{3,diag}) = 2(1 + O(g'))\frac{\Gamma_\phi}{\lambda}$ by the gap equation. By number conservation (see e.g. discussion before Definition 1.5), all diagrams contributing to F_1 contain at least one off-diagonal fermionic propagator, hence they all have at least one Γ_ϕ in factor. Since the one-point function of the Goldstone boson vanishes by construction, the Cooper pair $(\bar{\Psi}\sigma^1\Psi)(\xi)$ may not be directly connected to a Goldstone boson propagator. On the other hand, more complicated fermionic diagrams than the bubble diagram, potentially containing Goldstone bosons are possible. However, they all contain at least one more vertex, implying a further prefactor in $O(g)$.

3.8 Proof of Theorem 5: local transverse behavior of the Goldstone boson

We are interested in this subsection in large deviations for the random variable

$$X_\Omega := \text{Re} \int_\Omega d\xi (\bar{\Psi}\sigma(\theta)\Psi)(\xi) \quad (3.93)$$

– interpreted as the integral over Ω of the projection along the direction θ of the Goldstone boson –, where $\sigma(\theta) = \cos(\theta)\sigma^1 + \sin(\theta)\sigma^2$, and $\Omega \subset V$ is some volume comparable to a box of transition scale j_ϕ , say, Ω is a roughly cubic connected union of boxes $\Delta \in \mathbb{D}^{j_\phi}$ with dimensions $\approx \frac{L}{v_\phi} \times L \times L$, $L \approx \frac{v_\phi}{\Gamma_\phi}$. By rotation invariance, we may and shall assume that $\theta = 0$.

We let ℓ be the ratio $\frac{L}{v_\phi/\Gamma_\phi}$. The validity of the argument below extends in part to $\ell \gg 1$, so we simply assume that $\ell \gtrsim 1$. Note that $\text{Vol}(\Omega) \approx \ell^3 \frac{v_\phi^2}{\Gamma_\phi^3}$.

Standard large-deviation theory (see e.g. Cramer's theorem in [13], §2.2) implies the following large deviation bound. Let $\bar{X}_\Omega := \langle X_\Omega \rangle_{0;\lambda}$ be the average of X_Ω in the symmetry-broken measure along $\theta = 0$; as proved in §3.7, $\bar{X}_\Omega = \text{Vol}(\Omega) \langle (\bar{\Psi} \sigma^1 \Psi)(0) \rangle_{0;\lambda} \sim \text{Vol}(\Omega) \frac{\Gamma_\phi}{\lambda}$. Let

$$\Lambda(A) := \log \langle e^{AX_\Omega} \rangle_{0;\lambda} \quad (3.94)$$

be the *log-cumulant* of X_Ω , and

$$\tilde{\Lambda}(x) := \sup_{A \in \mathbb{R}} \left(Ax - \Lambda(A) \right) \quad (3.95)$$

its *Legendre transform*. Then, for $\eta > 0$,

$$\mathbb{P}[X_\Omega > \bar{X}_\Omega + \eta \frac{\Gamma_\phi}{\lambda} \text{Vol}(\Omega)] \leq e^{-\tilde{\Lambda}(\bar{X}_\Omega + \eta \frac{\Gamma_\phi}{\lambda} \text{Vol}(\Omega))}. \quad (3.96)$$

Similarly,

$$\mathbb{P}[X_\Omega < \bar{X}_\Omega - \eta \frac{\Gamma_\phi}{\lambda} \text{Vol}(\Omega)] \leq e^{-\tilde{\Lambda}(\bar{X}_\Omega - \eta \frac{\Gamma_\phi}{\lambda} \text{Vol}(\Omega))}. \quad (3.97)$$

We concentrate on the consequences of (3.96) in the sequel; similar bounds, obtained by substituting $\eta \rightarrow -\eta$, hold for $\mathbb{P}[X_\Omega < \bar{X}_\Omega - \eta \frac{\Gamma_\phi}{\lambda} \text{Vol}(\Omega)]$.

Note that $\Lambda(0) = 0$ and (by Jensen's inequality) $\Lambda(A) \geq A\bar{X}_\Omega$ for all A . As a consequence, $\min_{x \in \mathbb{R}} \tilde{\Lambda}(x) = \tilde{\Lambda}(\bar{X}_\Omega) = 0$, so that $\tilde{\Lambda}'(\bar{X}_\Omega) = 0$, and $\tilde{\Lambda}''(x) = 1/\Lambda''(A)$, where

$$A \equiv A(x) = \operatorname{argmax} \left(A \mapsto Ax - \Lambda(A) \right) = (\Lambda')^{-1}(x) \quad (3.98)$$

is the unique $A \in \mathbb{R}$ realizing the maximum of the function $A \mapsto Ax - \Lambda(A)$; in particular, $A(\bar{X}_\Omega) = 0$. Thus

$$\begin{aligned} -\log \left(\mathbb{P}[X_\Omega > \bar{X}_\Omega + \eta \frac{\Gamma_\phi}{\lambda} \text{Vol}(\Omega)] \right) &\geq \frac{1}{2} \eta^2 \left(\frac{\Gamma_\phi}{\lambda} \right)^2 \text{Vol}(\Omega)^2 \left(\max_{0 \leq A \leq A(\bar{X}_\Omega + \eta \frac{\Gamma_\phi}{\lambda} \text{Vol}(\Omega))} \Lambda''(A) \right)^{-1} \\ &= \frac{1}{2} \eta^2 \left(\frac{\Gamma_\phi}{\lambda} \right)^2 \text{Vol}(\Omega)^2 \left(\max_{0 \leq A \leq A(\bar{X}_\Omega + \eta \frac{\Gamma_\phi}{\lambda} \text{Vol}(\Omega))} \langle X_\Omega X_\Omega \rangle_{\lambda, \Omega, A}^c \right)^{-1}, \end{aligned} \quad (3.99)$$

where $\langle \cdot \rangle_{\lambda, \Omega, A}^c$ is the connected expectation w.r. to the perturbed measure $d\mu_{\lambda, \Omega, A} \propto e^{AX_\Omega} d\mu_{0;\lambda}$.

Now, define

$$A_\eta := A(\bar{X}_\Omega + \eta \frac{\Gamma_\phi}{\lambda} \text{Vol}(\Omega)); \quad (3.100)$$

By (3.98),

$$\langle X_\Omega \rangle_{\lambda, \Omega, A_\eta} = \Lambda'(A_\eta) \equiv \bar{X}_\Omega + \eta \frac{\Gamma_\phi}{\lambda} \text{Vol}(\Omega); \quad (3.101)$$

equivalently, $A_\eta = (\Lambda')^{-1}(\bar{X}_\Omega + \eta \frac{\Gamma_\phi}{\lambda} \text{Vol}(\Omega))$.

By construction, $\langle X_\Omega \rangle_{\lambda, \Omega, A_\eta}$ is equal to the sum of truncated expectation values $\sum_{n \geq 0} A_\eta^n \langle X_\Omega^{n+1} \rangle_{0; \lambda}^c$. If $n \geq 2$, the main contributions to $A_\eta^n \langle X_\Omega^{n+1} \rangle_{0; \lambda}^c$ are in the form of $(n+1)$ bubble diagrams connected through scale $\approx j_\phi$ Goldstone bosons to a fermionic polymer of scale $\approx j_\phi$, represented as the central gray blob in the Figure below.

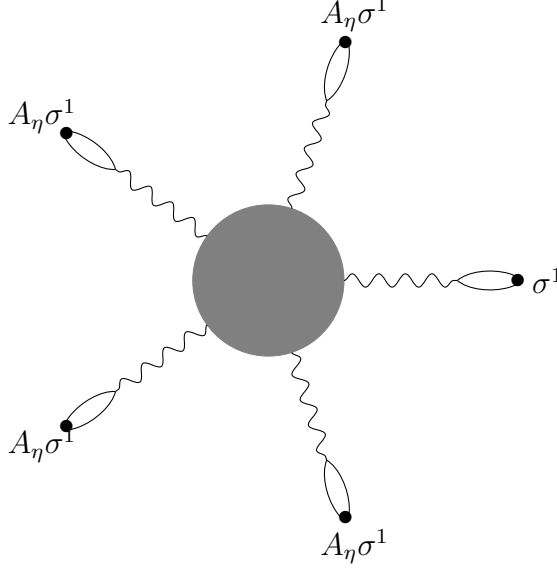


Fig. 3.8.1. Main contribution to $A_\eta^n \langle X_\Omega^{n+1} \rangle_{0; \lambda}^c$ for $n = 4$.

Similarly, the truncated expectation $\langle X_\Omega X_\Omega \rangle_{\lambda, \Omega, A_\eta}^c$ may be expanded into $\sum_{n \geq 0} A_\eta^n \langle X_\Omega^{n+2} \rangle_{0; \lambda}^c$.

Let

$$\begin{aligned} V_\Omega &:= \int \int_{\Omega \times \Omega} d\xi d\xi' \frac{1}{\lambda^2} \Sigma(\xi - \xi') \\ &\approx \frac{1}{\lambda^2} \text{Vol}(\Omega) \int_0^L \frac{g_\phi / 4\pi v_\phi^2}{r} 4\pi r^2 dr \approx \text{Vol}(\Omega) \frac{m^* \Gamma_\phi^2 L^2}{g^2 v_\phi^2} \approx \text{Vol}(\Omega) \ell^2 \frac{m^*}{g^2} \end{aligned} \quad (3.102)$$

be the Cooper pair two-point function (see (3.14) for the intuition, or Theorem 2 for a more precise statement) integrated over the volume Ω . Since $\text{Vol}(\Omega) \approx \ell^3 \frac{v_\phi^2}{\Gamma_\phi^3}$,

$$V_\Omega \approx \ell^5 \frac{m^* v_\phi^2}{g^2 \Gamma_\phi^3}.$$

A diagram as in the above Figure contributes at most A_η^n times : (i) $\frac{1}{\text{Vol}(\Omega)} V_\Omega \approx \ell^2 \frac{m^*}{g^2}$ per Goldstone boson propagator with one fixed extremity, terminated in the other direction by a bubble, all together: $O((\ell^2 \frac{m^*}{g^2})^{n+1})$; (ii) $g^{n+1} (2^{j_\phi/2})^{2(n+1)-4} (p_F^*)^{-2(n+1)} = \frac{g \Gamma_\phi}{(m^*)^3 v_\phi^4} \times \left(\frac{g}{m^* \Gamma_\phi} \right)^n$ (power-counting (2.123) for an amputated fermionic diagram with lowest scale j_ϕ and $2(n+1)$ external legs), times a non-dimensional localization factor breaking translation invariance, $\approx (\ell^{2j_\phi})^3 \approx \ell^3 \frac{\mu^3}{\Gamma_\phi^3} \approx \ell^3 \frac{(m^*)^3 v_\phi^6}{\Gamma_\phi^3}$, all together

: $O(\ell^3 \frac{g v_\phi^2}{\Gamma_\phi^2} (\frac{g}{m^* \Gamma_\phi})^n)$. Hence, assuming $\frac{A_\eta}{g \Gamma_\phi} \ll 1$ (which will be checked later on by self-consistency as soon as $\eta \ll 1$)

$$\sum_{n \geq 2} \frac{A_\eta^n}{n!} \langle X_\Omega^{n+1} \rangle_{0;\lambda}^c \lesssim \ell^5 \frac{m^* v_\phi^2}{g \Gamma_\phi^2} \exp_2(\ell^2 A_\eta / g \Gamma_\phi) \lesssim \ell^9 \frac{m^* v_\phi^2}{g^3 \Gamma_\phi^2} \left(\frac{A_\eta}{\Gamma_\phi}\right)^2 \quad (3.103)$$

where $\exp_2(t) := e^t - 1 - t \approx t^2 e^t$ if $|t| \ll 1$.

On the other hand, the terms of order $n = 0, 1$ are resp. $\langle X_\Omega \rangle_{0;\lambda} = \bar{X}_\Omega$ and $A_\eta \langle X_\Omega X_\Omega \rangle_{0;\lambda}^c \approx A_\eta V_\Omega \approx A_\eta \text{Vol}(\Omega) \ell^2 \frac{m^*}{g^2}$. Concluding:

$$\langle X_\Omega \rangle_{\lambda, \Omega, A_\eta} - \bar{X}_\Omega \approx A_\eta V_\Omega + O\left(\ell^9 \frac{m^* v_\phi^2}{g^3 \Gamma_\phi^2} \left(\frac{A_\eta}{\Gamma_\phi}\right)^2\right). \quad (3.104)$$

Comparing with (3.101), we get, neglecting the error term in (3.104):

$$A_\eta \approx \ell^{-2} g \Gamma_\phi \eta. \quad (3.105)$$

Taking this as the value for A_η , we check that the error term in (3.104) is $\lesssim \ell^5 m^* \left(\frac{v_\phi}{\Gamma_\phi}\right)^2 \frac{1}{g} \eta^2$, which is $\ll \left| \langle X_\Omega \rangle_{\lambda, \Omega, A_\eta} - \bar{X}_\Omega \right| = \eta \frac{\Gamma_\phi}{\lambda} \text{Vol}(\Omega) \approx \eta \frac{\Gamma_\phi}{\lambda} \ell^3 \frac{v_\phi^2}{\Gamma_\phi^3} \approx \ell^3 m^* \left(\frac{v_\phi}{\Gamma_\phi}\right)^2 \frac{1}{g} \eta$ provided $\ell^2 \eta \ll 1$.

Now the covariance $\max_{0 \leq A \leq A(\bar{X}_\Omega + \eta \frac{\Gamma_\phi}{\lambda} \text{Vol}(\Omega))} \langle X_\Omega X_\Omega \rangle_{\lambda, \Omega, A}^c$ in (3.99) is similarly computed as

$$\langle X_\Omega X_\Omega \rangle_\lambda^c + O\left(\ell^5 \frac{m^* v_\phi^2}{g \Gamma_\phi^2} \times \frac{\ell^2}{g \Gamma_\phi}\right) \exp_1(\ell^2 A_\eta / g \Gamma_\phi) \approx V_\Omega + O\left(\ell^7 \frac{m^* v_\phi^2}{g^2 \Gamma_\phi^3}\right) \exp_1(\ell^2 A_\eta / g \Gamma_\phi) \quad (3.106)$$

where $\exp_1(t) := e^t - 1 \approx t e^t$. The error term, computed using (3.105), is now $\lesssim \ell^7 \frac{m^* v_\phi^2}{g^2 \Gamma_\phi^3} \eta \ll V_\Omega \approx \ell^5 \frac{m^* v_\phi^2}{\Gamma_\phi^3} \frac{1}{g^2}$, provided $\ell^2 \eta \ll 1$ once again.

Concluding: assume $\ell^2 \eta \ll 1$, then

$$\begin{aligned} -\log\left(\mathbb{P}[X_\Omega > \bar{X}_\Omega + \eta \frac{\Gamma_\phi}{\lambda} \text{Vol}(\Omega)]\right) &\gtrsim \eta^2 \left(\frac{\Gamma_\phi}{\lambda}\right)^2 \left(\frac{\ell^3 v_\phi^2}{\Gamma_\phi^3}\right)^2 \frac{\Gamma_\phi^3 g^2}{\ell^5 m^* v_\phi^2} \\ &\approx \ell m v_\phi^2 \frac{1}{\Gamma_\phi} \eta^2 \approx \ell \frac{\mu}{\Gamma_\phi} \eta^2 \approx \ell 2^{j_\phi} \eta^2. \end{aligned} \quad (3.107)$$

For $\ell \approx 1$ one has proved Theorem 5. For ℓ larger one observes that the large deviation rate (3.107) increases like $\ell \propto \text{Vol}(\Omega)^{1/3}$, and not $\text{Vol}(\Omega)$ as expected from the discussion in the Introduction based on the effective potential approach. Note however that this volume cubic root prefactor is not reliable, since it is valid only for small deviations $\eta \ll \ell^{-2}$. Another method would be needed to study large transverse deviations of the Goldstone boson over a large volume.

4 Generalizations and perspectives

This work is meant to be the first of a series of articles investigating the superconducting phase transition and quantum fluctuations of superconducting materials in various situations. The spectacular experimental and theoretical advances of the last 30 years or so, see e.g. [27, 64], is a strong incentive to draw detailed predictions from our microscopic approach in a variety of situations.

A first generalization. As mentioned in the Introduction, our approach extends in a straightforward way to more general two-body potentials U as in (0.12). Substituting the kernel $\frac{\omega^2((\mathbf{p}_1-\mathbf{p}_3)/\hbar)}{(p_1^0-p_3^0)^2+\omega^2((\mathbf{p}_1-\mathbf{p}_3)/\hbar)}$ to the delta-interaction only changes numerical constants, since the phonon interaction is a *short-range* one. The same conclusion holds if one adds a small two-body potential \hat{v} with high enough infra-red cut-off.

Three-dimensional theory. The phase space analysis of the 3D model is more complicated because the sector counting of Proposition 2.5 is not available, due to the fact that fixing two sectors does *not* fix the remaining two sectors of a vertex any more. Thus a precise sector-counting argument is needed already in Regime I. However, it can be proved perturbatively that there is just *at most one sum over sectors per vertex* in any dimension, as proved here in §2.3.2 by following a loop; we plan to extend this argument non-perturbatively (see [56] for a first step in that direction). After resumming explicitly the leading contribution in the form of chains of Cooper pair bubbles as in dimension 2, remaining terms should be small by virtue of a $1/N$ argument. Consequently, we expect the present proof to extend more or less straightforwardly to the 3d case.

BCS theory at positive temperature. The finite-temperature formalism using Matsubara frequencies, as presented e.g. in Chapter 7 of the book by Fetter and Walecka, makes it possible to compute Green's function of the system in thermal equilibrium in terms of a modified functional integral with discretized energies p^0 now ranging in the set $\{\hbar\omega_n, n \in \mathbb{Z}\}$, $\omega_n := \frac{(2n+1)\pi}{\hbar\beta}$, where β is the inverse temperature. At first sight, the same scheme should produce similar conclusions when the lowest Matsubara frequencies are smaller than the energy gap Γ_ϕ , i.e. when $k_B T \ll \Gamma_\phi$. In the inverse regime ($k_B T \gg \Gamma_\phi$), Cooper pairing should be shown to be statistically unfavorable. Interesting things should occur in 3D around a critical temperature $T_c \approx \frac{\Gamma_\phi}{k_B}$, where one should be able to investigate more precisely the quantum second-order phase transition, in connection to ideas due to M. Salmhofer [61, 62].

Real time. The Hamiltonian dynamics may be discussed in a $(1+d)$ -dimensional quantum-field theoretic framework with real-time variable t using advanced and retarded propagators at temperature zero, or more generally the Keldysh formalism [59, 50] at $T > 0$. The major difficulty is now that the infra-red singularity is carried by a *paraboloid* in energy-momentum variables, $p_0 - \frac{1}{2m}|\mathbf{p}|^2 = \mu$, a two-dimensional manifold instead of a circle.

5 Appendix

We collect in this section some technical formulas and bounds required for the proof. An essential bound is Proposition 5.3 below, ensuring the convergence of the series of perturbations.

5.1 Grassmann integrals

We briefly recall here usual conventions regarding Grassmann integrals, see e.g. [57], §9.5. By definition, if ψ_1, \dots, ψ_n are Grassmann anticommuting variables, and $F = F(\psi_1, \dots, \psi_n)$ is a polynomial function, then $\int d\psi_n \cdots d\psi_1 F$ is the coefficient of $\psi_1 \cdots \psi_n$ in F . In particular, if $\psi, \bar{\psi}$ is a couple of conjugate Grassmann variables, i.e. $\psi = \frac{\psi_1 + i\psi_2}{\sqrt{2}}, \bar{\psi} = \frac{\psi_1 - i\psi_2}{\sqrt{2}}$, then

$$\int d\bar{\psi} d\psi \psi \bar{\psi} = 1, \quad (5.1)$$

and

$$\int d\bar{\psi} d\psi e^{-\bar{\psi}b\psi} = b, \quad \int d\bar{\psi} d\psi \psi \bar{\psi} e^{-\bar{\psi}b\psi} = 1 = \frac{1}{b} \cdot b. \quad (5.2)$$

In case there are several couples $(\psi_i, \bar{\psi}_i)_{i=1,2,\dots}$, the above rules generalized easily using some linear algebra,

$$\left(\prod_i \int d\bar{\psi}_i d\psi_i \right) e^{-\sum_{i,j} \bar{\psi}_i B_{ij} \psi_j} = \det(B), \quad \left(\prod_i \int d\bar{\psi}_i d\psi_i \right) \psi_k \bar{\psi}_\ell e^{-\sum_{i,j} \bar{\psi}_i B_{ij} \psi_j} = \det(B) (B^{-1})_{k,\ell}. \quad (5.3)$$

The measure $\frac{1}{\det(B)} \left(\prod_i \int d\bar{\psi}_i d\psi_i \right) e^{-\sum_{i,j} \bar{\psi}_i B_{ij} \psi_j}$ is called the (normalized) *Grassmann Gaussian measure with covariance kernel* B^{-1} , where $B = B(\psi, \bar{\psi}) := \sum_{i,j} \bar{\psi}_i B_{ij} \psi_j$.

5.2 Integration by parts formulas

Proposition 5.1 *1. Let ϕ be a (fermionic or bosonic) Gaussian field with translation-invariant covariance kernel C_ϕ and functional measure $d\mu(\phi)$. Then, letting $\mathcal{F} \equiv \mathcal{F}[\phi]$ be a functional of ϕ ,*

$$\int d\mu(\phi) \phi(\xi) \mathcal{F}[\phi] = \int d\xi' C_\phi(\xi - \xi') \cdot \int d\mu(\phi) \frac{\delta \mathcal{F}[\phi]}{\delta \phi(\xi')}. \quad (5.4)$$

2. Consider a smooth variation of the covariance kernel, $\varepsilon \mapsto C_\phi(\varepsilon)$ and the associated functional measures $d\mu_\varepsilon(\phi)$, with $C_\phi(0) \equiv C_\phi$. Then

$$\frac{d}{d\varepsilon} \left(\int d\mu_\varepsilon(\phi) \mathcal{F}[\phi] \right) \Big|_{\varepsilon=0} = \int d\xi \int d\xi' \int d\mu(\phi) \left[\frac{\partial C_\phi}{\partial \varepsilon}(\varepsilon=0; \xi - \xi') \frac{\delta^2}{\delta \phi(\xi) \delta \phi(\xi')} \right] \mathcal{F}[\phi]. \quad (5.5)$$

The proof of these elementary identities in a quantum field theoretic context can be found e.g. in [70]. They imply in particular the following elegant formula for *horizontal cluster expansions*, called Brydges-Kennedy-Abdesselam-Rivasseau (BKAR) formula. For that we first need some definitions. Introduce a partition of $\mathbb{R} \times \mathbb{R}^2$ into a disjoint union of "objects" o^j , which are clusters, i.e. connected unions of scale j boxes; let \mathcal{O}^j denote the set of objects. (The simplest example is when objects are elementary scale j boxes, and $\mathcal{O}^j = \mathbb{D}^j$). A *weakening function* $s^j : \mathcal{O}^j \times \mathcal{O}^j \rightarrow [0, 1]$ is a function assigning a weight to each link $\ell = (o_\ell, o'_\ell)$ between two different objects; by hypothesis, $s^j_{o, o'} = s^j_{o', o}$ ($o \neq o'$) and $s^j_{o, o} = 1$. Alternatively, s^j may be considered as a weakening function $s^j : \mathbb{D}^j \times \mathbb{D}^j \rightarrow [0, 1]$ which is a constant on a box: letting o_Δ being the cluster containing Δ , $s^j_{\Delta, \Delta'} := s^j_{o_\Delta, o_{\Delta'}}$. Then $C_\theta^j(s^j) : (\mathbb{R} \times \mathbb{R}^2) \times (\mathbb{R} \times \mathbb{R}^2) \rightarrow \mathbb{C}$ is the Hermitian kernel defined by

$$C_\theta^j(s^j; \xi, \xi') := \sum_{\Delta, \Delta' \in \mathbb{D}^j} \chi_\Delta(\xi) \chi_{\Delta'}(\xi') s^j_{\Delta, \Delta'} C_\theta^j(\xi, \xi'). \quad (5.6)$$

A weakening function s^j may be chosen independently for each scale $j = j_D, \dots, j'_\phi - 1$. The associated Grassmann Gaussian measure is denoted by $d\mu_\theta^*(\mathbf{s})$, where $\mathbf{s} := (s^{j_D}, \dots, s^{j'_\phi - 1})$. We now present the outcome of a single application of the BKAR formula at scale j , so that $s^{j'} \equiv 1$ if $j' \neq j$. The result is in terms of a sum over scale j forests, whose set is denoted by \mathcal{F}^j . Forests are disjoint unions of trees. We write $o \sim_{\mathbb{F}^j} o'$ ($\mathbb{F}^j \in \mathcal{F}^j, o, o' \in \mathcal{O}^j$) if o and o' are in the same connected component of \mathbb{F}^j .

Proposition 5.2 (BKAR formula) (see [54], Proposition 2.6) *Let $F^j \equiv F^j(\Psi^j, \bar{\Psi}^j)$ be a functional of the scale j fermion fields. Then*

$$\langle F^j \rangle_{\theta; \lambda} = \sum_{\mathbb{F}^j \in \mathcal{F}^j} \left[\prod_{\ell \in L(\mathbb{F}^j)} \int_0^1 dw_\ell \int_{o_\ell} d\xi_\ell \int_{o'_\ell} d\xi'_\ell \right] \frac{1}{\mathcal{Z}_\lambda^*} \int d\mu_\theta^*(s^j(\mathbf{w})) (\Psi, \bar{\Psi}) \text{Hor}^j \left(F^j(\Psi^j, \bar{\Psi}^j) e^{-\mathcal{L}_\theta(\Psi, \bar{\Psi})} \right), \quad (5.7)$$

where

$$\text{Hor}^j := \prod_{\ell \in L(\mathbb{F}^j)} D_\ell^j, \quad (5.8)$$

$$D_\ell^j := \sum_{\alpha_\ell \in \mathbb{Z}/2^j\mathbb{Z}} C_\theta^{j, \alpha_\ell}(s^j(\mathbf{w}); \xi_\ell, \xi'_\ell) \frac{\delta}{\delta \Psi^{j, \alpha_\ell}(\xi_\ell)} \frac{\delta}{\delta \bar{\Psi}^{j, \alpha_\ell}(\xi'_\ell)}, \quad (5.9)$$

and $s(\mathbf{w}) = (s_{o, o'}(\mathbf{w}))_{o, o' \in \mathcal{O}^j}$, $s_{o, o'}(\mathbf{w})$, $o \neq o'$ being the infimum of the w_ℓ for ℓ running over the unique path from o to o' in \mathbb{F}^j if $o \sim_{\mathbb{F}^j} o'$, and 0 else.

5.3 Local bounds for determinants

We prove here the statement (2.88) made in §2.3.2 concerning bounds for diagrams with a large number of vertices per box. Before we do so however, let us discuss this problem briefly in general terms, and cite a result (Proposition 5.3 below) proved in a different context in [45]. The proposition is not directly applicable in our context, so we shall give an independent proof of (2.88), which however relies on the same arguments.

The expansion produces multilinear expressions of the type

$$G(\boldsymbol{\xi}, \bar{\boldsymbol{\xi}}) := \int d\mu_{\theta}^*(\Psi^j, \bar{\Psi}^j) \left(\prod_{i=1}^n \Psi_{\sigma_i}^{j, \alpha_i}(\xi_i) \right) \left(\prod_{\bar{i}=1}^n \bar{\Psi}_{\bar{\sigma}_{\bar{i}}}^{j, \bar{\alpha}_{\bar{i}}}(\bar{\xi}_{\bar{i}}) \right), \quad (5.10)$$

$\sigma_i, \bar{\sigma}_{\bar{i}} = \uparrow, \downarrow$. Applying Wick's formula and taking signs into account, one gets

$$G(\boldsymbol{\xi}, \bar{\boldsymbol{\xi}}) = \det(A) \quad (5.11)$$

where

$$A = (a_{i, \bar{i}})_{1 \leq i, \bar{i} \leq n}, \quad a_{i, \bar{i}} = \delta_{\alpha_i, \bar{\alpha}_{\bar{i}}} C_{\sigma_i, \bar{\sigma}_{\bar{i}}}^{j, \alpha_i}(\xi_i, \bar{\xi}_{\bar{i}}). \quad (5.12)$$

Expanding naively the determinant, one gets a sum over $n!$ terms indexed by permutations $\pi \in \mathcal{P}_n$ of the set of \bar{i} -indices, making the sum over n naively divergent. Looking at this factorial into details, however, one sees that this apparent divergence comes from accumulations of large numbers of fields $\Psi^j(\xi_i), \bar{\Psi}^j(\bar{\xi}_i)$ inside boxes. Namely, assuming e.g. that the ξ_i 's and $\bar{\xi}_i$'s are all located in different boxes, Proposition 2.3 implies

$$\sum_{\pi \in \mathcal{P}_n} \prod_{i=1}^n |C_{\sigma_i, \bar{\sigma}_{\pi(i)}}^{j, \alpha_i}(\xi_i, \bar{\xi}_{\pi(i)})| \leq (2^{-j} p_F^*)^{2n} \left\{ \sup_{\Delta \in \mathbb{D}^j} \sum_{\Delta' \in \mathbb{D}^j} C_N \left(1 + d^j(\Delta, \Delta') \right)^{-N} \right\}^n = O(C^n (2^{-j} p_F^*)^{2n}) \quad (5.13)$$

for some constant C , since the sum between $\left\{ \right\}$ converges for $N > 3$. There remains to discard the possibility of *local factorials* in the numerator, i.e. combinatorial factors of the form $\prod_{\Delta} (n_{\Delta}!)$ to a certain power, where n_{Δ} is the number of fields contained in a box $\Delta \in \mathbb{D}^j$. This does happen in the case of bosonic theories, which requires more elaborated, truncated expansions of the exponentiated action, in order to produce converging series. However, here, due to the *fermionic* character of the theory, Pauli's principle *strongly suppresses* local accumulations of fields. As a matter of fact, one has the following

Proposition 5.3 (Local bounds for determinants) [45] *Consider an $n \times n$ complex-valued matrix $A = (a_{i, \bar{i}})_{1 \leq i, \bar{i} \leq n}$, $a_{i, \bar{i}} = \delta_{\alpha_i, \bar{\alpha}_{\bar{i}}} \tilde{C}_{\sigma_i, \bar{\sigma}_{\bar{i}}}^{j, \alpha_i}(\xi_i, \bar{\xi}_{\bar{i}})$ of the same form as (5.12). Assume that the kernel $\tilde{C}_{\sigma, \bar{\sigma}}^{j, \alpha}$ is smooth, and that it has a scale L quasi-exponential decay, i.e. that, for every integer $N \geq 0$ and multi-index $\boldsymbol{\kappa}$,*

$$|\nabla_{\boldsymbol{\xi}}^{\boldsymbol{\kappa}} \tilde{C}_{\sigma, \bar{\sigma}}^{j, \alpha}(\boldsymbol{\xi}, \bar{\boldsymbol{\xi}})| \leq C_{N, |\boldsymbol{\kappa}|} J^2 (L/v_F^*)^{-\kappa_0} L^{-(\kappa_1 + \kappa_2)} \left(1 + \frac{|\boldsymbol{\xi} - \bar{\boldsymbol{\xi}}|}{L/v_F^*} \right)^{-N} \quad (5.14)$$

for some $J > 0$ (compare with Proposition 2.3). Pave $\mathbb{R} \times \mathbb{R}^2$ by cubes Δ of side L and define n_Δ , resp. \bar{n}_Δ to be the number of ξ_i 's, resp. $\bar{\xi}_i$'s inside Δ . Then, for every couple of integers $N, r \geq 0$, there exists a constant $C_{N,r}$, such that

$$|\det(A)| \lesssim (C_{N,r})^n J^{2n} \prod_{\Delta} \prod_{\alpha \in \mathbb{Z}/2^j\mathbb{Z}} \frac{1}{(n_{\Delta,\alpha}!)^r (\bar{n}_{\Delta,\alpha}!)^r} \sup_{\pi \in \mathcal{P}_n} \prod_{i=1}^n \left(1 + \frac{|\xi_i - \bar{\xi}_{\pi(\bar{i})}|}{L/v_F^*}\right)^{-N}. \quad (5.15)$$

Proposition 5.3 applies in our context to the evaluation of determinants, with $J = 2^{-j} p_F^*$, $L = 2^j (p_F^*)^{-1}$ and $\tilde{C}_{\sigma,\bar{\sigma}}^{j,\alpha}(\xi, \bar{\xi}) = \int d\mu_\theta^*(\Psi^j, \bar{\Psi}^j) e^{-i(p^\alpha, \xi)} \Psi_\sigma^{j,\alpha}(\xi) \cdot \bar{\Psi}_{\bar{\sigma}}^{j,\alpha}(\bar{\xi}) e^{i(p^\alpha, \bar{\xi})}$ is the covariance kernel of the fields $\Psi^{j,\alpha}$, $\bar{\Psi}^{j,\alpha}$ accompanied by their sector oscillation, so that $|\nabla_\xi \tilde{C}_{\sigma,\bar{\sigma}}^{j,\alpha}(\xi, \bar{\xi})| = |(\nabla_\xi - ip^\alpha) C_{\sigma,\bar{\sigma}}^{j,\alpha}(\xi, \bar{\xi})|$. The above Proposition has been proven only for fields with a single component (in our context, lying in a single angular sector), however the extension to fields with arbitrary angular sectors is straightforward (as can be checked from the arguments below).

As mentioned before, we cannot use this result directly in the context of §2.3.2, because we want to bound sums of diagrams with a given loop structure, sector assignment and choice of scale j boxes for vertex locations. So let us rewrite briefly the main arguments of the proof of Proposition 5.3 and prove that they do apply to such sums of diagrams. Fix some integer $k \geq 0$ (later on to be identified with some multiple of r in (5.15)). The idea is, for each sector $\alpha \in \mathbb{Z}/2^j\mathbb{Z}$, to split each scale j box Δ into $\approx n_{\Delta,\alpha}/3^k$ equal sub-boxes δ of side length scaling like $(n_{\Delta,\alpha}/3^k)^{-1/3} \times 2^j$, centered in ξ_δ , containing each $n_{\delta,\alpha}$ fields, with $\sum_{\delta \subset \Delta} n_{\delta,\alpha} = n_{\Delta,\alpha}$. Then each α -sector propagator line $C_\theta^{j,\alpha}(\xi, \cdot)$ connecting a $\Psi^{j,\alpha}$ -field located in $\xi \in \delta \subset \Delta$ is rewritten using Taylor expansion as

$$\begin{aligned} C_\theta^{j,\alpha}(\xi, \cdot) &= e^{i(p^{j,\alpha}, \xi)} \left(\left\{ \sum_{|\kappa| < k} \frac{(\xi - \xi_\delta)^\kappa}{\kappa!} \nabla^\kappa \right\} (e^{-i(p^{j,\alpha}, \xi_\delta)} C_\theta^{j,\alpha}(\xi_\delta, \cdot)) \right. \\ &\quad \left. + \left\{ \sum_{|\kappa|=k} (\xi - \xi_\delta)^\kappa \int_0^1 dt \frac{(1-t)^{k-1}}{(k-1)!} \nabla^\kappa \right\} (e^{-i(p^{j,\alpha}, (1-t)\xi_\delta + t\xi)} C_\theta^{j,\alpha}((1-t)\xi_\delta + t\xi, \cdot)) \right) \end{aligned} \quad (5.16)$$

This leads to a rewriting of an individual Feynman diagram as a sum of Feynman diagrams with displaced vertices and differentiated $\Psi^{j,\alpha}$ -fields. Because of Pauli's constraint, $\left(\nabla^\kappa (e^{-i(p^{j,\alpha}, \xi_\delta)} \Psi_\sigma^{j,\alpha}(\xi_\delta)) \right)^2 = 0$. This means that Feynman diagrams with $n_{\delta,\alpha} \gg 3^k$ (3^k being roughly the number of terms on the first line of (5.16)) involve a large number of k -order derivative fields $\Psi^{j,\alpha}$ inside δ , enjoying by (2.11) a supplementary prefactor $O((2^{-j})^k)$, multiplied by $(\xi - \xi_\delta)^\kappa = O((2^j (n_{\Delta,\alpha}/3^k)^{-1/3})^k)$, all together a small factor $O((n_{\Delta,\alpha}/3^k)^{-k/3})$. Multiplying all these factors yields an overall factor

$$\lesssim C^n \prod_{\Delta} \prod_{\alpha} \prod_{\delta \subset \Delta} (n_{\Delta,\alpha}^{-1/3})^{\frac{k}{3}(n_{\delta,\alpha} - O(3^k))} \quad (5.17)$$

where $n = \sum_{\Delta} \sum_{\alpha} n_{\Delta, \alpha}$ is the total number of Ψ -fields, and $C \lesssim 3^{k^2/3}$. Summing all exponents corresponding to sub-boxes δ included in a given box Δ yields $n_{\Delta, \alpha}^{-ckn_{\Delta, \alpha}}$ for some constant $c > 0$, or equivalently, inverse factorials $(n_{\Delta, \alpha}!)^{-1}$ to a power $r \approx k$.

5.4 Cooper pair bubble and Σ -kernel estimates

Proof of (1.59). We need to show that, assuming $|q|_+ \gtrsim 2^{-j}\mu$,

$$|\mathcal{A}_q^{j \rightarrow}(\Upsilon_{3, \text{diag}}) - \mathcal{A}_0^{k \rightarrow}(\Upsilon_{3, \text{diag}})| \lesssim m^*, \quad k := \lfloor \log(\mu/|q|_+) \rfloor \quad (5.18)$$

Assume $q = (0, \mathbf{q})$ (the easy generalization to $q^0 \neq 0$ is left to the reader). Copying the derivation of (1.56), we have $\mathcal{A}_q^{j \rightarrow}(\Upsilon_{3, \text{diag}}) = \frac{1}{(2\pi)^2} \int d\mathbf{p} \chi^{j \rightarrow}(\mathbf{p}) f_{\mathbf{q}}(\mathbf{p}) + O(m^*)$, with

$$f_{\mathbf{q}}(\mathbf{p}) := \frac{1}{e_{|\Gamma|}^*(\mathbf{p} + \mathbf{q}) + e_{|\Gamma|}^*(\mathbf{p})} \left(\text{sgn}(e_{|\Gamma|}^*(\mathbf{p} + \mathbf{q})) + \text{sgn}(e_{|\Gamma|}^*(\mathbf{p})) \right). \quad (5.19)$$

If both signs are equal, then $f_{\mathbf{q}}(\mathbf{p}) = \left| \frac{1}{e_{|\Gamma|}^*(\mathbf{p} + \mathbf{q}) + e_{|\Gamma|}^*(\mathbf{p})} \right|$. Split $\int d\mathbf{p}(\dots)$ into $\int_{|p_{\perp}| \gg |q|}(\dots) + \int_{|p_{\perp}| \lesssim |q|}$. In the first regime, both signs are always equal, and $f_{\mathbf{q}}(\mathbf{p}) \simeq f_0(\mathbf{p})$; more precisely, letting θ be the angle (\mathbf{p}, \mathbf{q}) , and $q_{//} = \mathbf{q} \cdot \frac{\mathbf{p}}{|\mathbf{p}|}$,

$$\begin{aligned} & \left| \int_{|p_{\perp}| \gg |q|} d\mathbf{p} \chi^{j \rightarrow}(\mathbf{p}) \left(f_{\mathbf{q}}(\mathbf{p}) - f_0(\mathbf{p}) \right) \right| \lesssim \int_{|p_{\perp}| \gg |q|} d\mathbf{p} \frac{|e_{|\Gamma|}^*(\mathbf{p} + \mathbf{q}) - e_{|\Gamma|}^*(\mathbf{p})|}{\left(\frac{p_F^*}{m^*} p_{\perp}\right)^2} \\ & \approx m^* \int_{|p_{\perp}| \gg |q|} dp_{\perp} \int d\theta \frac{|q_{//}|}{p_{\perp}^2} \lesssim m^* |q| \int_{|p_{\perp}| \gg |q|} \frac{dp_{\perp}}{p_{\perp}^2} = O(m^*). \end{aligned} \quad (5.20)$$

In the opposite regime ($p_{\perp} \lesssim |q|$), $\text{sgn}(e_{|\Gamma|}^*(\mathbf{p} + \mathbf{q})) = \text{sgn}(e_{|\Gamma|}^*(\mathbf{p}))$ implies either (i) $|\cos(\theta)| \lesssim \frac{|p_{\perp}|}{|q|}$, which amounts to $\mathbf{p} \in \Omega_{\mathbf{q}}$, $\Omega_{\mathbf{q}} := \{\mathbf{p} \mid |\frac{\pi}{2} \pm \theta| \lesssim \frac{|p_{\perp}|}{|q|}\}$; (ii) or $\cos \theta \gtrsim \frac{|p_{\perp}|}{|q|}$, $e_{|\Gamma|}^*(\mathbf{p} + \mathbf{q}) \gtrsim \frac{1}{m^*} \left(2p_F^* |q| \cos(\theta) + |q|^2 \right) \gtrsim e_{|\Gamma|}^*(\mathbf{p})$ (briefly said, this is a sub-regime where \mathbf{q} dominates w.r. to \mathbf{p}).

The small integration volume in θ in regime (i) makes the integral restricted to $\Omega_{\mathbf{q}}$ convergent,

$$\begin{aligned} & \int_{(|p_{\perp}| \lesssim |q|) \cap \Omega_{\mathbf{q}}} d\mathbf{p} \chi^{j \rightarrow}(\mathbf{p}) |f_{\mathbf{q}}(\mathbf{p})| \lesssim p_F^* \int_{|p_{\perp}| \lesssim |q|} \frac{dp_{\perp}}{|e_{|\Gamma|}^*(\mathbf{p} + \mathbf{q})| + |e_{|\Gamma|}^*(\mathbf{p})|} O\left(\frac{|p_{\perp}|}{|q|}\right) \\ & \lesssim \frac{m^*}{|q|} \int_{|p_{\perp}| \lesssim |q|} dp_{\perp} = O(m^*), \end{aligned} \quad (5.21)$$

In sub-regime (ii), letting $\bar{\theta} := \frac{\pi}{2} - \theta$,

$$\begin{aligned} & \int_{(|p_{\perp}| \lesssim |q|) \cap \Omega_{\mathbf{q}}^c} d\mathbf{p} \chi^{j \rightarrow}(\mathbf{p}) |f_{\mathbf{q}}(\mathbf{p})| \lesssim \frac{m^* p_F^*}{|q|} \int dp_{\perp} \int_{\frac{|p_{\perp}|}{|q|}}^{\frac{\pi}{2}} \frac{d\bar{\theta}}{p_F^* \bar{\theta} + |q|} \\ & = \frac{m^* p_F^*}{|q|} \int_0^{\frac{\pi}{2}} \frac{d\bar{\theta}}{p_F^* \bar{\theta} + |q|} |q| \bar{\theta} = O(m^*) \end{aligned} \quad (5.22)$$

too. □

Proof of Lemma 1.3.

We must evaluate the second derivatives at zero momentum of the Cooper pair bubble diagram of §1.4, $\partial_{q^0}^2 \mathcal{A}_q^{j \rightarrow}(\Upsilon_3) \Big|_{q=0}$ and $\nabla^2 \mathcal{A}_q^{j \rightarrow}(\Upsilon_3) \Big|_{q=0}$.

This is a tedious task in Fourier coordinates. It is easier to use an argument in direct space, where the positivity argument (1.67) can be used. First

$$-\frac{d^2}{d(q^0)^2} \Big|_{q=0} \int d\xi |C^{j \rightarrow}(\xi)|^2 e^{-iq^0 \tau} = - \int d\xi \tau^2 |C^{j \rightarrow}(\xi)|^2, \quad (5.23)$$

$$-\sum_{i=1}^2 \frac{d^2}{d(q^i)^2} \Big|_{q=0} \int d\xi |C^{j \rightarrow}(\xi)|^2 e^{-i\mathbf{q} \cdot \mathbf{x}} = - \int d\xi |\mathbf{x}|^2 |C^{j \rightarrow}(\xi)|^2. \quad (5.24)$$

We now need an estimate of $C^{j \rightarrow}(\xi) = \sum_{k=j_D}^j C^k(\xi)$. The covariance function C^k is decomposed in [25] into $2^{k/2}$ anisotropic angular sectors of size $\sim 2^{-k/2} p_F^*$ along the Fermi circle. This makes it easy to understand where the major contribution to $C^{j \rightarrow}(\xi)$ comes. Decompose χ^k into $\sum_{\tilde{\alpha} \in \mathbb{Z}/2^j/2\mathbb{Z}} \tilde{\chi}^{k, \tilde{\alpha}}$, where the $(\tilde{\chi}^{k, \tilde{\alpha}})_{\tilde{\alpha} \in \mathbb{Z}/2^j/2\mathbb{Z}}$ are anisotropic as indicated, but otherwise similar to the $(\chi^{k, \alpha})_{\alpha \in \mathbb{Z}/2^j\mathbb{Z}}$ of section 2. Take $\xi = (\tau, \mathbf{x}) \equiv (\tau, x \mathbf{e}_1)$, where $(\mathbf{e}_1, \mathbf{e}_2)$ is an orthonormal basis, with \mathbf{e}_1 following the direction of some sector $\tilde{\alpha}$, and $x > 0$. Let $\tilde{\beta}$ be the index of some angular sector, and $\mathbf{p}^{k, \tilde{\beta}}$ the projection onto the Fermi sphere of some momentum contained in the given angular sector. Then (as proven in [25]), for every $\kappa \geq 0$, there exists $C_\kappa > 0$ s.t.

$$|C^{k, \tilde{\beta}}(\xi)| \leq C_\kappa (p_F^*)^2 2^{-3k/2} (1 + 2^{-k} \mu |\tau|)^{-\kappa} (1 + 2^{-k} p_F |x_{//}|)^{-\kappa} (1 + 2^{-k/2} p_F |x_\perp|)^{-\kappa}, \quad (5.25)$$

(compare with Proposition 2.3) where $x_{//}$ is the projection of \mathbf{x} along $\mathbf{p}^{k, \tilde{\beta}}$, and x_\perp its projection along the orthogonal direction. So $|C^{k, \tilde{\beta}}(\xi)|$ decreases quasi-exponentially outside a box of dimensions $\approx 2^k \mu^{-1} \times 2^k p_F^{-1} \times 2^{k/2} p_F^{-1}$ and volume $\approx \frac{1}{m^* \mu^2} 2^{5k/2}$. For $|\xi| \approx 2^j$, this means that the main contribution comes from sectors $(k, \tilde{\beta})$ with $k \simeq j$ and $\tilde{\beta} \simeq \tilde{\alpha}$. Then

$$\begin{aligned} C_{1,1}^{k, \tilde{\beta}}(\xi) &= (2\pi)^{-3} \int dp e^{ip \cdot \xi} \chi^{k, \tilde{\beta}}(p) \frac{-ip_0 - e^*(\mathbf{p})}{(p^0)^2 + (e_{|\Gamma|}^*(\mathbf{p}))^2} \\ &\sim -(2\pi)^{-2} 2^{-k/2} e^{-i\mathbf{p}^{k, \tilde{\beta}} \cdot \mathbf{x}} \int dp^0 \int p_F^* dp_\perp \chi^k(p_\perp) \frac{p_F^*}{m^*} \frac{p_\perp}{((p^0)^2 + (e_{|\Gamma|}^*(\mathbf{p}))^2)} e^{i\delta p \cdot \xi} \end{aligned} \quad (5.26)$$

where $\delta p := (p^0, \mathbf{p} - \mathbf{p}^{k, \tilde{\beta}})$ and (to leading order) $|\mathbf{p}| = p_F^* + p_\perp$ has been replaced with p_F^* . If $|\xi| \ll 2^j \mu^{-1}$, then the first-order Taylor expansion $e^{i\delta p \cdot \xi} \sim 1 + i\delta p \cdot \xi$ is a good approximation. By symmetry, the term of order 0 vanishes, so the maximum order of

magnitude of $|C_{1,1}^{k,\tilde{\beta}}(0, \mathbf{x})|$ is obtained not in a neighborhood of 0, but for $\mathbf{x} \approx 2^j p_F^{-1} \mathbf{e}_1$. Replacing $e^{-i\delta \mathbf{p} \cdot \mathbf{x}} - 1$ by $-i\delta \mathbf{p} \cdot \mathbf{x}$, one obtains for such \mathbf{x}

$$|C_{1,1}^{k,\tilde{\beta}}(0, \mathbf{x})| \approx 2^{-k/2} |\mathbf{x}| m^* \int dp^0 dp_\perp \approx 2^{-3j/2} (p_F^*)^2 \quad (5.27)$$

as expected from (5.25), whereas

$$|C_{1,1}^{k,\tilde{\beta}}(\xi)| \approx 2^{-5j/2} |\xi| (p_F^*)^3, \quad |\xi| \ll 2^j p_F^{-1}. \quad (5.28)$$

Hence (integrating over a box and summing over the $\approx 2^{j/2}$ angular sectors $\tilde{\beta}$) one may conjecture that

$$\int d\xi |\mathbf{x}|^2 |C_{1,1}^{j \rightarrow}(\xi)|^2 \approx 2^{j/2} \cdot \frac{1}{m^* \mu^2} 2^{5j/2} \cdot \left(2^j (p_F^*)^{-1} \times 2^{-3j/2} (p_F^*)^2\right)^2 = 2^{2j} \mu^{-1}. \quad (5.29)$$

Letting $2^{-j} \mu \approx \Gamma_\phi$ be near the transition scale, this yields $-\nabla^2 \mathcal{A}_q(\Upsilon_3) \Big|_{q=0} \approx \left(\frac{p_F^*}{m^*}\right)^2 \frac{m^*}{\Gamma_\phi^2} \text{Id}$, which is what one wanted to prove. Considering instead $\partial_{q^0}^2 \mathcal{A}_q(\Upsilon_3) \Big|_{q=0}$, one expands similarly $e^{ip^0 \tau} = 1 + ip^0 \tau + \dots$, replaces $e^{ip^0 \tau} - 1$ by $ip^0 \tau$ and obtains a bound of the same magnitude but without the dimensionful prefactor $v_\phi^2 \approx \left(\frac{p_F^*}{m^*}\right)^2$.

This is however not a rigorous proof, since there is some overlap between sectors, namely, e.g. $\int d\xi |\mathbf{x}|^2 C^{j,\tilde{\alpha}}(\xi) (C^{k,\tilde{\beta}}(\xi))^* \neq 0$ in general for neighboring sectors $(j, \tilde{\alpha})$, $(k, \tilde{\beta})$ with $|j - k|, |\tilde{\alpha} - \tilde{\beta}| = O(1)$. It is simpler – though less instructive – to integrate over the angular coordinate along the Fermi sphere; making computations for an arbitrary value of Γ and j will allow us to produce at the same time the asymptotics (0.55) for the one-point density kernel, and the desired order of magnitude for the second derivatives of $\mathcal{A}(\Upsilon_3)$. Let $\rho := |\mathbf{p}|$. We use the standard formula

$$\frac{1}{2\pi} \int d\theta e^{i\rho |\mathbf{x}| \cos(\theta)} = J_0(\rho |\mathbf{x}|) \sim_{|\mathbf{x}| \rightarrow \infty} \sqrt{\frac{2}{\pi \rho |\mathbf{x}|}} \cos(\rho |\mathbf{x}| - \frac{\pi}{4}) + O\left(\frac{1}{\rho |\mathbf{x}|}\right) \quad (5.30)$$

in terms of Bessel functions of the first kind, and neglect the ultra-violet cut-off at scale j_D . Then the theorem of residues yields

$$\begin{aligned} C_{1,1}^{j \rightarrow}(\xi) &= (2\pi)^{-2} \int d\mathbf{p} \operatorname{sgn}(p_\perp) f(p_\perp) \chi^{j \rightarrow}(p) e^{-|e_{|\Gamma|}^*(\mathbf{p})\tau| + i\mathbf{p} \cdot \mathbf{x}} \\ &= (2\pi)^{-1} \int dp_\perp \chi^{j \rightarrow}(p) \operatorname{sgn}(p_\perp) f(p_\perp) e^{-|e_{|\Gamma|}^*(p_\perp)\tau|} \cdot (p_F^* + p_\perp) J_0((p_F^* + p_\perp)|\mathbf{x}|) \end{aligned} \quad (5.31)$$

$$\begin{aligned} \sim_{|\mathbf{x}| \rightarrow \infty} (2\pi)^{-1} \sqrt{\frac{2}{\pi |\mathbf{x}|}} \int dp_\perp \chi^{j \rightarrow}(p) \operatorname{sgn}(p_\perp) f(p_\perp) e^{-|e_{|\Gamma|}^*(p_\perp)\tau|} \cdot \\ \cdot (p_F^* + p_\perp)^{1/2} \cos((p_F^* + p_\perp)|\mathbf{x}|). \end{aligned} \quad (5.32)$$

where $f(p_\perp) := \begin{cases} \frac{(e^* - e_{|\Gamma|}^*)(p_\perp)}{2e_{|\Gamma|}^*(p_\perp)} & (p_\perp \tau > 0) \\ \frac{(e_{|\Gamma|}^* + e^*)(p_\perp)}{2e_{|\Gamma|}^*(p_\perp)} & (p_\perp \tau < 0) \end{cases}$. Replacing $\chi^{j \rightarrow}(p)$ by $\chi(p) \equiv \lim_{j \rightarrow +\infty} \chi^{j \rightarrow}(p)$,

and letting (as a vestige of the smoothing due to ultra-violet cut-off) $C_{1,1}^{j \rightarrow}(0, \mathbf{x}) := \frac{1}{2} \lim_{\tau \rightarrow 0^+} \left(C_{1,1}^{j \rightarrow}(\tau, \mathbf{x}) + C_{1,1}^{j \rightarrow}(-\tau, \mathbf{x}) \right)$, so that the coefficient $f(p_\perp)$ is replaced by the even function $\tilde{f}(p_\perp) := \frac{1}{2}(f(p_\perp) + f(-p_\perp)) = \frac{1}{2} \frac{e^*(p_\perp)}{e_{|\Gamma|}^*(p_\perp)}$ in the above integrals, one obtains (0.55) in the limit $\Gamma \rightarrow 0$ by remarking that

$$\int_0^{+\infty} dp_\perp \chi(p) (p_F^* + p_\perp)^{1/2} e^{\pm i(p_F^* + p_\perp)|\mathbf{x}|} \sim_{|\mathbf{x}| \rightarrow \infty} -\frac{e^{\pm i p_F^* |\mathbf{x}|} (p_F^*)^{1/2}}{|\mathbf{x}|}. \quad (5.33)$$

Assume on the other hand that $|\mathbf{x}| \approx 2^{j_\phi} (p_F^*)^{-1}$. Hence one may (up to an exponentially small error) replace $\chi(p) (p_F^* + p_\perp)^{1/2}$ in the above expressions by $(p_F^*)^{1/2}$, and $\text{sgn}(p_\perp) \tilde{f}(p_\perp)$ by $\frac{p_\perp}{\sqrt{p_\perp^2 + p_\phi^2}}$, with $p_\phi := \frac{m^*}{p_F^*} \Gamma_\phi$. Hence

$$\begin{aligned} C_{1,1}(0, \mathbf{x}) &\sim \frac{C}{\sqrt{|\mathbf{x}|}} \text{Re} \left\{ e^{i p_F^* |\mathbf{x}|} (p_F^*)^{1/2} \int dp_\perp \frac{p_\perp}{\sqrt{p_\perp^2 + p_\phi^2}} e^{i p_\perp |\mathbf{x}|} \right\} \\ &\sim \frac{C}{\sqrt{|\mathbf{x}|}} \text{Re} \left\{ e^{i p_F^* |\mathbf{x}|} (p_F^*)^{1/2} \frac{-i p_\phi^2}{|\mathbf{x}|} \int \frac{e^{i p_\perp |\mathbf{x}|} dp_\perp}{(p_\perp^2 + p_\phi^2)^{3/2}} \right\} \\ &\sim \frac{C}{\sqrt{|\mathbf{x}|}} \sin(p_F^* |\mathbf{x}|) (p_F^*)^{1/2} p_\phi K_1(p_\phi |\mathbf{x}|) \end{aligned} \quad (5.34)$$

with $C = 2(2\pi)^{-1} \sqrt{\frac{2}{\pi}}$, where $K_1(p_\phi |\mathbf{x}|)$ is a modified Bessel function (exponentially decreasing at infinity for $|\mathbf{x}| \gg p_\phi^{-1}$), see [4] (7) p. 11. All together, one has found that $C_{1,1}(0, \mathbf{x})$ is equal for $|\mathbf{x}| \approx p_\phi^{-1}$ to $\approx (p_F^*)^{1/2} p_\phi^{3/2} \approx 2^{-3j_\phi/2} (p_F^*)^2$, in conformity with (5.27), times a fast oscillating phase function.

The above argument is easily adapted to prove that $|C_{1,1}(\tau, \mathbf{x})| \approx 2^{-3j_\phi/2} (p_F^*)^2$ for $|\tau| \approx \Gamma_\phi$. Namely, the change of variable $p_\perp \mapsto P := \sqrt{p_\perp^2 + p_\phi^2}$ ($p_\perp > 0$) reduces the problem to the evaluation of the Laplace transform of the function $P \mapsto \frac{P}{\sqrt{P^2 - p_\phi^2}} \mathbf{1}_{P > p_\phi}$, which is also equal to the function $p_\phi K_1(p_\phi |\mathbf{x}|)$, see [4] (29) p. 136. \square

We further prove eq. (1.87) and (1.88). The infra-red cut-off bound (1.88) actually plays a minor rôle for the proof of (1.87), so let us prove it first. We concentrate on spatial gradients $(\frac{\mu}{p_F^*} \nabla_{\mathbf{q}})^\kappa f(q)$, with $f = \mathcal{A}^{j \rightarrow}(\Upsilon_3)$, $\text{Pre}\Sigma^{j \rightarrow}$ or $\Sigma^{j \rightarrow}$, but the bounds we write down also hold for homogenized gradients $\nabla_q^\kappa := \nabla_{q^0}^{\kappa_0} (\frac{\mu}{p_F^*} \nabla_{q^1})^{\kappa_1} (\frac{\mu}{p_F^*} \nabla_{q^2})^{\kappa_2}$.

Let $|q|_+ \gg \Gamma_\phi$. Then $(\frac{\mu}{p_F^*} \nabla_{\mathbf{q}})^\kappa \mathcal{A}_q^{j \rightarrow}(\Upsilon_3) \lesssim \frac{m^*}{|q|_+^\kappa}$ as shown by following the arguments in the proof of (1.59); $1 - \lambda \mathcal{A}_q^{j \rightarrow}(\Upsilon_3, \text{diag}) \approx \lambda m^* \log(|q|_+/\Gamma_\phi)$; and $\frac{\mu}{p_F^*} \nabla_{\mathbf{q}} \text{Pre} \Sigma^{j \rightarrow}(q) = \frac{\mu}{p_F^*} \nabla_{\mathbf{q}} \frac{\lambda}{1 - \lambda \mathcal{A}_q^{j \rightarrow}(\Upsilon_3)} = \frac{\lambda}{(1 - \lambda \mathcal{A}_q(\Upsilon_3))^2} \lambda \frac{\mu}{p_F^*} \nabla_{\mathbf{q}} \mathcal{A}_q^{j \rightarrow}(\Upsilon_3) = O(\frac{1}{m|q|_+ \log^2(|q|_+/\Gamma_\phi)})$, from which by an easy induction (1.88) holds.

We now return to corrections to leading-order behavior of $\Sigma(q)$,

$$\Sigma(\xi) \sim_{|\xi|_+ \rightarrow \infty} \frac{1}{4\pi} \frac{g_\phi/v_\phi^2}{|\xi|_+} (1 + O(\frac{1}{\Gamma|\xi|_+})). \quad (5.35)$$

Error terms involve both the correction to leading-order term in (1.84) for $|q|_+ \lesssim \Gamma_\phi$, and a subleading contribution obtained by integrating over large transfer momenta q such that $\Gamma_\phi \ll |q|_+ \lesssim \hbar\omega_D$. In either case, the idea is to apply repeated integrations by parts on $f(q) = \Sigma(q)$ or $f(q) = \Sigma(q) - \frac{g_\phi}{q_0^2 + v_\phi^2 |\mathbf{q}|^2}$,

$$\left| \int dq e^{i(q,\xi)} f(q) \right| \lesssim \frac{1}{((\xi^1)^2 + (\xi^2)^2)^{|\kappa|/2}} \int dq |\nabla_{\mathbf{q}}^\kappa f(q)|,$$

where $\kappa \in \mathbb{N}$ is arbitrarily large and $\nabla_{\mathbf{q}}^\kappa = \partial_{q^0}^{\kappa_0} \prod_{i=1}^2 (\frac{1}{v_\phi} \partial_{q^i})^{\kappa_i}$. The contribution of large transfer momenta is easily bounded using (1.88): if $|\kappa| > 3$,

$$\int_{|q|_+ \gg \Gamma_\phi} dq |\nabla_{\mathbf{q}}^\kappa \Sigma(q)| = O(\frac{1}{m^* v_\phi^2 \Gamma_\phi^{\kappa-3}}). \quad (5.36)$$

So assume that $|q|_+ \lesssim \Gamma_\phi$; we leave it to the reader to check that

$$\nabla_{\mathbf{q}}^\kappa \left(\Sigma(q) - \frac{g_\phi}{q_0^2 + v_\phi^2 |\mathbf{q}|^2} \right) = \frac{O(g_\phi)}{\Gamma_\phi^2 |q|_+^{|\kappa|}} \quad (5.37)$$

for $|q|_+ \lesssim \Gamma_\phi$. Hence

$$\int_{|q|_+ \lesssim \Gamma_\phi} dq |\nabla_{\mathbf{q}}^2 \Sigma(q)| \lesssim (\frac{p_F^*}{m^*})^{-2} \frac{g_\phi}{\Gamma_\phi} \approx \frac{g_\phi}{v_\phi^2 \Gamma_\phi}, \quad (5.38)$$

from which, finally, (1.87) holds. \square

5.5 Error terms for Ward identities

We bound here the error terms "err." due to the propagator cut-offs neglected in §3.3. We consider to begin with the variation of the fermionic covariance kernel $C_\theta^{\rightarrow jD}(p) \equiv \chi^{\rightarrow jD}(|p|/\mu) C_\theta(p)$, $C_\theta(p) := \frac{1}{ip^0 - e^*(\mathbf{p})\sigma^3 - \Gamma(\theta)}$ under an infinitesimal gauge transformation α . The commutator $[\alpha(q), C_\theta^{\rightarrow jD}(p)]$ is a sum of two terms, $[\alpha(q), C_\theta(p)] \chi^{\rightarrow jD}(|p|/\mu) +$

$[\alpha(q), \chi^{\rightarrow jD}(|p|/\mu)]C_\theta(p)$. Since $\alpha(\xi)$ acts multiplicatively on fields, its Fourier transform $\alpha(q)$ acts by convolution,

$$\begin{aligned} [\alpha*, \chi^{\rightarrow jD}(\cdot)]f(p) &= \int dq \left\{ \alpha(q)\chi^{\rightarrow jD}(|p-q|/\mu) - \chi^{\rightarrow jD}(|p|/\mu)\alpha(q) \right\} f(p-q) \\ &= \int dq \left\{ \chi^{\rightarrow jD}(|p-q|/\mu) - \chi^{\rightarrow jD}(|p|/\mu) \right\} \alpha(q)f(p-q). \end{aligned} \quad (5.39)$$

Write $(\delta_\alpha)_{cut}I_{n-1}(\xi_1, \dots, \xi_{n-1})$ the contribution of this term to (3.53), and proceed as done in the proof of Ward identities, see §3.3 **B.**, namely, take the functional derivative $\frac{\delta}{\delta\alpha(\xi_n)}$, multiply by the low-momentum kernel $\Sigma^{k_+,n}(\xi_{ext,n} - \xi_n)$, and integrate w.r. to ξ_n . After a Fourier transform, this is equivalent to the expression

$$\int dq \Sigma^{k_+,n}(q) \left\{ \chi^{\rightarrow jD}(|p-q|/\mu) - \chi^{\rightarrow jD}(|p|/\mu) \right\} f(p-q). \quad (5.40)$$

The above integral is restricted to $|q|_+ \approx 2^{-k_+}\mu$. By symmetry, the difference in (5.40) vanishes to order 1 when $q \rightarrow 0$. Hence the kernel $\chi^{\rightarrow jD}(|p-q|/\mu) - \chi^{\rightarrow jD}(|p|/\mu)$ in (5.40) may be replaced by a second-order derivative bounded like $|q|_+^2 |\nabla_p^2 \chi^{\rightarrow jD}(|p|/\mu)| = O(2^{-2k_+}\mu)$. Thus the error term exhibits a squared spring term $2^{-2(k_+-j_+)}$ as in §3.3, and a further absolute small factor $O(2^{-2j_+})$.

Let us illustrate this on an example.

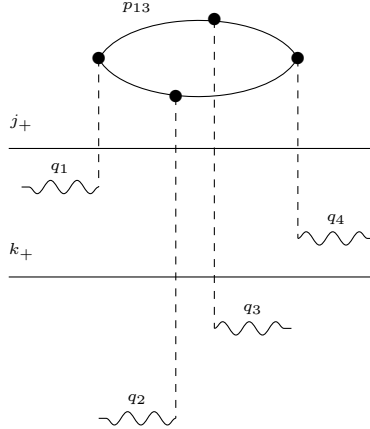


Fig. 5.5.1. An example of multi-scale diagram.

Internal momenta are p_{ij} , $(i, j) = (1, 2), (1, 3), (2, 4), (3, 4)$ connecting $\xi_{ext,i}$ with external transfer momentum q_i to $\xi_{ext,j}$ with external transfer momentum q_j . Let $p = p_{12}$. The amplitude of the amputated diagram Υ is given by an integral in p ,

$$\mathcal{A}(\Upsilon; \xi_{ext,1}) = \int dp \prod_{(i,j)} (\chi^{\rightarrow jD} C_\theta)(p_{ij}). \quad (5.41)$$

Let $f_{ij}(p) := \prod_{(i',j') \neq (i,j)} \chi(p_{i'j'}) \cdot \prod_{(i',j')} C_\theta(p_{i'j'})$. Then

$$(\delta_\alpha)_{cut} \mathcal{A}(\Upsilon; \xi_{ext,1}) = \sum_{(i,j)} \int dp \int dq \left\{ \chi^{\rightarrow jD}(|p-q|/\mu) - \chi^{\rightarrow jD}(|p|/\mu) \right\} \alpha(q) f_{ij}(p-q). \quad (5.42)$$

A similar analysis may be done for the variation under α of the *Goldstone boson* propagator $\Sigma^{j+\rightarrow}(p) = \chi_+^{j+\rightarrow}(|p|_+/\mu) \Sigma(p)$. This time, $\chi^{j+\rightarrow}(|p-q|_+/\mu) - \chi^{j+\rightarrow}(|p|_+/\mu)$ in (5.42) may be replaced by a second-order derivative bounded like $|q|_+^2 |\nabla_p^2 \chi^{j+\rightarrow}(|p|_+/\mu)| = O(2^{-2(k_+-j_+)})$, yielding precisely the desired squared spring factor.

5.6 Mayer expansion

We introduce here a variant of the BKAR formula already described in §5.2, to be used for the Mayer expansion (see §2.3.5). The idea is to test overlaps between polymers in $\mathcal{P}^{j+\rightarrow}$ with a *small* number of external legs, so as to extract leading-order translation-invariant quantities.

Let \mathcal{O} be the set of *polymers* in $\mathbb{P}^{j+\rightarrow}$. Among these polymers, there are polymers with $< N_0 = 8$ external legs, making up a subset $\mathcal{O}_1 \subset \mathcal{O}$. The complementary set \mathcal{O}_2 is made up of polymers with $\geq N_0$ external legs, which need no particular further treatment. The following variant of BKAR's formula, found originally in [1], is stated in the present form in [54]. We now denote by $\{\mathbb{P}_\ell, \mathbb{P}'_\ell\}$ a pair of polymers connected by a link $\ell \in L(\mathcal{O})$.

Proposition 5.4 (restricted 2-type cluster or BKAR2 formula) *Assume $\mathcal{O} = \mathcal{O}_1 \amalg \mathcal{O}_2$. Choose as initial object an object $o_1 \in \mathcal{O}_1$ of type 1, and stop the Brydges-Kennedy-Abdesselam-Rivasseau expansion as soon as a link to an object of type 2 has appeared. Then choose a new object of type 1, and so on. This leads to a restricted expansion, for which only the link variables z_ℓ , with $\ell \notin \mathcal{O}_2 \times \mathcal{O}_2$, have been weakened. The following closed formula holds. Let $\mathbf{S} : L(\mathcal{O}) \rightarrow [0, 1]$ be a link weakening of \mathcal{O} , and $F = F((\mathbf{S}_\ell)_{\ell \in L(\mathcal{O})})$ a smooth function. Let $\mathcal{F}_{res}(\mathcal{O})$ be the set of forests \mathbb{G} on \mathcal{O} , each component of which is (i) either a tree of objects of type 1, called unrooted tree; (ii) or a rooted tree such that only the root is of type 2. Then*

$$F(1, \dots, 1) = \sum_{\mathbb{G} \in \mathcal{F}_{res}(\mathcal{O})} \left(\prod_{\ell \in L(\mathbb{G})} \int_0^1 dW_\ell \right) \left(\left(\prod_{\ell \in L(\mathbb{G})} \frac{\partial}{\partial S_\ell} \right) F(S_\ell(\mathbf{W})) \right), \quad (5.43)$$

where $S_\ell(\mathbf{W})$ is either 0 or the minimum of the w -variables running along the unique path in \mathbb{G} from \mathbb{P}_ℓ to \mathbb{P}'_ℓ , and $\bar{\mathbb{G}}$ is the forest obtained from \mathbb{G} by merging all roots of \mathbb{G} into a single vertex.

The above Proposition is applied to the non-overlap function $F = \text{NonOverlap}$ in §2.3.5.

Index of notations

- $\mathcal{A}(\Upsilon)$, diagram amplitude 34
- $\mathcal{A}(\mathbb{P})$, polymer amplitude 83
 - \mathbb{D}^j , set of scale j boxes 62
 - $d\mu_{\theta;\lambda}$, symmetry-broken measure 33
 - $e^*(p)$, renormalized dispersion relation 30
 - g , non-dimensional coupling constant 9
 - g_ϕ^0 , pre-Goldstone boson coupling constant, 19
 - Hor^j , horizontal expansion operator, 81, 153
 - $I_{s.c.,//}^{j+\rightarrow}, I_{s.c.,\perp}^{j+\rightarrow}$, one-point function 132
 - j_D , highest momentum scale (Debye cut-off) 6
 - j_ϕ , transition scale, 17
 - \mathcal{L}_θ , action 33
 - LN, linking number 122
 - m , mass
 - μ , chemical potential
 - N_j number of scale j angular sectors 9,60,93
 - N_{ext} , 77
 - \mathbb{P} , polymer 75
 - p_\perp , transverse momentum coordinate 31
 - p_F , Fermi momentum 6
 - $p^{j,\alpha}$, momentum in $\mathcal{S}^{j,\alpha}$ 60
 - $\mathcal{S}^{j(\alpha,k)}$ angular sectors 60, 61
 - t^j , vertical expansion parameters 94
 - v_F , Fermi velocity 13
 - v_ϕ^0 , Goldstone pre-boson velocity 19
 - $\text{Vert}^j(\mathbb{P})$, vertical expansion parameter 94
 - α , angular sector 60
 - Γ , complex 25
 - $\Gamma^{//,\perp}$ or $\Gamma^{//,\perp}(\theta)$, 106
 - Δ , box 62
 - λ , coupling constant 6
 - $\bar{\Pi}$, Bethe-Salpeter kernel 55
 - $\bar{\Pi}^{disp}$, 54
 - Pre Σ , pre-Goldstone boson propagator 43
 - Σ , Goldstone boson propagator 43,139
 - Σ_F , Fermi circle 4
 - $\Upsilon_{3,diag}$, Cooper pair bubble diagram 38
 - $\Psi, \bar{\Psi}$, Nambu spinors 28
 - $\omega(N_{ext})$, degree of divergence 129
 - $|\cdot|$, fermionic norm 25
 - $C_\theta^*, C_\theta^{j(\alpha)}$, symmetry-broken covariance 30, 32
 - $d\mu_\theta^*$, symmetry-broken Gaussian measure 33
 - $e(p)$, dispersion relation 4
 - $e_{|\Gamma|}^*(p)$, 31
 - G , Green function 28
 - g_ϕ , Goldstone boson coupling constant, 19
 - $I_{(0,n)}^{j+\rightarrow}, I_{(k//,k_\perp)}^{j+\rightarrow}$, n -point functions 134,136
 - j_+ , bosonic scale 25
 - j'_ϕ , modified transition scale 14,92
 - $\mathcal{L}_\theta^\rightarrow(\mathbf{t})$, dressed action 66
 - m^* , renormalized mass 17
 - μ^* , renormalized chemical potential 17
 - $N_{ext,+}$, 140
 - $\mathbb{P}^{j\rightarrow}, \mathcal{P}^{j\rightarrow}$, (set of) lowest scale j polymers 77
 - p_c , 20
 - p_F^* , renormalized Fermi momentum 8
 - s^j , scale j cluster parameters 79
 - S , Mayer expansion parameters 97, 96
 - v_ϕ , Goldstone boson velocity 19
 - Z^j , wave-function renormalization 70
 - $\mathbb{F}, \mathbb{F}(\theta)$, Γ -matrix 18
 - $\mathbf{\Gamma}$, vector 25
 - Γ_ϕ , energy gap 18
 - χ_Δ , box cut-off function 62
 - $\tilde{\Pi}$, 48
 - $\tilde{\Pi}^{proj}$, 54
 - $\tilde{\Sigma}^{disp}$, 54
 - Σ_F^* , renormalized Fermi circle 31
 - $\Upsilon_{3,off}$, off-diagonal bubble diagram 37
 - $\Psi^{j(\alpha)}, \bar{\Psi}^{j(\alpha)}$ 32
 - ω_D , Debye energy 4
 - $|\cdot|_+$, bosonic norm 25

References

- [1] A. Abdesselam, V. Rivasseau. *Trees, forests and jungles: A botanical garden for cluster expansions*, Lecture Notes in Physics **446**, Springer Berlin/Heidelberg (1995).
- [2] A. Altland, B. Simons. *Condensed matter field theory*, Cambridge University Press (2010).
- [3] J. Bardeen, L. N. Cooper, J. R. Schrieffer. *Theory of superconductivity*, Phys. Rev. **108**, 1175– (1957).
- [4] H. Bateman. *Tables of Integral Transforms* (Vol. I), McGraw-Hill Book Company (1954).
- [5] K. van der Beek, F. Lévy-Bertrand. *Les vortex dans les supraconducteurs. Une matière molle au sein de la matière dure*, Reflets de la Physique, Société française de physique, January 2012.
- [6] J. Bellissard, J. Magnen, V. Rivasseau. *Supersymmetric analysis of a simplified two-dimensional Anderson model at small disorder*, Markov Process. Related Fields **9**, 261–278 (2003).
- [7] N. N. Bogoliubov, *On the theory of superfluidity*, J. Phys. **11**, 23– (1947).
- [8] N. N. Bogoliubov. *A new method in the theory of superconductivity I*, Soviet Phys. JETP **34**, 41–46 (1958).
- [9] D. Brydges. *A short course on cluster expansions*. In: *Critical phenomena, random systems, gauge theories*, Ecole d’été des Houches 1984, Elsevier (1986).
- [10] E. J. Candès, L. Demanet. *The curvelet representation of wave propagators is optimally sparse*, Comm. Pure Appl. Math. **58** (11), 1472–1528 (2005).
- [11] E. J. Candès, D. L. Donoho. *New tight frames of curvelets and optimal representations of objects with C^2 singularities*, Comm. Pure Appl. Math. **57** (2), 219–266 (2004).
- [12] P. G. De Gennes. *Superconductivity of Metals and Alloys*, Addison Wesley Publishing Company (1989).
- [13] A. Dembo, O. Zeitouni. *Large deviations techniques and applications*, Applications of Mathematics **38**, Springer (2010).
- [14] P. Di Francesco, P. Ginsparg. *2D gravity and random matrices*, Phys. Rep. **254**, 1– (1995).

- [15] M. Disertori, J. Magnen, V. Rivasseau. *Parametric Cutoffs for Interacting Fermi Liquids*, Ann. Henri Poincaré **14** (4), 925–945 (2013).
- [16] M. Disertori, V. Rivasseau. *A Rigorous Proof of Fermi Liquid Behavior for Helium Two-Dimensional Interacting Fermions*, Phys. Rev. Lett. **85**, 361– (2000).
- [17] M. Disertori, V. Rivasseau. *Interacting Fermi liquid in two dimensions at finite temperature. Part I: Convergent attributions*, Commun. Math. Phys. **215** (2), 251290 (2000).
- [18] M. Disertori, V. Rivasseau. *Interacting Fermi liquid in two dimensions at finite temperature. Part II: Renormalization*, Commun. Math. Phys. **215** (2), 291341 (2000).
- [19] *Constructive quantum field theory*, Proceedings of the 1973 Erice Summer School, ed. by G. Velo and A. Wightman, Lecture Notes in Physics **25**, Springer (1973).
- [20] J. Feldman, H. Knörrer, R. Sinclair, E. Trubowitz. *Superconductivity in a repulsive model*, Helv. Phys. Acta **70**, 154–191 (1997).
- [21] J. Feldman, J. Magnen, V. Rivasseau, R. Sénéor. *Construction and Borel summability of infrared Φ_4^4 by a phase space expansion*, Comm. Math. Phys. **109**, 437–480 (1987).
- [22] J. Feldman, J. Magnen, V. Rivasseau, E. Trubowitz. *Fermionic many-body models*, CRM Proceedings and Lecture Notes **7** (1994).
- [23] J. Feldman, J. Magnen, V. Rivasseau, E. Trubowitz. *An intrinsic $1/N$ expansion for many fermion systems*, Europhysics Letters **24**, 437-442 (1993).
- [24] J. Feldman, J. Magnen, V. Rivasseau, E. Trubowitz. *Ward identities and a perturbative analysis of a $U(1)$ Goldstone boson in a many fermion system*, Helv. Phys. Acta **66** (5), 498550 (1993).
- [25] J. Feldman, J. Magnen, V. Rivasseau and E. Trubowitz. *An infinite volume expansion for many Fermions Green's functions*, Helv. Phys. Acta **65**, 679 (1992).
- [26] A. Fetter, J. Walecka. *Quantum theory of many-particle systems*, McGraw-Hill (1971).
- [27] E. Fradkin. *Field theories of Condensed Matter Physics*, second edition, Cambridge Univeresity Press (2013).
- [28] R. L. Frank, C. Hainzl, R. Seiringer, J. P. Solovej. *Microscopic derivation of Ginzburg-Landau theory*, J. Amer. Math. Soc. **25** (3), 667713 (2012).

- [29] Y. Frishman, J. Sonnenschein. *Non-perturbative field theory. From two-dimensional conformal field theory to QCD in four dimensions*, Cambridge Monographs on Mathematical Physics, Cambridge University Press (2010).
- [30] H. Fröhlich. *Theory of the superconducting state. I. The ground state at the absolute Zero of temperature*, Phys. Rev. **79**, 845– (1950).
- [31] H. Fröhlich. *Interaction of electrons with lattice vibrations*, Proc. Roy. Soc. (London) **A215**, 291– (1952).
- [32] J. Fröhlich, T. Spencer. *The Kosterlitz-Thouless transition in two-dimensional abelian spin systems and the Coulomb gas*, Comm. Math. Phys. **81**, 527–602 (1981).
- [33] G. Gallavotti, K. Nicolò. *Renormalization theory in 4-dimensional scalar fields*, Comm. Math. Phys. **100**, 545–590 and **101**, 247–282 (1985).
- [34] K. Gawedzki, A. Kupiainen. *Massless lattice ϕ_4^4 theory: rigorous control of a renormalizable asymptotically free model*, Commun. Math. Phys. **99** (2) 197-252 (1985).
- [35] J. Glimm and A. Jaffe. *Quantum Physics, A Functional Point of View*, Springer (1987).
- [36] J. Glimm and A. Jaffe. *Positivity of the φ_3^4 Hamiltonian* Fortschr. Phys. **21**, 327–376 (1973) .
- [37] N. Goldenfeld. *Lectures on phase transitions and the renormalization group*, Addison-Wesley (1992).
- [38] J. Goldstone. *Field theories with "superconductor" solutions*, Nuovo Cim. **19**, 154– (1961).
- [39] L. P. Gor'kov. *On the energy spectrum of superconductors*, Sov. Phys. JETP. **34** (7), 505– (1958).
- [40] R. Gurau. *The $1/N$ expansion of colored tensor models*, Ann. Henri Poincaré **12**, 829–847 (2011).
- [41] R. Gurau, V. Rivasseau. *The $1/N$ expansion of colored tensor models in arbitrary dimension*, Europhysics Letters **95** (5).
- [42] C. Hainzl, R. Seiringer. *Low density limit of BCS theory and Bose-Einstein condensation of fermion pairs*, Lett. Math. Phys. **100** (2), 119138 (2012).
- [43] C. Hainzl, B. Schlein. *Dynamics of Bose-Einstein condensates of fermion pairs in the low density limit of BCS theory*, J. Funct. Anal. **265** (3), 399423 (2013).

- [44] C. Hainzl, E. Hamza, R. Seiringer, J. P. Solovej. *The BCS functional for general pair interactions*, Commun. Math. Phys. **281** (2), 349–367 (2008).
- [45] D. Iagolnitzer, J. Magnen. *Asymptotic completeness and multiparticle structure in field theories. II Theories with renormalization: the Gross-Neveu model*, Commun. Math. Phys. **111**, 81-100 (1987).
- [46] C. Kopper. *Mass generation in the large N nonlinear sigma-model*, Commun. Math. Phys. **202**, 89–126 (1999).
- [47] W. Kohn, J. M. Luttinger. *New mechanism for superconductivity*, Phys. Rev. Lett. **15**, 524–526 (1965).
- [48] C. Kopper, J. Magnen, V. Rivasseau. *Mass generation in the large N Gross-Neveu model*, Commun. Math. Phys. **169**, 121–180 (1995).
- [49] M. Le Bellac. *Quantum and statistical field theory*, Oxford Science Publications, Oxford University Press (1991).
- [50] M. Le Bellac. *Thermal field theory*, Cambridge University Press (1996).
- [51] A.J. Leggett. *Diatomic Molecules and Cooper Pairs*, in: A. Pekalski, J. A. Przystawa (eds), *Modern trends in the theory of condensed matter*, Lecture Notes in Physics **115**, Springer (1980).
- [52] J. M. Luttinger. *New mechanism for superconductivity*, Phys. Rev. **150**, 202–214 (1966).
- [53] J. Magnen, J. Unterberger. *The scaling limit of the KPZ equation in dimension 3 and higher*, to appear at: J. Stat. Phys.
- [54] J. Magnen, J. Unterberger. *From constructive theory to fractional stochastic calculus. (II) The rough path for $\frac{1}{6} < \alpha < \frac{1}{4}$: constructive proof of convergence*, Ann. Henri Poincaré **13**, 209–270 (2012).
- [55] V. Mastropietro. *Non-perturbative renormalization*, World Scientific (2008).
- [56] J. Magnen, V. Rivasseau. *A single scale infinite volume expansion for three-dimensional many fermion Green's functions*, Math. Phys. Electron. J. **1**, 1–28 (1995).
- [57] M. Peskine, D. Schröder. *An introduction to quantum field theory*, Addison-Wesley (1995).
- [58] G. Poirot. *Mean Green's function of the Anderson model at weak disorder with an infra-red cut-off*, Ann. Inst. H. Poincaré Phys. Théor. **70**, 101–146 (1999).

- [59] J. Rammer. *Quantum field theory of non-equilibrium states*, Cambridge University Press (2007).
- [60] V. Rivasseau. *From perturbative to constructive renormalization*, Princeton Series in Physics (1991).
- [61] M. Salmhofer. *Renormalization: an introduction*, Springer Verlag (1999).
- [62] W. Pedra, M. Salmhofer. *Determinant Bounds and the Matsubara UV Problem of Many-Fermion Systems*, Commun. Math. Phys. **282**, 797-818 (2008).
- [63] M. Salmhofer. *Continuous Renormalization for Fermions and Fermi Liquid Theory*, Commun. Math. Phys. **194** (2), 249–295 (1997).
- [64] E. Sandier, S. Serfaty. *Vortices in the magnetic Ginzburg-Landau model*, Progress in Nonlinear Differential Equations and their Applications **70**, Birkhäuser (2007).
- [65] J. Schrieffer. *Theory of superconductivity*, Advanced Books Classics (1983).
- [66] G. 't Hooft. *A planar diagram theory for strong interactions*, Nucl. Phys. **B 72**, 461– (1974).
- [67] D. R. Tilley, J. Tilley. *Superfluidity and superconductivity*, IOP Publishing Ltd. (1990).
- [68] M. Tinkham. *Introduction to superconductivity*, Dover Books (2004).
- [69] J. Unterberger. *Minkowski curvelets and wave equations*, arXiv:1204.2688.
- [70] J. Unterberger. *Mode d'emploi de la thorie constructive des champs bosoniques (avec une application aux chemins rugueux). A user's guide to bosonic constructive field theory*, Confluentes Mathematici **4**, 1– (2012).
- [71] F. Vignes-Tourneret. *Renormalisation des théories de champs non commutatives*, Thèse de doctorat de l'Université Paris 11, arXiv:math-ph/0612014.
- [72] K. G. Wilson. *Renormalization Group and Critical Phenomena. I. Renormalization Group and the Kadanoff Scaling Picture*, Phys. Rev. **B4**, 3174–3184 (1971).
- [73] K. G. Wilson and J. Kogut. *The renormalization group and the ε expansion*. Physics Reports **12**, 75–200 (1974).